Faculdade de Engenharia da Universidade do Porto

Production of C_4 dicarboxylic acids from lignin oxidation

Dissertation presented to Faculdade de Engenharia da Universidade do Porto for the degree of PhD in Chemical and Biological Engineering

by

Carlos Alberto Vega-Aguilar

Supervisor: Professor Alírio E. Rodrigues
Co-supervisor: Professor Filomena Barreiro

Laboratory of Separation and Reaction Engineering, Associate Laboratory LSRE-LCM

Department of Chemical Engineering, Faculty of Engineering, University of Porto

2021

FEUP-LSRE/LCM - Universidade do Porto

This thesis was financially supported by: Base-UIDB/50020/2020 and Programmatic-UIDP/50020/2020 Funding of LSRE-LCM, funded by national funds through FCT/MCTES (PIDDAC); Base Funding - UIDB/00690/2020 of CIMO - Centro de Investigação de Montanha—funded by national funds through FCT/MCTES (PIDDAC). COST Action LignoCOST (CA17128). PhD. Scholarship MICITT-PINN-CON-2-1-4-17-1-002 funded by the Costa Rican Science, Technology and Telecommunications Ministry.

Acknowledgements

First of all, I would like to thank God for giving me the opportunity of realizing this adventure I always dreamed about. I know every challenge He placed during this project was to improve my spirit, and I thank Him for being there and not letting me down.

I want to thank Prof. Alírio Rodrigues for all his help, support, and knowledge during these four years. It has been a pleasure to work under his guidance, trying to learn his point of view and way to work that certainly made him achieve an amazing and successful scientific career.

I owe my greatest gratitude to Prof. Filomena Barreiro, it was her dedication and availability the main reason why I chose Portugal as the place for my PhD studies. I really admire her perseverance, enthusiasm and knowledge, but also her warm hearth and kindness whenever I required something. Certainly, she is an example to follow, and I am grateful for having the opportunity to learn from her.

I really want to thank my lab mates in the lignin group: Carina Costa, Elson Gomes and Filipa Casimiro. You were always promt to help when needed, and during these years, I learned a lot from you, both professional and personal.

I want to express gratitude to the LSRE group (both students, post-doc researchers and professors), for their helpful advices, promptness, and guidance whenever needed. It was an amazing place to learn the do’s and don’ts of scientific research.

I also want to acknowledge the CIMO working group, as they kindly opened the doors of the beautiful city of Bragança during my short research stay in the IPB. I specially recognise Isabel Fernandez, Arantzazu Santamaria-Echart, João Pinto, Hélder Rafael and Stephany Rezende for helping me in the lab whenever I needed, and for all the nice conversations.

I don’t have the right words to thank Vanessa Vieira and Júlia Kessler. I can only say that you were the bright light in dark times that kept me going. I really thank for having you as my lovely friends.

I can’t forget the great times with Qian Shi and Asmaa Sharkawy during the first moments of the PhD programme. Thank you, my international friends, for your help and support in all these years. I hope we will meet again in the future, somewhere in the world.

I want to acknowledge the staff from DEQ and CEMUP for their readiness to help when needed.

This work was possible thanks to the financial support given by the Ministry of Science, Technology and Telecommunications of Costa Rica, under the PINN Programme. Also, I want to acknowledge the School of Chemistry and the OIACE, from the University of Costa Rica, for their support in these years. Also, I must recognise the UCR for the excellent academic preparation, that I confirmed when studying abroad.

To my closest Friends, both in Costa Rica and here in Portugal, I give you a big hug and a sincerely *Thank you!* for being there, supporting me and giving me courage and your love. Those chats, even at late hours, were perfect to light the spirit and forget the bad moments.

I want to express my eternal gratitude to all my family. Their gentle support during my entire life has been the driving force to achieve more than I have ever dreamed. Mom and Dad: thank you for being there whatever the circumstances and giving those words of courage and strength when were most needed. Glori, Fran: I really enjoy every funny talks, and I appreciate all the help you gave while I was outside my country. Above all, thanks for being there, side by side, with my parents!

Finally, but certainly not least, I thank my wife Priscila with my entire hearth. Her presence was the fuel that pushed me to achieve whatever I proposed. Thank you for all your motivation, peacefull conversations, patience and loving care. I love so much!

“Stubborn optimism needs to motivate you daily; you always need to bear in mind why you feel the future is worth fighting for.”

by Christiana Figueres

Former Executive Secretary of the United Nations Framework Convention on Climate Change 2010-2016.

Abstract

The work developed in this doctoral thesis aimed to obtain C_4 dicarboxylic acids (C_4-DCA) from lignin oxidation as an alternative for its valorisation. C_4-DCA are used in different industries, being considered as one of the 12 biobased building blocks for a circular bioeconomy. Among these acids, succinic acid has received great focus since it is used in the polymer, pharmaceutical, and food industries and can also be converted to biobased solvents. Wet peroxide oxidation is an attractive strategy for this valorisation, since it can deal with the lignin's complex heterogeneous structure and cleave the aromatic ring to produce different C_4-DCA. This oxidation can be enhanced even further with the use of heterogeneous catalysts (e.g., titanium silicalite-1 or TS-1) and innovative heating techniques (e.g., microwave heating).

The oxidation of lignin model compounds was analysed using hydrogen peroxide in the presence of a TS-1 catalyst. Vanillic acid was converted to C_4-DCA at different yields and selectivity, depending on the reaction conditions (i.e., temperature, pH, and reaction time). In acidic pH, the main product was succinic acid, while alkaline pH led to hydroxylated acids. Modified TS-1 catalysts with metallic ions (Fe, Co, and Cu) did not improve the productivity of C_4-DCA, except for Fe-TS1 in acidic pH that gave rise to a slightly higher succinic acid yield. Other model compounds produced succinic acid at lower yields under the same conditions.

As lignin's phenolic monomers differ in the presence of the methoxyl group, its effect was evaluated in the C_4-DCA production. This substituent proved to increase the reactivity towards peroxide oxidation, being syringic acid the more reactive molecule with higher selectivity for succinic acid, compared to the vanillic and *p*-hydroxybenzoic acids. However, *p*-hydroxybenzoic acid originated the highest succinic acid yield. When lignin was oxidised without a catalyst, hardwood lignin reacted faster and produced more succinic acid than softwood lignin.

When lignin was oxidized under peroxide conditions in the presence of TS-1 catalyst, kraft, and organosolv lignins led to higher conversion towards C_4-DCA. In all cases, the yields were associated to the reaction conditions, including pH, temperature, reaction time, H_2O_2 load, and catalyst load. Indulin AT (IAT) lignin produced the highest

succinic acid yield (11.3 wt%). Lignol (EOL) lignin produced the highest malic acid yield (19.5wt%) and the total C_4-DCA yields due to the less condensed structure and a high amount of *β-O-4* bonds typically found in organosolv lignins. TS-1 proved to be reusable and stable under the tested reaction conditions, increasing C_4-DCA yields compared to the non-catalysed reaction.

Finally, microwave-assisted oxidation showed good results in converting lignin to C_4-DCA. TS-1 and Fe-TS1 improved the production of succinic and malic acids for IAT and EKL, while Fe-TS1 accelerated the conversion in the first minutes. Microwave oxidation enhanced the non-catalytic oxidation of EOL lignin, producing a higher amount of succinic and malic acids when compared to conventional heating since microwave enhanced the cleavage of *β-O-4* bonds. However, conventional heating proved to originate better lignin conversion for prolonged times.

Overall, this work provided new prospects to obtain C_4-DCA from lignin oxidation, using a heterogeneous catalyst with good results for succinic and malic acids. It also provided experimental evidences of the chemical pathways to successfully convert lignin to added-value compounds.

Resumo

O trabalho desenvolvido nesta tese doutoral focou-se na obtenção de ácidos dicarboxílicos C_4 (ADC-C_4) a partir da oxidação da lenhina como uma alternativa para a sua valorização. Os ADC-C_4 são usados em diferentes industrias, e foram selecionados como um dos 12 blocos de construção de base biológica para a bio-economia circular. Entre esses ácidos, o ácido sucínico tem recebido um grande foco dado que é usado na industria dos polímeros, farmacêutica e alimentar, e também pode ser convertido em solventes de base biológica. A oxidação aquosa por peróxido de hidrogénio é uma estratégia atrativa para essa valorização, permitindo lidar com a estrutura complexa e heterogênea da lenhina, nomeadamente abrir o anel aromático para produzir os diferentes ADC-C_4. A oxidação pode ser melhorada ainda recorrendo ao uso de catalisadores heterogéneos (e.g., silicalita de titânio-1 ou TS-1), e técnicas inovadoras de aquecimento (e.g., aquecimento por micro-ondas).

A oxidação de compostos modelos da lenhina foi analisada usando peróxido de hidrogénio na presença do catalisador TS-1. O ácido vanílico foi convertido em ADC-C_4 com diferentes rendimentos e seletividades, dependendo nas condições de reação (temperatura, pH e tempo de reação). A pH ácido, o produto principal foi o ácido succínico, enquanto a pH básico foram produzidos ácidos hidroxilados. Os catalisadores TS-1 modificados com iões metálicos (Fe, Co e Cu) não melhoraram a produtividade dos ADC-C_4, exceto para o Fe-TS1 em pH ácido que originou um rendimento ligeiramente superior de ácido succínico. Os outros compostos modelo geraram rendimentos inferiores de ácido succínico nas mesmas condições de reação.

Como os monómeros fenólicos da lenhina diferem na presença do grupo metoxilo, o seu efeito na produção de ADC-C_4 foi avaliada. Este substituinte incrementou a reatividade na oxidação com peróxido de hidrogénio, sendo o ácido siríngico a molécula mais reativa e com maior seletividade para o ácido succínico, em comparação aos ácidos vanílico e *p*-hidroxibenzoico. Porém, o ácido *p*-hidroxibenzoico alcançou o rendimento mais elevado em de ácido succínico. Quando a lenhina foi oxidada sem catalisador, a lenhina de *hardwood* reagiu mais rápido e produziu mais ácido succínico que a lenhina de *softwood*.

Quando a lenhina foi oxidada com peróxido de hidrogénio em presença do catalisador TS-1, as lenhinas kraft e organosolv originaram uma melhor conversão para ADC-C_4. Em todas as situações, os rendimentos foram associados às condições de reação, incluindo pH, temperatura, tempo de reação, conteúdos de H_2O_2 e de catalisador. A lenhina Indulin AT (IAT) originou o maior rendimento de ácido succínico (11.3 wt%). A lenhina Lignol (EOL) conduziu a um maior rendimento de ácido málico (19.5wt%) e o um maior rendimento total de ADC-C_4 devido à presença de uma estrutura menos condensada e um maior conteúdo de ligações *β-O-4*, típico de lenhinas organosolv. O catalisador TS-1 provou ser reutilizável e estável nas condições de reação, aumentando os rendimentos de ADC-C_4 em comparação com a reação não catalisada.

Finalmente, a oxidação assistida por micro-ondas conduziu a bons resultados quanto à conversão da lenhina em ADC-C_4. Os catalisadores TS-1 e Fe-TS1 melhoraram a produção de ácidos succínico e málico a partir da IAT e EKL, enquanto Fe-TS1 acelerou a conversão nos primeiros minutos. A oxidação por micro-ondas melhorou a oxidação não catalítica da lenhina EOL, produzindo uma maior quantidade de ácidos succínico e málico quando comparada com o aquecimento convencional dado que as micro-ondas favorecem a clivagem das ligações *β-O-4*. Porém, o aquecimento convencional provou ser melhor no que respeita a conversão da lenhina para tempos prolongados.

Em síntese, este trabalho apontou uma nova possibilidade de obter ADC-C_4 a partir da oxidação da lenhina, usando um catalisador heterogéneo com bons resultados na obtenção de ácidos succínico e málico. Adicionalmente, forneceu evidências experimentais das vias químicas seguidas para converter com sucesso a lenhina em compostos com valor agregado.

Resumen

El trabajo desarrollado en esta tesis doctoral fue dirigido a la obtención de ácidos dicarboxílicos C_4 (ADC-C_4) a partir de la oxidación de lignina como una alternativa para su valorización. Los ADC-C_4 son usados en diferentes industrias, y fueron seleccionados como uno de los 12 bloques de construcción de origen biológico para una bioeconomía circular. Entre estos ácidos, el ácido succínico ha recibido una gran atención porque es usado en la industria de polímeros, farmacéutica y de alimentos, y también puede transformarse en bio-disolventes. La oxidación húmeda con peróxido es una estrategia atractiva para esta valorización, porque puede lidiar con la estructura compleja e heterogénea de la lignina, y romper el anillo aromático para producir diferentes ADC-C_4. Esta oxidación puede ser mejorada aún más con el uso de catalizadores heterogéneos (por ejemplo, silicalita de titanio-1, o TS-1), y técnicas innovadoras de calentamiento (por ejemplo, calentamiento por microondas).

La oxidación de compuestos modelo de lignina fue analizada usando peróxido de hidrógeno en la presencia del catalizador TS-1. El ácido vanílico fue convertido a ADC-C_4 con diferentes rendimientos y selectividades, dependiendo de las condiciones de reacción (incluyendo temperatura, pH y tiempo de reacción). En un pH ácido, el producto principal fue el ácido succínico, mientras que el pH alcalino se produjo ácidos hidroxilados. Los catalizadores TS-1 modificados con cationes metálicos (Fe, Co, y Cu) no mejoraron la productividad de ADC-C_4, excepto por el Fe-TS1 que en medio ácido produjo una cantidad ligeramente superior de ácido succínico. Otros compuestos modelo produjeron rendimientos menores de ácido succínico bajo las mismas condiciones.

Como los monómeros fenólicos de la lignina difieren entre sí por la presencia del grupo metoxilo, su efecto fue evaluado en la producción de ADC-C_4. Este substituyente incrementó la reactividad ante la oxidación con peróxido, siendo el ácido siríngico la molécula más reactiva con mayor selectividad ante el ácido succínico, en comparación a los ácidos vanílico y *p*-hidroxibenzoico. Sin embargo, el ácido *p*-hidroxibenzoico alcanzó el mayor rendimiento de ácido succínico. Cuando ligninas fueron oxidadas sin catalizador, la lignina de maderas duras reaccionó más rápido y produjo mayor cantidad de ácido succínico que ligninas de maderas blandas.

Cuando la lignina fue oxidada con peróxido de hidrógeno en presencia del catalizador TS-1, las ligninas kraft y organosolv alcanzaron mayores conversiones hacia ADC-C_4. En todos los casos, los rendimientos fueron asociados a las condiciones de reacción, incluyendo pH, temperatura, tiempo de reacción, cantidad de H_2O_2 y carga de catalizador. La lignina Indulin AT (IAT) produjo el mayor rendimiento de ácido succínico (11.3 wt%). Sin embargo, la lignina Lignol (EOL) produjo el mayor rendimiento de ácido málico (19.5 wt%) y el mayor rendimiento general de ADC-C_4 debido a la estructura menos condensada y una mayor cantidad de enlaces *β-O-4*, típicamente encontrados en ligninas organosolv. TS-1 probó ser un catalizador reutilizable y estable bajo las condiciones de reacción, aumentando los rendimientos de ADC-C_4 en comparación a la reacción no catalizada.

Finalmente, la oxidación asistida por microondas mostró buenos resultados en la conversión de lignina a ADC-C_4. Los catalizadores TS-1 y Fe-TS1 mejoraron la producción de ácidos succínico y málico para las ligninas IAT e EKL, mientras Fe-TS1 aceleró la conversión en los primeros minutos. La oxidación por microondas mejoró la oxidación no catalítica de la lignina EOL, produciendo una mayor cantidad de ácido succínico y málico cuando es comparada con el calentamiento convencional, ya que las microondas mejoran la ruptura de los enlaces *β-O-4*. Sin embargo, el calentamiento convencional obtuvo una mejor conversión de lignina en tiempos prolongados.

Este trabajo aportó una nueva posibilidad para obtener ADC-C_4 a partir de la oxidación de lignina, usando un catalizador heterogéneo con buenos resultados en la obtención de ácidos succínico y málico. También se aportó evidencia experimental de las rutas químicas para la conversión exitosa de ligninas a compuestos de valor añadido.

Abbreviations

AA	Atomic Absorption Spectrometry
ANOVA	Analysis of variance
ALK	Alkali lignin
ATR-FTIR	Attenuated Total Reflectance- Fourier Transform Infrared Spectroscopy
BDE	Bond Dissociation Energy
BDO	1,4-butanediol
BSTFA	N,O-Bis(trimethylsilyl)trifluoroacetamide
BTX	Benzene-toluene-xylene
C_4-DCA	C_4 dicarboxylic acids
CA	Carboxylic acids
CEMUP	Centro de Materiais da Universidade do Porto
CH	Conventional heating
CWPO	Catalytic wet peroxide oxidation
DC	Degree of condensation
DCA	Dicarboxylic acids
$Đ_M$	Polydispersity
DAD	Diode Arrange Detector
DMSO-d_6	Deuterated dimethylsulfoxide
EDS	Energy-dispersive X-ray spectroscopy
EKL	*E. globulus* kraft lignin isolated from black liquor
EOL	Lignol lignin
G	Guaiacyl group
GC-FID	Gas Chromatography with flame ionization detector
GC-MS	Gas Chromatography – Mass Spectrometry
GPC	Gel Permeation Chromatography
H	*p*-hydroxylphenyl group
HPLC	High Performance Liquid Chromatography

IAT	Indulin AT
k	Reaction rate constant
MCA	Monocarboxylic acids
MFI	Specific zeolite framework
M_n	Number-average molecular weight
M_w	Weight-average molecular weight
MW	Microwave
NMR	Nuclear magnetic resonance
PBS	Polybutelene succinate
pHBA	*p*-hydroxybenzoic acid
pKa	Logarithm of Acid dissociation constant
PS	Polystyrene
PTFE	Polytetrafluoroethylene
RI	Refraction Index detector
S	Syringyl group
SA	Syringic acid
SEM	Scanning Electron Microscopy
T	Temperature
TCA	Total carboxylic acids
THF	Tetrahydrofuran
TMCS	Trimethylchlorosilane
TS-1	Titanium silicalite - 1
UV	Ultraviolet
VA	Vanillic acid
XRD	Electron Backscattered Diffraction

Table of Contents

List of Figures

List of Tables

1. Introduction

This chapter presents a brief overview of the relevance of converting lignin, obtained as a side stream of the pulp and paper industry and lignocellulosic biorefineries, towards high-added value products, such as dicarboxylic acids. These acids can be used in several fields as a renewable feedstock, diminishing fossil fuel refinery dependence. The objectives related to the proposed tasks and the outline chosen for this Ph.D. thesis are also presented.

1.1. Motivation and Relevance

In recent years, fossil resources (i.e., crude oil, coal, and natural gas) have shown a growing but erratic behavior on their prices, as their availability is decreasing and the required extraction techniques are becoming more expensive. Moreover, environmental issues seeking a change in the traditional petrochemical industry, responsible for 30% of global industrial energy use and 16% of the world's direct CO_2 emissions (Takht Ravanchi and Sahebdelfar, 2014), looking to minimize waste materials, and developing cleaner policies (Jong and Jungmeier, 2015), are also points of concern. However, crude oil refining is the source for most raw materials used in textiles, pharmaceuticals, polymers, food, and commodity chemicals. Therefore, the manufacturing industry needs new sources of raw materials that will fill the gap left by the petrochemical refining industry if the world chooses to achieve a greener and circular economy.

In 2004, the "Top Value Added Chemicals from Biomass- Volume I" report included 12 building blocks as the base of the future biomass chemicals production (Werpy and Petersen, 2004). One of these building blocks is 1,4-dicarboxylic acids (including succinic, fumaric, maleic, and malic acids), mainly used as raw materials for other compounds, as butanediol, tetrahydrofuran, and γ-butyrolactone, which could be used primarily for polymer synthesis. These 1,4-dicarboxylic acids also have application in the pharmaceuticals and food industries. Most of these compounds can be obtained using biomass fermentation, but these techniques are still under development, or use substrates (e.g., starch) that compete with food sources.

Lignin, a by-product of the pulping industry, does not compete with food sources. This renewable resource, used as a low-value fuel in pulping plants (98% is burned to provide heat and energy), is considered a bottleneck in pulp production (Ahmad et al., 2020). Given its characteristics, lignin can be removed from black liquor and depolymerized to serve as a source of chemicals or to exploit its polymeric structure in materials without affecting the energy balance of the mill (Junghans et al., 2020; Westwood et al., 2016).

Research on depolymerization is currently focused on obtaining aromatic compounds from lignin. Still, recently, there has been some interest in lignin oxidation to achieve dicarboxylic acids (DCA), which could be an important way to provide a renewable source for these building blocks (Li et al., 2015; Liu et al., 2019; Sun et al., 2018; Vangeel et al., 2018; Xu et al., 2014). Some attempts to achieve these building blocks from lignin, mainly by catalytic oxidations were already attempted, but the conversion is inefficient, or it needs strong reaction conditions, such as very high temperatures or aggressive pH environments. Therefore, strategies to enhance DCA yields, especially succinic acid, which is used today for bio-based polymers and as a feedstock for bio-solvents, through catalytic conversion using catalysts and oxidation techniques not used before, opens a motivation for further investigation.

1.2. Objectives

The present work focuses on the production of C_4 dicarboxylic acids, mainly targeting succinic acid, through catalytic wet peroxide oxidation (CWPO) of lignin using H_2O_2 and a heterogeneous catalysts, trying to achieve the highest yield possible for each selected feedstock.

The specific objectives are:

- Evaluate the CWPO on lignin model compounds using H_2O_2 and a heterogeneous catalyst.
- Assess the effect of the methoxy substituents in the CWPO of lignin model compounds and lignin.
- Test the CWPO on lignin using H_2O_2 and a heterogeneous catalyst.
- Compare the lignin oxidation process using H_2O_2 and a heterogeneous catalyst (conventional batch reactor *versus* microwave reactor).

1.3. Outline

Therefore, this thesis comprises seven chapters where the different tasks are described, and the respective results discussed.

In **Chapter 1,** the motivation and relevance of the topic is discussed, including the main objectives of this work.

In **Chapter 2**, an overview of the most relevant and recent information regarding the lignin composition and oxidation techniques and primary products, including the different oxidizers and catalysts used for catalytic oxidation is presented. This chapter also covers the economic relevance of the C_4 dicarboxylic acids, which are the main target of the present work.

Chapter 3 concerns the study of vanillic acid oxidation as a model compound for lignin, using H_2O_2 as the oxidizer and TS-1 as the catalyst. Different approaches were used in this work, namely by testing different temperatures, pH, reaction time, and amount of catalyst. Also, TS-1 was modified with metal cations (Fe, Cu, Co) to enhance the production of the desired acids. All these catalysts (both original and modified) were characterized to evaluate the best catalyst for the oxidation process. In addition, a comparison between vanillic acid and two other model compounds (*p*-hydroxybenzoic acid and syringic acid) was performed to assess the effect of the structure modification on the C_4-DCA yield.

Chapter 4 refers the study of three lignin model compounds (vanillic acid, syringic acid, and *p*-hydroxybenzoic acid) to evaluate the effect of the methoxy substituents in the production of C_4 dicarboxylic acids. This work was expanded by including the oxidation of two different lignins (Indulin AT and lignin isolated from black liquor of *Eucalyptus globulus* pulping), to test which type of lignin is the more adequate for C_4-DCA production.

In **Chapter 5**, a study of lignin oxidation using TS-1 catalyst was performed, selecting four different lignins (Indulin AT, Alkali lignin, Lignol lignin, and lignin isolated from *E. globulus* black liquor). Each lignin was oxidized using different times, temperatures, pH values, H_2O_2 loading, and catalyst loading. Then, the catalyst was evaluated in a selected lignin to see how many cycles it could be used without leading to a decreasing in the C_4-DCA yield.

In **Chapter 6**, catalytic peroxide oxidation of selected lignins was done using a microwave reactor to achieve C_4 dicarboxylic acids. Different parameters were evaluated, such as time, temperature, and type of catalyst. Also, a comparison against oxidation performed in a closed reactor using conventional heating (presented in Chapter 5) was performed.

Finally, the most relevant remarks and suggestions for future work are presented in **Chapter 7**.

1.4. References

Ahmad, Z., Dajani, W.W. Al, Paleologou, M., Xu, C., 2020. Sustainable process for the depolymerization/oxidation of softwood and hardwood kraft lignins using hydrogen peroxide under ambient conditions. Molecules 25, 1–19. https://doi.org/10.3390/molecules25102329

Jong, E. De, Jungmeier, G., 2015. Biorefinery Concepts in Comparison to Petrochemical Refineries, in: Industrial Biorefineries and White Biotechnology. Elsevier B.V., pp. 3–33. https://doi.org/10.1016/B978-0-444-63453-5.00001-X

Junghans, U., Bernhardt, J.J., Wollnik, R., Triebert, D., Unkelbach, G., Pufky-Heinrich, D., 2020. Valorization of Lignin via Oxidative Depolymerization with Hydrogen Peroxide: Towards Carboxyl-Rich Oligomeric Lignin Fragments. Molecules 25. https://doi.org/10.3390/molecules25112717

Li, C., Zhao, X., Wang, A., Huber, G.W., Zhang, T., 2015. Catalytic Transformation of Lignin for the Production of Chemicals and Fuels. Chem. Rev. 115, 11559–11624. https://doi.org/10.1021/acs.chemrev.5b00155

Liu, C., Wu, S., Zhang, H., Xiao, R., 2019. Catalytic oxidation of lignin to valuable biomass-based platform chemicals: A review. Fuel Process. Technol. 191, 181–201. https://doi.org/10.1016/j.fuproc.2019.04.007

Sun, Z., Fridrich, B., De Santi, A., Elangovan, S., Barta, K., 2018. Bright Side of Lignin Depolymerization: Toward New Platform Chemicals. Chem. Rev. 118, 614–678. https://doi.org/10.1021/acs.chemrev.7b00588

Takht Ravanchi, M., Sahebdelfar, S., 2014. Carbon dioxide capture and utilization in petrochemical industry: potentials and challenges. Appl. Petrochemical Res. 4, 63–77. https://doi.org/10.1007/s13203-014-0050-5

Vangeel, T., Schutyser, W., Renders, T., Sels, B.F., 2018. Perspective on Lignin Oxidation: Advances, Challenges, and Future Directions. Top. Curr. Chem. 376, 30. https://doi.org/10.1007/s41061-018-0207-2

Werpy, T., Petersen, G., 2004. Top Value Added Chemicals from Biomass: Volume I -- Results of Screening for Potential Candidates from Sugars and Synthesis Gas., U.S. Department of energy. United States. https://doi.org/10.2172/926125

Westwood, N.J., Panovic, I., Lancefield, C.S., 2016. Chemical Modification of Lignin for Renewable Polymers or Chemicals, in: Fang, Z., Smith, R.L.J. (Eds.), Production of Biofuels and Chemicals from Lignin. Biofuels and Biorefineries. Springer, Singapore, pp. 183–216. https://doi.org/10.1007/978-981-10-1965-4_7

Xu, C., Arancon, R.A.D., Labidi, J., Luque, R., 2014. Lignin depolymerisation strategies: towards valuable chemicals and fuels. Chem. Soc. Rev. 43, 7485–7500. https://doi.org/10.1039/C4CS00235K

2. State-of-the-Art

This chapter presents a literature review about the main lignin characteristics, including composition, extraction methods, and depolymerization strategies needed to upgrade this feedstock to added-value compounds. Given the high interest in dicarboxylic acids, which can be obtained from lignin using a ring-opening reaction under harsh reaction conditions, a detailed revision of the main works using lignin and lignin model compounds to achieve C_4 dicarboxylic acids is included. Finally, this chapter describes the primary C_4 dicarboxylic acids, their current global market, production, and their use in the chemical industry.

2.1. Introduction

Modern chemistry is mainly based on C_2-C_4 petrochemical-derived alkene and aromatic platforms, later converted into many compounds and materials used commercially. However, economic, social, and environmental reasons have boost switching from a fossil feedstock to a renewable one, thus these chemical platforms must be substituted by new bio-based chemicals (Shanks and Keeling, 2017). World lignocellulosic biomass production is estimated at around 3-5 gigaton/year, with a capacity of supplying up to 9.2 billion tons of oil equivalents, which is around 87% of the global energy demand in the year 2004 (Murali et al., 2017). Modern biorefineries take advantage of this fact by modifying the different fractions of biomass (cellulose, hemicellulose, and lignin) with different thermochemical and biological methodologies to obtain chemical platforms to be used for the production of chemicals and materials at industrial scale (Kamm et al., 2008; Kohli et al., 2019). Among these platforms, 12 bio-based building blocks were chosen given their importance and interconversion into new chemicals and materials, one of the most promising are C_4 dicarboxylic acids (Werpy and Petersen, 2004). The following sections present a comprehensive description of the main topics related to lignin conversion into platform chemicals, focusing on C_4 dicarboxylic acids production.

2.2. Lignin as a feedstock for renewable materials and chemicals

Lignin is a biopolymer present in the cell wall of all vascular plants. It is a complex three-dimensional heterogeneous polymer, presenting from 15 to 36 wt% (while the rest is cellulose, hemicellulose, and other compounds). This material gives plants their rigidity, water-impermeability, and resistance against microbial attack (Kamm et al., 2008).

Lignin is bio-synthetized from three cinnamyl alcohol monomers: *p*-coumaryl alcohol, coniferyl alcohol, and sinapyl alcohol. When incorporated in the lignin structure, these monomers are called *p*-hydroxyphenyl (H), guaiacyl (G), and syringyl (S) units, respectively, and their chemical structures are represented in Figure 2.1. These monomers differ in the number of methoxy groups attached to the aromatic ring in the C-3 and C-5 positions (Kamm et al., 2008; Upton and Kasko, 2016).

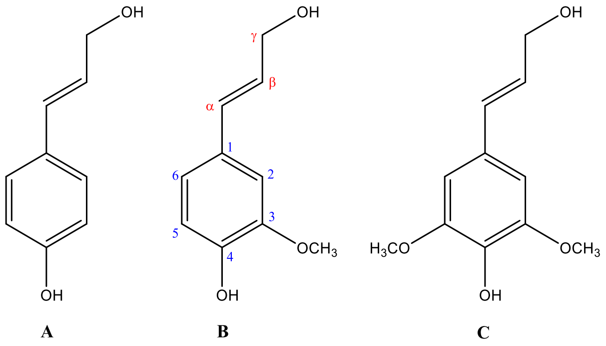

Figure 2.1 - Structure of the three main building blocks for lignin: **(a)** p-coumaryl alcohol (H), **(b)** coniferyl alcohol (G), **(c)** sinapyl alcohol (S)

The abundance of each monomer in lignin is related to plant taxonomy, as seen in Table 2.1. The relation between monomers is essential because each one has different chemical behavior and different possibilities of interlinking with other units (Kamm et al., 2008).

Table 2.1 - Abundance of cinnamyl alcohol monomers, depending on the plant taxonomy.

Monomer	**Coniferyl alcohol**	**Sinapyl alcohol**	***p*-coumaryl alcohol**
Softwood lignin	90-95%	0-1%	0.5-3.4%
Hardwood lignin	25-50%	50-75%	Traces
Grass lignin	25-50%	25-50%	10-25%

Source: Li et al., 2015

These three units are linked through ether and C-C linkages, like *β-O-4*, *α-O-4*, *β-5*, *β-β*, *5-5* and others, creating a cross-linked branched polymer. This polymer is difficult to extract from the source, and its reactivity is affected by the degree of cross-linking. A representative model of this cross-linked polymer can be seen in Figure 2.2. It is important to note that lignin structure can vary even within the same plant species (Dimmel, 2010; Kamm et al., 2008; C. Li et al., 2015).

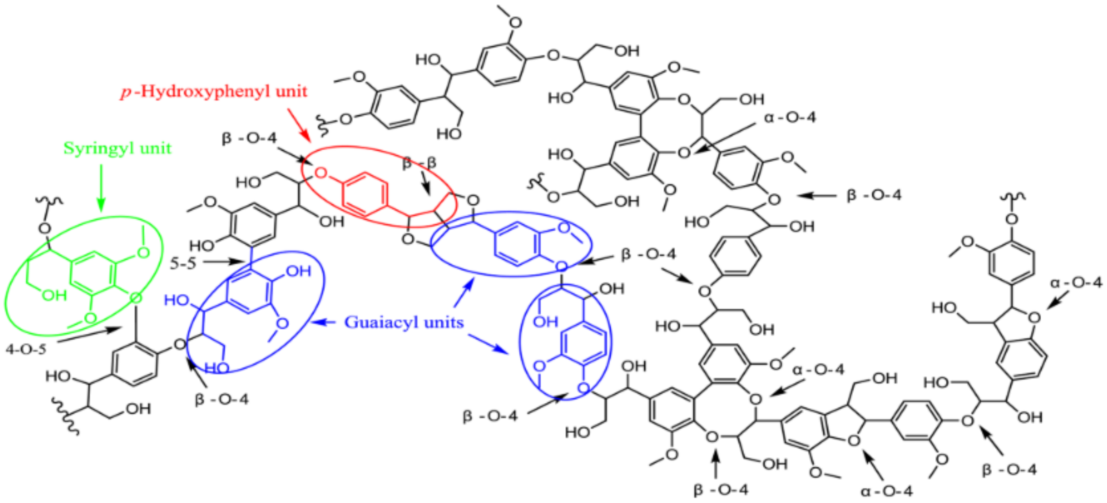

Figure 2.2 - Representative structure models of lignin.

Source: Li et al., 2015

The pulping process separates lignin from hemicellulose and cellulose, the primary feedstock for the pulp and paper industry. Mechanical and chemical procedures are used for pulping, and nowadays, kraft, soda, and sulfite pulping processes are widely used. Other methods for lignin separation are being researched and optimized, such as the organosolv, steam-explosion, and ammonia fiber expansion processes, especially for the biorefinery context (Berlin and Balakshin, 2014). The final lignin receives typically the name of the process used for pulping since the process considerably affects lignin’s final properties, which differs from the native lignin. The main properties of the most common lignins can be found in Table 2.2. The chemical pulping produces hydrolytic cleavage in lignin, usually by cleaving the *β-O-4* linkages, increasing the phenolic hydroxyl groups, and reducing the molecular mass, improving its solubility in some solvents. However, the depolymerization affects many C-C and C-O bonds and can cause a decrease in the aliphatic hydroxyls and oxygenated aliphatic moieties, while carboxyl groups and saturated aliphatic structures are produced. Also, the lignin fragments can undergo repolymerization or condensation reactions, increasing the degree of condensation and reducing the lignin’s solubility and reactivity (Berlin and Balakshin, 2014; Huang et al., 2020). As each process causes different chemical depolymerizations, the final lignin properties and structure will differ among processes. Then, each lignin can be used for different final uses and markets according to its final properties.

Table 2.2 - Comparison of various characteristics of lignin extracted using different processes.

Type of lignin	Properties
Kraft lignin	Soluble in alkali solution and highly polar organic solvents. Increase of 5–5 inter-subunit linkages, new functional groups, and linkages (stilbenes), high aliphatic/phenolic groups. Higher degree of condensation, M_w 1000- 3000 Da, polydispersity 2-4. Moderate purity, high hemicellulose content, low sulfur content. Industrial scale, high availability, low price.
Soda lignin	Soluble in alkali solution, partially soluble in organic solvents. Rich in vinyl ether and aryl-glycerol structures. Higher degree of condensation. Industrial scale, medium availability, low price. Moderate/low purity, free of sulfur.
Lignosulfonate lignin	Soluble in acidic and basic aqueous solutions, partially in polar organic solvents. Low purity, high sulfur content, medium hemicellulose content. Industrial scale, high availability, low price. M_w 36000- 61000 Da (softwood) and 5700-12000 Da (hardwood), polydispersity 4-9.
Organosolv lignin	Soluble in organic solvents. Increased amount of phenolic hydroxyl groups. High purity, very low sulfur content. M_w >1000 Da, polydispersity 2.4-6.4. Pilot/demo scale, low availability, high price.
Pyrolytic lignin	Soluble in organic solvents but poorly soluble in water. C_8 basic unit skeleton (rather than C_9 derived oligomers), very frequent C–C inter-subunit linkages. M_w 300- 600 Da, polydispersity 2.0-2.2.
Steam-explosion lignin	High content of phenolic hydroxyl groups. Lower content of methoxy groups. Frequent C–C inter-subunit linkages. Moderate/low purity. Demo/pilot scale. M_w 1100- 2300 Da, polydispersity 1.5-2.8.
Acidolysis lignin	Few carbohydrate impurities. Low molecular weight. Increased amount of hydroxyl groups and olefinic structures. Lower content in ether and ester linkages Industrial/pilot scale. M_w ~2000 Da, polydispersity ~3.

Source: (Abdelaziz et al., 2016; Behling et al., 2016; Berlin and Balakshin, 2014; Rodrigues et al., 2018)

The most common process used for pulping is the kraft process due to the stronger produced fibers and the efficient recovery of the chemicals (Abdelaziz et al., 2016). In this process, the lignin solubilizes in the alkaline solution, forming the black liquor. Most pulping industries burn the liquor to obtain power and steam, while some companies have incorporated separation processes to recover part of the soluble lignin (Kamm et al., 2008; Stevens and Verhé, 2004). Once recovered, lignin can be used in two main ways: (i) be subjected to oxidation and/or depolymerization processes to obtain added-value chemicals, or (ii) by incorporating it (directly, after chemical modification or depolymerization) as a component in new material’s formulations (Fang and Smith, 2016). The use of this lignin in another way rather than burning it for energy production must be based on additional profit for the pulping industry, since normally there is no production excess to justify the diversion from the burning kiln.

Globally, 130 million tons of industrial lignin are produced (Huang et al., 2020). However, it is underutilized as a feedstock, but different industry-required chemical compounds can be achieved through its depolymerization. Nowadays, there has been an interest to obtain aromatic building blocks (like benzene, toluene, and xylenes) given the aromatic nature of lignin that is not present in any other biological feedstock, e.g. cellulose or starch (Upton and Kasko, 2016). In a future biorefinery scheme, lignin should be converted to added-value products to achieve a technical and economically feasible system, and studies have shown the possible valorization steps and their incorporation opportunities into the biorefinery system (Liao et al., 2020).

There has been plenty of research looking for new and improved ways to depolymerize lignin and achieve high conversion to value-added chemicals, which could be found in detail in several recent review papers (Behling et al., 2016; Bourbiaux et al., 2021; Cao et al., 2019; C. Li et al., 2015; Liu et al., 2019; Ma et al., 2015; Mei et al., 2019; Rinaldi et al., 2016; Upton and Kasko, 2016; Wang et al., 2019; Xu et al., 2014). Figure 2.3 shows the main used processes to upgrade lignin to chemical compounds.

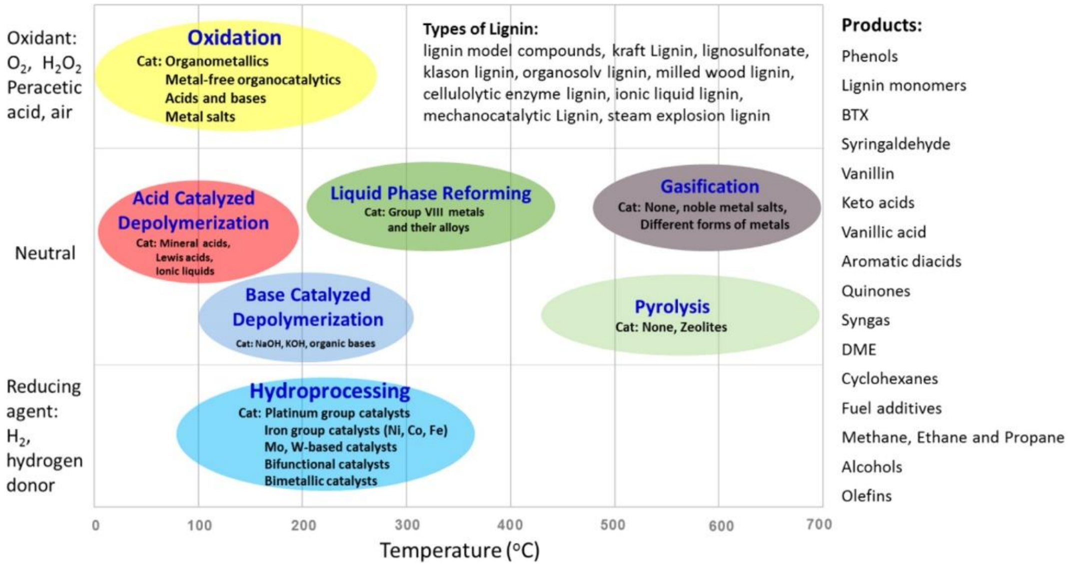

Figure 2.3 - Possible conversion processes of lignin and their conditions

Source: Li et al., 2015

Lignin depolymerization presents several technological challenges due to its heterogeneous structure, and usually produces oxygenated products (like phenol and vanillin) and other compounds, like non-condensable gases and lignin fragments. Also, depolymerization usually involves radical pathways that can produce new carbon-carbon bonds, creating recalcitrant structures which are difficult to upgrade to chemical compounds. The lignin chemical conversion can be done by two main processes: hydrogenolysis (pyrolysis in the presence of hydrogen) and oxidation (Upton and Kasko, 2016; Xu et al., 2014).

Currently, only three commercial products are obtained from lignin: vanillin, dimethyl sulfide, and dimethyl sulfoxide. All these products must be obtained more cheaply compared to an oil refinery to be commercially attractive. Phenol was commercially produced in the 1960s, but it was not competitive against the low production cost using fossil feedstock, like coal and oil (Upton and Kasko, 2016). Nowadays, there is much interest in upgrading lignin through low-cost oxidation processes, which will be discussed next.

2.3. Strategies for lignin depolymerisation and upgrading

Native lignin is already a molecule with a complex recalcitrant structure, which during the extraction is further modified, achieving condensed structures that hinders an easy depolymerization. Unfortunately, the main technical lignins (kraft, soda, and lignosulfonates) have high degrees of condensation where only around 10-15% of the bonds are *β-O-4* linkages, with new *C-C* bonds created (Rinaldi et al., 2016), compared to the 35-65% of *β-O-4* linkages present in lignins (Pandey and Kim, 2011). Other milder processes, such as organosolv, keep the structure closer to the native lignin but still imply some degradation (Rinaldi et al., 2016). These new modifications complicate the depolymerization and upgrading, causing the theoretical yield of monomers (mono-aromatics) obtained using low severity conditions from kraft and soda lignin to be just 1%. In comparison, organosolv lignins can reach up to 4%, compared to the native lignin, which can achieve 10-70% of the theoretical monomers, as seen in Figure 2.4. This information confirms that it is almost impossible to achieve a high individual yield of products in technical lignin valorization (Rinaldi et al., 2016).

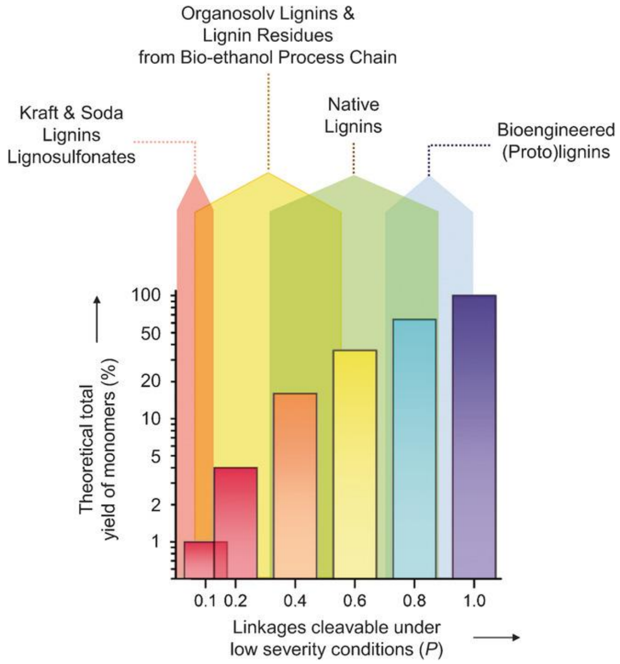

Figure 2.4 - Theoretical yield for monomers, based on the linkages available for cleavage under low severity conditions, for different types of lignins

Source: Rinaldi et al., 2016

A successful lignin valorization can be obtained through two possible pathways, represented in Figure 2.5 (Rinaldi et al., 2016). The first is a convergent funneling scheme (Figure 2.5.a), focusing on a single target compound. This approach is recommended for biological methods, where a specific metabolite is the microorganism's final product. The second approach (Figure 2.5.b) implies the existence of several depolymerization processes linked together. The first step would need mild depolymerization that is highly selective towards a high-value compound. One excellent example is the lignin valorization towards vanillin. The remaining material would follow a downstream process, requiring harsher conditions to break the more recalcitrant structure not valorized in the first step. Usually, this step will produce bulk chemicals, like organic acids, phenolics, and BTX. The remaining residues could be used to generate heat and power, perform a last catalytic cracking, or be used as a substitute for the asphalt fraction. The stepwise process ensures that the maximum benefit has been obtained from lignin. Many biorefineries have chosen this second approach due to the possibility of producing different types of added-value compounds and materials (Rodrigues et al., 2018).

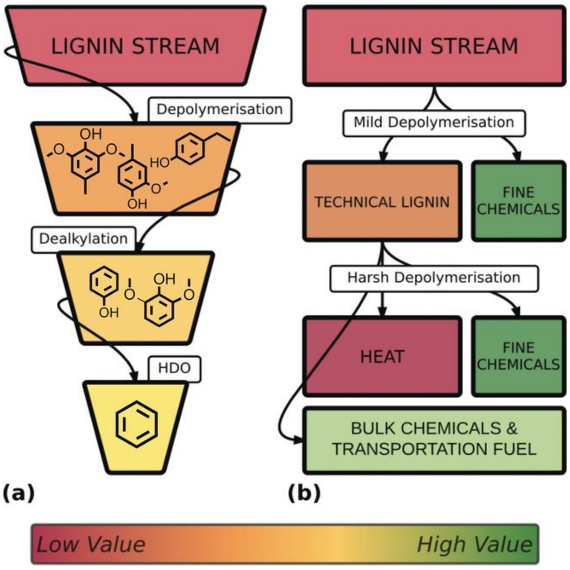

Figure 2.5 - Different approaches to depolymerize lignin: (a) funneling scheme for convergent generation of limited end-products (example with benzene); (b) stepwise approach through several depolymerization steps

Source: Rinaldi et al., 2016

Different strategies have been developed for lignin depolymerization and can be divided into cracking (pyrolysis, fast thermolysis, hydrogenation), hydrolysis, reduction, and oxidation reactions, using homogeneous, heterogeneous, or enzymatic catalysis (Behling et al., 2016). The main characteristics of these depolymerization techniques can be found in Table 2.3, together with the traditional products obtained after conversion.

Gasification and pyrolysis decompose lignin thermo-chemically in short times and high temperatures. Gasification converts lignin into syngas, used as fuel or upgraded into other compounds, while pyrolysis uses lower temperatures to achieve bio-oil with a mixture of compounds, including oxygenated aromatics, oxygenated aliphatic molecules, and hydrocarbons (Wang et al., 2019).

Hydrolysis is traditionally performed in aqueous media, with relatively milder conditions, to avoid char formation and lignin repolymerization (Abdelaziz et al., 2016). The selectivity and yield of the products depend on the solvent, temperature, time, catalyst type, among other parameters. Acid-catalyzed hydrolysis predominantly breaks *α-O-4* and *β-O-4* linkages with lower activation energy than phenolic ether bonds and *C-C* bonds. Base-catalyzed hydrolysis cleaves mainly *β*-O-4 bond, obtaining phenolic monomers and dimers. However, repolymerization and oligomerization can occur in base-catalyzed hydrolysis (Cao et al., 2019; Wang et al., 2019).

Table 2.3 - Catalytic conversion strategies for lignin

Lignin conversion strategies	Temperature range (ºC)	Catalysts	Products
Gasification	600-1200	CaO, MgO, K_2CO_3, Na_2CO_3, etc.	CO, CO_2, H_2, CH_4
Pyrolysis	450-650	K_2CO_3, Na_2CO_3, CaO, Al_2O_3, Fe_2O_3, Ni/Al_2O_3, Rh/CeO_2/SiO_2	Bio-gases (C_1-C_4 hydrocarbons), bio-oils, bio-chars
Acid hydrolysis	140-400	Mineral acids (HCl, H_2SO_4, H_3PO_4), Lewis acids, acidic zeolites, organic acids, acidic ionic liquids, etc.	Lignin monomers and dimers, including phenols, alkylphenols, aromatic aldehydes, aromatic acids, etc.
Base hydrolysis	180-330	NaOH, KOH, $Ca(OH)_2$, LiOH, Na_2CO_3, K_2CO_3, CaO, hydrotalcite, basic zeolites, basic ionic liquids, etc.	Lignin monomers and dimers, including phenols, alkylphenols, aromatic aldehydes, aromatic acids, etc.
Reductive conversion	130-450	Metals or bimetals (e.g., Ni, NiMo, CoMo, Ru, Rh, Pt, Pd, PdZn) on various supports (e.g., C, SiO_2, Al_2O_3, CeO_2, TiO_2, MgO, and zeolites), etc.	Phenols, alkylphenols, alkyl benzenes, linear and branched hydrocarbons, cyclic hydrocarbons.
Oxidative conversion	60-250	Metal chlorides (e.g., $CuCl_2$, $FeCl_3$, $CoCl_3$, $LaCl_3$), metal sulphates (e.g., $CuSO_4$, $CoSO_4$, $Fe_2(SO_4)_3$), metal oxides (e.g., CuO, Fe_2O_3, TiO_2), Pt or Pd supported on Al_2O_3, CeO_2, TiO_2, etc.	Aromatic and aliphatic alcohols, aldehydes, and acids.

Source: Wang et al., 2019

Reductive conversion requires H_2 or an H-donor in high temperatures and pressures to achieve hydrocarbons and phenols. It is a strategy with excellent selectivity in *C-O* and *C-C* bond cleavage, increasing the H/C ratio (Cao et al., 2019). However, it is expected char formation during the process (Abdelaziz et al., 2016). One of the most popular reductive reactions is hydrodeoxygenation (HDO), where the oxygen atom is removed from the oxygen-rich compounds present in lignin, increasing the stability and heating value of the products (Wang et al., 2019). However, reductive conversion is highly dependent on the catalyst type used for the reaction, many of them expensive or toxic.

Oxidative depolymerization has attracted more attention since it is a technique that presents a wide variety of final products (both aromatic and aliphatic). This strategy involves the cleavage of β-O-4 bonds, *C-C* bonds, aromatic rings, and other linkages present in lignin (Cao et al., 2019). Also, new functionalization is achieved during the reaction, especially by adding new acid and hydroxyl groups. Another advantage is the simple separation processes, which usually involves filtration or centrifugation (Behling et al., 2016). Given the higher interest in oxidative depolymerization, this topic is further explored in more detail.

2.3.1 Oxidative depolymerization

Initial studies regarding lignin oxidation were done to understand how, in pulp bleaching, the oxidizing agents removed the remaining lignin and destroyed chromophoric structures to achieve whiteness (Gellerstedt, 2010; Liu et al., 2019). However, studies have focused on obtaining several compounds in the last decades, mainly aromatic aldehydes like vanillin and syringaldehyde (Rodrigues et al., 2018), while other chemical compounds, like carboxylic acids, are still under preliminary research. Oxidation reactions are aided by hydroxyl groups in lignin and can cause cleavage of aromatic rings, aryl ether bond linkages, and other linkages inside lignin (Kang et al., 2013; Pandey and Kim, 2011). Catalysts are not entirely required for oxidation reactions, but if they are not used, reactions can be less effective, causing over-oxidation and leading to a reduced conversion and a wide range of by-products (Upton and Kasko, 2016).

During lignin oxidation, lower molecular weight compounds can be produced, which depending on the used conditions, could be susceptible to thermal decomposition to CO_2, H_2O, and other non-recoverable gases (Demesa et al., 2015). Most oxidation research has looked for new ways to obtain aromatic aldehydes and acids (Xu et al., 2014), but a broad schematic diagram with all the main products from oxidative depolymerization can be seen in Figure 2.6. The oxidation usually follows a radical pathway, leading to three possibilities: (i) side-chain cleavage, leading to aromatic structures like phenolic aldehydes, acids, and *p*-quinones; (ii) aromatic ring cleavage to produce aliphatic dicarboxylic acids; and (iii) biphenyl derivatives caused by condensation (Ma et al., 2015; W Schutyser et al., 2018). Several methods have been described to obtain these compounds, such as nitrobenzene oxidation, O_2 oxidation with Cu^{2+} or Fe^{3+} catalysts, H_2O_2 in the presence of heterogeneous catalysts, ozonolysis, and many others, involving different oxygen-based radicals with varied reactivities, producing a broad family of products (Behling et al., 2016; Pandey and Kim, 2011; Xiang and Lee, 2000).

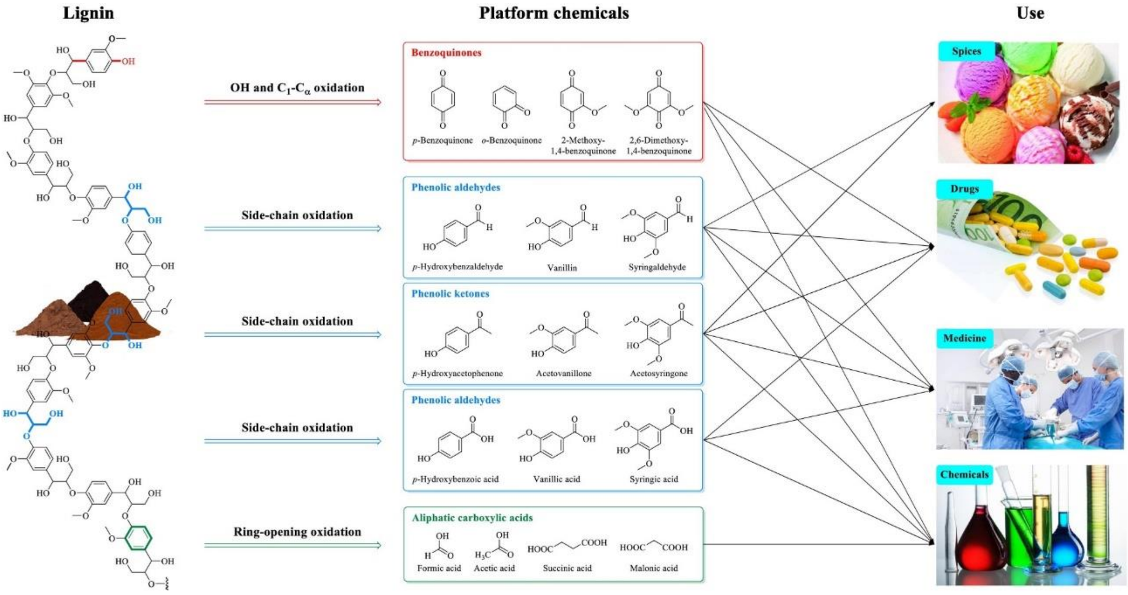

Figure 2.6 - Schematic diagram of lignin oxidative depolymerization to added-value chemicals

Source: Liu et al., 2019

The main lignin oxidizing agents are oxygen, chlorine, chlorine dioxide, peroxides, and peroxy acids (Gellerstedt, 2010; Ma et al., 2015). Chlorine (Cl_2) was the primary oxidant in pulp bleaching, with excellent efficiency but producing large amounts of organohalogens with high environmental pollution. Hypochlorite (^-OCl) and chlorine dioxide (ClO_2) has substituted Cl_2 in pulping processes (Gellerstedt, 2010), but for lignin conversion into added-value products, these oxidants are not used due to their relevant health and environmental problems (Liu et al., 2019; Ma et al., 2015). Oxygen (O_2) is extensively used in the oxidative valorization of lignin since it is inexpensive, readily available, and the main by-product is H_2O, with the great advantage of preserving the aromatic rings (W Schutyser et al., 2018). The structures that are more reactive with oxygen are phenolic units and ring-conjugated structures. Due to its weak oxidizing potential, O_2 needs an alkaline environment coupled with high O_2 pressure, high temperature, and vigorous mixing to react with the free phenolic hydroxyl groups from lignin (Ma et al., 2015). However, it has the disadvantage of being non-selective and causing over-oxidation (Das et al., 2012). Hydrogen peroxide (H_2O_2) is another green oxidant with excellent efficiency because it is a more potent oxidant than O_2, and it can be used even at acidic pH. It is less expensive than other strong oxidants, like $KMnO_4$ and O_3, however it is still more expensive than O_2. Usually, the main products are similar to the O_2 oxidation, but since it is a stronger oxidant, it is common to find phenolic acids and ring-opening reaction products instead of aromatic aldehydes and alcohols (Das et al., 2012; Ma et al., 2015). Ozone (O_3) is highly reactive and produces phenolic and non-phenolic compounds under 300 K, but at higher temperatures, it can produce aldehydes, ketones, and aliphatic carboxylic acids, with the drawback of needing to be generated *in situ* (Das et al., 2012; Figueirêdo et al., 2019; Ma et al., 2015). Peroxy acids, containing a –OOH group, are powerful oxidants for lignin, approaching the action of Cl_2. This oxidant interacts with aromatic rings and olefinic side chain structures, producing monomeric aromatics and aliphatic dicarboxylic acids (Gierer, 1986; Ma et al., 2015; Park et al., 2019). Nitrobenzene and CuO have also been used as oxidants, but mainly for analytical reasons without any commercial interest (Vangeel et al., 2018).

Oxidative depolymerization can be base or acidic catalyzed. The base catalysis cleaves most of the common *β-O-4* bonds, producing aromatic alcohols, aldehydes, and acids (Rodrigues et al., 2018; Wang et al., 2019). However, it requires high temperatures and pressures, producing an elevated amount of gases and by-products instead of aromatic compounds (Xu et al., 2014). Acid-catalyzed reactions require milder conditions, as they are kinetically favored, promoting the cleavage of *C-C* and *C-O* bonds. Despite the advantages over alkaline oxidation, this type of reaction is still under study and must be improved to achieve a mature technology (Xu et al., 2014).

Lignin oxidation has also been conducted using biochemical routes by several studies using microorganisms or enzymes. The main advantage is the high selectivity towards a target compound, but the main drawbacks are its low reaction rate, higher costs, and high sensitivity towards the reaction conditions (Abdelaziz et al., 2016). Different enzymes have been used, mainly laccases and manganese peroxidases, obtained mostly from organisms that degrade lignins, like fungus, yeast, and prokaryotes (Crestini et al., 2010). The main products from enzymatic oxidation of lignin model compounds are different aromatic alcohols, aldehydes, carboxylic acids, and even TFH (Abdelaziz et al., 2016). Aliphatic dicarboxylic acids can also be found using this technique. Muconic acid has been obtained using *E. coli* strains (Wu et al., 2017) and *P. putida* KT2440 (Chen and Wan, 2017; Vardon et al., 2015), while 2,4-pyridinedicarboxylic acid and 2,5-pyridinedicarboxylic acid were obtained using a mutant of *Rhodococcus jostii* RHA1 from lignin and vanillic acid (Mycroft et al., 2015). Vardon et al. (2015) converted the muconic acid to adipic acid by hydrogenation, achieving high-value chemical compounds.

Non-conventional methods have been reported for lignin oxidation with exciting results, namely mechanochemistry, microwave-assisted reaction, photocatalysis, and electrocatalysis.

Mechanochemistry is based on high energy micro-environments produced by the localized pressure and frictional heating caused by the kinetic energy and can reduce times, energy use, and solvent-free reactions (Behling et al., 2016; Cao et al., 2019). Mechanochemical treatment of lignin with KOH and toluene produced very high yields of vanillin and derivatives (Yao et al., 2018). Another transition metal-, solvent-free, base-assisted mechanochemical treatment obtained lower-molecular weight fragments from lignin, cellulose, and hemicellulose, confirming the cleavage of *β-O-4* bond (Kleine et al., 2013).

Microwave-assisted depolymerization applies high energy electromagnetic radiation directly inside the reaction medium, causing the rotation of the polar molecules and ionic conduction, releasing a substantial amount of heat and attaining higher temperatures in shorter times (Aguilar-Reynosa et al., 2017; Cao et al., 2019; Chio et al., 2019; H. Li et al., 2015). Since the heat is released *in situ*, microwaves avoid physical contact between the heating source and the material, avoiding surface overheating and causing a reduction in the reaction time (Chio et al., 2019). This technique has been used to study pyrolysis, liquefaction, and oxidative conversion of lignin and lignin model compounds to valuable compounds (Bartoli et al., 2020; H. Li et al., 2015). Microwave-assisted oxidative degradation of lignin with H_2O_2 showed that high-molecular-weight lignins were degraded at the same digestion rate as conventional heat but using lower temperatures or shorter times (Ouyang et al., 2015). Also, the lignin acquired a higher content of phenolic hydroxyl groups, lower methoxyl groups, and a lower degree of condensation, enhancing reactivity for further upgrading (Ouyang et al., 2010). Microwave irradiation increased carboxymethylation of lignin to provide a material with good Pb^{2+} adsorption properties compared to the conventional heating method (Li et al., 2018). This technique is still under development, and industrial-scale systems should be studied if scaling-up is desired for future biorefineries (Aguilar-Reynosa et al., 2017; Cao et al., 2019).

Photocatalysis has been widely studied to degrade aromatic compounds in wastewaters, but little research has targeted selective oxidative depolymerization of lignin towards value-added compounds. Holes or oxidative species created by photocatalysis will react with lignin to create free radical cations. Then, the *C-O* bond in *β-O-4* units is the most common linkage to be broken, but some progress has been achieved breaking *C-C* bonds as well (Xiang et al., 2020). Milder conditions, short times, sunline as the source of energy, and few residues are several advantages of the techniques, but one of the main drawbacks is achieving a good light activation through a typically dark lignin solution (Behling et al., 2016; Cao et al., 2019). Most of the research has been performed in lignin model compounds, but few examples with lignin have shown exciting results. UV-Fenton oxidation was performed in lignin isolated from eastern red cedar, obtaining different phenolic alcohols, aldehydes, and aliphatic carboxylic acids (Kang et al., 2019). Another photocatalytic oxidation produced aliphatic carboxylic acids by TiO_2/H_2O_2 oxidation of kraft lignin under UV light, achieving up to 7.8% of succinic acid and ~20% acetic acid (Suttipornphaisalkul et al., 2020).

Electrochemical approaches for lignin oxidation have proved to be highly selective, as well as highly dependent on the type of electrode used, applied current density, initial substrate loading, pH, and temperature (Behling et al., 2016). Oxidation can be controlled carefully, and vanillin has been the main focus of this methodology (Das et al., 2012). However, carboxylic acids (e.g., oxalic, formic, and acetic acids) can be obtained with vigorous electrochemical oxidation (Di Marino et al., 2019). Ko and collaborators (2019) prepared a very innovative photo-electro-biochemical compartment where lignin was oxidized using a TiO_2 photocatalyst, a Co-based electrocatalyst, and a lignin peroxidase enzyme as a biocatalyst under direct sunlight irradiation. The system used two membranes, one of Nafion and another of cellulose, to separate the different catalysts and compartments. This system achieved 98.7% selectivity in lignin depolymerization, producing up to 73% of coniferyl alcohol.

Even though oxidative depolymerization has several advantages and a promising future for lignin upgrading, several issues must be addressed before commercial processes are achieved. For example, several oxidation processes use harsh conditions with high temperatures and/or pressures with prolonged reaction times, expensive and/or toxic catalysts, and problems related to mass transfer due to low lignin solubility, which sometimes is overcome using non-ecofriendly solvents (Behling et al., 2016). Also, target compounds are usually produced in low yields (~10-11%), which need to be separated and/or isolated from the reaction mixture, while some lignin suffers recombination/repolymerization (Xu et al., 2014). Current research in oxidative depolymerization shows two significant challenges: (i) most of the substrates investigated are simplified lignin model compounds instead of lignin; and (ii) catalysts- and process-related challenges (including using homogeneous catalysts that are difficult to separate and regenerate, solvents that not necessarily are green or safe, reaction conditions that require expensive equipment, and product separation processes, among others) (Vangeel et al., 2018).

2.4 Ring-opening reactions in lignin oxidation: production of dicarboxylic acids

In the past years, there has been a particular interest in obtaining dicarboxylic acids (DCA) from renewable feedstocks, and lignin is a suitable raw material. To achieve DCA from lignin, oxidative cleavage of the aromatic ring must occur, performed under harsh depolymerization (Rinaldi et al., 2016). The first step to ring-opening reactions is oxidation to quinone structures, which are then opened to form dicarboxylic acids, mainly C_6 dicarboxylic acids (e.g., muconic acids and derivates). However, these acids are very unstable and are quickly degraded to C_2-C_4 acids. In very harsh depolymerization, complete mineralization to CO_2 and H_2O can occur (Ma et al., 2014). The product selectivity depends on the oxidizing agent, type of catalyst, the operational conditions (e.g., pressure, temperature, lignin concentration, and stirring rate), nature of the lignin, and reactor type (Asgari and Argyropoulos, 1998; Kang et al., 2013; Ma et al., 2014).

The chemical mechanism followed during pulp bleaching requires nucleophilic or electrophilic reactions to degrade lignin, producing small amounts of DCA. Any radical reaction should be avoided because it can damage the pulp. However, if the goal is to achieve a high percentage of DCA, the radical pathway should be chosen, and several catalysts can promote the radical formation, like many transition metal ions (Gellerstedt, 2010).

In the last 20 years, there have been at least 24 publications concerning C_4 dicarboxylic acids from lignin and lignin model compounds, as seen in Figure 2.7. These works have been done under catalytic and non-catalytic conditions, using different oxidants, i.e., O_2, O_3, H_2O_2, peracetic acid, and sodium percarbonate. Some of these works focused on lignin depolymerization towards aromatic monomers and reported the C_4-DCA as degradation products. Nowadays, this information is valuable to identify possible research lines and optimal conditions for lignin depolymerization. Given the differences between non-catalyzed and catalyzed reactions, each case will be discussed separately.

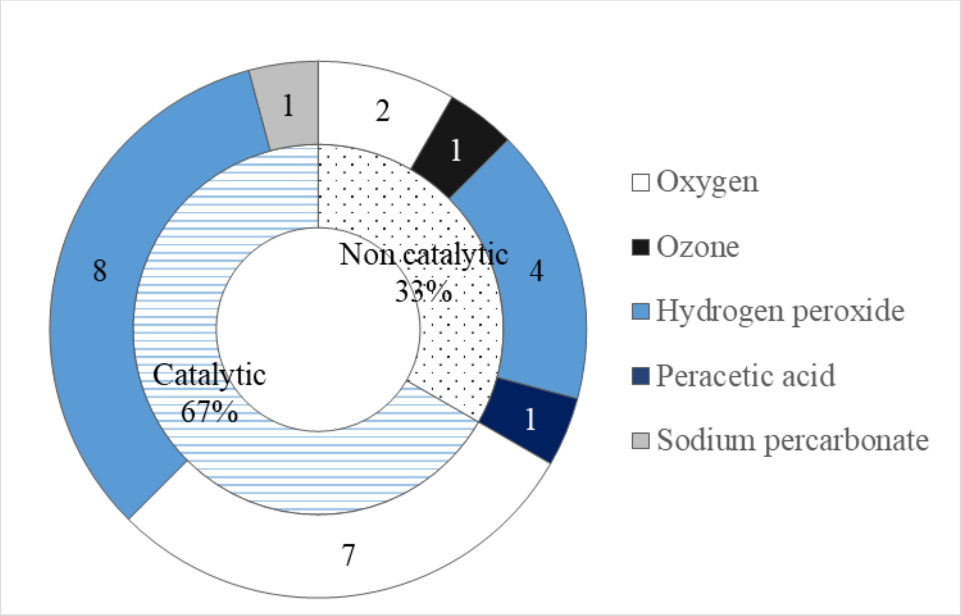

Figure 2.7 - Last 20-years publications regarding lignin and lignin model compound conversion to C_4-DCA

2.4.1 Non-catalytic conversion

As seen in Figure 2.7, 33% of the latest works regarding lignin depolymerization towards C_4-DCA were performed using non-catalyzed reactions. Even though molecular oxygen is widely used for lignin depolymerization to aromatic monomers, it can also be used for ring-opening reactions since it has a low cost and reduced toxicity. However, its oxidant power is lower than other oxidants, being less effective towards C_4-DCA (Cabral Almada et al., 2020; Demesa et al., 2015; Kang et al., 2013; C. Li et al., 2015). The different works that performed the non-catalytic conversion of lignin and lignin model compounds are detailed in Table 2.4.

Table 2.4 - Published works of lignin and lignin model compounds non-catalytic oxidation which reported C_4-DCA.

Substrate	**Oxidant**	**Solvent**	**Reaction conditions**	**Identified C_4-DCA and yield (%), if available**	**Source**
Lignin	O_2	Water	448-498 K, 5-15 bar, 1 h, pH 11	SU 3%, Traces of FU	(Demesa et al., 2015)
LignoBoost lignin	O_2	Water	393-473 K, 3-15 bar O_2, 30-40 min, alkaline pH	SU <0.5%	(Abdelaziz et al., 2019)
Pine pyrolytic lignin	O_3	Methanol	273 K, 1 bar, 15-240 min, acidic pH	SU 2.0%, MA 2.3 %	(Figueirêdo et al., 2019)
Spruce organosolv lignin	O_3	Acetone-water	423 K, 15 bar, 2.5-4.0 h	Muconic acid reported. C_4-DCA n.r.	(Evtuguin and Robert, 1997)
Aqueous and steam explosion autohydrolyzed corn stacks (AAM, SAM), organosolv material (OSM), Indulin AT	O_3	Gas phase	0-2 h	SAM: SU trace, MAL 0.02% OSM: - AAM: SU trace, MAL 0.03% Indulin AT:, MAL trace	(Quesada et al., 1999)
Alkali lignin, Organosolv lignin (preoxidated)	H_2O_2	Water	423-473 K, 200 bar, 0-5 min	SU (13%)	(Hasegawa et al., 2011)
Guaiacol, syringol, phenol	H_2O_2	Water	573 K, 10-60 s	Identified peaks for MA, SU, FU	(Suzuki et al., 2006)
Poplar precipitated lignin	H_2O_2	Water	353-433 K, 5-30 min, pH 2 and pH~13	Alkaline: SU 0.9% Acidic: SU 2.4%	(Xiang and Lee, 2000)
Lignin model compounds based on guaiacyl, syringyl, veratryl and methylsyringyl	H_2O_2/UV	Water	303 K, 60 min, pH 11	Identified: SU, MA, FU, MAL, TA, MeO-FU, MeO-MA, n-propyl-SU, propyl-MA, propyl-FU, HO-FU	(Sun et al., 1998)
Catechol	H_2O_2	Water	533-553 K, 90-170 bar, 0-2 min	41% C_4-DCA: TA 20%, FU 16%, MAL 22%	(Yin et al., 2015)
Hardwood kraft lignin	Peracetic acid	Acetic acid:H_2O_2	298 K, 1-8 h, acidic pH	Identified (<1%): SU, MA, Me-SU, FU	(Park et al., 2019)

Note: abbreviations used in the table: DCA=dicarboxylic acids, SU= succinic acid, MA= maleic acid, FU= fumaric acid, MAL= malic acid, TA= tartaric acid, n.r.= not reported.

Demesa et al. (2015) performed alkali lignin oxidation using molecular O_2, showing that succinic acid yield increased faster when the higher temperature was used, but the acids were decomposed if elevated temperatures were kept. Succinic acid, the only C_4-DCA quantified in Demesa's work, reached up to 3 wt%. The total carboxylic acid yield was affected positively by decreasing lignin concentration and increasing oxygen partial pressure; however, the authors did not specify the behavior for C_4-DCA.

Another oxidation using O_2 was performed by Abdelaziz et al. (2019) to obtain a depolymerized lignin which was used as a carbon source for growing different bacterial strains. After depolymerization, no more than 0.5% of succinic acid was observed, while the main products were smaller lignin fragments, organic monomers, and short-chain aliphatic acids (formic and acetic acids).

Figueirêdo et al. (2019) oxidized pyrolytic lignin using ozone, obtaining a small amount of succinic acid (2.0 wt%) and maleic acid (2.3 wt%). These acids were initially obtained as esters since the reaction was performed in methanol as solvent and hydrolyzed before quantification. Also, plenty of other carboxylic acids were found, such as formic, acetic, oxalic, propionic, malonic, and even traces of adipic acid, being all the acids accountable for 40% of the product oil obtained after lignin oxidation. Ozone proved to be an exciting oxidant for upgrading the pyrolytic lignin; however, its effect on technical lignin was not shown. Comparatively, previous works from other research groups using O_3 on technical lignins showed low yields of C_4-DCA (Evtuguin and Robert, 1997; Quesada et al., 1999). Also, the final product shows a complex mixture of different acids and phenolics, which should need an effective separation and purification process.

Hydrogen peroxide has received a strong focus when ring-opening reactions are the objective. It is more reactive than molecular oxygen, with the benefit of being environmentally benign, allowing milder conditions compared to O_2, and avoiding mass transfer barriers that appear between liquid and gas phases (Bhargava et al., 2006; Cheng et al., 2017; Guélou et al., 2003; Pandey and Kim, 2011). However, given that H_2O_2 is a weak acid, its reactivity is strongly associated with the pH, stable at acidic conditions but decomposing in alkaline conditions (Xiang and Lee, 2000; Yin et al., 2015). Lignin model compounds (guaiacol, syringol, and phenol) were oxidized using H_2O_2 as oxidant at 300ºC and short times (10-60 s) (Suzuki et al., 2006), and different C_1-C_6 dicarboxylic acids were identified but not quantified. Catechol was oxidized in a different system by

Yin et al. (2015), still at high temperatures and short times, reaching very high yields of tartaric, fumaric, and malic acids, with up to 41% of C_4-DCA. Both works determined that the oxidation route of these phenolic model compounds to DCA passes through *o*-benzoquinones and *p*-benzoquinones structures, yielding muconic and 2,5-dioxo-3-hexenoic acids, which are highly unstable and are degraded to C_4-DCA in the presence of a strong oxidant, such as H_2O_2.

Flow reactor oxidation of alkali lignin using H_2O_2 was performed by Hasegawa et al. (2011), obtaining up to 13 wt% of succinic acid when using very high temperature (200ºC) and short times (3.6 minutes). It was noticed that succinic acid was formed only above 150ºC, confirming that harsh conditions are required to achieve succinic acid in valuable yields, at least in a non-catalyzed reaction.

Finally, peracetic acid was also considered an oxidant for lignin ring-opening reactions since peroxy acids are powerful oxidants with a perhydroxyl group (-OOH), achieving good results under mild conditions and low by-products formation and side reactions (Ma et al., 2016). After hardwood kraft lignin oxidation, Park et al. (2019) identified succinic, maleic, and fumaric acids, but they were not quantified. Since the peracetic acid was prepared in situ, by adding acetic acid and hydrogen peroxide, it was determined that a specific ratio (1:1.5) enhanced the formation of DCA. As the experiments were performed at room temperature, lignin degradation reached only high-molecular weight fragments without complete degradation to DCA. Given the highly oxidative strength of peracetic acid and the dependence on temperature (Ma et al., 2016), it would be interesting to evaluate DCA in more severe conditions.

2.4.2 Catalytic conversion

Peroxide oxidation of lignin towards C_4-DCA can be performed using different types of catalysts, which can vary from expensive noble metals, cheaper zeolites, or even homogeneous metal ions, such as Fenton’s reagent, which uses transitions metals with at least two oxidation states, such as Fe, Mn, or Cu (Demesa et al., 2015). As noted in Figure 2.7, 67% of the latest publications about lignin conversion to C_4-DCA use catalytic conversion, and those works focused mainly on two oxidants: O_2 and H_2O_2, the latest with the higher amount of research and better results. Recently, Earth-abundant metals have gained interest as catalysts instead of using expensive noble metals due to their higher availability and lower prices (Bullock et al., 2020), and this trend can also be observed in the lignin oxidation towards DCA. The different publications, including catalytic conversion of lignin and lignin model compounds, are detailed in Table 2.5.

Several works have used homogeneous catalysis, mainly ions of transition metals, such as Cu^{2+} and Fe^{2+}. Although homogeneous catalysis was applied to O_2 oxidation, the C_4-DCA yields were very low (Rovio et al., 2012; Wu and Heitz, 1995), and in the last years, this oxidant has not being used with metal ions. Instead, several works involving H_2O_2 were published, especially using Fenton's reagent that mimics the lignin degradation achieved by fungi (Zeng et al., 2015). Oxidation of phenol yielded 8% of maleic acid, among others carboxylic acids and phenolics (Faisal, 2009), while lignin model compounds (phenolic aldehydes and alcohols) produced a small amount of maleic and fumaric acids (not more than 2%), along with other phenolics and acids, after being exposed to Fenton's and Fenton's/UV conditions (Kang et al., 2019). However, when lignin was oxidized using this methodology, no C_4-DCA was obtained. Zeng et al. (2015) achieved only adipic acid esters when oxidizing organosolv hardwood lignin and no C_4-DCA were reported. Therefore, it can be concluded that Fenton's catalysis approach is not efficient for depolymerizing lignin towards C_4-DCA.

Perovskite-type oxides (e.g., rutile, wurtzite, and chalcopyrite) could work as oxidation catalysts because they have high oxidative activity, robustness, and relative affordability (Ansaloni et al., 2017; Kang et al., 2013). These compounds can absorb/desorb oxygen on their surface and in the lattice, allowing them to oxidize in two main contact areas. The suprafacial type (related to the surface) works better under lower temperatures, while the interfacial type (in the lattice) works better in gas-phase oxidation. These perovskite-type oxides have the general formula ABO_3, where A are rare earth, alkaline earth, alkali, or large ion cations, and B are transition metals (Ansaloni et al., 2017; Ma et al., 2015). They proved to produce aromatic aldehydes but nearly no DCA. Ansaloni et al. (2017) tried $LaFeO_3$, $LaMnO_3$, and $CeFeO_3$, and C_4-DCA concentration (maleic and malic acids) showed no significant improvement related to the non-catalyzed experiment.

Table 2.5 - Published works of lignin and lignin model compounds catalytic oxidation which reported C_4-DCA.

Substrate	**Catalyst**	**Oxidant**	**Solvent**	**Reaction conditions**	**Identified C_4-DCA and yield (%), if available**	**Source**
Norway spruce wood chips	$CuSO_4 \cdot 5H_2O$ / phenanthroline	O_2	Water	393-413 K, 1-20 h, alkaline pH	Traces of FU, MAL, SU	(Rovio et al., 2012)
Alkaline lignin from *Populus tremuloides*	CuO, $CuSO_4$, $FeCl_3$	CuO, O_2	Water	433-493 K, 2-40 min, alkaline pH	CuO: MA 0.02%, FU 0.01% $O_2/Cu^{2+}/Fe^{3+}$: MA 0.05%, FU 0.08% O_2/Fe^{3+}: MA 0.06%, FU 12% O_2/Cu^{2+}: MA 0.04%, FU 0.07%	(Wu and Heitz, 1995)
Wheat straw lignin; Acetovanillone	Perovskite-type oxides ($LaFeO_3$, $LaMnO_3$, $CeFeO_3$)	Air	Water	423-473 K, 20-30 bar, 2 h	Traces of MA and MAL.	(Ansaloni et al., 2017)
Lignin	Phosphotungstic acid ($H_3PW_{12}O_4$) Phosphomolybdic acid ($H_3PMo_{12}O_{40}$)	O_2	Water	448-498 K, 5-15 bar, 1 h	Non catalyzed: 1.2 % SU With W: 1.8% SU With Mo: 1.2 % SU	(Demesa et al., 2017)
Lignin solution	Al-V-Mo (γ-Al_2O_3, V, Mo), Vanadium pyrophosphate	O_2	Water	600-700 K, 1 bar, max. 16 min, alkaline pH	Maleic anhydride 0.7%	(Lotfi et al., 2015)
Softwood Kraft lignin	1: V-Mo/Al_2O_3; 2: V-Mo/TiO_2; 3: V_2O_5/MnO_2; 4: MgO; 5: Mg-Si-Al-K; 6: WO_3/TiO_2; 7: V-Mo/HZSM-5; 8: V-W/HZSM-5	O_2	Gas phase	423-823 K, 0.2 s (contact time)	1: MA/FU: 4.7%, SU 1.8%; 2: MA/FU 7.0%, SU 1.2%; 3: MA/FU: 3.0%, SU 0.5%; 4: MA/FU: 0.09%; 5: MA/FU 0.3% 6: MA/FU: 1.8%; 7: MA/FU: 6.5%, SU 0.3%; 8: MA/FU: 5.3%, SU 0.8%	(Lotfi et al., 2016)
Washed and unwashed softwood kraft lignin,	Vanadium pyrophosphate (VPP), HZSM-5, VPP/HZSM-5	O_2	Gas phase	Test 1: 413-493 K, 10-20 % steam, 0-3% O_2 Test 2: 723-953 K, p_{amb}, 0-20% steam or 0-15.5% O_2	Test 1 (VPP): max 0.30% MA Test 2: max 0.20% MA (sand as catalyst)	(Lotfi et al., 2020)
Lignin (Poplar, High-S Poplar, Pine sawdust, Spruce Kraft, corn stover (CS) DMR-EH, DAP-EH, AAP-AE)	$LaMn_{0.8}Cu_{0.2}O_3$	O_2	Water	448 K, 20 bar (5 bar O_2), 0-60 min, alkaline pH	Spruce Kraft: SU <1% CS DMR-EH: SU <1%, MAL 2% CS DAP-EH: SU <1%, MAL 2% CS AAP-AE: SU <1%, MAL 2%	(Wouter Schutyser et al., 2018)
Loblolly pine, black oak and mixed hardwood materials	$Fe_2(SO_4)_3$	O_3	Water	445-550 K, 16-33 bar, 30 min	Only succinic was analyzed	(Mcginnis et al., 1983)
Guaiacol	TS-1 (titanium silicatite)	H_2O_2	Water	323-353 K, 24 h, alkaline pH (12-14)	MA 25.9%, FU 1.5%, MAL 3.1%	(Su et al., 2014)

Phenol	Fe-TS1, TS-1, Fe-ZSM-5, Fe-NaY, Fe-USY, Fe-silicalite	H_2O_2	Water	373 K, 10 bar, 12-120 min, pH=5.6	MA detected	(Ovejero et al., 2001)
Creosol, 4-methylcatechol, dimers (5-5' link, α-5 link, methylene dimer)	Metal salts (sulfates): Mn^{2+}, Cu^{2+}, Fe^{2+}, Mg^{2+}	H_2O_2	Water	353 K, 2 h, alkaline pH	Catechol: n.d.; Creosol: Me-SU 16.4%, Me-MA 14.2% ; 5-5' Dimer: Me-SU 2.0%, Me-MA 2.4% ; α-5' Dimer: SU 3.0%, MA 4.7%, Me-SU 3.1%, Me-MA 4.1%, MAL 11.4% ; 5-CH_3-5' Dimer: Me-SU 2.3%, Me-MA 3.9%	(Sun et al., 1999)
Hardwood organosolv lignin	Fe^{3+} (Fenton)	H_2O_2	Ethanol (supercritical)	Fenton mod,: T_{amb}, 30 min; Depolymerization: 523 K, 70 bar N_2, 3 h	No C_4-DCA reported. Adipic and levulinic acid reported.	(Zeng et al., 2015)
Syringaldehyde, 4-hydroxybenzaldehyde, 2-methoxyphenol, 2,6-dimethoxyphenol, eastern red cedar lignin	Fe^{3+} (Fenton), UV/Fenton, UV/TiO_2	H_2O_2	NH_3/ H_2O	30 min, pH=3.0	Fenton: 4-HBA: MA 1%, FU 15%; SA: FU 2%; 2-MP: n.d.; 2,6-MP: n.d. UV/Fenton: 4-HBA: FU 2%; SA: n.d.; 2-MP: n.d.; 2,6-MP: n.d. Lignin: No DCA	(Kang et al., 2019)
Phenol	Fe^{2+} (Fenton)	H_2O_2	Water	298 K, 4 h	MA: 8%	(Faisal, 2009)
Lignin dimer model compounds	CuO	H_2O_2	water	403-443 K, 20 min, alkaline pH, microwave reactor	SU 2.5%, FU 2.0%, MA 1.0%, MAL 0.5%	(Qu et al., 2020)
Diluted-acid corn stover lignin; steam-exploded spruce lignin; guaiacol; catechol; vanillin	Chalcopyrite ($CuFeS_2$)	H_2O_2	water	333 K, 0-5 h, pH 4 (acetate buffer)	DACSL: SU 7%, MAL 0.8% SESPL: SU 5.2%, MAL 0.3% Guaiacol: SU 5.2%, MAL 2.5% Catechol: SU 8.3%, MAL 5.9% Vanillin: SU 4.8%, MAL %	(Ma, 2016; Ma et al., 2014)
Lignin; model compounds	$CuFeS_2$	H_2O_2	Water	333 K, 5 h, pH=4.5	Max yields: SU 12%, FU 1%, MA 1%,	(Bi et al., 2018)
Lignin	$CuFeS_2$	H_2O_2 (acidic); Sodium percarbonate (neutral, alkaline)	Water	333-573 K, 1-6 h, pH 4 (acetate buffer) or NaOH 0.1-1.0 mol/L	H_2O_2/chalcopyrite: SU <0.5%, Traces of MA and MAL. Sodium percarbonate: Neutral: SU 1%; Alkaline: SU 0.5%. Traces of MA and MAL	(Cronin et al., 2017)

Note: abbreviations used in the table: DCA=dicarboxylic acids, SU= succinic acid, MA= maleic acid, FU= fumaric acid, MAL= malic acid, TA= tartaric acid, n.r.= not

Some compounds have transition metals in their structure with two different oxidation states, enhancing electron transfer in their surface and catalyzing the oxidation when using H_2O_2. Chalcopyrite ($CuFeS_2$), which holds in its structure different oxidation states (Fe^{2+}, Fe^{3+}, Cu^{+}, Cu^{2+}), was suggested first by Ma et al. (2014). Model compounds (guaiacol, catechol, and vanillin) achieved high C_4-DCA yields, being catechol the one with higher yields (malic acid 6%, succinic acid 8%). Biorefinery lignins also showed promising results, with 7% succinic acid and 1% malic acid for diluted-acid corn stover lignin, with lower yields for steam-exploded spruce lignin. Bi and coworkers (2018) used chalcopyrite nanoparticles on industrial lignin using an acidic pH, obtaining high yields for succinic acid (12%) and oxalic acid (30%), with low yields for fumaric and maleic acids (1 %, each). The authors also demonstrated that the individual yields and lignin conversion are highly dependent on the parameters of the condition used in the reaction, such as time, temperature, dosage of H_2O_2, and catalyst. However, when bagasse lignin was oxidized using chalcopyrite as the catalyst, low succinic acid yields were obtained (0.9%), even after 3 hours at 200ºC (Cronin et al., 2017). This result could be expected since bagasse lignin has a richer H ratio, and it has been reported that H groups are more resistant to oxidation and produce a lower amount of C_4-DCA than G groups. The presence of two transition metals enhanced the formation of radical species from H_2O_2, allowing the depolymerization of lignin to aromatic rings, which were oxidized to quinones and then cleaved to DCA (Bi et al., 2018). Copper oxide (CuO) has also been used as a catalyst with H_2O_2 oxidation of phenolic and non-phenolic lignin dimer model compounds using oil-bath and microwave heating (Qu et al., 2020). During this study, the authors found that the microwave irradiation interacts with the reaction intermediates that are sensitive to electromagnetic waves, increasing cleavage of the side chain and converting vanillin into vanillic acid, but causing no effect on veratraldehyde oxidation to veratric acid or in the ring cleavage reaction to produce dicarboxylic acids. Therefore, no difference was observed between conventional heating and microwave heating regarding the C_4-DCA yields.

Sodium percarbonate ($Na_2CO_3 \cdot 1.5\ H_2O_2$) in alkaline conditions was also used with bagasse lignin (both as the catalyst and the oxidizer), and it achieved approximately 1% succinic acid, traces of maleic and fumaric acids, and other aromatic compounds and low-molecular-weight carboxylic acids (Cronin et al., 2017). Under the same reaction conditions, it behaved better than chalcopyrite, but the overall reaction was not successful in obtaining high yields of C_4-DCA.

Peracetic acid was used on lignin under mildly acidic conditions (30-60ºC, 0.5-8 h) and Nb_2O_5 as a catalyst, achieving several low molecular aromatic compounds but no DCA. However, there has not been any more research using higher temperatures, which could help cleave the aromatic ring and produce DCA (Ma et al., 2016).

It has been reported that the use of two heteropoly acids, i.e., phosphotungstic acid ($H_3PW_{12}O_{40}$) and phosphomolybdic acid ($H_3PMo_{12}O_{40}$), under high O_2 pressure and high temperature (175-225°C). Both catalysts were compared to a non-catalyzed experiment, being observed that there was not a significant increase in succinic acid production (max. yield 1.8% for $H_3PW_{12}O_4$, 1.2% for $H_3PMo_{12}O_{40}$, and 1.2% for non-catalyzed reaction). Others DCA were not studied or reported. These catalysts have higher costs (compared to other traditional catalysts) and are difficult to recover (Demesa et al., 2017).

Molecular oxygen can also be used in gas-phase oxidation with several catalysts. Aluminium-vanadium-molybdenum oxides (Al-V-Mo) and vanadium pyrophosphate (VPP) were used in a fluidized bed in the presence of O_2, but only VPP produced small amounts of maleic acid (1.5%wt), obtained from maleic anhydride hydrolyzed in water (Lotfi et al., 2015). In their subsequent work, Lotfi et al. (2016) tested eight different catalysts (V-Mo/Al_2O_3, V-Mo/TiO_2, V_2O_5/MnO_2, MgO, Mg-Si-Al-K, WO_3/TiO_2, V-Mo/HZSM-5, V-W/HZSM-5) in a fluidized bed using O_2 and a high-temperature ramp. All of the catalysts produced a small amount of DCA (succinic and/or maleic/fumaric acids), but it was V-W/HZSM-5 that produced the most (nearly 2% of succinic and 12% of maleic/fumaric acid). This result confirmed the idea that V^{5+} activates the aromatic rings in monomeric units (after depolymerization), enhancing the electrophilicity and favoring the attack of two O_2 molecules. This intermediate opens and rearranges to produce maleic anhydride, later hydrolyzed in water (Lotfi et al., 2016). The latest work using unwashed lignin and VPP, HZSM-5, and VPP/HZSM-5 catalysts produced mainly formic, acetic, and malonic acids, with very low percentages of maleic acid (maximum 0.30% using washed lignin, and 0.20% with unwashed lignin) (Lotfi et al., 2020).

Su et al. (2014) oxidized guaiacol with H_2O_2 and Titanium silicalite 1 (TS-1) in mild alkaline conditions (25-85ºC, 24 h), obtaining high percentages of maleic and oxalic acids, with small percentages of fumaric and malic acids. TS-1 is a zeolite with an MFI structure, with no more than 3% TiO_2 in its structure. Its hydrophobic properties permit non-polar compounds oxidation in an aqueous medium and have been widely used for cyclohexanone ammoximation to caprolactam and production of propylene oxide. Its better reactivity in peroxide oxidation is based on the adsorption of H_2O_2 in the Ti tetrahedral sites to form Ti-OOH groups that act as the active species (Clerici, 2015; Gamba et al., 2009; Xia et al., 2017). TS-1 was previously reported for efficient catechol oxidation using H_2O_2 under mild aqueous conditions, but no DCA were quantified after the oxidation (Sengupta et al., 2013). Phenol was oxidized using TS-1 and modified Fe-TS-1 with H_2O_2, identifying maleic acid among other smaller carboxylic acids and aromatic compounds, but no quantitative data for maleic acid was provided (Ovejero et al., 2001). This work reported that the modified Fe-TS-1 showed the best catalytic activity compared to the other catalysts (TS-1, homogeneous Fe^{2+} or Fe^{3+}, and Fe-NaY). Other works oxidizing furfural had reported good yields on maleic acid (Alba-Rubio et al., 2017; Rodenas et al., 2018).

2.5 C_4 dicarboxylic acids: an industrial perspective

Dicarboxylic acids with four carbons (C_4-DCA) have become an important research topic in recent years. These compounds are identified by having a carboxylic acid group on each of the two terminal carbon atoms. The C_4-DCA that have shown a higher prevalence in lignin oxidation are succinic, malic, maleic, fumaric, and tartaric acids, as shown in Figure 2.8. Their status, concerning production, average price, and current use, is shown in Table 2.6.

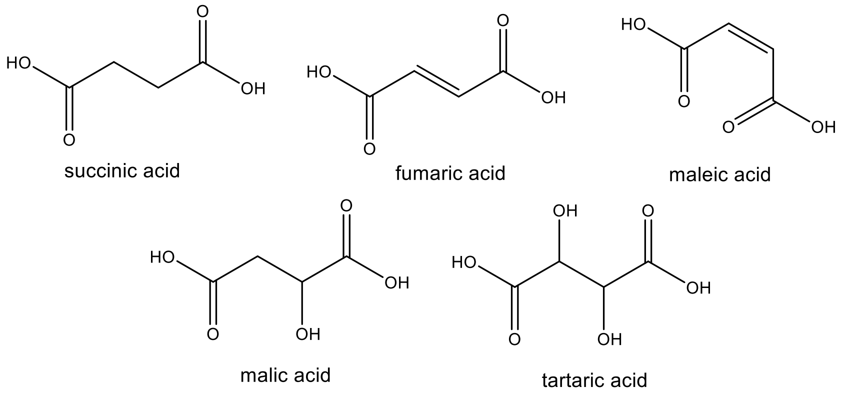

Figure 2.8 - Structure of the primary C_4 dicarboxylic acids (C_4-DCA) found after lignin oxidation

Table 2.6 - Status for C_4 dicarboxylic acids market.

Acid	Current production technology	Annual production	Average price (USD/ton)	Main applications	References
Succinic	Hydrogenation of petrochemical maleic anhydride, sugar fermentation	50 kt/year	2500 (petro) – 2860 (bio)	Food additive, pharmaceutical industry, foaming agent, surfactant, chemical precursor, polymer production.	(Cok et al., 2014; Du et al., 2015; Gérardy et al., 2020; Höfer, 2015; Jong and Jungmeier, 2015; Litsanov et al., 2014; Werpy and Petersen, 2004)
Malic	Hydration of petrochemical maleic anhydride, enzymatic process from fumaric acid	60 kt/year	1700-2500	Food industry, metal cleaning, textile finishing, electrode plating, paints, chemical precursor.	(Chi et al., 2016; Du et al., 2015; Gérardy et al., 2020; Kamm et al., 2008; Martin-Dominguez et al., 2018; West, 2017)
Maleic	Hydrolysis of petrochemical maleic anhydride	2800 kt/year (maleic anhydride)	1400-1600	Resins and co-monomer, pesticides and growth inhibitors production.	(Lohbeck et al., 2000; Na, 2015; Oils and Chain, 2019)
Fumaric	Hydrolysis and isomerization of petrochemical maleic anhydride, fermentation and enzymatic processes	240 kt/year	1280-1700	Food and beverage additive, intermediate for polyester resins, L-malic and L-aspartic acid.	(Du et al., 2015; Gérardy et al., 2020; Goldberg and Rokem, 2014; Lohbeck et al., 2000; Martin-Dominguez et al., 2018)
Tartaric	Decomposition of calcium tartrate	60 kt/year	3000	Food, pharmaceutical and viniculture industries, fire retardant, antioxidant, electronics.	(Grand View Research, 2015; Plantier-Royon et al., 2004; UN COMTRADE Statistics Database and Kassaian, 2018)

In the “Top Value Added Chemicals from Biomass- Volume I” report (Werpy and Petersen, 2004), the 1,4-diacids were selected as one of the 12 building blocks that will be the base of the chemical production derived from biomass. These building blocks will be the chemical raw material of the future high-value biobased chemicals and materials to substitute petrochemicals as raw materials. Most of the current research focuses on obtaining these building blocks from renewable resources and converting them effectively into new materials and chemicals.

In the past years, there has been a growing market for biomass-derived C_4-DCA, as seen in Table 2.6, while the price is decreasing as more efficient technology is used, approaching petrochemical-derived C_4-DCA prices. Nowadays, many of these C_4-DCA are obtained from petrochemical routes, whose price has increased in recent years. Since these C_4-DCA are used mainly as intermediates, it is essential to note that, for bulk chemicals with prices over 1 USD/kg, the price is widely affected by the cost of raw material, and in this case, it is expected to expect higher prices as petroleum price increases (Goldberg and Rokem, 2014).

There is a more detailed description for each C4-DCA in the following subsections, including its current sources, markets, and main uses.

2.5.1 Succinic acid

Succinic acid is used for several applications, including industrial applications (57.1%), pharmaceuticals (15.9%), food and beverages (13.1%), and others (13.9%) (Saxena et al., 2017). It is currently produced mainly by hydrogenation of petrochemical maleic anhydride and later hydration. It can also be obtained as a side-product from adipic acid production, by oxidation of 1,4-butanediol, and by carbonylation of ethane or ethylene glycol. The leading producers are DSM (The Netherlands), Gavid Petrochemical Industries (Israel), Mitsubishi Chemical Corp. and Kawasaki Kasei Chemicals (Japan), and Anqing Hexing Chemical and Anhui Sunsing Chemicals (China) (Gérardy et al., 2020; Höfer, 2015; Kohli et al., 2019).

In the United States, the actual succinic acid market is approximately 4.5 x 10^5 tonnes with an average price of 2.8 USD/kg, while nearly 0.5 million metric tonnes of bio-succinic acid production facilities have been installed or under construction. Bio-succinic acid fermentation is done by yeasts and bacteria that can accumulate succinic acid using fermentable sugars, like dextrose, as their carbon source under an anaerobic process (Höfer, 2015). This bio-succinic acid must have a production cost equal to or lower than 0.55 USD/kg to match petrochemical production. Even today, there is a greater demand than production, which cannot be matched by petrochemical production (Du et al., 2015; Jong and Jungmeier, 2015; Kamm et al., 2008).

There is a growing industry related to bio-succinic acid, produced by fermentation. Four leading companies appeared in the 2010 decade to fill the bio-based succinic acid gap, installing production plants that produced succinic acid by fermentation using bacteria strains from rumen or by engineered microorganisms. These four companies were: BioAmber (Canada), Reverdia (Joint venture of DSM and Roquette, Italy), Myriant (USA), and Succinity (Joint venture of BASF and Corbion Purac, Spain), being the biggest producer was BioAmber, which upgraded their facilities to produce near 230 kt/year with sales over 12 million USD in 2017 (Carlson et al., 2016; Cok et al., 2014). Global production was expected to increase rapidly in the following years, reaching production values between 94 -500 kt by 2025 (Gérardy et al., 2020). However, BioAmber declared bankruptcy in the year 2018 (McCoy, 2018). Myriant and Succinity are not running anymore, and Reverdia is probably the only company still in the market (Li and Mupondwa, 2021). Shandong Landian Biological Technology (China) is also a prominent player in the market, but no production information is available (Gérardy et al., 2020). Most of the plants failed to survive mainly due to costly technologies which were not ready for commercialization, high production costs, low productivity, difficulties on the precise control of the microorganisms, problems regarding the separation of succinic acid from the fermentation broth, the sensibility to the oil price, and the emergence of cheap succinic acid derived from shale gas in the last years (Gérardy et al., 2020; Iglesias et al., 2020; Li and Mupondwa, 2021).

Succinic acid has several applications in the industry. In the chemical industry, it can be used as a surfactant, detergent extender, foaming agent, ion chelator in plating. It can be used as an acidulant, flavoring additive, and antimicrobial agent in the food industry. However, it can also be used as an intermediate for producing other chemicals and materials, like resins, as seen in Figure 2.9 (Du et al., 2015; Gérardy et al., 2020; Nghiem et al., 2017; Saxena et al., 2017).

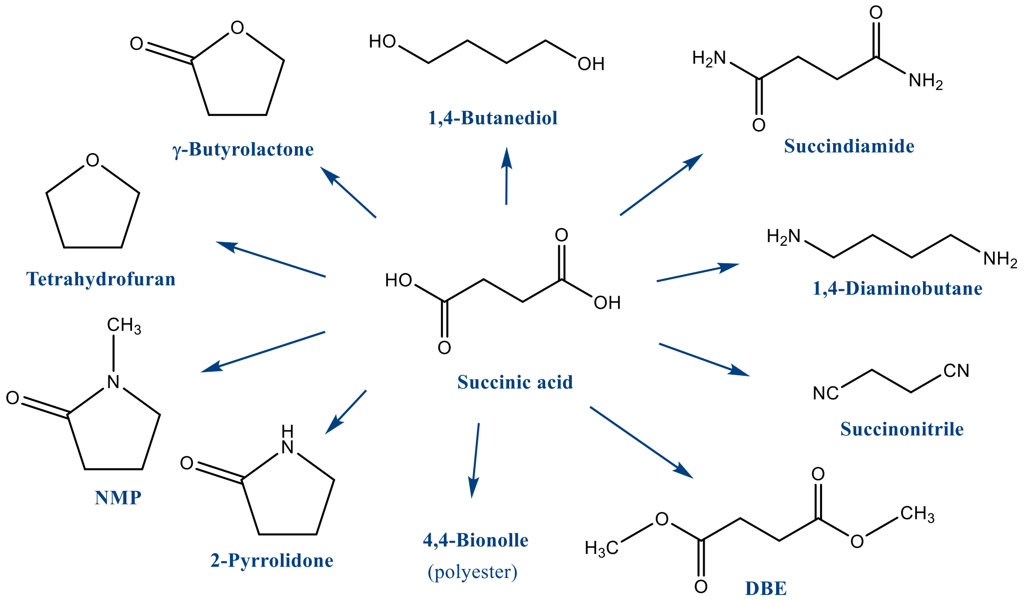

Figure 2.9 - Conversion of succinic acid to other chemicals

Source: Modified from Werpy & Petersen, 2004

There is a great interest in substituting adipic acid (used for polymer production) with succinic acid, which has a shorter carbon chain but can be obtained from renewable resources, while adipic acid cannot. At this moment, the succinic acid market is less than 2% of the total adipic acid market, so there is plenty of room for expansion. The price is one of the main factors to consider because the difference between petrochemical adipic acid and bio-succinic acid is around 450 USD/t. This price gap should be reduced before any attempt at industrial substitution should be achieved (Grotkjaer, 2015).

Succinic acid can be converted through hydrogenation/reduction to 1,4-butanediol (BDO), which is a raw material for several polymers, like polybutylene terephthalate (PBT) and polybutylene succinate (PBS). PBS production requires not only BDO but succinic acid as well. This bio-polymer, and its modified derivatives, show similar properties to polypropylene and polyvinylchloride and can be produced using the same existing processing equipment. Furthermore, 40% of the world production of BDO is used to produce tetrahydrofuran (THF), which is later used for polymer production (Spandex®, poly(tetramethylene ether glycol)), as a solvent in PVC cements, pharmaceuticals, and coatings, and as a reaction solvent. Another chemical derivative is γ-butyrolactone (GBL), which is used as a chemical intermediate in pyrrolidone solvent production. (Cok et al., 2014; Gérardy et al., 2020; Höfer, 2015; Iglesias et al., 2020; Jong et al., 2011; Kamm et al., 2008; Kohli et al., 2019; Litsanov et al., 2014; Werpy and Petersen, 2004).

Succinic acid can also be converted to derivate compounds, like succinate esters and salts, sulfosuccinates and sulfosuccinamates, and pyrrolidones. These compounds have applications as additives or main ingredients in the food industry, pharmaceuticals, fuels, and cosmetics (Litsanov et al., 2014). Recently, there is increasing research on biodegradable polymer production from succinate esters to produce poly(3-hydroxybutyrate) and other polymers using biotechnological routes (Tang and Chen, 2018).

It was expected that in the year 2020, the succinic acid market volume would achieve 600 kt/year. BDO global market would produce 316 kt/year (52.7% of the market share). PBS and PBST would have an 82 kt/year market (13.7% market share) and polyester polyols 51 kt/year (8.5% market share). Other applications, such as food, pharmaceuticals, resins, and cosmetics, would have a market volume lower than 30 kt/year (<4% market share) (Nghiem et al., 2017). However, the failure of the bio-succinic acid plants could have diminished the expected market volume growth.

2.5.2 Fumaric acid

Fumaric acid can be produced via biotechnological processes (fermentation and enzymatic processes), but the petrochemical routes have better yields and lower prices. It is currently produced from oil-based maleic anhydride or by isomerization of maleic acid. It can also be produced by fermentation using several fungi species in aerobic and anaerobic conditions, using common sugars as a carbon source, while other enzymes can interconvert maleic acid to fumaric acid (Du et al., 2015; Gérardy et al., 2020; Goldberg and Rokem, 2014; Lohbeck et al., 2000).

The global production of fumaric acid was 225 kt/year in 2012, with a price of 1280-1700 USD/ton, and expected production of 346 kt/year is expected in 2020, which shows a slight growth due to food industry demands for natural acidulant and flavoring agents (Gérardy et al., 2020; Martin-Dominguez et al., 2018). The petrochemical process is the primary producer, and currently, more facilities are being constructed under this technology. The principal production plants are located in Asia, being the most important Changzhou Yabang Chemical Co. Ltd. (China), Changmao Biochemical Engineering Company Limited (China), Nippon Shokubai (Japan), and Yongsan Chemicals (Korea) (Gérardy et al., 2020).

Fumaric acid is widely used in several fields, as seen in Figure 2.10. The food industry is the main market, with 33% of the world's consumption in 2009. It is primarily used as a food and beverage additive, as an acidulant, preservative, and flavoring agent, but also as an intermediate for L-malic acid and L-aspartic acid, which are used in beverages, health drinks, and cosmetics (Goldberg and Rokem, 2014; Martin-Dominguez et al., 2018). It is also used in paper and pulp industries, as an acid sizing agent but with decreasing use (Goldberg and Rokem, 2014). Moreover, it is used as an intermediate in unsaturated polyester resins (UPEs) production, given the two carboxylic acids and the *trans* double bond, creating very compact polymers with multiple intermolecular interactions. These polymers show higher mechanical and thermal properties than polymers prepared from maleic acid (however, the latter are preferred when low-cost polymers are needed) (Lohbeck et al., 2000; Martin-Dominguez et al., 2018).

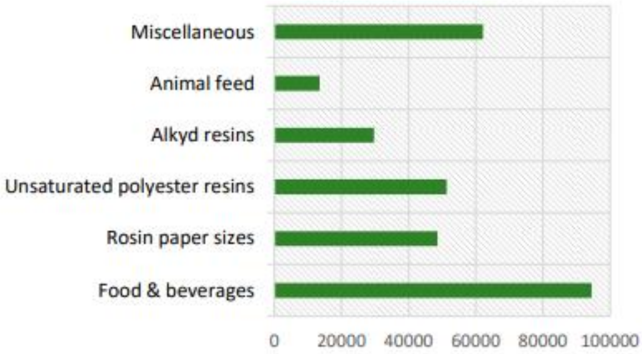

Figure 2.10 - Fumaric acid consumption regarding its applications (in t/year)

Source: Martin-Dominguez et al. 2018

Fumaric acid also produces alkyd resins, obtained after condensation of polyols and polyacids and then modified with long fatty acids, oils, and other compounds. These thermoplastic resins are used mainly in the coating industry (Martin-Dominguez et al., 2018).

It is also utilized in animal feed (as a hydrogen sink in the rumen of cattle) and cosmetic and pharmaceuticals use (Martin-Dominguez et al., 2018). One of the main advantages of fumaric acid over maleic acid is its innocuous nature, and resins made with fumaric acid show better physical properties (Du et al., 2015; Lohbeck et al., 2000).

2.5.3 Maleic acid

Maleic acid is mainly produced by hydrolysis of maleic anhydride in water. It is not a much-utilized chemical, used mainly for resins and as co-monomer (as maleic acid esters), for example, in polyester and alkyd resins, lacquers, plasticizers, copolymers, and lubricants. It can also be used to produce pesticides (Captan, Malathion) and growth inhibitors (maleic acid hydrazide). It is not used in the food industry because it has a critical toxicological activity, being irritant and corrosive on the skin, mucous membrane, and eyes (Lohbeck et al., 2000).

Maleic acid is produced from the hydrolysis of oil-based maleic anhydride, which is obtained from catalytic oxidation of hydrocarbons in the gas phase, normally benzene (up to 1980s), and nowadays, other C_4 hydrocarbons, such as *n*-butane and *n*-butene (Gérardy et al., 2020; Lohbeck et al., 2000). Currently, the leading companies producing maleic anhydride are displayed in Table 2.7.

Table 2.7 - Main producers for maleic anhydride, year 2015

Company	**Location**	**Capacity (kt/year)**	**% of total**
Huntsman Corporation	United States	154	5.5
Jiangsu Yabang Group	China	150	5.4
Bohai Chemicals	China	140	5.0
Sasol/Huntsman	Germany	105	3.8
Polynt	Italy	101	3.6

Source: Zhao 2015

The total world capacity of maleic anhydride production in 2015 was 2800 kt/year, and it is expected that in the following years, many Chinese plants will increase their capacity or build new plants, adding more than 1000 tonnes. Most of this new production capacity will use butane-based technology, which will reach 43% of the total processes, while the other 57% will use the normal benzene-based process (Na, 2015). However, it is said that most of these Chinese plants have overcapacity and are running at 50-60% of their total capacity. Around November 2017, the European prices of maleic anhydride were about 1200-1300 €/t (ICIS, 2018).

The interest in obtaining maleic acid from renewable routes has been studied in the last years, and several processes based on biomass-derived platform oxidation have been suggested. Among them, the most promising are gas-phase oxidation of butanol and levulinic acid using O_2, liquid-phase oxidation of 5-hydroxymethylfurfural using O_2, and furfural oxidation (by liquid-phase or gas-phase O_2 oxidation, liquid-phase H_2O_2 oxidation, or electrochemically). However, the problem with these routes is that most of these biomass-derived platform chemicals are not commercially available yet, their price is higher than the petrochemical routes, or the technology is still under development. Only furfural is an already available bio-based platform with a competitive price (Iglesias et al., 2020).

Maleic acid converts to fumaric acid when heated at 120ºC, and under strong heating (at approximately 450ºC), it gets dehydrated to form maleic anhydride (Whelan, 1994). In 1990, Du Pont developed a method to convert maleic acid to succinic acid in the presence of H_2, then converted to γ-butyrolactone and finally to THF (Wittcoff et al., 2004).

2.5.4 Malic acid

L-malic acid was initially extracted from eggshells, fruits, and apple juice, but this technique implied higher costs against petrochemical routes. Nowadays, it is produced by hydrating petrochemical maleic anhydride or fumaric acid at high temperature and pressure, giving a racemic mixture of *L*- and *D*- isomers, although only *L*- isomer is present in Krebs' cycle. Purification by recrystallization and resolution gives a high purity L-malic acid. The primary producers worldwide are Fuso (Japan), Changmao Biochemical Engineering Company Limited (China), Yongsan Chemicals (Korea), and Thirumalai Chemicals (India). (Du et al., 2015; Gérardy et al., 2020; West, 2017).

Since the malic acid is an intermediate of the tricarboxylic acid cycle (TCA), it can also be produced enzymatically from fumaric acid by purified fumarase enzymes or microbial cells with this enzyme (Chi et al., 2016; Kamm et al., 2008). A novel route obtains *L*-malic acid from poly(*β*-*L*-malic acid) (PMA), which is synthesized by the fungus *A. pullulans*, which is hydrolyzed at 85ºC in acidic conditions, giving a very promising route with economic advantages (West, 2017). However, these biological routes are still expensive and involve many steps, not being commercially available yet.

In 2016, the global production of *L*-malic acid was 162 kt/year, and it was expected a 5.1% growth to the year 2020 (Martin-Dominguez et al., 2018). The retail price of malic acid ranges from 4000-4400 USD/t (West, 2017). This high price is related to the current production methods, avoiding an increased use of malic acid (Chi et al., 2016).

Malic acid is used mainly as an acidulant in the food industry because it has a better acid taste and less bitterness than citric acid. It is also used as a flavor enhancer and antimicrobial agent in food and can be found as calcium, ferric, and zinc salts to enhance mineral content in drinks and foods. Malic acid can be used in metal cleaning and finishing, textile finishing, electrode plating, and paints (Chi et al., 2016).

As a chemical precursor, malic acid can be used to produce 1,2,4-butanetriol (used as intermediate for alkyd resins) and 3-hydroxybutyrolactone (used for pharmaceuticals). It is also used to synthetized the biodegradable polymer PMA (Chi et al., 2016; Kamm et al., 2008). Malic acid can be transformed to maleic and fumaric acid under heating at different temperatures (Pomogailo et al., 2010).

2.5.5 Tartaric acid

Tartaric acid is widely used as an additive in the food industry (bakery, sugar confectionery, and drinks), building industry (concrete and plaster), pharmaceutical and cosmetic industry (formulation of medicines and cosmetics), textile printing, and enology (adjustment of final acidity in wines). Also, *L*-tartaric acid can be used as a raw material to synthesize other chiral molecules (Garcia et al., 2020; Goldberg and Rokem, 2017; Plantier-Royon et al., 2004).

Tartaric acid is a by-product of the winemaking industry since it is found naturally as tartrates in grapes. During fermentation, it precipitates as hydrogen potassium tartrate (commonly called tartar or cream of tartar) or sometimes as calcium tartrate mixed with dead yeast. Then, the salt is collected from the tank and purified to obtain an approximate yield of 100-350 g/hL. Typically, tartaric acid is widely available in wine lees (100-150 kg/ton) and grape pomace (50-75 kg/ton) (Ahmad et al., 2020; Fu et al., 2017; Plantier-

Royon et al., 2004). A synthetic route produces a racemic mixture of tartaric acid from petrochemical maleic anhydride (Goldberg and Rokem, 2017).

The global market for tartaric acid in 2017 was 216 million USD, and it is expected to grow 5.8%. However, its price has varied since it is considered a by-product of the winery industry, in which productivity depends on the climate and other variables (Garcia et al., 2020; Goldberg and Rokem, 2017). Since this acid is easily obtainable from winery by-products, and the technology is commercially available and non-expensive, tartaric acid arouses low interest for new bio-based methods for its production, with few attempts to obtain this compound using alternative biological pathways with various bacteria (Goldberg and Rokem, 2017).

2.6 Final remarks

Lignin, as a readily available feedstock, has significant possibilities to be upgraded to value-added compounds. However, given the complex structure and deep recalcitrance in most technical lignins, specific depolymerization processes must be used to achieve the target compounds efficiently. Catalytic oxidative depolymerization is a valuable strategy to accomplish these requirements.

Recent interest in dicarboxylic acids, especially in four carbons acids, makes appealing the use of lignin as a renewable feedstock for its production. The ring-opening reaction, needed for cleaving the aromatic ring, requires a strong oxidant and specific reaction conditions to achieve good selectivity without having over-oxidation and losing the carbon source as low-molecular-weight compounds, like formic acid and CO_2. With the complexity of lignin reactivity, this fact places complex challenges to obtain valuable C_4-DCA yields and makes the developed process attractive to incorporate in future biorefineries.

Catalytic peroxide oxidation could be an exciting solution to enhance the oxidation potential without employing more aggressive reaction conditions. Although many studies have been performed using heterogeneous catalysts and H_2O_2 to produce C_4-DCA, most were tested in lignin model compounds, and few have achieved good results using real lignin. Therefore, more research is required to address an efficient route to depolymerize and upgrade lignin into valuable C_4-DCA.

2.7 References

Abdelaziz, O.Y., Brink, D.P., Prothmann, J., Ravi, K., Sun, M., García-Hidalgo, J., Sandahl, M., Hulteberg, C.P., Turner, C., Lidén, G., Gorwa-Grauslund, M.F., 2016. Biological valorization of low molecular weight lignin. Biotechnol. Adv. 34, 1318–1346. https://doi.org/10.1016/j.biotechadv.2016.10.001

Abdelaziz, O.Y., Ravi, K., Mittermeier, F., Meier, S., Riisager, A., Lidén, G., Hulteberg, C.P., 2019. Oxidative Depolymerization of Kraft Lignin for Microbial Conversion. ACS Sustain. Chem. Eng. 7, 11640–11652. https://doi.org/10.1021/acssuschemeng.9b01605

Aguilar-Reynosa, A., Romaní, A., Ma. Rodríguez-Jasso, R., Aguilar, C.N., Garrote, G., Ruiz, H.A., 2017. Microwave heating processing as alternative of pretreatment in second-generation biorefinery: An overview. Energy Convers. Manag. 136, 50–65. https://doi.org/10.1016/j.enconman.2017.01.004

Ahmad, B., Yadav, V., Yadav, A., Rahman, M.U., Yuan, W.Z., Li, Z., Wang, X., 2020. Integrated biorefinery approach to valorize winery waste: A review from waste to energy perspectives. Sci. Total Environ. 719, 137315. https://doi.org/10.1016/j.scitotenv.2020.137315

Alba-Rubio, A.C., Fierro, J.L.G., León-Reina, L., Mariscal, R., Dumesic, J.A., López Granados, M., 2017. Oxidation of furfural in aqueous H_2O_2 catalysed by titanium silicalite: Deactivation processes and role of extraframework Ti oxides. Appl. Catal. B Environ. 202, 269–280. https://doi.org/10.1016/j.apcatb.2016.09.025

Ansaloni, S., Russo, N., Pirone, R., 2017. Wet Air Oxidation of Industrial Lignin Case Study: Influence of the Dissolution Pretreatment and Perovskite-type Oxides. Waste and Biomass Valorization 0, 1–15. https://doi.org/10.1007/s12649-017-9947-4

Asgari, F., Argyropoulos, D.S., 1998. Fundamentals of oxygen delignification . Part II . Functional group formation / elimination in residual kraft lignin. Can. J. Chem. 76, 1606–1615. https://doi.org/10.1139/cjc-76-11-1606

Bartoli, M., Rosi, L., Frediani, P., Frediani, M., 2020. Bio-oils from microwave assisted pyrolysis of kraft lignin operating at reduced residual pressure. Fuel 278, 118175. https://doi.org/10.1016/j.fuel.2020.118175

Behling, R., Valange, S., Chatel, G., 2016. Heterogeneous catalytic oxidation for lignin valorization into valuable chemicals: What results? What limitations? What trends? Green Chem. 18, 1839–1854. https://doi.org/10.1039/c5gc03061g

Berlin, A., Balakshin, M., 2014. Industrial Lignins, in: Gupta, V.K., Tuohy, M.G., Kubicek, C.P., Saddler, J., Xu, F. (Eds.), Bioenergy Research: Advances and Applications. Elsevier, Amsterdam, pp. 315–336. https://doi.org/10.1016/B978-0-444-59561-4.00018-8

Bhargava, S.K., Tardio, J., Prasad, J., Föger, K., Akolekar, D.B., Grocott, S.C., 2006. Wet oxidation and catalytic wet oxidation. Ind. Eng. Chem. Res. 45, 1221–1258. https://doi.org/10.1021/ie051059n

Bi, Z., Li, Z., Yan, L., 2018. Catalytic oxidation of lignin to dicarboxylic acid over the $CuFeS_2$ nanoparticle catalyst. Green Process. Synth. 7, 306–315. https://doi.org/10.1515/gps-2017-0056

Bourbiaux, D., Pu, J., Rataboul, F., Djakovitch, L., Geantet, C., Laurenti, D., 2021. Reductive or oxidative catalytic lignin depolymerization: An overview of recent advances. Catal. Today 373, 24–37. https://doi.org/10.1016/j.cattod.2021.03.027

Bullock, R.M., Chen, J.G., Gagliardi, L., Chirik, P.J., Farha, O.K., Hendon, C.H., Jones, C.W., Keith, J.A., Klosin, J., Minteer, S.D., Morris, R.H., Radosevich, A.T., Rauchfuss, T.B., Strotman, N.A., Vojvodic, A., Ward, T.R., Yang, J.Y., Surendranath, Y., 2020. Using nature's blueprint to expand catalysis with Earth-abundant metals. Science 369. https://doi.org/10.1126/science.abc3183

Cabral Almada, C., Kazachenko, A., Fongarland, P., Da Silva Perez, D., Kuznetsov, B.N., Djakovitch, L., 2020. Oxidative depolymerization of lignins for producing aromatics: variation of botanical origin and extraction methods. Biomass Convers. Biorefinery. https://doi.org/10.1007/s13399-020-00897-6

Cao, Y., Chen, S.S., Zhang, S., Ok, Y.S., Matsagar, B.M., Wu, K.C.-W.C.W., Tsang, D.C.W., 2019. Advances in lignin valorization towards bio-based chemicals and fuels: Lignin biorefinery. Bioresour. Technol. 291, 121878. https://doi.org/10.1016/j.biortech.2019.121878

Carlson, A., Coggio, B., Lau, K., Mercogliano, C., Millis, J., 2016. Industrial production of succinic acid. Chem. Fuels from Bio-Based Build. Blocks 173–190.

https://doi.org/10.1017/CBO9781107415324.004

Chen, Z., Wan, C., 2017. Biological valorization strategies for converting lignin into fuels and chemicals. Renew. Sustain. Energy Rev. 73, 610–621. https://doi.org/10.1016/j.rser.2017.01.166

Cheng, C., Wang, J., Shen, D., Xue, J., Guan, S., Gu, S., Luo, K.H., 2017. Catalytic oxidation of lignin in solvent systems for production of renewable chemicals: A review. Polymers (Basel). 9, 38–50. https://doi.org/10.3390/polym9060240

Chi, Z., Wang, Z.P., Wang, G.Y., Khan, I., Chi, Z.M., 2016. Microbial biosynthesis and secretion of l-malic acid and its applications. Crit. Rev. Biotechnol. 36, 99–107. https://doi.org/10.3109/07388551.2014.924474

Chio, C., Sain, M., Qin, W., 2019. Lignin utilization: A review of lignin depolymerization from various aspects. Renew. Sustain. Energy Rev. 107, 232–249. https://doi.org/10.1016/j.rser.2019.03.008

Clerici, M.G., 2015. The Activity of Titanium Silicalite-1 (TS-1): Some Considerations on Its Origin. Kinet. Catal. 56, 453–458. https://doi.org/10.7868/s045388111504005x

Cok, B., Tsiropoulos, I., Roes, A.L., Patel, M.K., 2014. Succinic acid production derived from carbohydrates: An energy and greenhouse gas assessment of a platform chemical toward a bio-based economy. Biofuels, Bioprod. Biorefining 8, 16–29. https://doi.org/10.1002/bbb.1427

Crestini, C., Crucianelli, M., Orlandi, M., Saladino, R., 2010. Oxidative strategies in lignin chemistry: A new environmental friendly approach for the functionalisation of lignin and lignocellulosic fibers. Catal. Today 156, 8–22. https://doi.org/10.1016/j.cattod.2010.03.057

Cronin, D.J., Zhang, X., Bartley, J., Doherty, W.O.S.S., 2017. Lignin Depolymerization to Dicarboxylic Acids with Sodium Percarbonate. ACS Sustain. Chem. Eng. 5, 6253–6260. https://doi.org/10.1021/acssuschemeng.7b01208

Das, L., Kolar, P., Sharma-Shivappa, R., 2012. Heterogeneous catalytic oxidation of lignin into value-added chemicals. Biofuels 3, 155–166. https://doi.org/10.4155/BFS.12.5

Demesa, A.G., Laari, A., Sillanp, M., Koiranen, T., 2017. Valorization of lignin by partial wet oxidation using sustainable heteropoly acid catalysts. Molecules 22, 1–11. https://doi.org/10.3390/molecules22101625

Demesa, A.G., Laari, A., Turunen, I., Sillanpää, M., 2015. Alkaline Partial Wet Oxidation of Lignin for the Production of Carboxylic Acids. Chem. Eng. Technol. 38, 2270–2278. https://doi.org/10.1002/ceat.201400660

Di Marino, D., Jestel, T., Marks, C., Viell, J., Blindert, M., Kriescher, S.M.A., Spiess, A.C., Wessling, M., 2019. Carboxylic Acids Production via Electrochemical Depolymerization of Lignin. ChemElectroChem 6, 1434–1442. https://doi.org/10.1002/celc.201801676

Dimmel, D., 2010. Overview, in: Heitner, C., Dimmel, D.R., Schmidt, J.A. (Eds.), Lignin and Lignans: Advances in Chemistry. Boca Raton, pp. 1–48.

Du, G., Liu, L., Chen, J., 2015. White Biotechnology for Organic Acids, in: Pandey, A., Höfer, R., Taherzadeh, M., Nampoothiri, K.M., Larroche, C. (Eds.), Industrial Biorefineries & White Biotechnology. Elsevier, pp. 409–444. https://doi.org/10.1016/B978-0-444-63453-5.00013-6

Evtuguin, D., Robert, D., 1997. The detection of muconic acid type structures in oxidized lignins by13C NMR spectroscopy. Wood Sci. Technol. 31, 423–431. https://doi.org/10.1007/BF00702564

Faisal, I., 2009. Oxidation of Phenolic Wastewater by Fenton’s Reagent. Iraqi J. Chem. Pet. Eng. 10, 1–5.

Fang, Z., Smith, R.L., 2016. Production of Biofuels and Chemicals from Lignin. https://doi.org/10.1007/978-981-10-1965-4

Figueirêdo, M.B., Deuss, P.J., Venderbosch, R.H., Heeres, H.J., 2019. Valorization of Pyrolysis Liquids: Ozonation of the Pyrolytic Lignin Fraction and Model Components. ACS Sustain. Chem. Eng. 7, 4755–4765. https://doi.org/10.1021/acssuschemeng.8b04856

Fu, J., Vasiliadou, E.S., Goulas, K.A., Saha, B., Vlachos, D.G., 2017. Selective hydrodeoxygenation of tartaric acid to succinic acid. Catal. Sci. Technol. 7, 4944–4954. https://doi.org/10.1039/c7cy01374d

Gamba, A., Tabacchi, G., Fois, E., 2009. TS-1 from First Principles. J. Phys. Chem. A 113, 15006–15015. https://doi.org/10.1021/jp905110s

Garcia, A.C., Sánchez-Martínez, C., Bakker, I., Goetheer, E., 2020. Sustainable Electrochemical Production of Tartaric Acid. ACS Sustain. Chem. Eng. 8, 10454–10460. https://doi.org/10.1021/acssuschemeng.0c02493

Gellerstedt, G., 2010. Chemistry of pulp bleaching, in: Heitner, C., Dimmel, D.R., Schmidt, J.A. (Eds.), Lignin and Lignans: Advances in Chemistry. Boca Raton, pp. 393–438. https://doi.org/doi:10.1201/EBK1574444865-c11

Gérardy, R., Debecker, D.P., Estager, J., Luis, P., Monbaliu, J.-C.M., 2020. Continuous Flow Upgrading of Selected C 2 –C 6 Platform Chemicals Derived from Biomass. Chem. Rev. 120, 7219–7347. https://doi.org/10.1021/acs.chemrev.9b00846

Gierer, J., 1986. Chemistry of delignification. Wood Sci. Technol. 20, 1–33. https://doi.org/10.1007/bf00350692

Goldberg, I., Rokem, J.S., 2017. Organic and Fatty Acid Production, Microbial ☆, in: Reference Module in Life Sciences. Elsevier, pp. 358–382. https://doi.org/10.1016/B978-0-12-809633-8.13083-3

Goldberg, I., Rokem, J.S., 2014. Fumaric Acid Biosynthesis and Accumulation, in: Bioprocessing of Renewable Resources to Commodity Bioproducts. pp. 409–434. https://doi.org/10.1002/9781118845394.ch15

Grand View Research, 2015. Tartaric acid Market Analysis By Application (Food & Beverages, Wine, Pharmaceuticals, Antacids) And Segment Forecasts To 2020.

Grotkjaer, T., 2015. Commercial Development of Fermentation Processes, in: Villadsen, J. (Ed.), Fundamental Bioengineering. Wiley-VCH Verlag GmbH & Co. KGaA, Weinheim, Germany, pp. 499–546. https://doi.org/10.1002/9783527697441.ch17

Guélou, E., Barrault, J., Fournier, J., Tatibouët, J.M., 2003. Active iron species in the catalytic wet peroxide oxidation of phenol over pillared clays containing iron. Appl. Catal. B Environ. 44, 1–8. https://doi.org/10.1016/S0926-3373(03)00003-1

Hasegawa, I., Inoue, Y., Muranaka, Y., Yasukawa, T., Mae, K., 2011. Selective production of organic acids and depolymerization of lignin by hydrothermal oxidation with diluted hydrogen peroxide. Energy and Fuels 25, 791–796. https://doi.org/10.1021/ef101477d

Höfer, R., 2015. Sugar- and Starch-Based Biorefineries, in: Industrial Biorefineries &

White Biotechnology. Elsevier, pp. 157–235. https://doi.org/10.1016/B978-0-444-63453-5.00005-7

Huang, D., Li, R., Xu, P., Li, T., Deng, R., Chen, S., Zhang, Q., 2020. The cornerstone of realizing lignin value-addition: Exploiting the native structure and properties of lignin by extraction methods. Chem. Eng. J. 402, 126237. https://doi.org/10.1016/j.cej.2020.126237

ICIS, 2018. Europe Chemicals Outlook.

Iglesias, J., Martínez-Salazar, I., Maireles-Torres, P., Martin Alonso, D., Mariscal, R., López Granados, M., 2020. Advances in catalytic routes for the production of carboxylic acids from biomass: A step forward for sustainable polymers. Chem. Soc. Rev. 49, 5704–5771. https://doi.org/10.1039/d0cs00177e

Jong, E. de, Higson, A., Walsh, P., Wellisch, M., 2011. Biobased Chemicals - Value Added Products from Biorefineries, IEA Bioenergy-Task 42 Biorefinery. https://doi.org/10.1126/science.1179713

Jong, E. De, Jungmeier, G., 2015. Biorefinery Concepts in Comparison to Petrochemical Refineries, in: Industrial Biorefineries and White Biotechnology. Elsevier B.V., pp. 3–33. https://doi.org/10.1016/B978-0-444-63453-5.00001-X

Kamm, B., Gruber, P.R., Kamm, M., 2008. Biorefineries-Industrial Processes and Products: Status Quo and Future Directions, Biorefineries-Industrial Processes and Products: Status Quo and Future Directions. https://doi.org/10.1002/9783527619849

Kang, J., Irmak, S., Wilkins, M., 2019. Conversion of lignin into renewable carboxylic acid compounds by advanced oxidation processes. Renew. Energy 135, 951–962. https://doi.org/10.1016/j.renene.2018.12.076

Kang, S., Li, X., Fan, J., Chang, J., 2013. Hydrothermal conversion of lignin: A review. Renew. Sustain. Energy Rev. 27, 546–558. https://doi.org/10.1016/j.rser.2013.07.013

Kleine, T., Buendia, J., Bolm, C., 2013. Mechanochemical degradation of lignin and wood by solvent-free grinding in a reactive medium. Green Chem. 15, 160–166. https://doi.org/10.1039/C2GC36456E

Ko, M., Pham, L.T.M., Sa, Y.J., Woo, J., Nguyen, T.V.T., Kim, J.H., Oh, D., Sharma, P., Ryu, J., Shin, T.J., Joo, S.H., Kim, Y.H., Jang, J.W., 2019. Unassisted solar lignin valorisation using a compartmented photo-electro-biochemical cell. Nat. Commun. 10, 1–10. https://doi.org/10.1038/s41467-019-13022-7

Kohli, K., Prajapati, R., Sharma, B., 2019. Bio-Based Chemicals from Renewable Biomass for Integrated Biorefineries. Energies 12, 233. https://doi.org/10.3390/en12020233

Li, C., Zhao, X., Wang, A., Huber, G.W., Zhang, T., 2015. Catalytic Transformation of Lignin for the Production of Chemicals and Fuels. Chem. Rev. 115, 11559–11624. https://doi.org/10.1021/acs.chemrev.5b00155

Li, H., Qu, Y., Xu, J., 2015. Microwave-Assisted Conversion of Lignin. pp. 61–82. https://doi.org/10.1007/978-94-017-9612-5_4

Li, X., Mupondwa, E., 2021. Empirical analysis of large-scale bio-succinic acid commercialization from a technoeconomic and innovation value chain perspective: BioAmber biorefinery case study in Canada. Renew. Sustain. Energy Rev. 137, 110587. https://doi.org/10.1016/j.rser.2020.110587

Li, Y., Zhao, R., Pang, Y., Qiu, X., Yang, D., 2018. Microwave-assisted synthesis of high carboxyl content of lignin for enhancing adsorption of lead. Colloids Surfaces A Physicochem. Eng. Asp. 553, 187–194. https://doi.org/10.1016/j.colsurfa.2018.05.029

Liao, Y., Koelewijn, S.F., van den Bossche, G., van Aelst, J., van den Bosch, S., Renders, T., Navare, K., Nicolaï, T., van Aelst, K., Maesen, M., Matsushima, H., Thevelein, J.M., van Acker, K., Lagrain, B., Verboekend, D., Sels, B.F., 2020. A sustainable wood biorefinery for low-carbon footprint chemicals production. Science (80-.). 367, 1385–1390. https://doi.org/10.1126/science.aau1567

Litsanov, B., Brocker, M., Oldiges, M., Bott, M., 2014. Succinic Acid, in: Bisaria, V.S., Kondo, A. (Eds.), Bioprocessing of Renewable Resources to Commodity Bioproducts. John Wiley & Sons, Inc., Hoboken, NJ, USA, pp. 435–472. https://doi.org/10.1002/9781118845394.ch16

Liu, C., Wu, S., Zhang, H., Xiao, R., 2019. Catalytic oxidation of lignin to valuable biomass-based platform chemicals: A review. Fuel Process. Technol. 191, 181–201. https://doi.org/10.1016/j.fuproc.2019.04.007

Lohbeck, K., Haferkorn, H., Fuhrmann, W., Fedtke, N., 2000. Maleic and Fumaric Acids, in: Ullmann's Encyclopedia of Industrial Chemistry. Wiley-VCH Verlag GmbH & Co. KGaA. https://doi.org/10.1002/14356007.a16_053

Lotfi, S., Bahrpaima, K., Boffito, D.C., Patience, G.S., 2020. Gas–Solid Oxidation of Unwashed Lignin to Carboxylic Acids. Energy & Fuels 34, 9683–9696. https://doi.org/10.1021/acs.energyfuels.0c01519

Lotfi, S., Boffito, D.C., Patience, G.S., 2016. Gas–solid conversion of lignin to carboxylic acids. React. Chem. Eng. 1, 397–408. https://doi.org/10.1039/C6RE00053C

Lotfi, S., Boffito, D.C., Patience, G.S., 2015. Gas-Phase Partial Oxidation of Lignin to Carboxylic Acids over Vanadium Pyrophosphate and Aluminum-Vanadium-Molybdenum. ChemSusChem 8, 3424–3432. https://doi.org/10.1002/cssc.201501036

Ma, R., 2016. Dicarboxylic acids platform chemicals for valorization of biorefinery lignin. Washington State University. https://doi.org/10.1029/2002GL016535

Ma, R., Guo, M., Lin, K.T., Hebert, V.R., Zhang, J., Wolcott, M.P., Quintero, M., Ramasamy, K.K., Chen, X., Zhang, X., 2016. Peracetic Acid Depolymerization of Biorefinery Lignin for Production of Selective Monomeric Phenolic Compounds. Chem. - A Eur. J. 22, 10884–10891. https://doi.org/10.1002/chem.201600546

Ma, R., Guo, M., Zhang, X., 2014. Selective Conversion of Biorefinery Lignin into Dicarboxylic Acids. ChemSusChem 7, 412–415. https://doi.org/10.1002/cssc.201300964

Ma, R., Xu, Y., Zhang, X., 2015. Catalytic Oxidation of Biorefinery Lignin to Value-added Chemicals to Support Sustainable Biofuel Production. ChemSusChem 8, 24–51. https://doi.org/10.1002/cssc.201402503

Martin-Dominguez, V., Estevez, J., Ojembarrena, F.D.B., Santos, V.E., Ladero, M., 2018. Fumaric Acid Production : A Biorefinery Perspective. Fermentation 4, 22. https://doi.org/10.3390/fermentation4020033

McCoy, M., 2018. Succinic acid maker BioAmber is bankrupt. Chem. Eng. News 96, 4.

Mcginnis, G.D., Wilson, W.W., Prince, S.E., Chen, C.C., 1983. Conversion of Biomass into Chemicals with High-Temperature Wet Oxidation. Ind. Eng. Chem. Prod. Res. Dev. 22, 633–636. https://doi.org/10.1021/i300012a022

Mei, Q., Shen, X., Liu, H., Han, B., 2019. Selectively transform lignin into value-added chemicals. Chinese Chem. Lett. 30, 15–24. https://doi.org/10.1016/j.cclet.2018.04.032

Murali, N., Srinivas, K., Ahring, B.K., 2017. Biochemical Production and Separation of Carboxylic Acids for Biorefinery Applications. Fermentation 3, 22. https://doi.org/10.3390/fermentation3020022

Mycroft, Z., Gomis, M., Mines, P., Law, P., Bugg, T.D.H.H., 2015. Biocatalytic conversion of lignin to aromatic dicarboxylic acids in Rhodococcus jostii RHA1 by re-routing aromatic degradation pathways. Green Chem. 17, 4974–4979. https://doi.org/10.1039/C5GC01347J

Na, Z., 2015. Maleic Anhydride Chain - World Market Overview. APIC 2015, 24.

Nghiem, N., Kleff, S., Schwegmann, S., 2017. Succinic Acid: Technology Development and Commercialization. Fermentation 3, 26. https://doi.org/10.3390/fermentation3020026

Oils, B., Chain, F., 2019. Europe Chemicals Outlook 2019.

Ouyang, X., Huang, X., Ruan, T., Qiu, X., 2015. Microwave-assisted oxidative digestion of lignin with hydrogen peroxide for TOC and color removal. Water Sci. Technol. 71, 390–396. https://doi.org/10.2166/wst.2014.535

Ouyang, X., Lin, Z., Deng, Y., Yang, D., Qiu, X., 2010. Oxidative Degradation of Soda Lignin Assisted by Microwave Irradiation. Chinese J. Chem. Eng. 18, 695–702. https://doi.org/10.1016/S1004-9541(10)60277-7

Ovejero, G., Sotelo, J.L., Martínez, F., Melero, J.A., Gordo, L., 2001. Wet Peroxide Oxidation of Phenolic Solutions over Different Iron-Containing Zeolitic Materials. Ind. Eng. Chem. Res. 40, 3921–3928. https://doi.org/10.1021/ie000896g

Pandey, M.P., Kim, C.S., 2011. Lignin Depolymerization and Conversion: A Review of Thermochemical Methods. Chem. Eng. Technol. 34, 29–41. https://doi.org/10.1002/ceat.201000270

Park, S.Y., Cho, S.M., Kim, J.C., Hong, C., Kim, S.H., Ryu, G.H., Choi, I.G., 2019. Effects of peracetic acid and hydrogen peroxide concentration on kraft lignin degradation at room temperature. BioResources 14, 4413–4429. https://doi.org/10.15376/biores.14.2.4413-4429

Plantier-Royon, R., Massicot, F., Sudha, A.V.R.L., Portella, C., Dupont, L., Mohamadou, A., Aplincourt, M., 2004. Synthesis of functionalized bis-amides of L-(+)-tartaric acid and application as copper (II) ligands. Comptes Rendus Chim. 7, 119–123. https://doi.org/10.1016/j.crci.2003.10.009

Pomogailo, A.D., Kestelman, V.N., Dzhardimalieva, G.I., 2010. Monomeric and Polymeric Carboxylic Acids, in: Macromolecular Metal Carboxylates and Their Nanocomposites. pp. 7–25. https://doi.org/10.1007/978-3-642-10574-6_2

Qu, C., Ito, K., Katsuyama, I., Mitani, T., Kashimura, K., Watanabe, T., 2020. Directly Microwave-Accelerated Cleavage of C−C and C−O Bonds of Lignin by Copper Oxide and H_2O_2. ChemSusChem 13, 4510–4518. https://doi.org/10.1002/cssc.202000502

Quesada, J., Rubio, M., Gómez, D., 1999. Ozonation of Lignin Rich Solid Fractions from Corn Stalks. J. Wood Chem. Technol. 19, 115–137. https://doi.org/10.1080/02773819909349603

Rinaldi, R., Jastrzebski, R., Clough, M.T., Ralph, J., Kennema, M., Bruijnincx, P.C.A., Weckhuysen, B.M., 2016. Paving the Way for Lignin Valorisation: Recent Advances in Bioengineering, Biorefining and Catalysis. Angew. Chemie - Int. Ed. 55, 8164–8215. https://doi.org/10.1002/anie.201510351

Rodenas, Y., Mariscal, R., Fierro, J.L.G.G., Martín Alonso, D., Dumesic, J.A., López Granados, M., 2018. Improving the production of maleic acid from biomass: TS-1 catalysed aqueous phase oxidation of furfural in the presence of γ-valerolactone. Green Chem. 20, 2845–2856. https://doi.org/10.1039/C8GC00857D

Rodrigues, A.E., Pinto, P.C. de O.R., Barreiro, M.F., Esteves da Costa, C.A., Ferreira da Mota, M.I., Fernandes, I., 2018. An Integrated Approach for Added-Value Products from Lignocellulosic Biorefineries. Springer International Publishing, Cham. https://doi.org/10.1007/978-3-319-99313-3

Rovio, S., Kallioinen, A., Tamminen, T., Hakola, M., Leskelä, M., Siika-ahoa, M., 2012. Catalysed alkaline oxidation as a wood fractionation technique. BioResources 7, 756–776.

Saxena, R.K., Saran, S., Isar, J., Kaushik, R., 2017. Production and Applications of Succinic Acid, in: Current Developments in Biotechnology and Bioengineering.

Elsevier, pp. 601–630. https://doi.org/10.1016/B978-0-444-63662-1.00027-0

Schutyser, Wouter, Kruger, J.S., Robinson, A.M., Katahira, R., Brandner, D.G., Cleveland, N.S., Mittal, A., Peterson, D.J., Meilan, R., Román-Leshkov, Y., Beckham, G.T., 2018. Revisiting alkaline aerobic lignin oxidation. Green Chem. 20, 3828–3844. https://doi.org/10.1039/C8GC00502H

Schutyser, W, Renders, T., Van den Bosch, S., Koelewijn, S.F., Beckham, G.T., Sels, B.F., 2018. Chemicals from lignin: an interplay of lignocellulose fractionation, depolymerisation, and upgrading. Chem. Soc. Rev. 47, 852–908. https://doi.org/10.1039/C7CS00566K

Sengupta, S., Basu, J.K., Ghosal, D., 2013. Oxidation of Catechol using Titanium Silicate (TS-1) Catalyst: Modeling and Optimization. Bull. Chem. React. Eng. Catal. 8, 167–177. https://doi.org/10.9767/bcrec.8.2.4759.167-177

Shanks, B.H., Keeling, P.L., 2017. Bioprivileged molecules: creating value from biomass. Green Chem. 19, 3177–3185. https://doi.org/10.1039/C7GC00296C

Stevens, C. V., Verhé, R.G., 2004. Renewable Bioresources Scope and Modification for Non-Food Applications. John Wiley & Sons Ltd, West Sussex.

Su, J., Yang, L., Liu, R.N., Lin, H., 2014. Low-temperature oxidation of guaiacol to maleic acid over TS-1 catalyst in alkaline aqueous H_2O_2 solutions. Chinese J. Catal. 35, 622–630. https://doi.org/10.1016/S1872-2067(14)60039-5

Sun, Y.-P.P., Nguyen, K.L., Wallis, A.F.A.A., 1998. Ring-Opened Products from Reaction of Lignin Model Compounds with UV-Assisted Peroxide. Holzforschung 52, 61–66. https://doi.org/10.1515/hfsg.1998.52.1.61

Sun, Y., Fenster, M., Yu, A., Berry, R.M., Argyropoulos, D.S., 1999. The effect of metal ions on the reaction of hydrogen peroxide with Kraft lignin model compounds. Can. J. Chem. 77, 667–675. https://doi.org/10.1139/v99-036

Suttipornphaisalkul, M., Wright, P., Kamwilaisak, K., 2020. Succinic acid production from lignin by photo-oxidation. Eng. Appl. Sci. Res. 47, 36–46. https://doi.org/10.14456/easr.2020.3

Suzuki, H., Cao, J., Jin, F., Kishita, A., Enomoto, H., Moriya, T., 2006. Wet oxidation of lignin model compounds and acetic acid production. J. Mater. Sci. 41, 1591–1597. https://doi.org/10.1007/s10853-006-4653-9

Tang, X., Chen, E.Y.-X., 2018. Chemical synthesis of perfectly isotactic and high melting bacterial poly(3-hydroxybutyrate) from bio-sourced racemic cyclic diolide. Nat. Commun. 9, 2345. https://doi.org/10.1038/s41467-018-04734-3

UN COMTRADE Statistics Database, Kassaian, J.-M., 2018. Tartaric acid, Ullmann's Encyclopedia of Industrial Chemistry. Wiley-VCH Verlag GmbH & Co. KGaA, Weinheim, Germany. https://doi.org/10.1002/14356007.a26_163

Upton, B.M., Kasko, A.M., 2016. Strategies for the conversion of lignin to high-value polymeric materials: Review and perspective. Chem. Rev. 116, 2275–2306. https://doi.org/10.1021/acs.chemrev.5b00345

Vangeel, T., Schutyser, W., Renders, T., Sels, B.F., 2018. Perspective on Lignin Oxidation: Advances, Challenges, and Future Directions. Top. Curr. Chem. 376, 30. https://doi.org/10.1007/s41061-018-0207-2

Vardon, D.R., Franden, M.A., Johnson, C.W., Karp, E.M., Guarnieri, M.T., Linger, J.G., Salm, M.J., Strathmann, T.J., Beckham, G.T., 2015. Adipic acid production from lignin. Energy Environ. Sci. 8, 617–628. https://doi.org/10.1039/C4EE03230F

Wang, H., Pu, Y., Ragauskas, A., Yang, B., 2019. From lignin to valuable products–strategies, challenges, and prospects. Bioresour. Technol. 271, 449–461. https://doi.org/10.1016/j.biortech.2018.09.072

Werpy, T., Petersen, G., 2004. Top Value Added Chemicals from Biomass: Volume I -- Results of Screening for Potential Candidates from Sugars and Synthesis Gas., U.S. Department of energy. United States. https://doi.org/10.2172/926125

West, T.P., 2017. Microbial Production of Malic Acid from Biofuel-Related Coproducts and Biomass. Fermentation 3, 14. https://doi.org/10.3390/fermentation3020014

Whelan, A., 1994. Polymer Technology Dictionary, 1st ed. Springer Netherlands. https://doi.org/10.1007/978-94-011-1292-5

Wittcoff, H.A., Reuben, B.G., Plotkin, J.S., 2004. Industrial Organic Chemicals, 2nd ed. John Wiley & Sons, Inc., Hoboken, NJ, USA. https://doi.org/10.1002/0471651540

Wu, G., Heitz, M., 1995. Catalytic mechanism of Cu^{2+} and Fe^{3+} in alkaline O_2 oxidation of lignin. J. Wood Chem. Technol. 15, 189–202. https://doi.org/10.1080/02773819508009507

Wu, W., Dutta, T., Varman, A.M., Eudes, A., Manalansan, B., Loqué, D., Singh, S., 2017. Lignin Valorization: Two Hybrid Biochemical Routes for the Conversion of Polymeric Lignin into Value-added Chemicals. Sci. Rep. 7, 1–13. https://doi.org/10.1038/s41598-017-07895-1

Xia, C., Peng, X., Zhang, Y., Wang, B., Lin, M., Zhu, B., Luo, Y., Shu, X., 2017. Environmental-Friendly Catalytic Oxidation Processes Based on Hierarchical Titanium Silicate Zeolites at SINOPEC, in: Karamé, I. (Ed.), Green Chemical Processing and Synthesis. InTech, pp. 119–150. https://doi.org/10.5772/intechopen.68389

Xiang, Q., Lee, Y.Y., 2000. Oxidative cracking of precipitated hardwood lignin by hydrogen peroxide. Appl. Biochem. Biotechnol. 84–86, 153–162. https://doi.org/10.1385/ABAB:84-86:1-9:153

Xiang, Z., Han, W., Deng, J., Zhu, W., Zhang, Y., Wang, H., 2020. Photocatalytic Conversion of Lignin into Chemicals and Fuels. ChemSusChem 13, 4199–4213. https://doi.org/10.1002/cssc.202000601

Xu, C., Arancon, R.A.D., Labidi, J., Luque, R., 2014. Lignin depolymerisation strategies: towards valuable chemicals and fuels. Chem. Soc. Rev. 43, 7485–7500. https://doi.org/10.1039/C4CS00235K

Yao, S.G., Mobley, J.K., Ralph, J., Crocker, M., Parkin, S., Selegue, J.P., Meier, M.S., 2018. Mechanochemical Treatment Facilitates Two-Step Oxidative Depolymerization of Kraft Lignin. ACS Sustain. Chem. Eng. 6, 5990–5998. https://doi.org/10.1021/acssuschemeng.7b04597

Yin, G., Jin, F., Yao, G., Jing, Z., 2015. Hydrothermal Conversion of Catechol into Four-Carbon Dicarboxylic Acids. Ind. Eng. Chem. Res. 54, 68–75. https://doi.org/10.1021/ie5036447

Zeng, J., Yoo, C.G., Wang, F., Pan, X., Vermerris, W., Tong, Z., 2015. Biomimetic fenton-catalyzed lignin depolymerization to high-value aromatics and dicarboxylic acids. ChemSusChem 8, 861–871. https://doi.org/10.1002/cssc.201403128

3. Vanillic acid catalytic wet peroxide oxidation

Lignin can be depolymerized and used as a feedstock to obtain renewable raw materials, providing a green alternative to fossil counterparts. C_4 dicarboxylic acids (DCA), e.g., succinic, malic, maleic, and fumaric acids, can be obtained from lignin catalytic wet peroxide oxidation. These acids have applications in the pharmaceuticals, food industry and act as solvents. However, a prior evaluation of the catalyst titanium silicalite (TS-1) for C_4-DCA production must be performed using simpler model compounds, assessing the best oxidation conditions.

In this Chapter, the oxidation of vanillic acid (VA) was studied under catalytic wet peroxide oxidation (CWPO) conditions, using TS-1. The effect of temperature, pH, and reaction time was studied. In a second phase, catalyst modification with transition metal oxides (Fe, Co, Cu) was tested. Results concerning the yields of each C_4-DCA are presented and discussed accordingly to the studied effect, showing that acidic pH led to the best succinic acid production while alkaline pH produced mainly hydroxylated acids Modified catalysts did not improve the yields, except for Fe-TS1 in acidic pH. Finally, a comparison between the three model compounds is presented, showing that vanillic acid achieved the best results compared to the other models.

This Chapter is adapted from Vega-Aguilar, C.A.; Barreiro, M.F.; Rodrigues, A.E., "Catalytic wet peroxide oxidation of vanillic acid as a lignin model compound towards the renewable production of dicarboxylic acids". *Chemical Engineering Research and Design*, **2020**, 159. DOI 10.1016/j.cherd.2020.04.021

3.1 Introduction

Lignin is a three-dimensional heterogeneous biopolymer providing plants with properties like rigidity, water-impermeability, and resistance against microbial attack (Kamm et al., 2008). Lignin structure can be envisaged based on three monomeric units: *p*-hydroxyphenyl, guaiacyl, and syringyl linked together through ether and C-C bonds, creating a cross-linked polymeric structure (Kamm et al., 2008; Li et al., 2015). A promising route towards renewable chemicals and fuels is lignin depolymerization. Nevertheless, the lignin complex structure hinders its application, encouraging the quest for innovative and more effective depolymerization strategies (Xu et al., 2014).

Lignin can be depolymerized by several processes, including acid/base-catalyzed depolymerization, pyrolysis, hydrotreatment, oxidation, reforming, and gasification (Erdocia et al., 2017; Li et al., 2015). Lignin oxidation can cause the cleavage of lignin aromatic rings and aryl ether bonds, which is an interesting way to obtain low-molecular-weight chemical compounds (Abdelaziz et al., 2018; Kang et al., 2013; Pandey and Kim, 2011). In this context, the most studied oxidants are molecular oxygen, nitrobenzene, metal oxides, and hydrogen peroxide (H_2O_2) (Li et al., 2015; Pandey and Kim, 2011). Among them, oxidation with H_2O_2 is a highly promising strategy, especially in the presence of catalysts, enabling mild reaction conditions and shorter reaction times (Cheng et al., 2017). Hydrogen peroxide is more reactive than oxygen, even at alkaline or acidic conditions, with the benefit of being considered an environmentally benign chemical (Ma et al., 2015; Pandey and Kim, 2011).

Currently, dicarboxylic acids (DCA) are produced from petrochemical routes or edible biomass fermentation and find uses in the pharmaceutical industry, polymer synthesis, as a food additive, or used as chemical precursors of other compounds (Höfer, 2015). In the current context of biomass valorization, C_4-DCA, which includes succinic, fumaric, maleic, and malic acids, were listed among the 12 building blocks to be produced via this synthetic route (Werpy and Petersen, 2004).

DCA are among the products obtained from lignin wet peroxide oxidation (CWPO) after cleavage of the aromatic ring. The product selectivity depends on the oxidizing agent, catalyst type, process conditions, and reactor type (Kang et al., 2013; Ma et al., 2015). In the context of DCA from lignin, several studies have been carried out using wet peroxide oxidation, with and without catalyst (Cronin et al., 2017; Hasegawa et al., 2011; Kang et al., 2019; Ma et al., 2015; Su et al., 2014; Yin et al., 2015; Zeng et al., 2015). However, many of the lignin oxidation processes, including the catalyzed ones, are not selective enough to favor the production of a specific DCA, generating a mixture of DCA, introducing the need for additional steps of separation and purification.

Titanium silicalite-1 (TS-1) catalyst, a synthetic zeolite with an MFI framework structure, currently used in the chemical industry, has shown good catalytic activity for oxidation reactions using H_2O_2 (Přech, 2018). The increased H_2O_2 reactivity is related to several TS-1 characteristics, including microporosity, hydrophobic nature, and the presence of titanium atoms, which reduces the electron density of the O-O bonds, making the oxidant more susceptible to nucleophilic attack (Clerici, 2015; Přech, 2018). TS-1 catalyst has already been tested in guaiacol peroxide oxidation under mild alkaline conditions, producing different DCA, mainly maleic, malic, and oxalic acids (Su et al., 2014). These results pointed out the interest to proceed with the testing of TS-1 with other lignin model compounds, namely with the ones with higher complexity.

Catalyst modification with transition metals (Fe, Mn, Co, Cu, Ni) is reported as a strategy to enhance the oxidation activity by increasing hydroxyl radical's formation (Schutyser et al., 2018; Védrine, 2017). Comparatively, with precious metals (Pd, Au), transition metals have lower prices, provide easy reaction conditions, and promising results for lignin depolymerization (Zeng et al., 2015). Transition metals can be used as homogeneous and heterogeneous catalysts, constituting an exciting strategy to modify the TS-1 catalyst.

The objective of the present work was to study the oxidation of vanillic acid (VA) to produce C_4-DCA, using H_2O_2 as the oxidizing agent in the presence of a TS-1 catalyst. Comparatively, with other lignin model compounds found in previous oxidation studies with TS-1, VA shares a similar aromatic structure to guaiacyl, the most common structural unit in softwood lignins, representing the behavior of the aromatic ring-opening reactions toward the production of C_4-DCA. VA can also be found as a product of lignin oxidation with O_2, which is a necessary process to achieve aromatic compounds (Rodrigues et al., 2018). In a second phase of the work, the TS-1 catalyst was modified with transition metals (Fe, Co, Cu) and tested in the oxidation reaction. The effect of pH and reaction time on maleic, fumaric, tartaric, succinic, and malic acids production yield was studied. Moreover, the occurrence of degradation products was checked. Finally, a comparison between three model compounds (vanillic acid, syringic acid, and p-hydroxybenzoic acid) was studied to analyze the best substrate for C_4-DCA production.

3.2 Materials and methods

3.2.1 Materials

Vanillic acid (97%), DL-malic acid (≥99.0%), fumaric acid (≥99.0%), maleic acid (>99%), *p*-hydroxybenzoic acid (>99%), syringic acid (>95%), succinic acid (≥99.0%), L-(+)-tartaric acid (≥99.5%), malonic acid (>99%), oxalic acid dihydrate (≥99.0%), lactic acid solution (85%, p.a.), $FeCl_3 \cdot 6H_2O$ (97%) and $Co(NO_3)_2 \cdot 6H_2O$ (99%) were purchased from Sigma-Aldrich Co. LLC. Other reagents were purchased from different suppliers: formic acid (Chem-labs, >99%), acetonitrile (VWR, HPLC grade), sulfuric acid (Chem-labs, 95-97%), sodium hydroxide (Merck, p.a.), hydrogen peroxide solution (Fluka, >30% p.a.), $Cu(NO_3)_2 \cdot 3H_2O$ (Merck, p.a.). Catalyst TS-1 was bought to ACS Materials, LLC. All reactants were used as received without further purification.

3.2.2 Oxidation Procedure

VA was oxidized using closed steel reactors (20 mL) comprising an inner PTFE vial, where 5.00 mL of a 10.0 g/L vanillic acid solution, 0.500 mL of a 30 wt% H_2O_2 solution, and 5.0 mg of TS-1 catalyst were placed (10 wt%, VA-basis). The added oxidant amount was estimated based on oxygen stoichiometric demand for complete VA oxidation to CO_2 and H_2O. After adding all reactants and catalyst, pH was adjusted to the desired value using NaOH 2.0 mol/L or H_2SO_4 2.0 mol/L for the acid and alkaline medium, respectively. The reactors were then closed and heated to 145±1 ºC, using a heating plate equipped with a thermocouple, and the mixture was kept under stirring (600 rpm) for the required reaction time. After the desired reaction time, the reactors were quenched in an ice water bath, and samples were recovered for analysis. The effect of pH (4.0-12.0) and reaction time (0-6 h) on selected DCA was studied. Moreover, the formation of DCA degradation products was checked. Experiments were done in triplicate, except when indicated. The 20 mL reactor was used as a first step to study the process. By using this low-volume system, it was possible to control the reaction conditions, especially temperature, accurately. A 145 ºC temperature was chosen after validating the dependence of temperature on C_4-DCA yield and VA conversion.

The conducted experiments covered a pH range where several lignins are soluble in an aqueous solution, avoiding mass transfer problems. Moreover, the catalyst does not act in the lignin structure but in the H_2O_2 O-O bond, to form hydroxyl radicals. These radicals are soluble in an aqueous solution and are responsible for the ring-opening reaction.

3.2.3 Quantification of VA, C_4-DCA

Quantification of VA, DCAs (maleic, fumaric, tartaric, succinic, and malic acids), and degradation products (malonic, oxalic, formic, acetic, and lactic acids) was done by high-performance liquid chromatography (HPLC). The apparatus was a Shimadzu UFLC equipped with a Diode Array Detector (210, 260 nm) and a Phenomenex® Rezex™ ROA H^+ column (300x7.8 mm) conditioned at 50 ºC. The solvent programming (flowrate of 0.5 mL/min) was as follows: 0.0-10.0 min H_2SO_4 4 mmol/L; 20.0-42.5 min: 15% acetonitrile in H_2SO_4 4 mmol/L; 47.5-100.0 min: H_2SO_4 4 mmol/L. For injection (injection volume 20 μL), samples from the oxidation reaction were acidified with H_2SO_4 2 mol/L to pH~2, diluted as needed, and filtered through a 0.22 μm pore-size filter. The target DCA, degradation products, and VA were quantified using calibration curves prepared from available commercial standards, which can be found in Appendix A, Table A.1.

Gel permeation chromatography (GPC) analysis was used to evaluate molecular weight changes due to the used oxidation procedures with the modified catalysts. Calibration was done using polystyrene (PS) standards. More details about the applied method can be found elsewhere (Costa et al., 2018), and the HPLC equipment corresponds to the one mentioned above. The calibration curve can be found in Appendix A, Table A.1.

3.2.4 Carboxylic acids yield and VA conversion

The information obtained in HPLC quantification was used to determine the individual carboxylic acid (CA_i) yields (Equation 3.1) and VA conversion (Equation 3.2). Total C_4-DCA yield was obtained as the sum of the individual C_4-DCA yields (succinic, fumaric, maleic, malic, and tartaric).

$$VA\ conversion\ (mol\%) = \frac{[VA]_O - [VA]_f}{[VA]_O} x100 \qquad \text{Equation 3.1}$$

where $[VA]_0$ is the initial VA concentration, and $[VA]_f$ is the VA final concentration.

$$CA_i\ Yield\ (mol\%) = \frac{[CA_i]_f}{[VA]_O} x100 \qquad \text{Equation 3.2}$$

Where $[CA_i]_f$ is the molar concentration of the individual C_4-DCA (CA_i=maleic, fumaric, tartaric, succinic, or malic acid) or degradation product (CA_i = malonic, oxalic, formic, or lactic acids).

VA conversion and DCA yield were expressed as average±standard deviation.

3.2.5 Catalyst Modification Procedure

According to the methodology described elsewhere, catalyst modification with transition metals (Fe, Cu, and Co) was done using a modified wet impregnation method (Prasetyoko et al., 2010). Briefly, the TS-1 catalyst was placed in a solution containing a sufficient amount of the cation salt ($FeCl_3 \cdot 6H_2O$, $Cu(NO_3)_2 \cdot 3H_2O$, $Co(NO_3)_2 \cdot 6H_2O$), to yield materials with a loading of 2 wt% of the corresponding oxide (Fe_2O_3, CuO, and CoO, respectively). The suspension was heated at 80 ºC for 3 h under stirring, followed by water evaporation overnight at 100 ºC. After that, the obtained product was calcined at 550 ºC for 3 h to obtain the modified catalyst.

3.2.6 Catalyst Characterisation

Modified catalysts were analyzed by Scanning Electron Microscopy (SEM), Energy-dispersive X-ray Spectroscopy (EDS), and Electron Backscattered Diffraction analysis (XRD) after being produced and applied in the oxidation process. The catalysts used in the oxidation process were washed with hot water and dried at 80 ºC overnight before characterization.

SEM and EDS were performed using a High Resolution (Schottky) Environmental Scanning Microscope with X-Ray Microanalysis and Electron Backscattered Diffraction analysis (Quanta 400 FEG ESEM / EDAX Genesis X4M). EDS was done at high vacuum, 15 keV, 10 mm working distance, and a 50 Lsec collection time. For that, samples were coated with Au/Pd by sputtering using the SPI Module Sputter Coater equipment (15 mA, 80 s).

XRD was done in a diffractometer PANalytical EMPYREAN, using CuKα1,2 (1.5406 Å) radiation. Diffraction patterns were collected over a range of $4^{\circ}<2\Theta<70^{\circ}$, using 0.5º diverging and antidiverging slits, 0.04 rad Soller slits (receiving and scattering), step size of 0.0167º, and a 30 min total time. The X-ray tube worked at 45 kV and 40 mA. Crystallinity percentages were calculated based on peak intensity at $2\Theta=23.04^{\circ}$. TS-1 non-modified catalyst was given a 100% crystallinity.

In addition to morphological characterizations, atomic absorption (AA) was used to check the leaching of the transition metals from the modified catalysts. For that, the samples were centrifuged and digested using 10% of concentrated HNO_3. The analysis was done using a GBC 932plus equipment, following the Flame Methods Manual for Atomic Absorption by GBC Scientific Equipment PTY Ltd.

3.3 Results and discussion

3.3.1 Oxidation with TS-1 Catalyst

3.3.1.1 Effect of Temperature and pH Conditions

Concerning pH conditions, the studied range was 4.0-12.0 at 145 ºC, during 2 hours, following preliminary results pointed out the higher DCA yield at this temperature. The production yield of C_4-DCA (maleic, fumaric, tartaric, succinic, and malic acids) and the VA conversion are registered in Figure 3.1. The highest reactivity was achieved for basic pHs, with complete VA conversion over pH 10.5. At an acidic medium, a complete VA conversion was not reached for the tested time. When pH increased, the more robust oxidation level leads to the rupture of the aromatic ring and its conversion to hydroxylated DCAs, like malic and tartaric acids. In pH 4.0, no hydroxylated acids were obtained, and VA conversion was lower than the alkaline pH oxidation.

No catalyst was recovered after the reaction at a pH of 12, indicating that very high pHs are not recommended to be used with TS-1 catalysts.

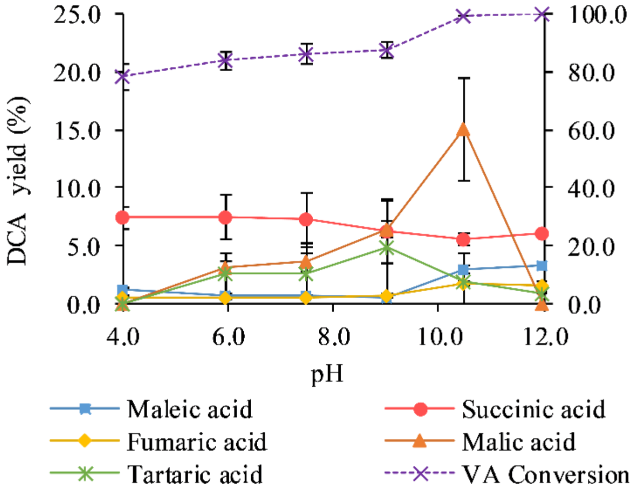

Figure 3.1 - Effect of pH in C_4 dicarboxylic acids (DCA) yield and vanillic acid (VA) conversion, with TS-1 (145 °C, 2.0 h)

Considering temperature, VA conversion increased with temperature increase; behavior validated using a temperature range of 80-145 °C (Figure 3.2). Moreover, catalyzed and non-catalyzed reactions were compared at pH conditions of 10.5 and 4.0, confirming that TS-1 catalyst improved conversion, especially under alkaline conditions at lower temperatures. VA conversion for the non-catalyzed reaction rise with temperature increase, starting from 32% at 80 °C to full conversion at 145 °C. The catalyzed reaction gives rise to higher conversion at lower temperatures (80 °C and 100 °C). At higher temperatures (120 °C and 145 °C), there is no difference between catalyzed and non-catalyzed reactions for alkaline pH, while for acidic pH, the non-catalyzed reaction led to better VA conversion. Also, for the non-catalyzed reactions, a final solution with intense dark color, together with the presence of sediments resulting from the condensation of different compounds, was observed. This observation indicates that VA was oxidized to quinones, molecules with high color intensity, corresponding to the first stage described in Figure 3.3. These oxidized structures reacted with each other to produce condensation products instead of promoting ring-opening reactions to form

DCAs. As seen in Figure 3.2b, in all cases, C_4-DCA production was higher for the catalyzed reaction than for the non-catalyzed one.

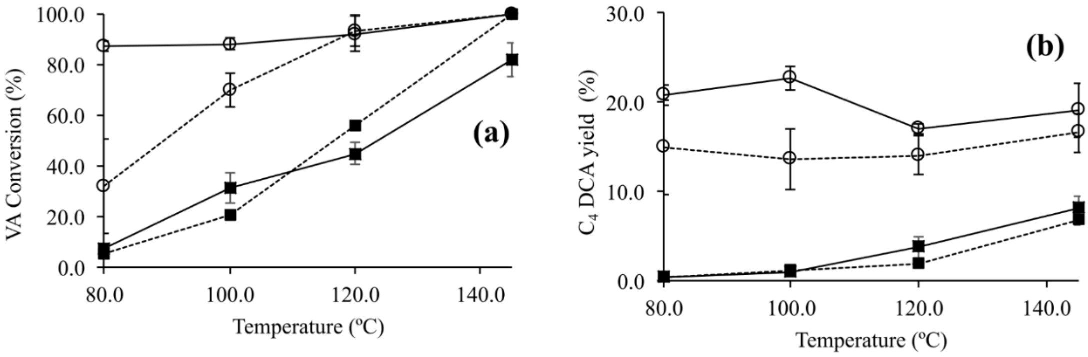

Figure 3.2 **-** (a) Vanillic acid (VA) and (b) C_4-DCA conversion at pH 10.5 (o) and pH 4.0 (■), for catalyzed (—) and non-catalyzed (**---**) oxidations (3.0 h, by duplicate)

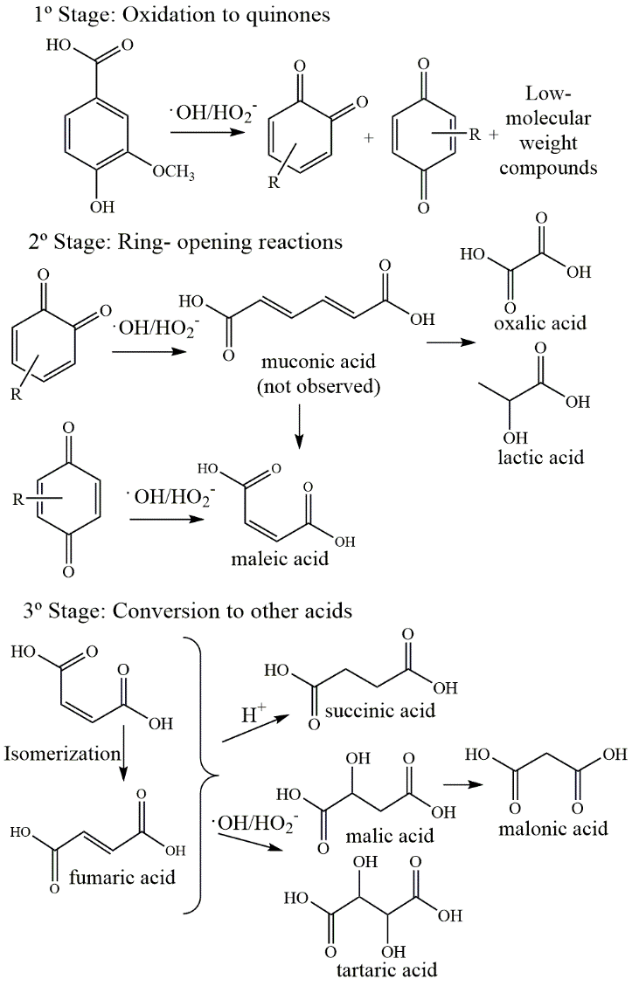

Figure 3.3 - Steps for vanillic acid oxidation.

(Modified with permission from Cronin et al. *(*2017) Copyright 2017. American Chemical Society)

The higher reactivity of the catalyzed reaction was due to the improvement in the H_2O_2 nucleophilic attack capability. This effect is achieved when H_2O_2 is adsorbed on the catalyst's tetrahedral Ti active sites, forming Ti-OOH species and increasing the partial negative charges of the oxygen atoms (Xia et al., 2017). The microporosity and the hydrophobic nature of the pores are also important factors, enhancing Ti-OOH formation, avoiding solvation of Ti atoms and active species (Clerici, 2015).

Hydrogen peroxide reactivity depends on pH since it can act as a nucleophile or electrophile species (Xiang and Lee, 2000). In wet peroxide oxidation, the active species for the compound's oxidation are hydroxyl radicals (HO•) and hydroperoxyl anions (HOO^-). These compounds can later degrade to molecular oxygen, decreasing their reactivity (Yin et al., 2015). Hydrogen peroxide can decompose during oxidation reactions; it is stable in acidic conditions but quickly decomposes to H_2O, O_2, and OH^- above pH= 6.0 (maximum decomposition occurs at its pK_a). Moreover, it is sensitive to temperature and the presence of transition metal ions (Xiang and Lee, 2000). Phenolic units are stable to alkaline peroxide but become reactive against hydroxyl radicals derived from H_2O_2 decomposition (Sun et al., 1999). Molecular O_2 was not studied in this work as an oxidant agent due to its low reactivity compared to H_2O_2, avoiding the ring-opening reactions to obtain DCA.

3.3.1.2 Effect of Reaction Time in C_4-DCA Production under Alkaline and Acidic Conditions

Given the results of the previous section, pH 4.0 and pH 10.5 were chosen for acidic and alkaline conditions, respectively, together with the temperature of 145 ºC, to study the production of C_4-DCA from VA. For alkaline conditions, complete VA conversion was achieved in less than 30 min, and C_4-DCA production reached the highest yield at 2 hours, being malic acid the one presented at a higher amount (Figure 3.4a). However, after 3 hours, the yield of malic, fumaric, maleic, and succinic acids decreased, which suggested that these DCA were degraded to low-molecular-weight compounds. Tartaric acid concentration remained almost constant after a time frame of 2.5 h. Malonic acid, an intermediate product in the C_4-DCA degradation process, decreased through time, while lactic, acetic, and formic acids, also degradation products according to Figure 3.3, increased their concentration until 3 hours, but then decreased, confirming the degradation of the C_4-DCA (Figure 3.4b). This observation indicates that H_2O_2 is highly reactive at alkaline pH and high temperatures. After prolonged reaction times, an over-oxidation of the already produced C_4-DCA occurs, originating low-molecular-weight degradation products, like malonic, oxalic, lactic, acetic, and formic acids. Therefore, the oxidation reaction should be performed at short times to avoid the loss of C_4-DCA products. Also, the high nucleophilic capacity of H_2O_2 at alkaline pH causes the hydroxylation of double bonds in both maleic and fumaric acids, leading to malic and tartaric acids' formation, avoiding the production of succinic acid at higher yields. In this work, succinic acid was identified (up to 5,6 mol%), while Su et al. (2014) reported guaiacol alkaline peroxide oxidation with TS-1 at 80ºC shown no production of succinic acid, but higher maleic acid yield (up to 27.7 mol%). Looking to achieve high yields for succinic acid, as according to step c) in Figure 3.3, a source of H^+ should be included, which is not the case of alkaline oxidation.

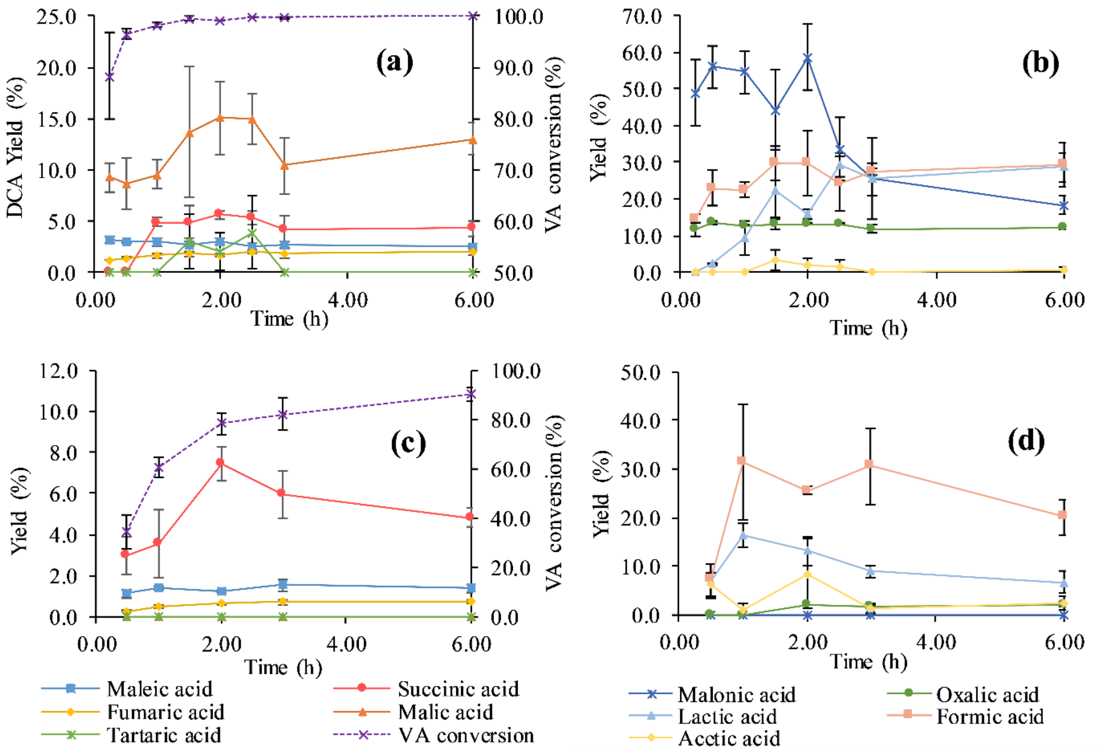

Figure 3.4 - Effect of time in vanillic acid (VA) oxidation. **(a)** C_4 dicarboxylic acid (C_4-DCA) yield, VA conversion, and **(b)** degradation products yield at pH 10.5; **(c)** C_4-DCA yield, VA conversion, and **(d)** degradation products yield at pH 4.0. (All reactions at 145 ºC).

According to Figure 3.3, vanillic acid is firstly oxidized to *o*- and *p*-quinones, which react with free radicals to produce ring-opening reactions, obtaining maleic acid. Maleic acid is isomerized to fumaric acid if heated at 120 ºC in an aqueous solution (Whelan, 1994), producing malic acid at higher temperatures (Gao et al., 2018). This observation indicates that during the transition of maleic to fumaric acid, the double bond is more labile to be hydroxylated, explaining why malic and tartaric acids were present at higher amounts at higher temperatures, especially after several minutes of reaction. The hydroxylated acids were at lower amounts (max. 2.9 mol%) in Su et al. (2014) work, which used lower temperatures.

The abundance of C_4-DCA production under acid conditions was different from alkaline pH, as shown in Figure 3.4c; the more abundant acid was succinic (7.4 mol%), accompanied by small quantities of maleic and fumaric acids. Malic and tartaric acids were not detected after 6 hours of reaction. As seen in Figure 3.3, when acidic pH is selected, the already produced maleic/fumaric acids avoid the hydroxylation reaction towards malic/tartaric acids. Still, the H^+ source promotes saturation of the double bonds to produce succinic acid at higher selectivity. Previous publications (Bi et al., 2018; Cronin et al., 2017; Ma et al., 2014) show that succinic acid can be obtained from lignin and lignin model compounds (guaiacol, catechol, vanillin) using peroxide oxidation under acidic pH in the presence of different catalysts. Nevertheless, none of the cited works used TS-1 catalyst in an acidic medium to obtain succinic acid. In this work, the highest succinic acid yield was achieved after 2.0 h reaction at 145 ºC (7.4 mol%; 5.2 wt%), similarly to the ones reported by Ma et al. (Ma et al., 2014), using $FeCuS_2$ catalyst to oxidize guaiacol (5.4 wt%) and catechol (4.5 wt%).

Under acidic conditions, lower degradation products were obtained, comparatively with alkaline conditions (Figure 3.4d). Lactic and formic acids concentration did not increase through reaction time, as it happened in alkaline oxidation. These facts show that the oxidation level was weaker in this case, being the produced C_4-DCA better preserved, avoiding the extensive degradation observed in the alkaline oxidation. Therefore, according to the desired C_4-DCA, different pH conditions should be selected. If succinic acid is the target, VA oxidation should be performed at an acidic medium to avoid maleic/fumaric acids oxidation to their hydroxylated derivatives.

3.3.2 Oxidation with Modified TS-1 Catalyst

3.3.2.1 Catalyst Modification with Transition Metal Oxides

Transition metals, like Co, Fe, Cu, Mn, and Ni, have been widely studied because of their capability to activate the peroxide oxidation; as homogeneous (soluble salts) or heterogeneous (metal oxides, supported metal oxides, or as part of compounds, such as $CuFeS_2$) catalysts (Leary and Schmidt, 2010; Ma et al., 2014; Sun et al., 1999; Vangeel et al., 2018; Védrine, 2017; Zeng et al., 2015). These metals can enhance the production of free reactive radicals, converting VA to quinones and causing ring-opening reactions, producing DCA (Bi et al., 2018). They can increase H_2O_2 reactivity, which is important at acidic pHs, like in Fenton's reaction, which uses Fe^{2+}/Fe^{3+} ion pair as a catalyst with a reactivity peak at pH=2.8-3.0 (Wang et al., 2012).

A 2 wt% metallic oxide loading was selected based on the work of Widiarti et al. (2012), which reported that higher loads would cover the TS-1 surface, blocking access to the pores. If this blockage occurs, the H_2O_2 will not access Ti^{4+} sites to release the HO• and HO_2^- radicals, decreasing the activity of the modified catalyst and enhancing H_2O_2 dismutation to H_2O and O_2. This behavior was previously observed with Cu/TS-1 (Widiarti et al., 2012) and Fe/TS-1 (Prasetyoko et al., 2010) catalysts. In this work, modifications with Cu, Co, and Fe have been chosen.

As seen in the SEM images (Figure 3.5, Pre-oxidation), all modified catalysts presented no metal oxide crystals visible on the particle's surface. XRD results (Figure 3.6) showed that the MFI structure was not affected after impregnation with the metal, namely the characteristic diffraction lines of TS-1 (2Θ=23.04, 23.23, 23.65, 23.88, 24.36) were present, at the same peak height, in all modified catalysts. Crystallinity percentage, after modification with the selected metals, did not change (Table 3.1). No diffraction lines were assigned to the modified catalysts' metal oxides due to their low percentage in the matrix. The Ti/Si ratio of the original catalyst (Ti/Si ratio=0.023) was kept after the metal impregnation, as reported in Table 3.1.

Table 3.1 - Transition metal-modified TS-1 catalyst's physical properties.

Reaction condition	Ti/Si ratio*			Crystallinity (%)**		
	Cu/TS-1	Co/TS-1	Fe/TS-1	Cu/TS-1	Co/TS-1	Fe/TS-1
After modification	0.024	0.019	0.026	100	91	100
pH 10.5	0.032	0.034	0.026	60	27	46
pH 4.0	0.023	0.019	0.024	100	97	91

* Non-modified TS-1 Ti/Si ratio: 0.023; ** Based on peak intensity at 2Θ=23.04º. TS-1 non-modified catalyst=100 % crystallinity.

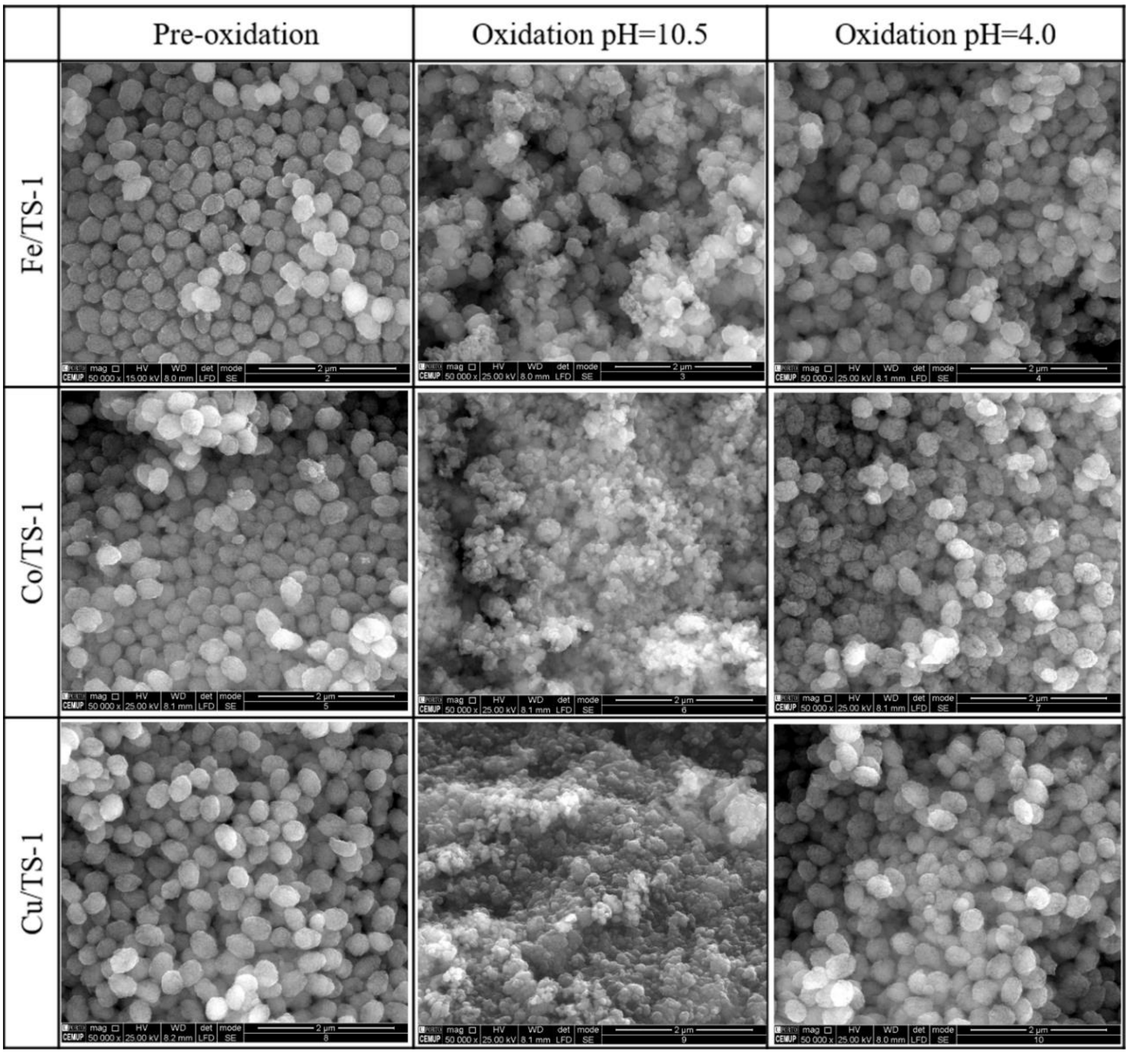

Figure 3.5 - SEM images from modified TS-1 catalysts (50000X).

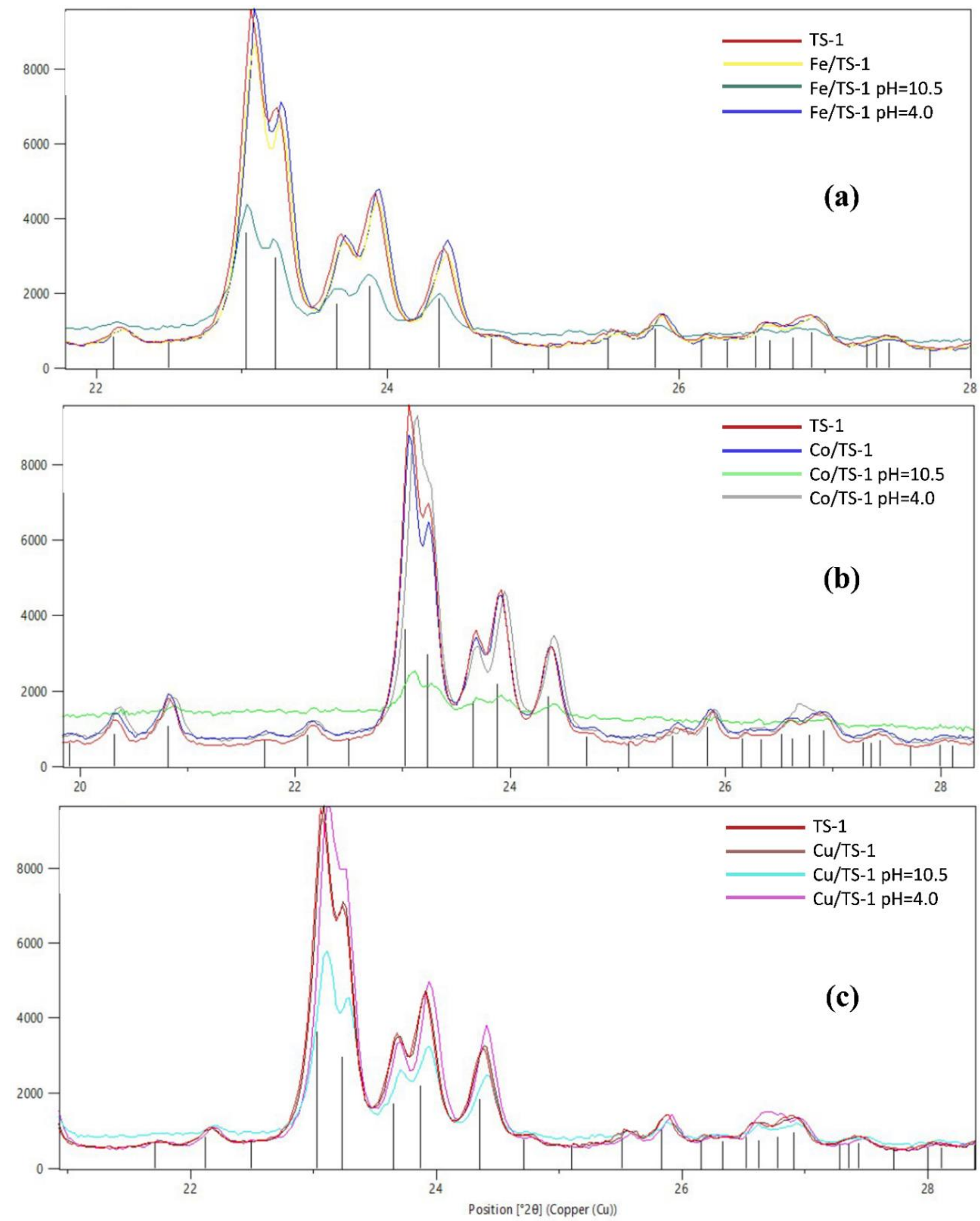

Figure 3.6 - XRD Diffractograms for modified TS-1 catalysts: **(a)** Fe/TS-1; **(b)** Co/TS-1; **(c)** Cu/TS-1.

(Each figure includes the modified non-used catalyst, the catalyst used under acidic and alkaline conditions, and the original TS-1 diffractogram as a comparison)

3.3.2.2 C_4-DCA Production under Alkaline and Acidic Conditions

To compare the effect of the catalyst modification with metallic ions, reactions were done at 145 ºC for 2 h, which was the time and temperature where the highest yield for succinic acid was obtained. All the modified catalysts give rise to complete VA conversion at alkaline conditions, but the production yield of the targeted C_4-DCA was not improved (Figure 3.**7**a). Only maleic and fumaric acids were produced at similar yields, comparatively with the non-modified TS-1 catalyst, and tartaric acid was not detected. A prominent bubbling was observed when the Co/TS-1 and Cu/TS-1 catalyst were added to the reaction medium, indicating that H_2O_2 is quickly degraded to O_2, skipping the release of the active radicals needed for the ring-opening reactions. Since TS-1 can only activate H_2O_2 and not O_2 (Přech, 2018), lower productivity is expected when H_2O_2 is degraded to O_2. All these oxidations produced dark-colored solutions, and organic sediments in the Co/TS-1 reaction may be derived from VA oxidized derivatives condensation reactions. The condensation reactions gave rise to higher molecular-weight compounds, confirmed by GPC analyses (Figure 3.8). Lower over-oxidation occurred because lower degradation products yields were obtained (Figure 3.7c,e), confirming that modified catalysts enhanced oxidant degradation instead of promoting the oxidation of VA into C_4-DCA.

Under acidic conditions, VA conversion was improved when using Cu/TS-1 and Fe/TS-1, achieving complete conversion after 2 hours at 145 ºC. With Co/TS-1 catalyst, only 57% conversion was achieved, while for TS-1 non-modified catalyst, 78% conversion was reached. The higher activity for Cu/TS-1 catalyst was expected due to the intermediate reduction potential of Cu^{2+} (Schutyser et al., 2018), which is confirmed by the higher formic acid production, a degradation product of VA oxidation (Figure 3.7f). A higher amount of malic acid was also observed, suggesting the conversion of the original maleic/fumaric acids into this compound, avoiding the conversion to succinic acid, even at acidic pH. Fe/TS-1 improved VA oxidation due to iron capacity to act as a Fenton's catalyst, enhancing HO• and HO_2• radicals formation through the mixture of Fe^{2+}/Fe^{3+} ions (Wang et al., 2012). Malic acid was also produced with Fe/TS-1 and Cu/TS-1 catalysts (Figure 3.7b), suggesting that this oxidation was more potent than the one with non-modified TS-1.

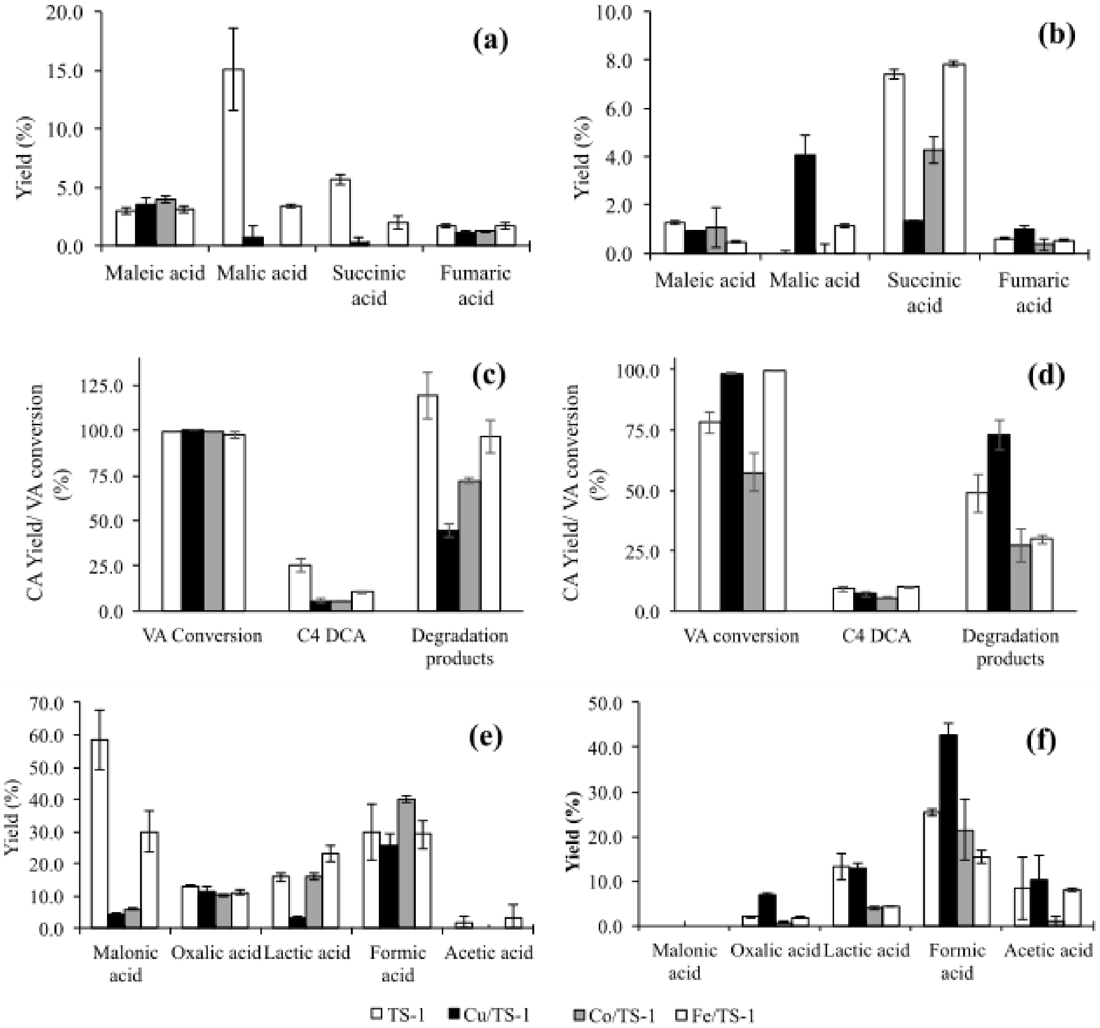

Figure 3.7 - Yields achieved with modified catalysts, and comparison with non-modified catalyst, under different pHs. C_4-DCA yields at **(a)** pH=10.5 and **(b)** pH=4.0; VA conversion and acid yields at **(c)** pH=10.5 and **(d)** pH=4.0; Degradation products at **(e)** pH=10.5 and **(f)** pH=4.0 (145 °C, 2.0 h).

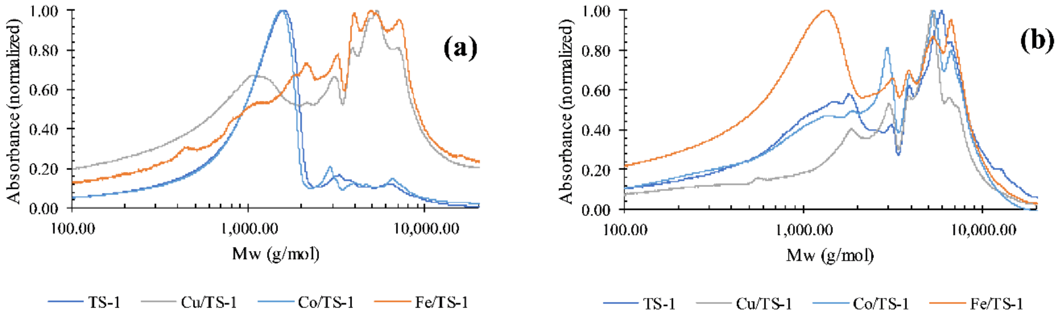

Figure 3.8 - GPC analysis for vanillic acid oxidation using modified TS-1 catalysts, under different pH. Vanillic acid oxidation with non-modified TS-1 GPC curve is shown as a comparison for each curve. **(a)** pH 4.0, **(b)** pH 10.5. (Reaction conditions 145ºC, 2.0 h)

The Fe/TS-1 catalyst was the only modified catalyst form providing a high yield of succinic acid (7.9 mol%), slightly higher than with the non-modified TS-1. Moreover, lower amounts of degradation products were detected, showing that oxidation was more selective than the other modified catalysts. Iron has been reported as the less reactive of the three tested metals (Schutyser et al., 2018). This lower reactivity lowers H_2O_2 degradation but generating the needed radicals to open the aromatic ring. However, the appearance of malic acid, which was not present in the non-modified TS-1 experiment, shows that even with lower reactivity, the Fe catalyst produces more free radicals than the non-modified TS-1 catalyst. Under acidic oxidation, higher molecular weight compounds were produced mainly when Fe and Cu catalysts were used but at lower amounts compared to alkaline oxidation (Figure 3.8b). Moreover, no organic sediments nor colored solutions were observed under this pH condition.

3.3.2.3 Effect of Reaction Conditions in the Modified Catalysts

The modified catalysts suffered degradation after alkaline oxidation (Figure 3.5), resulting in particles with smaller diameters and loss of organization. EDS analysis showed that the Ti/Si ratio was higher after alkaline oxidation (Table 3.1), suggesting that the internal zeolite structure was affected, and Si atoms were leached out from the catalyst structure. XRD results showed that alkaline oxidation leads to significant MFI crystallinity losses. This effect can be observed as a decrease in the intensity of the TS-1 characteristic peaks (Figure 3.6), thus reducing the crystallinity percentage (Table 3.1). A higher crystallinity loss was observed for the Co/TS-1 catalyst. Titanosilicates zeolites, including TS-1, are reported as resistant to concentrated mineral acids but not to alkaline pHs due to desilication development (Přech, 2018). To avoid catalyst degradation, the recommended NaOH concentration should be lower than 0.2 mol/L since higher levels can cause total disruption of the framework (Přech, 2018).

After acidic oxidation, the catalyst particles did not show any structural changes (Figure 3.5), and XRD results confirmed that crystallinity was maintained (Table 3.1), pointing out that an acidic environment is safer for TS-1 catalyst structure.

In an acidic or alkaline environment, soluble ions were quantified by atomic absorption analysis to check the leaching of metallic ions. Fe/TS-1 catalyst showed no leaching, while Co/TS-1 and Cu/TS-1 showed leaching in acidic pH (5 mg/L and 13 mg/L, respectively), and Cu/TS-1 leaching at alkaline pH (5 mg/L). CuO has the lowest solubility in alkaline medium (pH around 8-9) at 145 ºC and high solubility in acidic and alkaline pH, explaining the observed leaching (Palmer, 2005). Therefore, Co/TS-1 and Cu/TS-1 catalysts did not enhance DCA yield and showed low chemical stability due to leachate of metals, disabling their possible use until no procedure to avoid leaching could be carried out. Only Fe/TS-1 showed to be a stable catalyst in both media. Stability increase could be achieved if different metal salts, selected among the ones that have been proven to be insoluble in alkaline or acidic pH, are chosen, which should be done individually according to each metallic ion. It is not recommended to increase calcination temperature due to possible sintering of the TS-1 catalyst.

3.3.3 Oxidation with other lignin model compounds

Based on previous results, the recommended conditions for oxidation using TS-1 were 145ºC, a neutral pH, and a 2-hours reaction time. Three model compounds (vanillic acid, p-hydroxybenzoic acid and syringic acid) were evaluated using these parameters.

As seen in Figure 3.9, there was an important difference between the conversion and the production of C_4-DCA when modifying the substrate. In VA oxidation at pH=7, the primary acid is still succinic acid (8.5 mol%), but other acids appeared, mainly malic (5.0 mol%) and tartaric acids (6.1 mol%), which are produced due to the hydroxylation of the double bond present in maleic and fumaric acids. These two last acids were quantified in minimal percentages. This behavior was expected from the results in Figure 3.1.

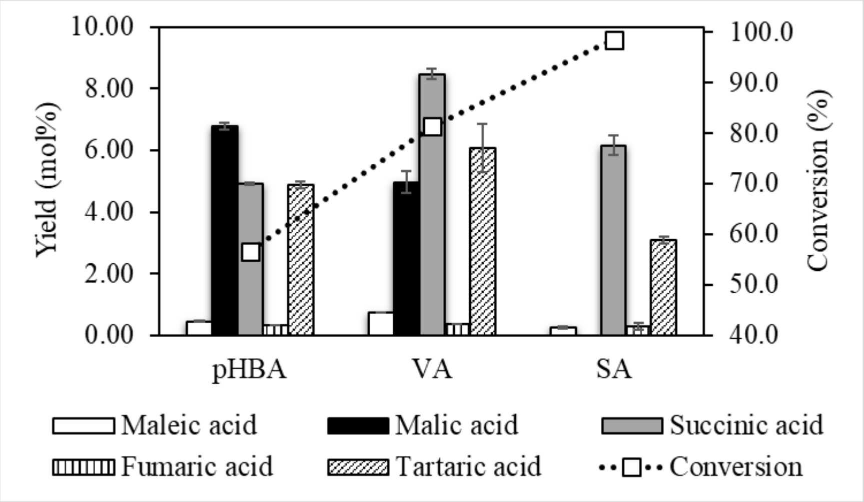

Figure 3.9 – Oxidation of three model compounds: p-hydroxybenzoic acid (pHBA), vanillic acid (VA), and syringic acid (SA) using TS-1 at 145ºC and neutral pH

Compared to VA, pHBA showed a much lower conversion since it has no methoxy substituents in its structure and has been reported to have a lower reactivity towards oxidation (Casimiro et al., 2019). pHBA showed less succinic acid (4.9 mol%) than VA, and higher yields of malic (6.8 mol%) and tartaric acids (4.9 mol%), and small percentages of maleic and fumaric acids.

On the other hand, SA showed an almost complete conversion since this acid has a strong reactivity against oxidation (Casimiro et al., 2019). However, when evaluating the main C_4-DCA produced, there is an interesting difference in the type and yields of the products. Succinic acid is still the primary acid, but it has a lower yield (6.2 mol%) than VA. Moreover, only tartaric acid was observed in high quantities (3.1 mol%) but in lower yields than VA and pHBA oxidation. It was also noted that SA oxidation produced a clear colorless solution instead of the VA and pHBA solutions. Even though SA is very reactive and is degraded faster, the degradation will be targeted into low-molecular-weight compounds and even CO_2 and H_2O, and it will not produce much of C_4-DCA. However, this fact must be confirmed in a kinetic study, evaluating products through time.

The fact that methoxy substituents are located in the aromatic ring could probably prevent hydroxylation of the produced double-bonded C_4-DCA, avoiding malic and tartaric acids and helping to increase the presence of succinic acid as the main product. In addition, increasing methoxy substituents in the aromatic ring enhance oxidation reactivity, achieving higher conversion. However, to ensure this fact, a more detailed study should be performed evaluating model compounds' oxidation through time because it could provide a path to select the best lignin type to obtain C_4-DCA.

3.4 Conclusions

The use of TS-1 catalyst in the catalytic wet peroxide oxidation of VA enhanced the production of C_4-DCA compared with the non-catalyzed reaction. The type of produced acids depends mainly on the used temperature, pH, and reaction time. An alkaline medium caused an over-oxidation of VA, giving rise to hydroxylated acids, like malic and tartaric, together with high degradation levels. The primary produced acid was succinic in acidic pH, and a lower amount of degradation products was observed. Therefore, VA oxidation acted similarly to other lignin model compounds, where the oxidation of the aromatic ring is the first step, getting open to produce C_4-DCA. However, these C_4-DCA can quickly degrade to low-molecular-weight compounds, especially under alkaline conditions and long reaction times. If succinic acid is the target compound, acidic oxidation should be selected.

When TS-1 catalyst is modified with Fe, Co, and Cu oxides, the productivity of C_4-DCA was not improved under alkaline pH due to the high degradation of H_2O_2 to O_2, associated mainly with Co and Cu oxides. Fe/TS-1 and Co/TS-1 catalysts increased VA conversion and oxidative reaction in acidic pH, but only Fe/TS-1 showed a slight improvement in succinic acid production and stability against leaching. Leaching in Cu and Co catalysts was observed, and their use is not recommended. Under alkaline oxidation, modified TS-1 catalysts suffered desilication and loss of external structure, but not in acid conditions. Thus, it is recommended to carry out oxidations with TS-1 catalyst at acidic or neutral pH.

Finally, different model compounds produced C_4-DCA in varied yields when using the best oxidation conditions (pH=7, 145ºC, 2h). pHBA was proved to be the least reactive compound, while SA was fully converted. However, a higher succinic acid yield was obtained with VA oxidation. The amount of the methoxy substituents affect the reactivity of the compounds, and therefore the selection of the best lignin to achieve C_4-DCA could be affected by this fact. A more detailed analysis should be performed, evaluating compounds through time.

3.5 References

Abdelaziz, O.Y., Li, K., Tunå, P., Hulteberg, C.P., 2018. Continuous catalytic depolymerisation and conversion of industrial kraft lignin into low-molecular-weight aromatics. Biomass Convers. Biorefinery 8, 455–470. https://doi.org/10.1007/s13399-017-0294-2

Bi, Z., Li, Z., Yan, L., 2018. Catalytic oxidation of lignin to dicarboxylic acid over the $CuFeS_2$ nanoparticle catalyst. Green Process. Synth. 7, 306–315. https://doi.org/10.1515/gps-2017-0056

Casimiro, F.M., Costa, C.A.E.E., Botelho, C.M., Barreiro, M.F., Rodrigues, A.E., 2019. Kinetics of oxidative degradation of lignin-based phenolic compounds in batch reactor. Ind. Eng. Chem. Res. 58, 16442–16449. https://doi.org/10.1021/acs.iecr.9b02818

Cheng, C., Wang, J., Shen, D., Xue, J., Guan, S., Gu, S., Luo, K.H., 2017. Catalytic oxidation of lignin in solvent systems for production of renewable chemicals: A review. Polymers (Basel). 9, 38–50. https://doi.org/10.3390/polym9060240

Clerici, M.G., 2015. The Activity of Titanium Silicalite-1 (TS-1): Some Considerations on Its Origin. Kinet. Catal. 56, 453–458. https://doi.org/10.7868/s045388111504005x

Costa, C.A.E.E., Pinto, P.C.R.R., Rodrigues, A.E., 2018. Lignin fractionation from E. Globulus kraft liquor by ultrafiltration in a three stage membrane sequence. Sep. Purif. Technol. 192, 140–151. https://doi.org/10.1016/j.seppur.2017.09.066

Cronin, D.J., Zhang, X., Bartley, J., Doherty, W.O.S.S., 2017. Lignin Depolymerization to Dicarboxylic Acids with Sodium Percarbonate. ACS Sustain. Chem. Eng. 5, 6253–6260. https://doi.org/10.1021/acssuschemeng.7b01208

Erdocia, X., Ruiz, E., Romero, I., Diaz, M.J., Castro, E., Labidi, J., 2017. Lignin characterization from two different pretreatments in bioethanol production processes from olive tree pruning. Chem. Eng. Trans. 61, 421–426. https://doi.org/10.3303/CET1761068

Gao, Z., Chen, W., Chen, X., Wang, D., Yi, S., 2018. Study on the Isomerization of Maleic Acid to Fumaric Acid without Catalyst. Bull. Korean Chem. Soc. 39, 920–924. https://doi.org/10.1002/bkcs.11499

Hasegawa, I., Inoue, Y., Muranaka, Y., Yasukawa, T., Mae, K., 2011. Selective Production of Organic Acids and Depolymerization of Lignin by Hydrothermal Oxidation with Diluted Hydrogen Peroxide. Energy & Fuels 25, 791–796. https://doi.org/10.1021/ef101477d

Höfer, R., 2015. Sugar- and Starch-Based Biorefineries, in: Industrial Biorefineries & White Biotechnology. Elsevier, pp. 157–235. https://doi.org/10.1016/B978-0-444-63453-5.00005-7

Kamm, B., Gruber, P.R., Kamm, M., 2008. Biorefineries-Industrial Processes and Products: Status Quo and Future Directions, Biorefineries-Industrial Processes and Products: Status Quo and Future Directions.

https://doi.org/10.1002/9783527619849

Kang, J., Irmak, S., Wilkins, M., 2019. Conversion of lignin into renewable carboxylic acid compounds by advanced oxidation processes. Renew. Energy 135, 951–962. https://doi.org/10.1016/j.renene.2018.12.076

Kang, S., Li, X., Fan, J., Chang, J., 2013. Hydrothermal conversion of lignin: A review. Renew. Sustain. Energy Rev. 27, 546–558. https://doi.org/10.1016/j.rser.2013.07.013

Leary, G., Schmidt, J.A., 2010. The Chemistry of Lignin-Retaining Bleaching : Oxidative Bleaching Agents, in: Heitner, C., Dimmel, D.R., Schmidt, J.A. (Eds.), Lignins and Lignans: Advances in Chemistry. CRC Press, Boca Raton, pp. 439–469. https://doi.org/10.1201/EBK1574444865-c12

Li, C., Zhao, X., Wang, A., Huber, G.W., Zhang, T., 2015. Catalytic Transformation of Lignin for the Production of Chemicals and Fuels. Chem. Rev. 115, 11559–11624. https://doi.org/10.1021/acs.chemrev.5b00155

Ma, R., Guo, M., Zhang, X., 2014. Selective Conversion of Biorefinery Lignin into Dicarboxylic Acids. ChemSusChem 7, 412–415. https://doi.org/10.1002/cssc.201300964

Ma, R., Xu, Y., Zhang, X., 2015. Catalytic Oxidation of Biorefinery Lignin to Value-added Chemicals to Support Sustainable Biofuel Production. ChemSusChem 8, 24–51. https://doi.org/10.1002/cssc.201402503

Palmer, A., 2005. Solubility of copper oxides in water and steam. 14Th Int. Conf. Prop. Water Steam Kyoto.

Pandey, M.P., Kim, C.S., 2011. Lignin Depolymerization and Conversion: A Review of Thermochemical Methods. Chem. Eng. Technol. 34, 29–41. https://doi.org/10.1002/ceat.201000270

Prasetyoko, D., Royani, C.E., Fansuri, H., Ramli, Z., Nur, H., 2010. Catalytic performances of Fe_2O_3/TS-1 Catalyst in Phenol Hydroxylation Reaction. Indones. J. Chem. 10, 149–155.

Přech, J., 2018. Catalytic performance of advanced titanosilicate selective oxidation catalysts – a review. Catal. Rev. - Sci. Eng. 60, 71–131. https://doi.org/10.1080/01614940.2017.1389111

Rodrigues, A.E., Pinto, P.C. de O.R., Barreiro, M.F., Esteves da Costa, C.A., Ferreira da Mota, M.I., Fernandes, I., 2018. An Integrated Approach for Added-Value Products from Lignocellulosic Biorefineries. Springer International Publishing, Cham. https://doi.org/10.1007/978-3-319-99313-3

Schutyser, W., Kruger, J.S., Robinson, A.M., Katahira, R., Brandner, D.G., Cleveland, N.S., Mittal, A., Peterson, D.J., Meilan, R., Román-Leshkov, Y., Beckham, G.T., 2018. Revisiting alkaline aerobic lignin oxidation. Green Chem. 20, 3828–3844. https://doi.org/10.1039/C8GC00502H

Su, J., Yang, L., Liu, R.N., Lin, H., 2014. Low-temperature oxidation of guaiacol to maleic acid over TS-1 catalyst in alkaline aqueous H_2O_2 solutions. Chinese J. Catal. 35, 622–630. https://doi.org/10.1016/S1872-2067(14)60039-5

Sun, Y., Fenster, M., Yu, A., Berry, R.M., Argyropoulos, D.S., 1999. The effect of metal ions on the reaction of hydrogen peroxide with Kraft lignin model compounds. Can. J. Chem. 77, 667–675. https://doi.org/10.1139/v99-036

Vangeel, T., Schutyser, W., Renders, T., Sels, B.F., 2018. Perspective on Lignin Oxidation: Advances, Challenges, and Future Directions. Top. Curr. Chem. 376, 30. https://doi.org/10.1007/s41061-018-0207-2

Védrine, J., 2017. Heterogeneous Catalysis on Metal Oxides. Catalysts 7, 341. https://doi.org/10.3390/catal7110341

Wang, C., Liu, H., Sun, Z., 2012. Heterogeneous Photo-Fenton Reaction Catalyzed by Nanosized Iron Oxides for Water Treatment. Int. J. Photoenergy 2012, 1–10. https://doi.org/10.1155/2012/801694

Werpy, T., Petersen, G., 2004. Top Value Added Chemicals from Biomass: Volume I -- Results of Screening for Potential Candidates from Sugars and Synthesis Gas., U.S. Department of energy. United States. https://doi.org/10.2172/926125

Whelan, A., 1994. Polymer Technology Dictionary, 1st ed. Springer Netherlands. https://doi.org/10.1007/978-94-011-1292-5

Widiarti, N., Ediati, R., Fansuri, H., Prasetyoko, D., 2012. Preparation, Characterization and Catalytic Activity of CuO/TS-1 on Benzene Hydroxylation Reaction. MAKARA Sci. Ser. 15, 135–147. https://doi.org/10.7454/mss.v15i2.1063

Xia, C., Peng, X., Zhang, Y., Wang, B., Lin, M., Zhu, B., Luo, Y., Shu, X., 2017.

Environmental-Friendly Catalytic Oxidation Processes Based on Hierarchical Titanium Silicate Zeolites at SINOPEC, in: Karamé, I. (Ed.), Green Chemical Processing and Synthesis. InTech, pp. 119–150. https://doi.org/10.5772/intechopen.68389

Xiang, Q., Lee, Y.Y., 2000. Oxidative cracking of precipitated hardwood lignin by hydrogen peroxide. Appl. Biochem. Biotechnol. 84–86, 153–162. https://doi.org/10.1385/ABAB:84-86:1-9:153

Xu, C., Arancon, R.A.D., Labidi, J., Luque, R., 2014. Lignin depolymerisation strategies: towards valuable chemicals and fuels. Chem. Soc. Rev. 43, 7485–7500. https://doi.org/10.1039/C4CS00235K

Yin, G., Jin, F., Yao, G., Jing, Z., 2015. Hydrothermal Conversion of Catechol into Four-Carbon Dicarboxylic Acids. Ind. Eng. Chem. Res. 54, 68–75. https://doi.org/10.1021/ie5036447

Zeng, J., Yoo, C.G., Wang, F., Pan, X., Vermerris, W., Tong, Z., 2015. Biomimetic fenton-catalyzed lignin depolymerization to high-value aromatics and dicarboxylic acids. ChemSusChem 8, 861–871. https://doi.org/10.1002/cssc.201403128

4. Effect of methoxy substituents in lignin and lignin model compounds wet peroxide oxidation

Three main phenyl propane units (*p*-coumaryl alcohol, coniferyl alcohol, and sinapyl alcohol) compose lignin, whose difference lay in the presence and location of the methoxy substituents in the aromatic structure. These substituents affect not only the chemical structure but also the reactivity. Based on this behavior, lignins with various structures can produce different C_4-DCA, but there has not been reported a clear connection suggesting which lignin is better for each C_4-DCA.

In this Chapter, the effect of the methoxy substituents in C_4-DCA production using peroxide oxidation on lignin model compounds (*p*-hydroxybenzoic acid, vanillic acid, and syringic acid) and hardwood and softwood lignin samples was studied. Conversion rates and yields for each C_4-DCA are presented and then compared between the different lignin models and lignins to suggest a better lignin towards C_4-DCA. Results showed that methoxy substituents increased reactivity and had higher selectivity to succinic acid, but with lower yields. Hardwood lignin produced higher yields of succinic acid, and reacted faster.

This Chapter is adapted from Vega-Aguilar, C.A.; Barreiro, M.F.; Rodrigues, A. E., "Effect of methoxy substituents on wet peroxide oxidation of lignin and lignin model compounds: Understanding the pathway to C_4 dicarboxylic acids". *Industrial & Engineering Chemistry Research*, **2021**, 60, 3543-3553. DOI 10.1021/acs.iecr.0c05085

4.1 Introduction

Lignocellulosic biomass biorefinery has proven to be a favorable alternative to reduce the fossil fuel dependence of the chemical industry (Gillet et al., 2017). Lignin is present in all lignocellulosic biomass, at contents that vary depending on their source. Structurally, it is composed of three phenyl propane units, known as *p*-hydroxyphenyl (H), guaiacyl (G), and syringyl (S) units (Li et al., 2015). Those units can be identified in lignin structure, respectively, as derivatives of *p*-coumaryl alcohol, coniferyl alcohol, and sinapyl alcohol moieties. The main difference between these structures relies on the methoxy substituents located in the *ortho* position relative to the hydroxyl group in the phenolic ring, as shown in Figure 4.1a. The abundance of each monomer in the lignin is related to plant taxonomy, as shown in Table 4.1. The ratio between monomers is relevant because each monomer has a different chemical behavior and distinct interlinking possibilities (Brunow, 2005). Most of the links between monomers are alkyl- and aryl-ether linkages (60-70%), C-C linkages (~25-35%), and some ester bonds (<5%), being the most common ones the *β-O-4*, *α-O-4*, *β-β*, *β-5*, 5-5, *β-1* and the *4-O-5*, which leads to a complex heterogeneous structure that is difficult to isolate and depolymerize (Ponnusamy et al., 2019; Upton and Kasko, 2016). Kraft lignin is obtained from kraft pulping processes, which modifies the structure of native lignin through cleavage of *α* and *β* ether bonds, but also causing condensation as carbon-carbon bonds. In these processes, lignin is burnt to produce energy and recover chemicals. However, kraft lignin can also be valorized into value-added products (Evstigneyev and Shevchenko, 2019; Upton and Kasko, 2016).

Table 4.1**-** Approximate composition (%) of some lignin classes, depending on the plant taxonomy.

Phenylpropane units	Guaiacylpropane	Syringylpropane	*p*-hydroxyphenylpropane
Softwood lignin	95%	1%	4%
Hardwood lignin	50%	50%	2%
Grass lignin	70%	25%	5%

Reprinted with permission from Brunow, G.(2005). Copyright 2008. John Wiley and Sons.

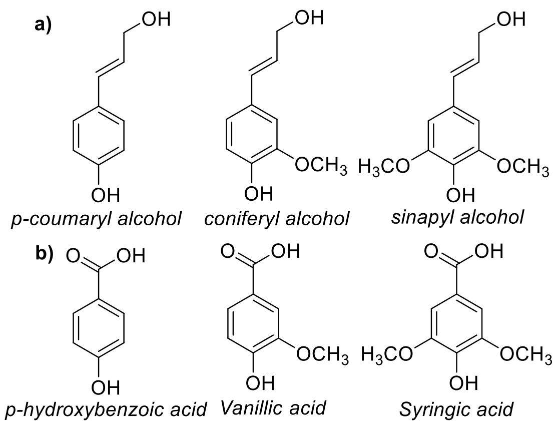

Figure 4.1 - Structures of **a)** monolignol monomers and **b)** model compounds used for this work

Lignin has been proposed as a feedstock for several products after depolymerization, which can be achieved by oxidation, reduction, pyrolysis, hydrotreatment, enzymatic hydrolysis, and many other chemical and biological treatments (Li and Zheng, 2020; Sun et al., 2018; Tarabanko and Tarabanko, 2017; Wendisch et al., 2018). Phenolic products, such as phenol, vanillin, syringaldehyde, and catechol, have been the main focus of lignin depolymerization (Rodrigues et al., 2018; Wendisch et al., 2018). However, due to lignin higher availability and low commercial use, the study of this renewable raw material as a feedstock for the production of a diversity of aliphatic compounds (e.g., adipic acid, succinic acid, cyclohexane), which are nowadays produced by petrochemical routes or biochemical pathways using fermentable sugars, is becoming of high interest (Li et al., 2015). Strong oxidative depolymerization can cause a ring-opening reaction, producing several C_1 to C_6 acids, especially dicarboxylic acids (DCA), like adipic, muconic, succinic, maleic, and oxalic acids (Bi et al., 2018; Cronin et al., 2017b; Hasegawa et al., 2011; Zeng et al., 2015). Peroxide oxidation has been considered more efficient for aromatic ring cleavage than O_2 oxidation because it avoids mass-transfer limitations. Moreover, H_2O_2 releases free radicals, which enhance lignin degradation at shorter times with less severe conditions (Bhargava et al., 2006; Ma et al., 2015). Several of these dicarboxylic acids have shown relevance as feedstocks for polymers, cosmetics, and the food industry. They are currently under study to enhance their production through chemical and biological lignin depolymerization (Ma et al., 2015). C_4-DCA (succinic, maleic, malic, fumaric, and tartaric acids) (Figure 4.2), the main diacids obtained in the oxidation, and oxalic acid, have great importance as renewable building blocks for the future high-value biobased chemicals and materials (Werpy and Petersen, 2004, pp. 22–26). In particular, succinic acid has gotten special interest due to its application in the chemical industry (as a surfactant, ion chelator, etc.), food industry (acidulant, flavoring additive, and anti-microbial agent), and as an intermediate for chemical and materials production (Du et al., 2015).

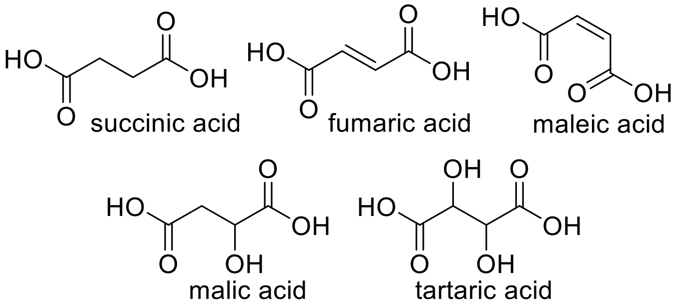

Figure 4.2- Structures of C_4 dicarboxylic acids (DCA).

Initial studies on lignin model compounds and lignin oxidation revealed the formation of C_4-DCA after ring-opening reaction in the alkaline pulping and peroxide bleaching processes (Gierer, 1986). Those studies were used to explain lignin degradation through the pulping process but were not focused on DCA production. Therefore, the quantities reported in those works were negligible or not specified at all. More recently, different works presented the non-catalyzed production of dicarboxylic acids from lignin and lignin model compounds oxidation using H_2O_2. However, none of these studies focused on analyzing the impact of the model compounds' structural features in the DCA yields (Hasegawa et al., 2011; Sun et al., 1998; Suzuki et al., 2006; Xiang and Lee, 2000). A higher DCA (oxalic, malonic, and succinic acids) yield has been related to a lower aromatic to aliphatic functional groups ratio when bagasse lignin was catalytically oxidized with H_2O_2 and sodium percarbonate or chalcopyrite (Cronin et al., 2017a). Ma et al. (2018) reported the oxidative conversion of several biorefinery lignins to monomeric phenols and dicarboxylic acids (described as a mixture of C_2-C_6 acids) using chalcopyrite-catalyzed peroxide oxidation, showing that DCA yield increased as the methoxy group content and aromatic hydroxyl groups increased (Ma et al., 2018). However, this model did not discriminate C_4-DCA from other acids, especially from C_2-C_3 acids, which are degradation products of C_4-DCA formation. In fact, until now, there is no clear evidence showing the best lignin structural unit to obtain a specific dicarboxylic acid by peroxide oxidation. This evidence can point out the most appropriate lignin for depolymerization towards a lignin-based chemicals platform.

In the present work, the effect of the methoxy substituents in the aromatic ring was studied to obtain dicarboxylic acids, focused on C_4-DCA (mainly succinic, malic, fumaric, maleic, and tartaric acids), and specifically succinic acid. This effect was analyzed on *p*-hydroxybenzoic, vanillic, and syringic acids, which are lignin model compounds resembling the lignin structural monomeric units, namely by presenting a different number of methoxy substituents in the *ortho* position to the phenolic OH group, as shown in Figure 4.1b. Moreover, this study was extended to two kraft lignins with different G:S:H ratios (a hardwood and a softwood sample).

4.2 Materials and methods

4.2.1 Materials

All chemical reagents were purchased from commercial sources and used without further purification. The following reagents were purchased from Sigma-Aldrich Co. LLC.: *p*-hydroxybenzoic acid (>99%), vanillic acid (97%), syringic acid (>95%), DL-malic acid (≥99.0%), fumaric acid (≥99.0%), maleic acid (>99%), malonic acid (>99%), oxalic acid dihydrate (≥99.0%), succinic acid (≥99.0%), acetic acid glacial (>99%), N,O-bis(trimethylsilyl)trifluoroacetamide (≥99.0%), trimethylchlorosilane (>98%), pyridine (>99.0%). Other reagents were purchased from different suppliers: formic acid (Chem-labs, >99%), acetonitrile (VWR, HPLC grade), sulfuric acid (Chem-labs, 95-97% p.a.), sodium hydroxide (Merck, p.a.), hydrogen peroxide solution (Fluka, >30% p.a.). Gases Helium (ALPHAGAZ™ 1 He) and argon (ALPHAGAZ™ Ar 1) were supplied by Air Liquide.

Two lignins were used: Indulin AT, a softwood lignin, commercialized by MeadWestvaco Corporation, USA, with an S:G:H ratio of 0:97:3 (Constant et al., 2016). The hardwood lignin was isolated from the black liquor obtained from a *Eucalyptus globulus* kraft pulping mill (The Navigator Company, Portugal). This lignin has an S:G:H ratio of 65:29:6 (Costa et al., 2018). Table 4.2 show some properties of these two studied lignins.

Table 4.2 - Properties of the studied lignins

Lignin	Lignin isolated from kraft black liquor (hardwood) (Costa et al., 2018)	Indulin AT (softwood) (Constant et al., 2016; Rohde et al., 2019)
S:G:H ratio	65:29:6	0:97:3
Total lignin (wt%)	66	92.2
Weight average molecular weight (M_w) (g/mol)	10323	4290
Number average molecular weight (M_n) (g/mol)	8768	530

4.2.2 Experimental methods

4.2.2.1 Oxidation procedure

Oxidation reactions were conducted in a glass-jacketed 1 dm^3 Büchi autoclave (Figure 4.3). A Lauda E300 thermostatic bath was used to control heating, keeping the reactor at 393-413 K. All model compounds (vanillic acid [VA], syringic acid [SA], and *p*-hydroxybenzoic acid [pHBA]) were used at a concentration of 10 g/L and an initial pH of 7.0, adjusted with NaOH or H_2SO_4 1.0 mol/L, as needed. Lignin samples (10 g/L) were solubilized in a 0.1 mol/L phosphate buffer to ensure complete solubilization throughout the reaction. The solution (400 mL) was placed in the batch reactor, closed, and pressurized with helium. Heating was applied to reach the desired temperature. A 40 mL-aliquot of 30 vol% H_2O_2 was loaded into the feed vessel, closed and pressurized with He. When the temperature was steady, H_2O_2 was introduced into the reactor, and the reaction started. Samples were taken manually for 4 hours at intervals of 10-30 minutes. The stirring speed was fixed at 800 rpm, and a maximum pressure of 9.0 bar was used. Signals of the thermocouple and pressure inside the reactor were recorded using an acquisition board and LabVIEW software. All experiments were done in duplicate. The protocol used for the Büchi reactor utilization can be found in Appendix B.

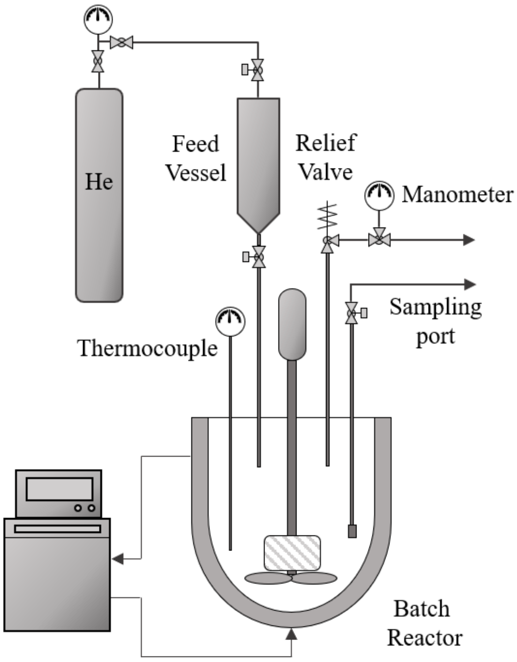

Figure 4.3- Scheme of the set-up used for the oxidation reactions.

All the reactions were done using 40 mL of a 30 vol% H_2O_2 (0.39 mol), which provide the molar quantities needed to achieve complete mineralization of the three used model compounds, according to Equation 4.1 (VA, 0.023 mol, which need 0.38 mol H_2O_2), Equation 4.2 (pHBA, 0.028 mol, which need 0.39 mol H_2O_2) and Equation 4.3 (SA, 0.019 mol, which need 0.34 mol H_2O_2). Even so, H_2O_2 cannot be considered the limiting reagent because not all the model compound molecules were mineralized but converted to low molecular-weight compounds. The same amount of oxidant was used for lignin since preliminary tests showed that a higher amount of oxidant caused C_4-DCA degradation. The oxidant was added precisely when the solution was at the setpoint temperature and the system pressurized to avoid H_2O_2 degradation while heating.

$$C_8H_8O_4 + 16\ H_2O_2 \ \rightarrow 8\ CO_2 + 20\ H_2O \qquad \text{Equation 4.1}$$

$$C_7H_6O_3 + 14\ H_2O_2 \ \rightarrow 7\ CO_2 + 17\ H_2O \qquad \text{Equation 4.2}$$

$$C_9H_{10}O_5 + 18\ H_2O_2 \ \rightarrow 9\ CO_2 + 23\ H_2O \qquad \text{Equation 4.3}$$

4.2.3 Analytical methods

4.2.3.1 Samples preparation for chromatographic analysis and lignin quantification

Model compound-oxidation samples in aqueous solution were acidified with H_2SO_4 2 mol/L to pH~2, diluted as needed, and filtered through a 0.22 μm pore-size filter. Lignin samples were acidified to pH~2, then heated at 40°C to coagulate the acid-insoluble lignin, followed by centrifugation at 5000 rpm for 15 minutes. The insoluble lignin was dried at 100°C overnight to quantify the acid-insoluble lignin. The acidic supernatant was used for carboxylic acid and acid-soluble lignin quantification. Acid-soluble lignin was measured by UV spectrophotometry at 240 nm, based on a calibration curve done with the acid-soluble lignin from the original lignin. Lignin conversion was calculated as the sum of the acid-insoluble and acid-soluble lignins. The pH was recorded for all samples before acidification using a calibrated VWR pH110 equipment. The gaseous compounds were not quantified in this study.

4.2.3.2 Quantification by High-Performance Liquid Chromatography (HPLC)

Carboxylic acids were quantified by high-performance liquid chromatography (HPLC) using a Shimadzu UFLC, equipped with a Diode Array Detector (210 and 260 nm), refraction index detector (RI) and a Phenomenex® Rezex™ ROA H^+ column (300 mm x 7.8 mm) and precolumn (50 mm x 7.8 mm). The column was operated at 50°C, using a gradient flow of 4 mmol/L H_2SO_4 and a solution of 15% acetonitrile in 4 mmol/L H_2SO_4, a flow rate of 0.5 mL/min, and an injection volume of 20 μL. Carboxylic acids were identified and quantified using calibration curves prepared with standards of each acid, which can be found in Appendix A, Table A.2.

Quantified acids are expressed as *C_4-DCA* (succinic, malic, maleic, fumaric, and tartaric acids), *Other DCA* (malonic and oxalic acids), *Total DCA* (C_4-DCA + Other DCA), and *MCA* (monocarboxylic acid: acetic and formic acid). *Aromatic CA* (carboxylic acids) is the sum of pHBA, VA, and SA.

4.2.3.3 Gas Chromatography-Mass Spectroscopy (GC-MS) analysis

Qualitative analysis of the compounds produced at low concentrations was done with GC-MS to understand the degradation pathway of lignin and model compounds to C_4-DCA. For that, a 1.0 mL sample (prefiltered through a 0.22 µm filter) was lyophilized in a glass tube. The solids were dissolved in 150 µL of pyridine. Then 150 µL of BSTFA and 50 µL of TMCS were added. The mixture was mixed and placed in an oil bath at 80ºC for 30 minutes to allow complete silylation. The samples were immediately cooled in an ice bath and diluted to 1.0 mL with anhydrous acetonitrile. Derivatized samples were analyzed in a Shimadzu GC-MS – TQ8040, fitted with a Restek Rxi-5Sil MS column (30 m x 0.25 mm x 0.25 µm), injection port at 250ºC, 1 µL splitless injection, and a temperature program starting at 100ºC (hold 2 min), a ramp of 3ºC/min to 180ºC, hold for 5 min, ramp of 3ºC/min to 200 ºC, hold for 5 min, and a final ramp of 15ºC/min to 250ºC, and hold for 3 min. The mass spectrometer ion source was at 250ºC, and the interface temperature was at 260ºC. The resulting peaks were analyzed using the NIST library. The major components were identified by comparison with standard compounds.

4.3 Results and discussion

4.3.1 Oxidation of model compounds: *p*-hydroxybenzoic acid (pHBA), vanillic acid (VA), and syringic acid (SA)

The model compounds presented different behaviors when oxidized using H_2O_2 at 140ºC. Figure 4.4 shows that both VA and SA reached a nearly complete conversion at 40 min (99 wt% and 100 wt%, respectively). However, pHBA got a lower conversion, namely 88 wt%, never being total, even after 4 hours of reaction (even with enough H_2O_2 to reach complete mineralization, showing that the remaining oxidant was used to oxidize the produced compounds instead of pHBA). Table 4.3 summarizes the conversion rates for each tested model compound at 140ºC, where SA and VA showed higher conversion rates, while for pHBA, the lowest one was observed (88 wt%). It has been reported that SA is more reactive than VA when oxidized using O_2 at alkaline pH (Casimiro et al., 2019; Schutyser et al., 2018). However, when H_2O_2 at neutral pH is used, which has higher oxidant power, no significant differences between SA and VA conversions were detected.

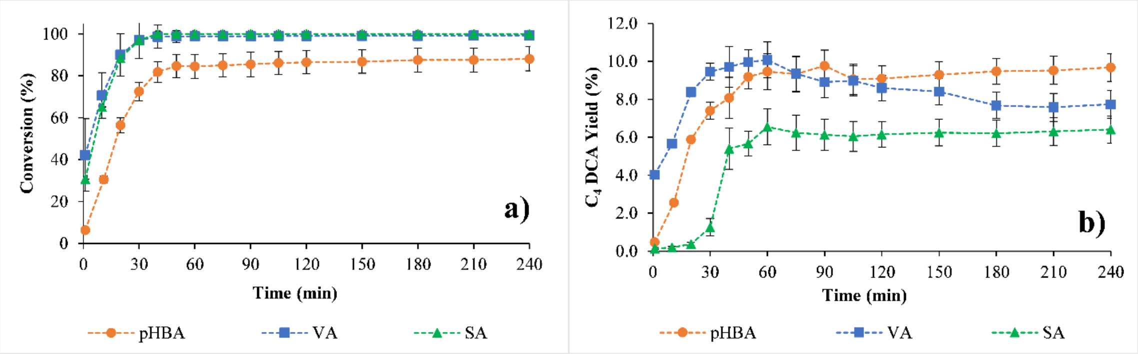

Figure 4.4 - **(a)** Model compound conversion and **(b)** C_4-DCA yield, at T=140°C.

Table 4.3 - Reaction rate constants (k) for model compound conversion, at 140°C and 120°C, based on a pseudo first-order kinetic equation.

	p-hydroxybenzoic acid	Vanillic acid	Syringic acid
$k_{140°C}$ (s^{-1})	$(7.2 \pm 0.3) \times 10^{-4}$	$(1.7 \pm 0.2) \times 10^{-3}$	$(1.8 \pm 0.2) \times 10^{-3}$
$k_{120°C}$ (s^{-1})	$(3.2 \pm 0.4) \times 10^{-4}$	$(3.4 \pm 0.2) \times 10^{-4}$	$(5.1 \pm 0.2) \times 10^{-4}$

Lower reaction rates were found at 120°C, as seen in Table 4.3. There was no significant difference between VA and pHBA oxidation at this temperature, while SA oxidation occurred faster, confirming its higher reactivity. Therefore, it can be concluded that pHBA maintained the low reactivity even at higher temperatures, while SA showed the most increased reactivity.

The phenolic OH bond's strength explains most of the reactivity observed for the model compounds because it is the initial site where the compound reacts against a radical (Barclay and Vinqvist, 2003). After the phenolic OH bond is cleaved by accepting a radical, the radical is delocalized in the aromatic ring, which is reorganized as a quinone to be further oxidized and suffer ring-opening reactions (Barclay and Vinqvist, 2003). The Bond Dissociation Energy (BDE) for the phenolic OH bond, a parameter that measures the energy needed to cause the rupture of the bond, is affected by the presence of activating and deactivating groups in the aromatic ring, which can or not stabilize the radical by resonance and/or inductive effects. A compound with a lower BDE would show a higher reactivity against an oxidant because the OH bond would be cleaved easily, and the aromatic ring would be further oxidized to a quinone structure (Barclay and

Vinqvist, 2003; Mohajeri and Asemani, 2009). As the aromatic ring becomes activated, the radical is easily dislocated in the aromatic structure, reacting more against H_2O_2 oxidation (Sun et al., 1999). The highest BDE is presented by pHBA (85.15 kcal/mol) when compared to VA (79.41 kcal/mol) and SA (79.42 kcal/mol) (Mohajeri and Asemani, 2009) because the latter two compounds have methoxy groups in the *ortho* position to the phenolic OH (Figure 4.1b), which act as electron donors, stabilizing the radical in the aromatic ring. Even though SA has two methoxy groups and VA only one, there is no significant difference between the two compounds due to the intramolecular hydrogen bond formed between the phenolic hydrogen and the methoxy oxygen in SA, stabilizing the phenolic OH bond (Mohajeri and Asemani, 2009). It is expected that the real BDE for each model compound in solution is lower than the reported one because the reactions were carried out, at all moments, at a pH higher than the respective pK_{a1} (pHBA=4.57, VA=4.42, SA=4.34) (Lide, 2009; Ragnar et al., 2000). Over pK_{a1}, the carboxylic acid group was unprotonated, acting as a weak electron donor group by inductive effect, thus stabilizing the radical in the aromatic ring (Smith and March, 2006). In the opposite case, i.e., if the carboxylic group is protonated, it acts as a deactivating group, slightly destabilizing the radical in the aromatic ring.

After 40 minutes of reaction, and for the three compounds, the first-order kinetic model did not fit the experimental data. At this point, a change in the pH was observed; namely, it decreased from pH 7 to 4.0-5.5 and then increased to pH 6.3-7.4 (Figure 4.5). These facts evidenced a change in the reactions taking place after this time. The degraded model compounds were oxidized to other compounds, namely dicarboxylic acids, while the remaining model compounds continued to be oxidized but at a lower rate. However, after 40 minutes, model compounds conversion reached more than 96% of the total conversion, i.e., the conversion registered for 240 minutes reaction time, confirming that the expressed kinetic constant rate explained the primary behavior of the model compound conversion.

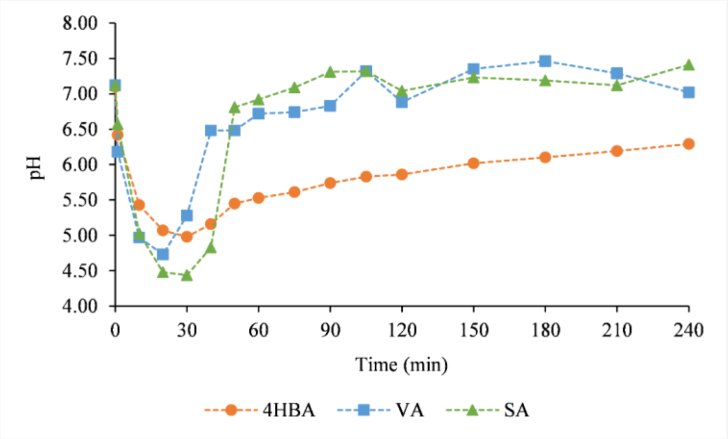

Figure 4.5 - pH behavior for model compounds oxidation at 140°C.

As the reaction proceeded, VA and pHBA solutions turned darker due to the production of chromophoric compounds, such as quinones and condensed aromatic rings. The condensation reactions occurred in these model compounds due to the *ortho* available position, having two available positions in pHBA and just one in VA since these positions were activated for addition and condensation reactions. When SA was oxidized, an initial darker color was produced while heating the mixture to the reaction temperature, caused by the presence of quinones produced by autooxidation. However, as soon as the H_2O_2 was added, they were quickly degraded, and the color disappeared after a short time. As SA has no available *ortho* positions to the phenolic OH, no condensation reactions occurred, and no darker solutions were formed (Barclay and Vinqvist, 2003).

The methoxylated model compounds were oxidative demethoxylated during the oxidation's first steps, resulting in hydroxyl groups in the aromatic structure. Demethoxylation is achieved when a hydroxyl radical attacks the position where the methoxyl group is linked, remaining this radical as a hydroxyl group while the methoxyl group is released as methanol (Gierer et al., 1994; Santos et al., 2016). This step was observed in VA and SA, where 3,4-dihydroxybenzoic acid (protocatechuic acid) was detected during the first minutes of reaction by GC-MS analysis. This compound is more reactive than VA and SA, having a lower BDE (74.44 kcal/mol) (Mohajeri and Asemani, 2009), so it was oxidized faster to *o*-quinones. This compound was also found in pHBA oxidation, suggesting that the hydroxyl radical attacked the carbon adjacent to the OH group. Interestingly, no 3,4,5-trihydroxybenzoic acid was found in any oxidation, suggesting that as soon as the 3,4-dihydroxybenzoic acid was obtained, it was oxidized to *o*-quinone instead of oxidizing the remaining *ortho* position to the trihydroxy acid.

4.3.2 Ring-opening reaction main products: C_4 dicarboxylic acids

Amongst the different compounds produced during the oxidation process, C_4-DCA were the main components in the mixture. They resulted from the aromatic ring-opening reaction, which required a strong oxidant. Figure 4.4b shows how the concentration of total C_4-DCA (which is the sum of succinic, maleic, malic, tartaric, and fumaric acids) changed through time, reaching the higher yield at 60 min for SA, at 50-60 min for VA, while for pHBA the highest yield was achieved at 90 min.

However, C_4-DCA were not the only acids produced. Other carboxylic acids, like formic, acetic, malonic, and oxalic acids, were identified and quantified, and their total concentration is presented conjunctly as "Other CA" in Figure 4.6. Most of these acids corresponded to degradation products of C_4-DCA, indicating an over-oxidation. These acids increased their concentration through time, mainly when pHBA was used as the starting compound, with the highest yield, 24.2 wt%, achieved at 75 min. VA gave rise to 17.3 wt% at 20 min, while SA to 12.9 wt% at 150 min. The remaining carbon, not quantified in this graphic representation, corresponds to gases losses (mainly CO_2) and non-quantified products in the solution.

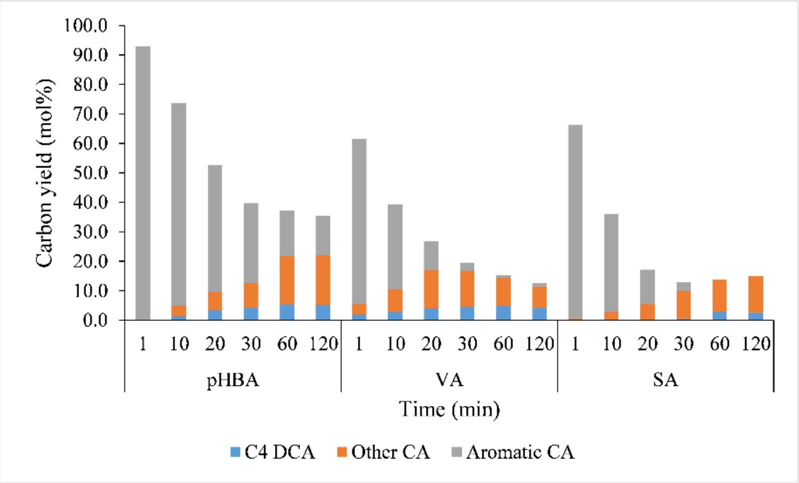

Figure 4.6 - Carbon yield by families, based on the carbon proportion.

(C_4-DCA: succinic, malic, maleic, tartaric and fumaric acids; Other CA: malonic, oxalic, acetic and formic acids; Aromatic CA: VA, SA, pHBA)

All the performed reactions started at neutral pH because it has been reported that many dicarboxylic acids are degraded at acidic conditions, even at lower temperatures (Cronin et al., 2017a; Di Marino et al., 2019). In contrast, many hydroxylated acids are obtained at alkaline pH, which can be further oxidized to low-molecular-weight acids, as mentioned in Chapter 3. Also, at alkaline conditions, more condensation products have been observed. The principal observed C_4-DCA was succinic acid in all cases, with a lower amount of maleic acid in pHBA and tartaric acid in VA oxidations, as seen in Figure 4.7. Malic, fumaric, and tartaric acids were detected in small quantities in all cases.

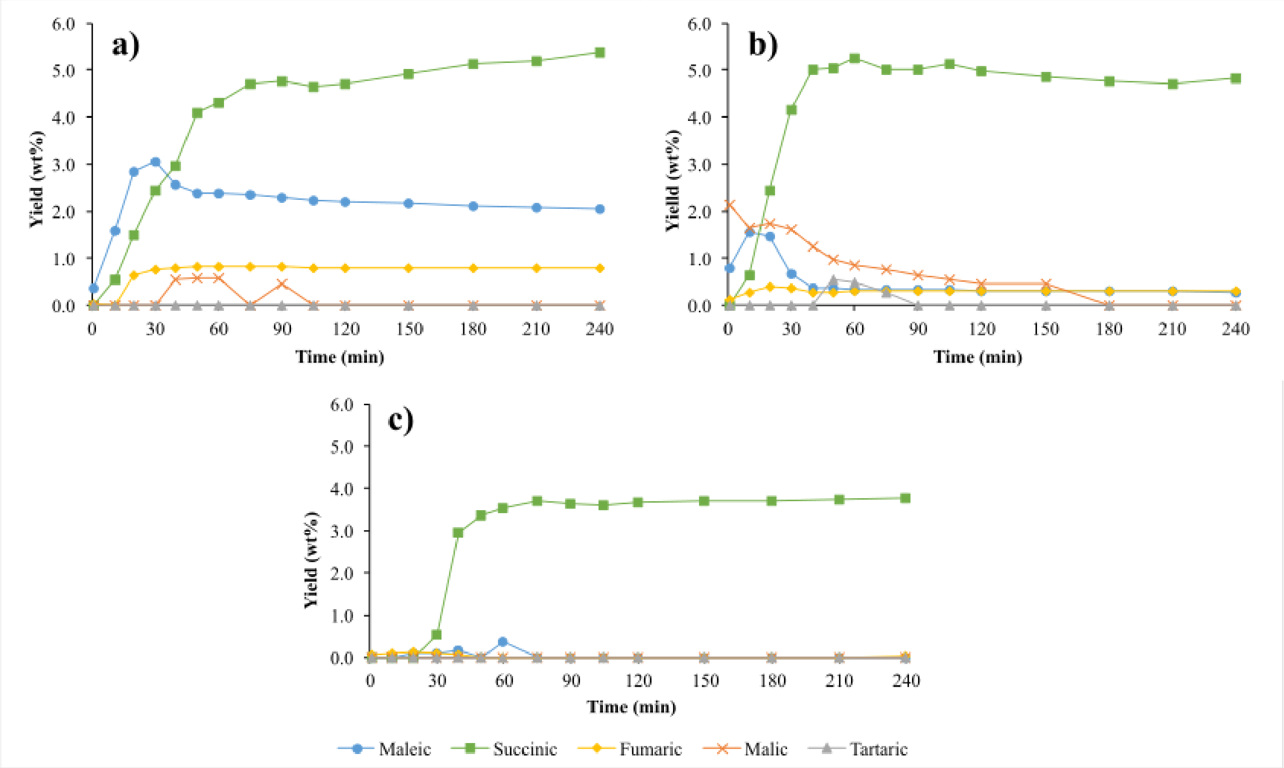

Figure 4.7 - C_4-DCA yield for model compound oxidation: **(a)** pHBA, **(b)** VA, **(c)** SA, at 140ºC.

In pHBA oxidation, the primarily obtained acid was succinic acid (5.4 wt%), while the production of maleic and fumaric acid up to 3.0 wt% and 0.8 wt%, respectively, was observed. During the first 90 minutes, traces of malic acid were detected, being the signal very close to the limit of quantification, explaining its appearance and disappearance in several samples. After 90 minutes, the signal disappeared utterly. Maleic acid concentration increased during the first 30 minutes and then decreased, being converted to other compounds, such as fumaric, malic, and succinic acids.

In VA oxidation, succinic acid was also the highest produced acid, achieving a maximum of 5.3 wt% at 60 min, then stabilizing up to 240 min. Malic acid was observed at the first minutes, with the highest amount of 2.1 wt%, thus decreasing slowly until its disappearance after 180 min. Fumaric acid reached the highest yield (0.4 wt%) at 20 minutes, maintaining this percentage for the remaining time. Tartaric acid was also found at low concentrations for several minutes. The presence of tartaric and malic acids was associated with the hydroxylation of the double bond present in the maleic acid, which was the first obtained acid after the ring cleavage when *p*-quinone structures were oxidized, which was proved in Chapter 3. Maleic acid behavior was similar to the one observed in the pHBA reaction, increasing its concentration in the first 20 minutes, then decreasing due to conversion to other compounds.

In SA oxidation, succinic acid was practically the only C_4-DCA present in the mixture, with the highest amount of 3.8 wt%. For several minutes, small quantities of maleic (0.4 wt%) and fumaric (0.1 wt%) were observed, but these compounds disappeared after 60 min of reaction. No hydroxylated acids were quantified during the analyzed reaction time.

GC-MS analysis identified more compounds (presented in Table 4.4 and their chemical structures in Figure 4.8). Different carboxylic acids were found, most of them precursors (e.g., isocitric, *cis*-aconitic, and 2,5-furandicarboxylic acids) or derivatives from the already quantified DCA (e.g., itaconic, tartronic, glycolic, and glyceric acids). These compounds' presence was directly related to the oxidized model compounds and therefore correlated to the original structure. With this data, it was possible to establish the oxidation pathway for each model compound and, consequently, to study the effect of the methoxy substituents in the aromatic structure towards the production of C_4-DCA.

Table 4.4 **-** Compounds identified by GC-MS for pHBA, VA, and SA oxidation at 140ºC.

#	**Compound name**	**Model compound/time (min)**								
		pHBA			**VA**			**SA**		
		30	**60**	**120**	**30**	**60**	**120**	**30**	**60**	**120**
1	Oxalic acid	++++	++++	++++	++++	++++	++++	++	++	++
2	3-Hydroxypropionic acid	-	-	-	+++	+++	+++	++	++	++
3	Malonic acid	++	+	tr	+++	++	++	+	+	+
4	Glycerol	tr	tr	+	++++	++++	++++	tr	tr	tr
5	Maleic acid	-	-	-	+	+	+	-	-	-
6	2-keto isovaleric acid	-	-	-	-	-	-	+	tr	tr
7	Succinic acid	+++	+++	+++	++++	++++	++++	++	+++	++
8	Glyceric acid	-	-	-	+++	++	++	tr	+	+
9	Itaconic acid	++	+++	++	+	+	+	-	tr	+
10	Fumaric acid	++	++	+++	++	++	++	tr	-	tr
11	Isocitric acid lactone	+++	+++	+++	tr	tr	tr	-	tr	tr
12	2-hydroxyacetic acid (glycolic acid)	+	tr	tr	++	tr	tr	-	-	-
13	Malic acid	++++	+++	+++	+++	+	+	tr	tr	tr
14	2-methylsuccinic acid	-	tr	tr	tr	tr	tr	tr	tr	tr
15	2,4-dihydroxybutanoic acid	-	-	-	tr	tr	tr	-	-	tr
16	2-(hydroxymethyl)butanoic acid	-	-	-	-	-	tr	-	tr	+
17	Dihydroxymalonic acid	tr	++	-	tr	tr	tr	-	-	-
18	2,3,4-butanaldehyde	tr	+	+	tr	tr	tr	-	-	-
19	Adipic acid	-	-	-	tr	tr	tr	-	-	tr
20	D-xylonic acid delta-lactone	+	++	++	+	++	++	-	-	-
21	Vanillin	-	-	-	-	-	-	-	tr	-
22	2-Hydroxyisobutyric acid	-	-	-	-	-	-	-	tr	tr
23	2-hydroxyhexanoic acid	+++	+++	+++	+++	++	+	-	-	-
24	2,3,4-Trihydroxybutyric acid	tr	tr	tr	tr	tr	tr	-	tr	tr
25	3-Methylene-1,4-butanediol	tr	tr	tr	-	-	-	-	-	-

Table 4.4 - (Continuation) Compounds identified by GC-MS for pHBA, VA, and SA oxidation at 140ºC.

26	Dimethyl ester of tartaric acid	-	-	-	tr	tr	tr	-	-	-
27	2,3,3-trihydroxy-2-propenoic acid	+	tr	tr	++	tr	tr	-	+	tr
28	2-hydroxypentanedioic acid	-	-	-	tr	tr	tr	-	tr	tr
29	Tartaric acid	++++	++++	+++	+++	++	++	-	+++	+++
30	Tartronic acid	tr	+	+	+	-	-	-	-	-
31	5-(1,2-dihydroxyethyl)-4-hydroxydihydrofuran-2(3H)-one	-	-	-	tr	tr	tr	-	-	-
32	2,3-Dimethylsuccinic acid	-	-	-	-	-	-	tr	-	-
33	Dihydroxyacetic acid	tr	+	+	-	-	-			
34	*p*-Hydroxybenzoic acid	++++	++++	++++	-	-	-	tr	-	tr
35	2,5-furandicarboxylic acid	+	tr	tr	tr	tr	tr	tr	tr	tr
36	(Z)-2,4-dihydroxypenta-2,4-dienoic acid	-	-	-	-	-	-	tr	-	-
37	2,3-dihydroxypropenoic acid	-	-	-	tr	tr	tr	-	-	-
38	2,3-dihydroxypentanedioic acid	+	+	+	+	tr	tr	-	tr	tr
39	2,4-dihydroxypentanedioic acid	tr	tr	tr	-	-	-	tr	-	-
40	2-ketosuccinic acid (oxalacetic acid)	+	tr	tr	-	-	-	-	tr	tr
41	Propane-1,2,3-tricarboxylic acid	tr	+	+	+	-	-	tr	++	++
42	2-methyl-4-hydroxybutanoic acid	tr	tr	tr	-	-	-	-	-	-
43	*cis*-aconitic acid	+	tr	tr	tr	tr	tr	tr	tr	tr
44	Vanillic acid	tr	tr	tr	++++	++++	++++	-	tr	-
45	2,4-dihydroxybenzoic acid	+	tr	tr	-	-	-	-	-	-
46	2,3,4-trihydroxypentadienoic acid	-	-	-	tr	tr	tr	-	tr	-
47	3,4-dihydroxybenzoic acid	++++	++++	++++	tr	tr	tr	+	tr	tr
48	Isocitric acid (1-hydroxyl-1,2,3-propanetricarboxylic acid)	+++	++++	++++	+	tr	tr	-	tr	tr
49	Syringic acid	-	-	-	-	-	-	++++	tr	tr
50	m-hydroxybenzoic acid	++++	+++	+++	-	-	-	tr	-	-

* Symbology: "+" to "++++": relative peak height in GC-MS chromatogram, "tr": traces, "-": not observed.

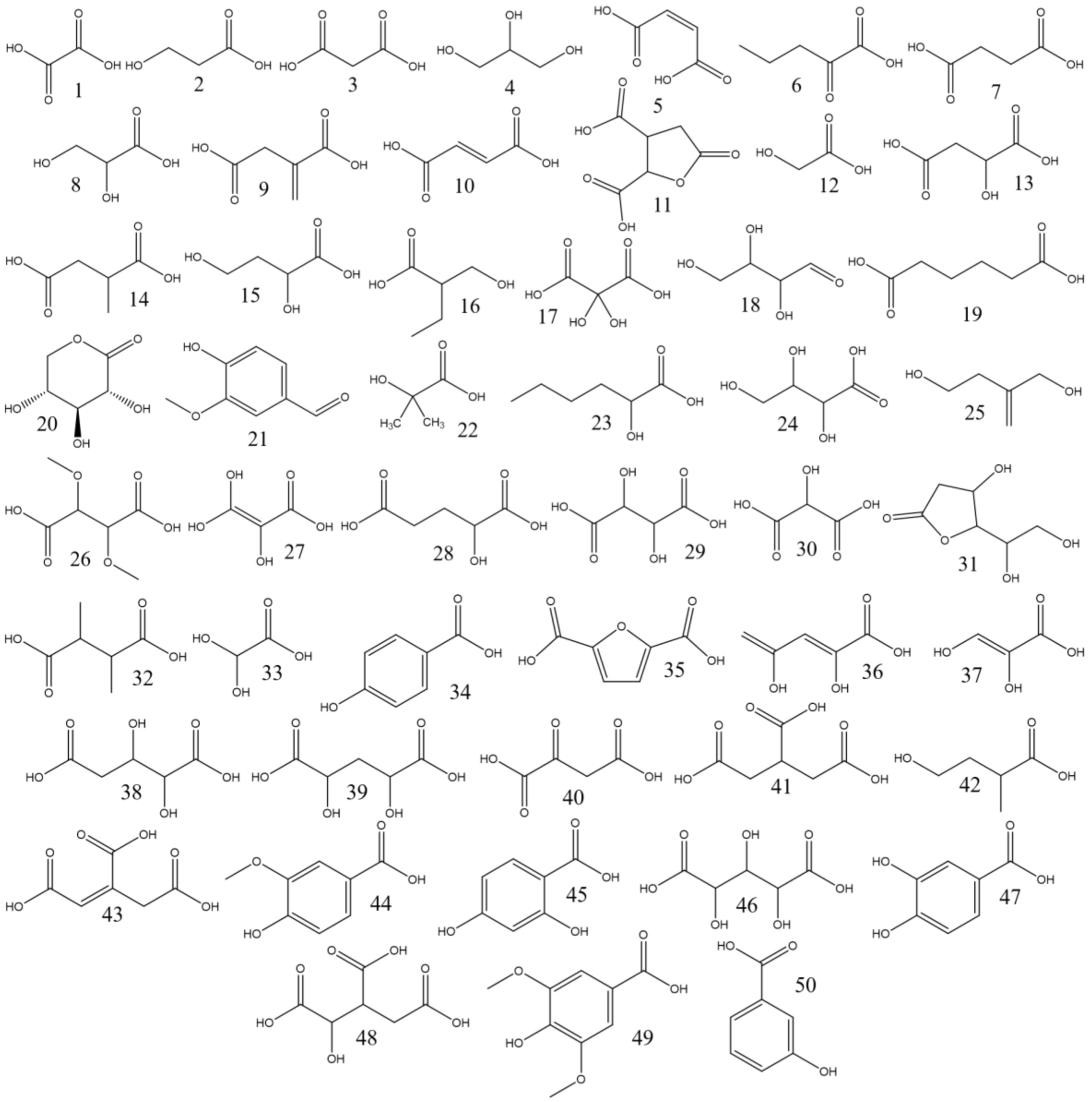

Figure 4.8 - Chemical structures of the compounds detected by GC-MS analysis for pHBA, VA, and SA oxidation with H_2O_2 at 140ºC.

Figure 4.9 shows the oxidation pathway for pHBA, which was identified after a detailed analysis of the data included in Table 4.4. Since the hydroxyl group in pHBA activated the aromatic ring, the first step in the oxidation was the hydroxylation in the *ortho* position, forming 3,4-dihydroxybenzoic acid, as confirmed by Kang et al. (Kang et al., 2019). Later, the hydroxyl groups were oxidized to an *o*-benzoquinone structure, which suffered a ring-opening reaction, to obtain a muconic acid derivative (Suzuki et al., 2006; Zeng et al., 2015). After decarboxylation, several 6-carbon dicarboxylic acids were obtained, like *cis*-aconitic acid or 2,5-furandicarboxylic acid. These compounds were very reactive, and *cis*-aconitic acid was decarboxylated to itaconic acid or converted to isocitric acid, being oxidized and decarboxylated to succinic acid. Most of these compounds showed a high response in the GC-MS, confirming their presence along the reaction course.

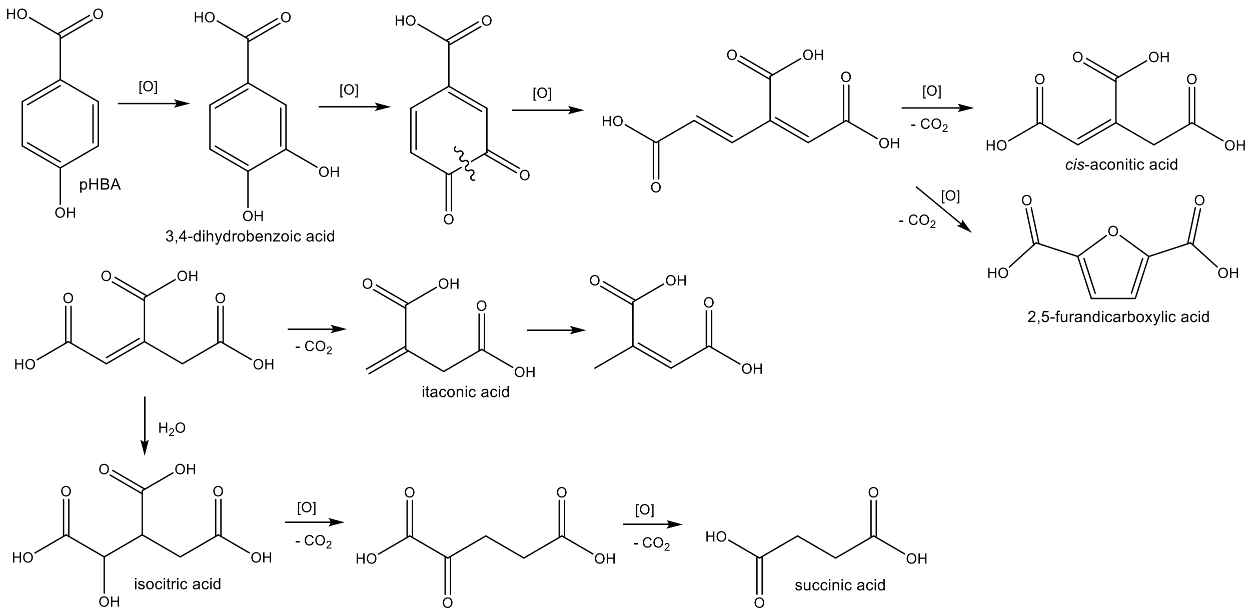

Figure 4.9 - Proposed pathway for p-hydroxybenzoic acid oxidation to achieve succinic and itaconic acid.

pHBA can also react through a *p*-benzoquinone structure, as detailed in Figure 4.10. To form the *p*-benzoquinone structure, the pHBA must be firstly oxidized to 3,4-dihydroxybenzoic acid and then decarboxylated to 2,4-dihydroxyphenol, which could be then oxidized to a *p*-benzoquinone derivative. Later, this structure underwent a ring-opening reaction and a rearrangement to obtain maleic and oxalic acids as the main products.

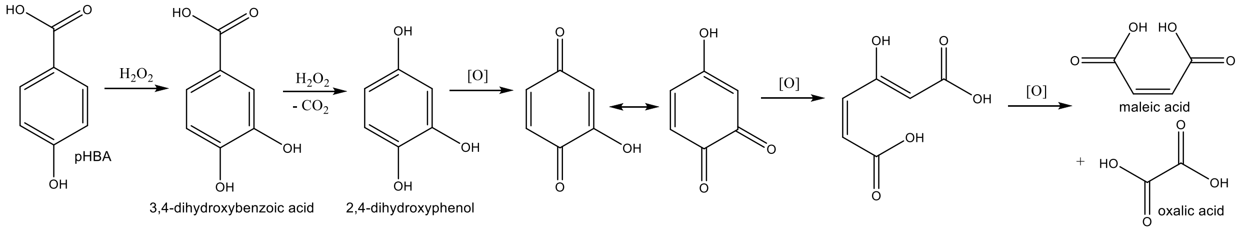

Figure 4.10 - Proposed pathway for p-hydroxybenzoic acid oxidation to achieve maleic and oxalic acid.

Due to the double bond in maleic acid, this compound could be later oxidized to other compounds, such as malic acid and tartaric acid, as shown in Figure 4.11. These acids could be further degraded to lower-molecular weight compounds, such as malonic acid, tartronic acid, 2,3,3-trihydroxy-2-propenoic acid, and formic acid.

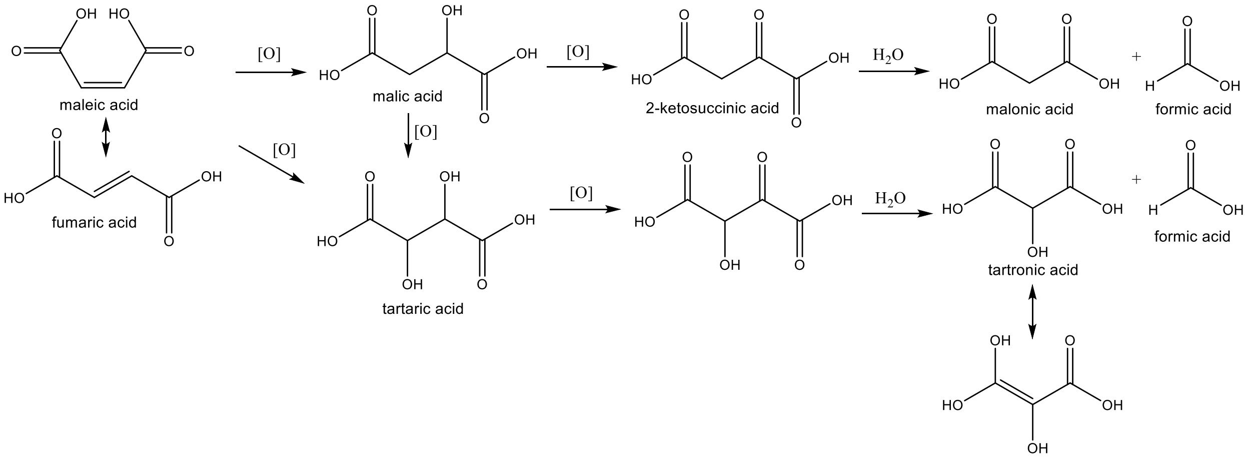

Figure 4.11 - Proposed pathway for maleic acid conversion.

The proposed pathway has been established for *p*-hydroxybenzoic acid oxidation, but it can also explain vanillic and syringic acids' oxidation. However, some changes should be mentioned to elucidate the observed differences in the produced compounds and their respective yields due to the methoxy substituents' presence.

Vanillic acid has a methoxy group in the *ortho* position to the OH group. However, one of the first steps in the oxidation was the demethoxylation, as suggested by several authors (Gierer et al., 1994; Santos et al., 2016; Sun et al., 1998), forming 3,4-dihydroxybenzoic acid, as shown in Figure 4.12a. This compound was the starting point of the oxidation in the pathway shown in Figure 4.9 for pHBA, therefore avoiding the aromatic ring's hydroxylation step. Both VA and pHBA followed the same reaction pathway, expecting to obtain the same products, especially for C_4-DCA, as confirmed by the results presented in Figure 4.7 and Table 4.4. The main difference lay in the obtained yield for C_4-DCA, which was higher for VA oxidation and derived from the higher reactivity of the aromatic ring due to the methoxy group's presence as an activating group, as explained before.

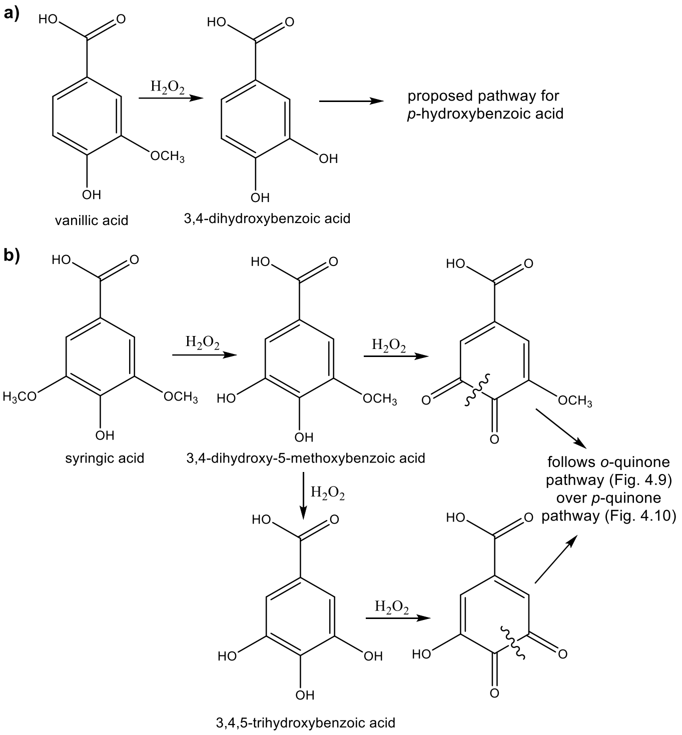

Figure 4.12 - Proposed pathways for **(a)** vanillic acid and **(b)** syringic acid.

SA oxidation behaved slightly differently, having as the main product succinic acid accompanied by lower amounts of other C_4-DCA. The small traces of maleic and fumaric acids were explained because when the molecule was demethoxylated, it formed 3,4,5-trihydroxybenzoic acid or 3,4-dihydroxy-5-methoxybenzoic acid, compounds that were easily oxidized to *o*-quinone derivatives (Figure 4.12b). Decarboxylation had been reported in the first steps for SA oxidation (Santos et al., 2016), but their products were not observed in the present study. The possibility of reaction through the *o*-quinone pathway (Figure 4.9) is higher than through the *p*-quinone pathway (Figure 4.10) because various *o*-quinone derived structures were produced, leading to a higher succinic acid yield and a lower amount of maleic and fumaric acids. The absence of maleic and fumaric acids explained the non-appearance of malic and malonic acids obtained from hydroxylation and further decarboxylation of fumaric/maleic acids, shown in Figure 4.11. Similar behavior concerning the low yield of maleic and fumaric acids was observed by Sun et al. (Sun et al., 1998) when lignin model compounds were oxidized with H_2O_2 using UV radiation. Also, SA oxidation generated propane-1,2,3-tricarboxylic acid (Table 4.4), which was more stable than *cis*-aconitic acid due to the lack of an unsaturated bond, avoiding the production of succinic acid at yields as high as the ones observed for VA and pHBA oxidation.

Summarizing, it can be concluded that syringic acid oxidation produced mainly succinic acid at a higher selectivity. However, vanillic acid produced succinic acid yielding higher (5.3 wt%) than syringic acid oxidation (3.8 wt%). The oxidation of pHBA gave rise to the highest succinic acid yield (up to 5.7 wt% after 4 hours), but mixed with other acids at higher concentrations, with the disadvantage of needing several hours to achieve a competitive yield when compared to the faster reaction undergone by VA and SA. Regarding other C_4-DCA, only VA produced malic acid at significant yields, while pHBA produced unsaturated C_4-DCA.

4.3.3 Oxidation of hardwood

Lignin was oxidized to evaluate using real samples the behavior observed with model compounds. For that reason, two lignins with different proportions of structural units, one from softwood and another from hardwood, were chosen. Both lignins are derived from the kraft pulping process, avoiding any difference associated with the pulping process. Indulin AT, selected as the softwood lignin, is commercialized by MeadWestvaco Corporation, USA, having an S:G:H ratio of 0:97:3 (Constant et al., 2016). The hardwood lignin was isolated from a black liquor obtained from a *Eucalyptus globulus* kraft pulping mill (The Navigator Company, Portugal), presenting an S:G:H ratio of 65:29:6 (Costa et al., 2018). The two lignins were chosen to represent kraft hardwood and softwood lignins. Since it was not possible to find hardwood and softwood lignins from the same provider, thus guaranteeing the application of the same process, this option was considered adequate to conduct the present study. Both lignins were solubilized in a 0.1 mol/L phosphate buffer to ensure that the lignin was at a pH around 7 during the oxidation process, avoiding precipitation in an acidic environment. However, this buffer caused a partial degradation of peroxide inside the reactor, lowering its oxidation potential.

Figure 4.13 summarizes the results obtained for Indulin AT (softwood lignin) conversion after 4 hours, which was 68%. The amount of monocarboxylic acids (obtained from lignin degradation into C_4-DCA) increased up to 14 wt% after 4 hours. Malic and succinic acids were the main obtained DCA; the malic acid yield was high at the reaction starting (8.0 wt% at 10 min), but then decreased to 1.0 wt% after 4 hours, while succinic acid yield increased slowly, reaching a maximum of 2.5 wt% at the end of the reaction

(240 min). Small quantities of maleic and fumaric acids were also observed but at yields lower than 0.30 wt%.

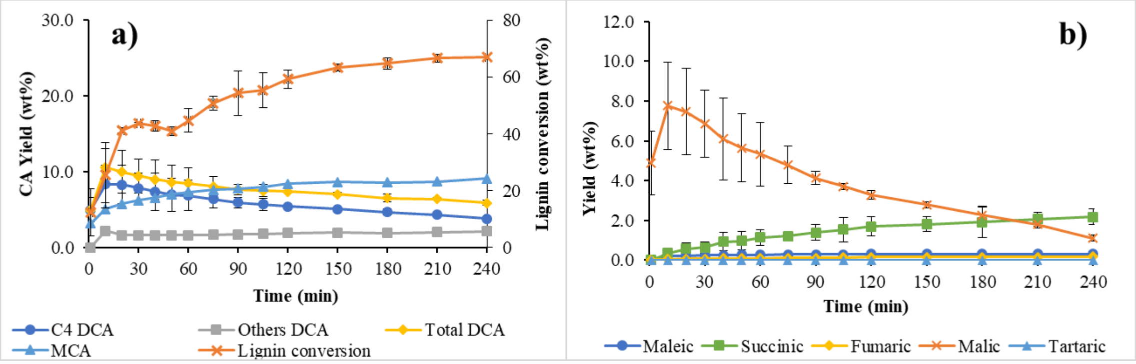

Figure 4.13 - Indulin AT lignin oxidation with H_2O_2, at 140°C; **(a)** CA yield (C_4-DCA [dicarboxylic acids], other DCA, and monocarboxylic acids [MCA]) and lignin conversion, and **(b)** C_4-DCA yield.

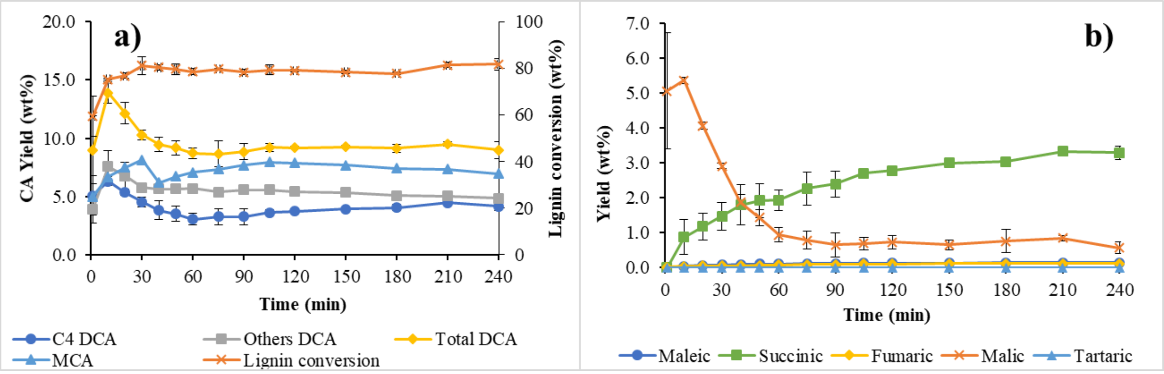

Figure 4.14 - Hardwood lignin oxidation with H_2O_2, at 140°C; **(a)** CA yield (C_4-DCA [dicarboxylic acids], other DCA and monocarboxylic acids [MCA]) and lignin conversion, and **(b)** C_4-DCA yield.

Figure 4.14 illustrates that *E. globulus* kraft lignin (hardwood lignin) oxidation reached a total conversion of 83% after 30 minutes, then remaining practically constant. C_4-DCA were also produced in the first minutes, while the monocarboxylic acids yield increased, but only slightly compared to softwood lignin. The main obtained DCA were also malic and succinic acids. Malic acid showed the same behavior as the one observed for Indulin AT lignin, i.e., achieving a high yield at the starting of the reaction (5.3 wt% at 10 min) but then decreasing quickly to 0.5 wt% after 4 hours. Succinic acid yield increased, reaching a maximum of 3.2 wt%. Small quantities of maleic and fumaric acids were detected but at yields lower than 0.13 wt%.

The presence of malic acid during the first minutes of the reaction was associated with the high content of guaiacyl units in both lignins, which resulted in similar to the one observed for VA oxidation. In this case, softwood lignin was composed mainly of guaiacyl units and produced more malic acid than hardwood lignin, which has an S:G ratio of 65:29. However, the higher yield of malic acid observed during the reaction starting phase in both lignins, comparatively with VA oxidation, could be caused by the solution's slightly different pH conditions. When lignins were oxidized, the buffer kept the pH around 6.5-7.0 during the overall reaction avoiding lignin precipitation. In contrast, in the model compounds oxidation, which was done without a buffer, the medium was quickly acidified and then back to neutral pH (Figure 4.5). When the reaction took place at higher pH, there was a higher chance to obtain hydroxylated compounds in the peroxide oxidation, as previously reported in Chapter 3. During the first minutes of model compound oxidation, the acidic pH could prevent the malic acid formation at high yields, converting any produced malic acid to succinic acid. Even though malic acid was obtained at high yields during the first minutes of lignin oxidation, it was quickly converted to succinic acid or degraded to low-molecular-weight compounds due to the slightly acidic environment.

E. globulus kraft lignin gave rise to the highest conversion in the first 30 minutes, while Indulin AT needed more than 210 minutes to reach the highest conversion, but without attaining the level achieved for hardwood lignin. It has been reported that hardwood lignins are more reactive towards peroxide oxidation when compared to softwood lignins due to structural differences (Hasegawa et al., 2011; Ma et al., 2018). Since the hardwood lignin had a higher S:G ratio, it became more reactive against peroxide oxidation due to the high content of S units, which was also observed in SA comparatively to VA.

VA showed higher succinic acid yield than SA oxidation, so softwood lignin was expected to result in higher succinic acid yield, based only on the lower S:G ratio (due to higher content on guaiacyl units). However, due to S groups' higher reactivity, hardwood lignin (with a higher S:G ratio) had a higher reactivity and was degraded easier. This fact helped open the lignin structure, making more lignin fractions available for further oxidation towards DCA and presenting a slightly better succinic acid yield, as observed in Figure 4.14. It was also noticed that *E. globulus* kraft lignin oxidation produced succinic acid faster than Indulin AT lignin, while malic acid was also degraded more quickly. In several works, lignin peroxide oxidation using lignins with a high S:G ratio showed a higher yield for dicarboxylic acids than lignins based on guaiacyl moieties (softwood lignins), especially under acidic pH (Bi et al., 2018; Ma et al., 2018, 2014; Xiang and Lee, 2000). Ma et al. (Ma et al., 2018) reported that a higher amount of methoxy groups in lignin had a positive effect on the total dicarboxylic acid yield (quantified in their work as C_2-C_6 DCA, and not only C_4-DCA), while the presence of these groups had a negative influence in lignin depolymerization to monomeric phenolic compounds. Although methoxy groups apparently hindered lignin depolymerization to phenolic compounds, they activated the aromatic ring creating electron-rich areas that competed with the alkyl side chains between aromatic lignin monomeric units enhancing ring-opening reactions. Hardwood lignin showed a higher yield of total DCA, as seen in Figure 4.13a. and Figure 4.14a. Therefore, this work's findings corroborated the model proposed by Ma et al. for DCA production, even though that model was not entirely focused on C_4-DCA. Still, DCA yield changed through time, especially with softwood lignin (due to malic acid degradation), which was not considered in their model. They evaluated a specific point of the reaction time and not the variations along time giving rise to DCA production and degradation.

In conclusion, the *E. globulus* kraft lignin seems to be a better lignin than Indulin AT to obtain succinic acid by peroxide oxidation. It was degraded faster than Indulin AT lignin, produced malic acid, and other acids at lower yields, and gave rise to succinic acid at higher yields through a faster reaction. This finding confirmed that lignins with a higher S:G ratio could be better for peroxide oxidation and ring-opening reactions towards C_4-DCA, especially succinic acid. However, it should be noted that a more detailed analysis should include the different bonding structures of lignin, which varies from biomass to biomass, and the used pulping techniques. Namely, lignins with high condensation degrees have been reported as very stable towards oxidation. Future works must be conducted to increase and optimize C_4-DCA yields, considering the type and origin of lignin, the reactor design, and the presence of catalysts. Moreover, the profit exploitation of lignin must consider a cascade of products in its value chain, for which C_4-DCAs can contribute.

4.4 Conclusions

This study demonstrated that *p*-hydroxybenzoic acid, vanillic acid, and syringic acid peroxide oxidation produced C_4 dicarboxylic acids (succinic, malic, fumaric, maleic, and tartaric acids) at different contents, yields, and kinetics, which was justified by the different amounts of methoxy groups present in the aromatic structure. SA had the higher reactivity towards oxidation, while pHBA had the lower one due to the activation effect of the methoxy groups in the aromatic ring. The observed succinic acid yield followed the relation pHBA>VA>SA but needing longer times for pHBA to reach a competitive yield. VA and pHBA produced other C_4-DCA besides succinic acid, being SA oxidation much more selective towards succinic acid.

When two lignins with different S:G:H ratios were oxidized, softwood lignin (Indulin AT) produced a lower amount of succinic acid than hardwood lignin (lignin obtained from *Eucalyptus globulus* black liquor). Moreover, the hardwood lignin reacted faster than the softwood lignin due to the higher reactivity observed in syringyl units. Both lignins produced malic acid at an initially high yield, then converted to other compounds during the reaction time. Summarizing, it can be concluded that lignins richer in syringyl groups have a higher reactivity towards peroxide oxidation reactions. They are converted faster, producing succinic acid at higher yields, justified by the activation effect of methoxy groups in aromatic rings.

4.5 References

Barclay, L.R.C., Vinqvist, M.R., 2003. Phenols as Antioxidants, in: Rappoport, Z. (Ed.), The Chemistry of Phenols. John Wiley & Sons, Ltd, Chichester, UK, pp. 839–908. https://doi.org/10.1002/0470857277.ch12

Bhargava, S.K., Tardio, J., Prasad, J., Föger, K., Akolekar, D.B., Grocott, S.C., 2006. Wet oxidation and catalytic wet oxidation. Ind. Eng. Chem. Res. 45, 1221–1258. https://doi.org/10.1021/ie051059n

Bi, Z., Li, Z., Yan, L., 2018. Catalytic oxidation of lignin to dicarboxylic acid over the $CuFeS_2$ nanoparticle catalyst. Green Process. Synth. 7, 306–315.

https://doi.org/10.1515/gps-2017-0056

Brunow, G., 2005. Lignin Chemistry and its Role in Biomass Conversion, in: Kamm, B., Gruber, P.R., Kamm, M. (Eds.), Biorefineries-Industrial Processes and Products. Wiley-VCH Verlag GmbH, Weinheim, Germany, pp. 151–163. https://doi.org/10.1002/9783527619849.ch21

Casimiro, F.M., Costa, C.A.E.E., Botelho, C.M., Barreiro, M.F., Rodrigues, A.E., 2019. Kinetics of oxidative degradation of lignin-based phenolic compounds in batch reactor. Ind. Eng. Chem. Res. 58, 16442–16449. https://doi.org/10.1021/acs.iecr.9b02818

Constant, S., Wienk, H.L.J., Frissen, A.E., Peinder, P. De, Boelens, R., Van Es, D.S., Grisel, R.J.H., Weckhuysen, B.M., Huijgen, W.J.J., Gosselink, R.J.A., Bruijnincx, P.C.A., 2016. New insights into the structure and composition of technical lignins: A comparative characterisation study. Green Chem. 18, 2651–2665. https://doi.org/10.1039/c5gc03043a

Costa, C.A.E.E., Pinto, P.C.R.R., Rodrigues, A.E., 2018. Lignin fractionation from E. Globulus kraft liquor by ultrafiltration in a three stage membrane sequence. Sep. Purif. Technol. 192, 140–151. https://doi.org/10.1016/j.seppur.2017.09.066

Cronin, D.J., Dunn, K., Zhang, X., Doherty, W.O.S.S., 2017a. Relating Dicarboxylic Acid Yield to Residual Lignin Structural Features. ACS Sustain. Chem. Eng. 5, 11695–11705. https://doi.org/10.1021/acssuschemeng.7b03164

Cronin, D.J., Zhang, X., Bartley, J., Doherty, W.O.S.S., 2017b. Lignin Depolymerization to Dicarboxylic Acids with Sodium Percarbonate. ACS Sustain. Chem. Eng. 5, 6253–6260. https://doi.org/10.1021/acssuschemeng.7b01208

Di Marino, D., Jestel, T., Marks, C., Viell, J., Blindert, M., Kriescher, S.M.A., Spiess, A.C., Wessling, M., 2019. Carboxylic Acids Production via Electrochemical Depolymerization of Lignin. ChemElectroChem 6, 1434–1442. https://doi.org/10.1002/celc.201801676

Du, G., Liu, L., Chen, J., 2015. White Biotechnology for Organic Acids, in: Pandey, A., Höfer, R., Taherzadeh, M., Nampoothiri, K.M., Larroche, C. (Eds.), Industrial Biorefineries & White Biotechnology. Elsevier, pp. 409–444. https://doi.org/10.1016/B978-0-444-63453-5.00013-6

Evstigneyev, E.I., Shevchenko, S.M., 2019. Structure, chemical reactivity and solubility of lignin: a fresh look. Wood Sci. Technol. 53, 7–47. https://doi.org/10.1007/s00226-018-1059-1

Gierer, J., 1986. Chemistry of Delignification- Part 2: Reactions of lignins during bleaching. Wood Sci. Technol. 20, 1–33. https://doi.org/10.1007/BF00350692

Gierer, J., Yang, E., Reitberger, T., 1994. On the significance of the superoxide radical (O2-/HO2·) in oxidative delignification, studied with 4-t-butylsyringol and 4-t-butylguaiacol part i. the mechanisrn of aromatic ring opening. Holzforschung 48, 405–414. https://doi.org/10.1515/hfsg.1994.48.5.405

Gillet, S., Aguedo, M., Petitjean, L., Morais, A.R.C., da Costa Lopes, A.M., Łukasik, R.M., Anastas, P.T., 2017. Lignin transformations for high value applications: towards targeted modifications using green chemistry. Green Chem. 19, 4200–4233. https://doi.org/10.1039/C7GC01479A

Hasegawa, I., Inoue, Y., Muranaka, Y., Yasukawa, T., Mae, K., 2011. Selective production of organic acids and depolymerization of lignin by hydrothermal oxidation with diluted hydrogen peroxide. Energy and Fuels 25, 791–796. https://doi.org/10.1021/ef101477d

Kang, J., Irmak, S., Wilkins, M., 2019. Conversion of lignin into renewable carboxylic acid compounds by advanced oxidation processes. Renew. Energy 135, 951–962. https://doi.org/10.1016/j.renene.2018.12.076

Li, C., Zhao, X., Wang, A., Huber, G.W., Zhang, T., 2015. Catalytic Transformation of Lignin for the Production of Chemicals and Fuels. Chem. Rev. 115, 11559–11624. https://doi.org/10.1021/acs.chemrev.5b00155

Li, X., Zheng, Y., 2020. Biotransformation of lignin: Mechanisms, applications and future work. Biotechnol. Prog. 36, 1–21. https://doi.org/10.1002/btpr.2922

Lide, D.R., 2009. CRC Handbook of Chemistry and Physics, 90th Edition (CD-ROM Version 2010), Journal of the American Chemical Society. https://doi.org/10.1021/ja906434c

Ma, R., Guo, M., Zhang, X., 2014. Selective Conversion of Biorefinery Lignin into Dicarboxylic Acids. ChemSusChem 7, 412–415.

https://doi.org/10.1002/cssc.201300964

Ma, R., Xu, Y., Zhang, X., 2015. Catalytic Oxidation of Biorefinery Lignin to Value-added Chemicals to Support Sustainable Biofuel Production. ChemSusChem 8, 24–51. https://doi.org/10.1002/cssc.201402503

Ma, R., Zhang, X.X., Wang, Y., Zhang, X.X., 2018. New insights toward quantitative relationships between lignin reactivity to monomers and their structural characteristics. ChemSusChem 11, 2146–2155. https://doi.org/10.1002/cssc.201800550

Mohajeri, A., Asemani, S.S., 2009. Theoretical investigation on antioxidant activity of vitamins and phenolic acids for designing a novel antioxidant. J. Mol. Struct. 930, 15–20. https://doi.org/10.1016/j.molstruc.2009.04.031

Ponnusamy, V.K., Nguyen, D.D., Dharmaraja, J., Shobana, S., Banu, J.R., Saratale, R.G., Chang, S.W., Kumar, G., 2019. A review on lignin structure, pretreatments, fermentation reactions and biorefinery potential. Bioresour. Technol. 271, 462–472. https://doi.org/10.1016/j.biortech.2018.09.070

Ragnar, M., Lindgren, C.T., Nilvebrant, N.-O., 2000. pK a -Values of Guaiacyl and Syringyl Phenols Related to Lignin. J. Wood Chem. Technol. 20, 277–305. https://doi.org/10.1080/02773810009349637

Rodrigues, A.E., Pinto, P.C. de O.R., Barreiro, M.F., Esteves da Costa, C.A., Ferreira da Mota, M.I., Fernandes, I., 2018. An Integrated Approach for Added-Value Products from Lignocellulosic Biorefineries. Springer International Publishing, Cham. https://doi.org/10.1007/978-3-319-99313-3

Rohde, V., Böringer, S., Tübke, B., Adam, C., Dahmen, N., Schmiedl, D., 2019. Fractionation of three different lignins by thermal separation techniques-A comparative study. GCB Bioenergy 11, 206–217. https://doi.org/10.1111/gcbb.12546

Santos, G.T.A.D., Santos, P.S.M., Duarte, A.C., 2016. Vanillic and syringic acids from biomass burning: Behaviour during Fenton-like oxidation in atmospheric aqueous phase and in the absence of light. J. Hazard. Mater. 313, 201–208. https://doi.org/10.1016/j.jhazmat.2016.04.006

Schutyser, W., Kruger, J.S., Robinson, A.M., Katahira, R., Brandner, D.G., Cleveland, N.S., Mittal, A., Peterson, D.J., Meilan, R., Román-Leshkov, Y., Beckham, G.T., 2018. Revisiting alkaline aerobic lignin oxidation. Green Chem. 20, 3828–3844. https://doi.org/10.1039/C8GC00502H

Smith, M.B., March, J., 2006. March's Advanced Organic Chemistry, 6th Ed. ed, March's Advanced Organic Chemistry. John Wiley & Sons, Inc., Hoboken, NJ, USA. https://doi.org/10.1002/0470084960

Sun, Y.-P.P., Nguyen, K.L., Wallis, A.F.A.A., 1998. Ring-Opened Products from Reaction of Lignin Model Compounds with UV-Assisted Peroxide. Holzforschung 52, 61–66. https://doi.org/10.1515/hfsg.1998.52.1.61

Sun, Y., Fenster, M., Yu, A., Berry, R.M., Argyropoulos, D.S., 1999. The effect of metal ions on the reaction of hydrogen peroxide with Kraft lignin model compounds. Can. J. Chem. 77, 667–675. https://doi.org/10.1139/v99-036

Sun, Z., Fridrich, B., De Santi, A., Elangovan, S., Barta, K., 2018. Bright Side of Lignin Depolymerization: Toward New Platform Chemicals. Chem. Rev. 118, 614–678. https://doi.org/10.1021/acs.chemrev.7b00588

Suzuki, H., Cao, J., Jin, F., Kishita, A., Enomoto, H., Moriya, T., 2006. Wet oxidation of lignin model compounds and acetic acid production. J. Mater. Sci. 41, 1591–1597. https://doi.org/10.1007/s10853-006-4653-9

Tarabanko, V., Tarabanko, N., 2017. Catalytic Oxidation of Lignins into the Aromatic Aldehydes: General Process Trends and Development Prospects. Int. J. Mol. Sci. 18, 2421. https://doi.org/10.3390/ijms18112421

Upton, B.M., Kasko, A.M., 2016. Strategies for the conversion of lignin to high-value polymeric materials: Review and perspective. Chem. Rev. 116, 2275–2306. https://doi.org/10.1021/acs.chemrev.5b00345

Vega-Aguilar, C.A., Barreiro, M.F., Rodrigues, A.E., 2020. Catalytic wet peroxide oxidation of vanillic acid as a lignin model compound towards the renewable production of dicarboxylic acids. Chem. Eng. Res. Des. 159, 115–124. https://doi.org/10.1016/j.cherd.2020.04.021

Wendisch, V.F., Kim, Y., Lee, J.H., 2018. Chemicals from lignin: Recent depolymerization techniques and upgrading extended pathways. Curr. Opin. Green

Sustain. Chem. 14, 33–39. https://doi.org/10.1016/j.cogsc.2018.05.006

Werpy, T., Petersen, G., 2004. Top Value Added Chemicals from Biomass: Volume I -- Results of Screening for Potential Candidates from Sugars and Synthesis Gas., U.S. Department of energy. United States. https://doi.org/10.2172/926125

Xiang, Q., Lee, Y.Y., 2000. Oxidative cracking of precipitated hardwood lignin by hydrogen peroxide. Appl. Biochem. Biotechnol. 84–86, 153–162. https://doi.org/10.1385/ABAB:84-86:1-9:153

Zeng, J., Yoo, C.G., Wang, F., Pan, X., Vermerris, W., Tong, Z., 2015. Biomimetic fenton-catalyzed lignin depolymerization to high-value aromatics and dicarboxylic acids. ChemSusChem 8, 861–871. https://doi.org/10.1002/cssc.201403128

5. Lignin wet peroxide oxidation with TS-1

Lignin valorisation towards added-value products has become a relevant topic to consolidate a future circular bioeconomy. In this context, lignin oxidation to C_4 dicarboxylic acids by catalytic wet peroxide oxidation is emerging as a value-added strategy, supported by the extensive use of these building blocks in several industrial fields. After testing the catalytic properties of Titanium Silicalite 1 (TS-1) catalyst for C_4-DCA production on lignin model compounds, oxidation experiments should be performed on technical lignins to assess the best reaction conditions.

In this chapter, four lignins from different sources (Indulin AT, Lignol, Aldrich Alkali and *E. globulus* kraft lignins) were oxidised using H_2O_2 and TS-1 catalyst under different operating conditions (temperature, pH, time, H_2O_2, and TS-1 load). Lignin conversion and individual C_4-DCA yields are presented and discussed accordingly to the studied effect and the type of lignin used for oxidation, showing that Indulin AT produced the highest succinic acid yield, while Lignol achieved the highest malic acid yield. All reaction conditions affected the C_4-DCA yields. The TS-1 reusability was also tested after several cycles, being confirmed as reusable and stable in the reaction conditions.

This Chapter is adapted from Vega-Aguilar, C.A.; Barreiro, M.F.; Rodrigues, A. E., “Lignin conversion into C_4 dicarboxylic acids by catalytic wet peroxide oxidation using titanium silicalite-1”. *Industrial Crops and Products*, **2021**, 173, 114155. DOI: 10.1016/j.indcrop.2021.114155

5.1 Introduction

Lignin is obtained as a by-product in pulp mills, where it is burned in the recovery boiler to produce energy and heat. However, this step is usually considered a bottleneck in pulp production (Ahmad et al., 2020; Mathias, 1993). Consequently, using part of this residual lignin as a raw material for conversion to added-value products would improve the sustainability of the pulping industry without affecting pulp production and the energy balance of the mill (Junghans et al., 2020; Rodrigues et al., 2018; Silva et al., 2009).

The physical and chemical properties of technical lignins change depending on the feedstock source, the pulping process, and the isolation method (Kienberger et al., 2021). Lignin structure is based on three monomers: *p*-hydroxyphenyl (H), guaiacyl (G), and syringyl (S), which are present in different ratios and linked differently depending on the biomass origin (Kamm et al., 2008; Upton and Kasko, 2016). Softwood lignin usually has a high G:H ratio and no S units. Units are linked by *β-O-4* (43-50%), *5-5'* (10-25%), *β-5 + α-O-4* (9-12%) linkages, among others. Hardwood is an S:G:H lignin with a higher S content. Units are linked by *β-O-4* (50-65%), *5-5'* (4-10%), *α-O-5* (4-8%), and *α-O-5'* (6-8%) linkages, among others (Rodrigues Pinto et al., 2011). These structural differences introduce challenges for the depolymerisation and upgrading of the recalcitrant lignin matrix. Cooking methods focused on high-quality cellulose, such as Kraft, sulfite, and alkaline processes, use harsh conditions to achieve their objective, causing strong modifications in the lignin structure (Sun et al., 2018). The alkali process cleaves many of the ester and ether bonds between lignin and carbohydrates, and also some of the lignin *C-C* bonds (Kim et al., 2016). Kraft process produces a highly modified and partially fragmented lignin, with α-aryl ether and β-aryl ether linkages cleavage, recondensation reactions, and sulphur incorporation (Li et al., 2015; Sun et al., 2018). Other milder extraction processes, such as ionic liquid extraction, organosolv, and milled-wood lignin, cause fewer modifications to the lignin structure. Organosolv uses organic solvents, such as primary alcohols, alone or mixed with water at high temperatures and pressures, and produces lignins with structures closer to the native one, with slight modifications like cleavage of *β-O-4* linkages, repolymerizations, and formation of new *C-C* bonds (Sun et al., 2018).

Depolymerisation is an important route to achieve new products from the lignin. Oxidative lignin depolymerisation has several advantages, leading to the incorporation of new functional groups (e.g., alcohol, aldehydes, and carboxylic groups) and production of low-molecular-weight fractions, giving rise to added-value products such as phenolics, dicarboxylic acids, and others. However, it remains challenging to overcome the low selectivity towards target products and circumvent the over-oxidation to gaseous compounds (Ahmad et al., 2020; Liu et al., 2019). C_4 dicarboxylic acids, currently derived from petrochemical sources and carbohydrates fermentation routes, are used in several fields as final products (e.g. food additives) and as raw materials for pharmaceuticals and polymer industries (Zhang et al., 2020). They are also pointed out as the biomass-derived building blocks for future development of a greener chemistry (Jong et al., 2011; Werpy and Petersen, 2004). Therefore, achieving C_4 dicarboxylic acids from lignin would allow the attainment of added-value products without competing with food and fossil resources.

Non-catalytic lignin oxidative depolymerisation has been previously reported with succinic and maleic acids yields lower than 3% (Abdelaziz et al., 2019; Demesa et al., 2015; Figueirêdo et al., 2019; Hasegawa et al., 2011). Better results were obtained with catalytic oxidation, especially in the presence of heterogeneous catalysts, such as perovskite-type oxides, chalcopyrite, and heteropoly acids (i.e., phosphotungstic and phosphomolybdic acids) (Ansaloni et al., 2017; Bi et al., 2018; Cronin et al., 2017; Demesa et al., 2017; Ma et al., 2014). The use of Fenton reagent (Fe^{2+}/H_2O_2) gave rise up to 8% maleic acid with phenol (Faisal, 2009), although with other lignin model compounds, the yield was lower than 2% (Kang et al., 2019). When lignin was used, no C_4-DCA were obtained (Zeng et al., 2015), suggesting that this oxidation methodology is not an efficient strategy for lignin depolymerisation towards C_4-DCA. Perovskite-type oxides have also been tested due to their oxidative activity and the presence in their structure of transition metals with two different oxidation states. However, catalysts like $LaFeO_3$, $LaMnO_3$, and $CeFeO_3$ showed no improvement for C_4-DCA production comparatively with non-catalysed experiments (Ansaloni et al., 2017). Chalcopyrite ($CuFeS_2$) has been used with lignin and lignin model compounds with good results. Namely, catechol oxidation yielded 6% malic acid and 8% succinic acid, and diluted-acid corn stove lignin oxidation yielded 7% succinic acid and 1% malic acid (Ma et al., 2014). Chalcopyrite nanoparticles in acidic pH enhanced succinic acid yield up to 12% when an industrial lignin was oxidized, accompanied by low fumaric and maleic acids yields (Bi et al., 2018), confirming that acid yields are dependent on the used oxidation reaction conditions. Heteropoly acids (i.e., phosphotungstic acid ($H_3PW_{12}O_{40}$) and phosphomolybdic acid ($H_3PMo_{12}O_{40}$)) showed low improvement for succinic acid yield, with disadvantages such as higher costs and recovering difficulties (Demesa et al., 2017). Other catalysts based on V and Mo oxides or pyrophosphates (deposited in materials like Al_2O_3, TiO_2, and HZSM-5), used in lignin gas-phase oxidation gave rise to no more than 2% of succinic acid (Lotfi et al., 2016, 2015). In most of these studies, significant amounts of oxalic, formic, and acetic acids were obtained (as degradation products of lignin over-oxidation). Still, the final yield and C_4-DCA type varied according to the used catalyst and applied reaction conditions. In most of these works, succinic acid yield varied between trace levels up to 2-3 wt% (lignin-basis), while maleic and fumaric acids were reported to be obtained at contents less than 1%.

Different oxidants, such as O_2, H_2O_2, O_3, and peroxy acids, have enough oxidative power to break down most ether linkages and some C-C linkages (Ma et al., 2018a). However, to cause ring-opening reactions to achieve dicarboxylic acids, a strong oxidant is needed (Sun and Argyropoulos, 1996). O_2 oxidation occurs only in alkaline conditions and is usually intended for mild oxidation to achieve aldehydes. Its oxidative power is relatively low to origin ring-opening reactions at high yields (Cabral Almada et al., 2020; Li et al., 2015). Peroxide oxidation is more active than O_2 oxidation by eliminating liquid/gas mass transfer barriers and releasing free radicals, allowing faster oxidations in milder and cleaner conditions (Bhargava et al., 2006; Cheng et al., 2017). H_2O_2 oxidation causes the cleavage of *β-O-4* linkages, forming non-condensed structures, especially in softwood lignins. In hardwood lignins, demethoxylation of S units to G units happens, which could be repolymerized, increasing the condensed OH structures (Ahmad et al., 2020). These small fragments can further have the aromatic ring cleaved to dicarboxylic acids. Ozone can also be used for lignin oxidation, leading to ring-opening reactions and generating C_4-DCA (Figueirêdo et al., 2019). However, O_3 handling can be complex since it has to be generated *in situ* (Ahmad et al., 2020). Recently, electrochemical depolymerisation was used for lignin oxidation, releasing O_2 and H_2O_2 *in situ*; however, this technique leads to small amounts of C_4-DCA (Di Marino et al., 2019).

Among the catalysts enhancing H_2O_2 oxidative power, titanium silicalite-1 catalyst (TS-1) has been used for lignin model compounds peroxide oxidation to C_4-DCA with good results. Namely, it was reported that guaiacol is oxidised mainly to maleic acid, while vanillic acid is primarily converted to succinic acid, an important feedstock for renewable polymer production (Su et al., 2014). This catalyst has an MFI zeolite structure, with less than 3% TiO_2 and hydrophobic properties, allowing the oxidation of non-polar compounds in aqueous medium, such as phenolic compounds (Clerici, 2015; Gamba et al., 2009). The active species in the TS-1 catalysed peroxide oxidation is the Ti-OOH group, which shows better reactivity than H_2O_2 (Clerici, 2015).

Under the current state of the art, the catalytic peroxide oxidation of lignin to C_4-DCA using TS-1 catalyst is still lacking. Given the reported advantages of this catalyst towards the production of C_4-DCA, namely the previous studies conducted with model compounds, its use to improve the production yield of target acids (e.g. succinic acid) from lignin is a promising strategy towards circular economy. Therefore, in this work, lignins from different origins (Indulin AT, Lignol, Alkali and *E. globulus* kraft lignins) were oxidised using H_2O_2 and TS-1 catalyst focusing C_4-DCA production, especially succinic acid. Moreover, the stability of the TS-1 catalyst to the applied reaction conditions, taking as reference 5 consecutive utilizations, was also be studied.

5.2 Materials and methods

5.2.1 Materials

All chemical reagents were purchased from commercial sources and used without further purification: formic acid (Chem-labs, >99%), sulfuric acid (Chem-labs, 95-97% p.a.), sodium hydroxide (Merck, p.a.), hydrogen peroxide solution (Fluka, >30% p.a.), N,N-dimethylformamide (VWR, ≥99.9%) and lithium chloride (VWR, AnalaR NORMAPUR). Catalyst TS-1 (ref. #: MSTS1001, lot number: 130117; H^+ cation) was acquired from ACS Materials, LLC.

Four different lignins were studied: Alkali lignin (ALK), commercialised by Aldrich (product number 471003, batch #09724CE); Indulin AT (IAT), commercialised by MeadWestvaco Corporation, USA; a lignin isolated from an industrial black liquor obtained from a Portuguese *Eucalyptus globulus* Kraft pulping mill (The Navigator

Company, Portugal) (EKL); and a lignin produced by an ethanol organosolv process from *Eucalyptus globulus* (EOL), supplied by Lignol Innovations, Canada.

5.2.2 Oxidation Procedure

Lignins were oxidised in closed steel reactors (20 mL), described in Chapter 3 (Section 3.2.2.), using 5.00 mL of a 10.0 g/L lignin solution (dissolved in ultra-pure water), 0.500 mL of a 30 wt% H_2O_2 solution, and 5.0 mg of TS-1 catalyst (10 wt%, lignin-basis). The effect of pH (4.0-10.0), temperature (100-160ºC), reaction time (0-8 h), catalyst amount (0-15 wt%), and H_2O_2 volume (0.25-0.75 mL) on the selected DCA (succinic, fumaric, maleic, malic, tartaric, acetic, oxalic, and formic acids) yield was studied. Experiments were done in duplicate. The study of the effect of each parameter was performed under the following specific reaction conditions: pH effect (2 h, 140ºC, 10% catalyst, 0.50 mL H_2O_2), temperature effect (2 h, pH 7, 10% catalyst, 0.50 mL H_2O_2), reaction time effect (pH 7, 140ºC, 10% catalyst, 0.50 mL H_2O_2); catalyst amount effect (2 h, pH 7, 140ºC, 0.50 mL H_2O_2), and H_2O_2 volume effect (2 h, pH 7, 140ºC, 10% catalyst).

Reutilization of the TS-1 catalyst was done through its use in consecutive experiments. For that, the catalyst was washed with acidified water, centrifuged at 3500 rpm for 30 minutes, and then transferred, dispersed in 1.0 mL of water, to the reaction flask for the subsequent reaction. After the 5th run, the catalyst was dried at 100ºC overnight and then analysed by SEM.

5.2.3 Lignin quantification

Oxidized lignin samples were acidified to pH~2, heated at 40°C to coagulate the acid-insoluble lignin, then centrifuged at 3500 rpm for 30 minutes. The acidic supernatant was used for carboxylic acid and acid-soluble lignin quantification. The insoluble lignin was resolubilised in an alkaline solution. Acid-soluble and insoluble lignin solutions were analysed by UV spectrophotometry at 240 nm, and quantified based on a calibration curve done with the acid-soluble and insoluble lignin obtained from the respective original lignin, respectively. Lignin conversion was calculated as the sum of the acid-insoluble and the acid-soluble lignins. Calibration curves for acid-soluble and insoluble lignins can be found in Fig A.1, in Appendix A.

5.2.4 Carboxylic acids quantification

Carboxylic acids were quantified by high-performance liquid chromatography (HPLC) analysis using a Shimadzu UFLC, equipped with a Diode Array Detector (210 nm), a refractive index detector (RI), and a Phenomenex® Rezex™ ROA H^+ column (300 mm x 7.8 mm) and precolumn (50 mm x 7.8 mm). The analysis was performed at 50°C using isocratic mode (4 mmol/L H_2SO_4) at a flowrate of 0.5 mL/min and an injection volume of 20 µL. Carboxylic acids were identified and quantified using calibration curves prepared from individual standards. Samples were diluted as needed and filtered through a 0.22 µm pore-size filter before injection. Calibration curves can be found in Table A.2, in Appendix A.

Quantified acids are expressed as *C_4-DCA* (succinic, malic, maleic, fumaric, and tartaric acids), *Total DCA* (C_4-DCA + malonic acid + oxalic acid), and *MCA* (monocarboxylic acids: acetic and formic acid).

5.2.5 Lignin molecular weight determination

Gel permeation chromatography (GPC) was used to evaluate lignin molecular weight and polydispersity index. Calibration was done using polystyrene (PS) standards, in the molecular weight range comprised between 162 and 50 000 g/mol (calibration curve can be seen in Fig A.3, in Appendix A). A Shimadzu UFLC, equipped with a Diode Array Detector (280 nm) was used with two Agilent columns in series: first an OligoPore column (300 x 7.5 mm, 6 µm nominal partical size) and then a MesoPore column (300 x 7.5 mm, 3 µm nominal partical size). Prior to this arrange, a OligoPore pre-column (300 x 7.5 mm) was used. Analysis was performed at 70ºC, using dimethylformamide with 0.5 wt% LiCl, at 0.8 mL/min. More details about the applied method can be found elsewhere (Costa et al., 2018).

5.2.6 ATR-FTIR spectroscopic analysis of lignin

Attenuated total reflectance- Fourier transform Infrared Spectroscopy (ATR-FTIR) measurements were carried out using a JASCO FT/IR-6800 spectrometer (JASCO Analytical Instruments, USA), equipped with a MIRacle™ Single Reflection (ZnSe crystal plate; PIKE Technologies, USA). The analysis was performed using 256 scans, in the 4000-700 cm^{-1} region, with a 4 cm^{-1} resolution.

5.2.7 Catalyst characterization

Scanning electron microscopy (SEM) and Energy-dispersive X-ray spectroscopy (EDS) were used to analyse the physical structure of the catalyst before and after oxidations, especially when it was reused. The analysis was performed in the Materials Centre of the University of Porto (CEMUP), following the procedure and equipment reported in Chapter 3 (Section 3.2.6). Briefly, samples were coated with Au/Pd (15 mA, 80s), then analysed in a Quanta 400 FEG ESEM/EDAX Genesis X4M equipment, using high vacuum, 15 keV, 10 mm working distance and a 50 Lsec collection time.

5.3 Results and discussion

5.3.1 Lignin characterization

The studied lignins correspond to products available from commercial processes. Alkali (ALK), Indulin AT (IAT), and ethanol organosolv lignin (EOL) were received in powder form, and no further purification or treatments were done. Regarding *E. globulus* kraft lignin (EKL), received as black liquor, it was isolated by the acid precipitation method (Costa et al., 2018).

The selected lignins are products of different pulping processes and proceed from distinct biomass feedstocks. IAT and EKL are softwood and hardwood Kraft lignins, respectively. ALK is an alkali softwood, and EOL a hardwood organosolv (ethanol) lignin. The different pulping processes and feedstock origin affects lignin's physical and chemical properties, influencing their reactivity towards oxidation and thus the production (type and yield) of C_4-DCA.

The main characteristics of the used lignins are reported in Table 5.1. Molecular weight (in weight and number; M_w and M_n, respectively) and polydispersity index (M_w/M_n) were obtained in the present work. The other features, namely S:G:H ratio, lignin content and ash content, are reference values obtained from literature. Concerning molecular weight, all the studied lignins have similar M_w (around 8300-13600 g/mol) but variable M_n and polydispersity index ($Đ_M$). EKL has low polydispersity, while EOL was the lignin with the highest value. ALK lignin was the only water-soluble lignin, while IAT, EOL, and EKL needed an alkaline medium to get fully solubilised. Thus, to achieve a stable 10 g/L aqueous solution, lignins were firstly solubilised at pH 11 and then carefully acidified to pH 7. No precipitation of insoluble lignin fractions was noticed for all studied samples.

Table 5.1 - Properties of the studied lignins (ALK, IAT, EOL, and EKL).

Lignin	M_w (g/mol)	M_n (g/mol)	$Đ_M$	S:G:H ratio	Lignin content (%)	Ash content (%)
ALK	9646	1807	5.34	0:98:2(•)	93.7 (♦)	1.30 (♦)
IAT	11521	3027	3.81	0:97:3(■)	92.2(■)	2.6(■)
EOL	13678	1849	7.40	70:30:0(*)	98.5(*)	0.11(*)
EKL	8354	8096	1.03	65:29:0.6(▲)	59.0(▲)	37.5(▲)

Note: marked data was obtained from: •Ma et al., 2018; ♦Sigma-Aldrich, 2006; *Costa et al., 2014; ■Constant et al., 2016; ▲Costa et al., 2018.

The ATR-FTIR analysis showed typical bands for softwood and hardwood lignins, as observed in Figure 5.1. The bands are described according to Faix (1992) and Cateto et al. (2009). All lignins show a broad band at ~3400 cm^{-1} corresponding to the O-H stretch of O-H groups. Bands at 2983-2834 cm^{-1} appear for all lignins, related to C-H stretch of $–CH_3$ and $–CH_2$- groups. The band at 1594 cm^{-1} is related to aromatic skeletal vibration plus C=O stretch, higher for hardwood lignins (EOL and EKL). Band at 1510 cm^{-1} correspond to aromatic skeletal vibrations. The band at 1456 cm^{-1} correspond to C-H asymmetric deformations in $–CH_3$ and $–CH_2$- groups. Bands below 1430 cm^{-1} should be interpreted carefully, since there is a contribution of various vibration modes for each band in this region. At 1422 cm^{-1} the aromatic skeletal vibration is combined with C-H in-plane deformation. Band at 1213 cm^{-1} corresponds to C-C, C-O and C=O stretches. Guaiacyl units (G) characteristic vibrations (primarily in softwood ALK and IAT) include 1266 cm^{-1} (G ring and C=O stretch) and 855 cm^{-1} (C-H out-of-plane vibration in G) (Boeriu et al., 2004). Syringic units (S) vibrations (only in hardwood EOL and EKL) include 1323 cm^{-1} (S ring joined to G ring condensed) and 830 cm^{-1} (C-H out-of-plane in S) (Ma et al., 2018b). At 1108-1133 cm^{-1}, aromatic C-H in-plane deformation appears, combined with secondary alcohols and C=O stretch (higher values for G lignins). The 1080 cm^{-1} band is related to C-O deformation in secondary alcohols and aliphatic ethers, particularly in ALK. Band at 1030-1040 cm^{-1} corresponds to aromatic C-H in-plane deformation with higher prevalence in G lignins, combined with C-O deformation in primary alcohols and C=O stretch (unconjugated).

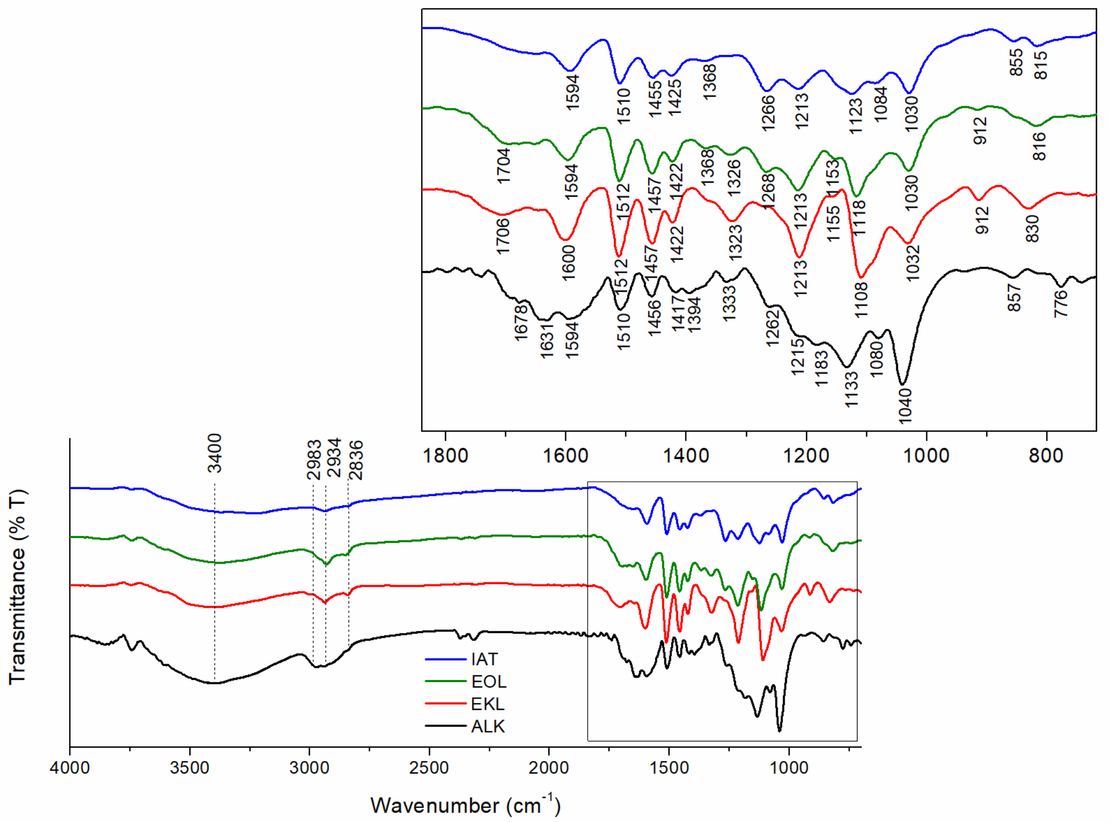

Figure 5.1 - ATR-FTIR analysis for the studied lignins

5.3.2 TS-1 catalysed lignin oxidation

Hydrogen peroxide oxidation is reported to depend on several factors, such as pH conditions, temperature, reaction time, and H_2O_2 load, directly impacting the conversion rate and the obtained target compounds (type and yield) (Bi et al., 2018). To evaluate how these factors influenced the catalytic wet peroxide oxidation of the studied lignins, different oxidation tests were conducted by modifying each factor at a time.

5.3.2.1 Lignin conversion

Lignin has a complex structure that must be depolymerized, i.e. broken into smaller fragments, to be converted into C_4-DCA and other compounds. Therefore, it is necessary to evaluate lignin conversion under different parameters, such as temperature, pH, time, and H_2O_2 load. In this study, lignin conversion was determined by quantification of the remaining lignin after oxidation, which was extracted after adding diluted acid and centrifuged, remaining in solution the soluble lignin. Insoluble lignin was re-solubilized in an alkaline solution, and both lignins were quantified by UV spectrophotometry. Lignin conversion was calculated against the original lignin placed in the reactor.

It is known that high temperatures affect the oxidative power of H_2O_2, allowing the release of hydroxyl radicals, which can be decomposed at these high temperatures (Xiang and Lee, 2000). The temperature effect was quite notable on lignin conversion, as can be seen in Figure 5.2(a), with conversion increasing with temperature increase for all lignins, up to 140 ºC where the maximum conversion was achieved (80.3%, 91.9%, 93.6%, and 97.5%, respectively for ALK, EOL, EKL, and IAT). When 160ºC were used no significant differences were noticed. The molecular weight decrease with temperature rise can be observed in Figure 5.3a, compatible with depolymerisation occurrence (structure reduction to smaller fragments). At higher temperatures, a prevalence of lignin fragments of low molecular weight was perceived comparatively with the original lignin, especially for AKL and IAT, pointing out that the molecular weight profile for 140 and 160 ºC is quite similar corroborating, the maintenance of the lignin conversion after 140 ºC. Moreover, for the EOL lignin signs of repolymerization at high temperatures are noticed. Data for EKL at 100ºC is not shown since the lignin was not well dissolved in the solvent.

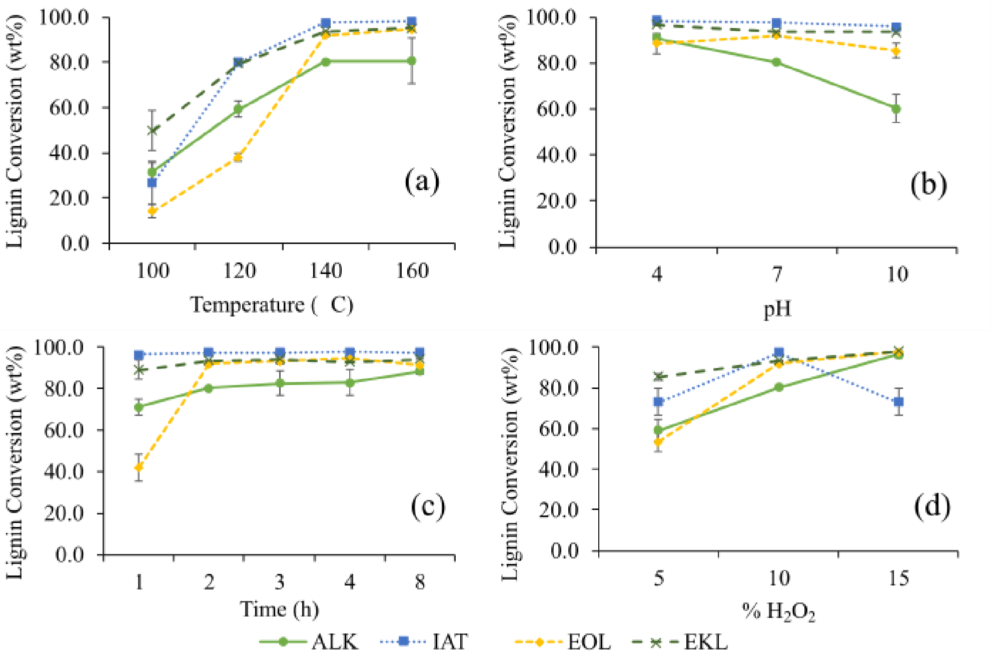

Figure 5.2 - Lignin conversion by catalytic wet peroxide oxidation. Effect of: **(a)** Temperature; **(b)** pH; **(c)** time; **(d)** H_2O_2 percentage.

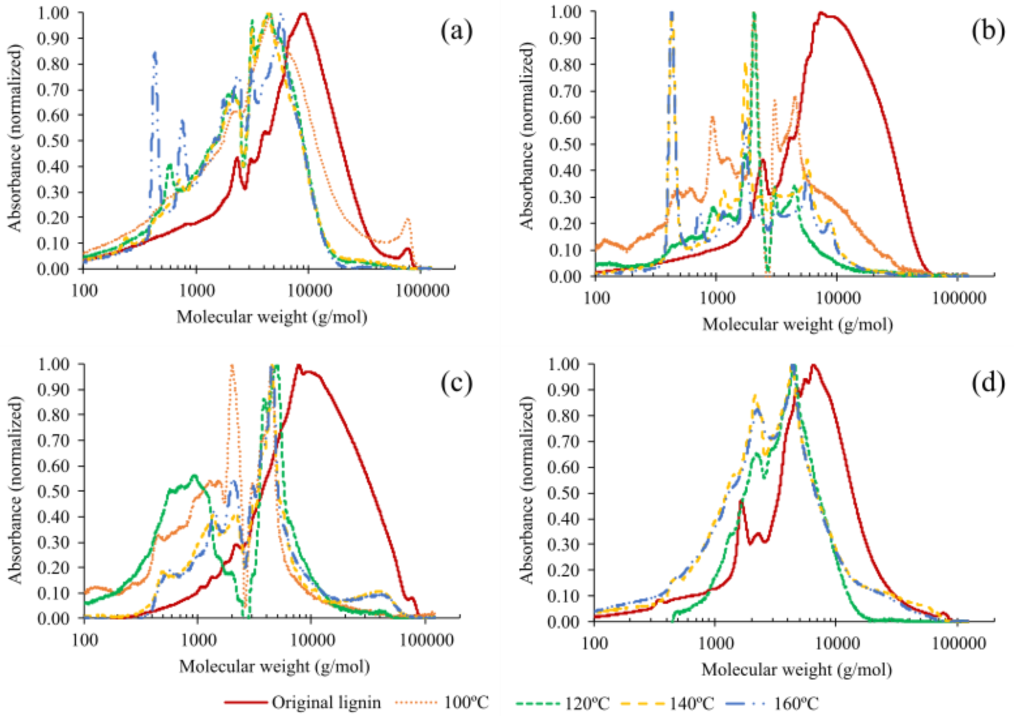

Figure 5.3 - Gel permeation chromatograms for lignins (**(a)** ALK, **(b)** IAT, **(c)** EOL, **(d)** EKL) oxidised at different temperatures (100, 120, 140, and 160 ºC).

Peroxide oxidation also has a high dependence on the pH medium; H_2O_2 is a weak acid, and thus its reactivity changes with pH. H_2O_2 is stable at acidic pH, while it quickly decomposes at alkaline conditions to molecular O_2 and H_2O. It can act as a nucleophile under alkaline conditions and electrophile in acidic medium (Xiang and Lee, 2000; Yin et al., 2015). pH conditions also affect the oxidation pathway of the phenolic structures, namely by the attack to hydroxyl radicals with the formation of an anionic radical (alkaline pH), a cationic radical (acidic pH), or a neutral radical, releasing an OH^-, $H^{+,}$ or H_2O group, respectively (Gierer et al., 1992).

Alkaline pH gave rise to lower lignin conversions (especially for ALK lignin) (Figure 5.2b). The lignin phenolic structures were stable to H_2O_2 oxidation at this pH, inhibiting radicals formation from the H_2O_2 homolytic decomposition, which is responsible for aromatic moieties degradation (Gierer, 1986). Recoupling of aromatic structures was also favoured, generating larger aromatic compounds with high absorptivity (Gierer et al., 1992). This fact may explain the lower lignin conversion at alkaline pH due to repolymerization reactions. Moreover, H_2O_2 is quickly decomposed at alkaline pH to water and O_2 (Suttipornphaisalkul et al., 2020). In acidic and neutral pH, redox and disproportionation reactions were more frequent, allowing the formation of hydroxylated and demethoxylated products, and, therefore, to a higher level of lignin depolymerisation to short fragments and, in a later stage, to the compounds of interest.

The testing of the lignin oxidation at different times was done at 140ºC and pH 7 in the range 1-8 hours. Lignin conversion was already observed in the first hours for kraft lignins (IAT and EKL), as can be observed in Figure **5**.2c. EOL gave rise to low conversion in the first hour, probably due to its high condensed structure (Costa et al., 2014), which needed longer oxidation times to break the structure to smaller fragments. Comparatively with the other lignins, ALK conducted to lower conversions, never reaching 100%. Alkaline pretreatment depolymerised lignin by cleaving the ether linkages and leaving instead available OH phenolic groups, which are the main cause for lignin re-condensation, reaching a very condensed and recalcitrant structure (Bao et al., 2020; Ma et al., 2018b). ATR-FTIR confirmed the presence of the available OH groups by the presence of different bands. Band at 1040 cm^{-1} shows a high intensity compared to the other lignins, being related to C-O in primary alcohols. Band at 1086 cm^{-1} is related to secondary alcohols and ethers, and it is only present in ALK and IAT. Finally, bands at 1108-1133 cm^{-1} are associated to a combination of C-H in S units and secondary alcohols and C=O (Cateto et al., 2009). This band is present in EKL and EOL (as hardwood lignins) but is also present in ALK, mainly by the presence of OH groups. Also, ALK showed a more intense band at 3400 cm^{-1}, associated to O-H groups. It has been reported that higher ether linkages content helps to activate the aromatic ring (Ma et al., 2018b). Since alkaline-pretreated lignin has a lower amount of ether linkages, the depolymerisation of the aromatic moieties become lower, causing that ALK presented a low reactivity towards oxidation. Therefore the ring-opening reaction of these aromatic compounds yields lower amounts of C_4-DCA.

The amount of H_2O_2 available for oxidation is a relevant parameter for reaching good conversions, avoiding over-oxidation of the already produced compounds. As seen in Figure 5.2d, lignin conversion increased as the H_2O_2 available to react also increased. EOL and ALK lignins were the ones leading to lower conversions for low H_2O_2 contents due to their higher condensed structure (Costa et al., 2014; Ma et al., 2018b), while the conversion of the EKL lignin was higher due to the higher reactivity of softwood kraft lignins in peroxide oxidations, as explained in Chapter 4.

5.3.2.2 C_4-DCA yields

Once the lignin has been depolymerised into smaller fragments, ring-opening reactions occur yielding C_4-DCA compounds. The parameters tested for lignin conversion (temperature, pH, time and H_2O_2 percentage) were also analysed in the production yield of the acids (succinic, malic, maleic, fumaric, and tartaric acids).

The best lignin conversions to C_4-DCA were obtained for the higher tested temperatures, as seen in Figure 5.4a. Namely, the best C_4-DCA yield was achieved at 140ºC for most lignins (IAT, EOL, and EKL), following the same behaviour observed for lignin conversion. Only ALK showed a slightly higher yield at 160ºC. ALK lignin has a low reactivity towards oxidation (Ma et al., 2018b), therefore needing a higher temperature to be depolymerised and oxidised. Malic and succinic acids were the main obtained acids, while maleic and fumaric acids were observed for all temperatures, but at very low yields. Tartaric acid was obtained mainly at high temperatures. IAT provided the higher succinic acid yield, with 11.3 wt%, compared to EOL (9.7 wt%), EKL (7.6 wt%), and ALK (5.8 wt%). Regarding malic acid, EOL gave rise to the highest yield (19.5 wt%), compared to IAT (10.1 wt%), ALK (6.6 wt%), and EKL (5.5 wt%). In all cases, the succinic acid yield was higher for the catalysed reaction, when compared to the non-catalysed one, being up to four times higher in the best-case scenario (as compared with the non-catalysed reaction, Figure 5.5). In contrast, for malic acid, the results were similar for the two oxidation methods (Figure 5.4a and Figure 5.5a). Moreover, in most cases, acetic acid yields were similar for the non-catalysed and catalysed reactions, with formic acid yields being higher for the catalysed reaction (Figure 5.6 and Figure 5.7).

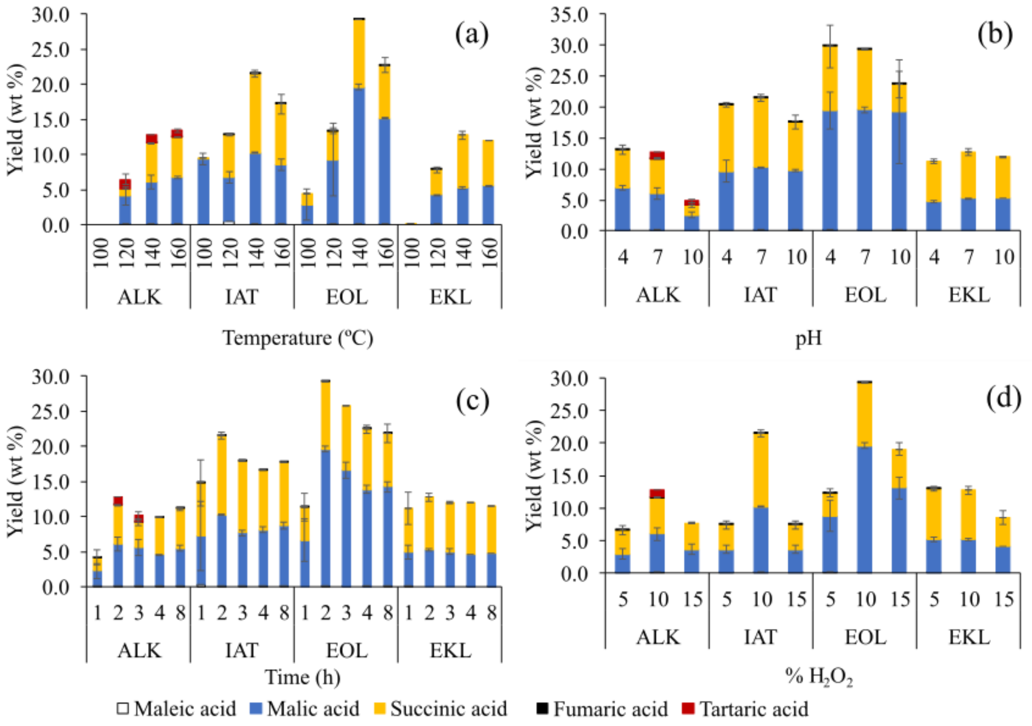

Figure 5.4 - C_4-DCA yield in catalytic wet peroxide oxidation. Effect of: **(a)** Temperature; **(b)** pH; **(c)** time; **(d)** H_2O_2 percentage.

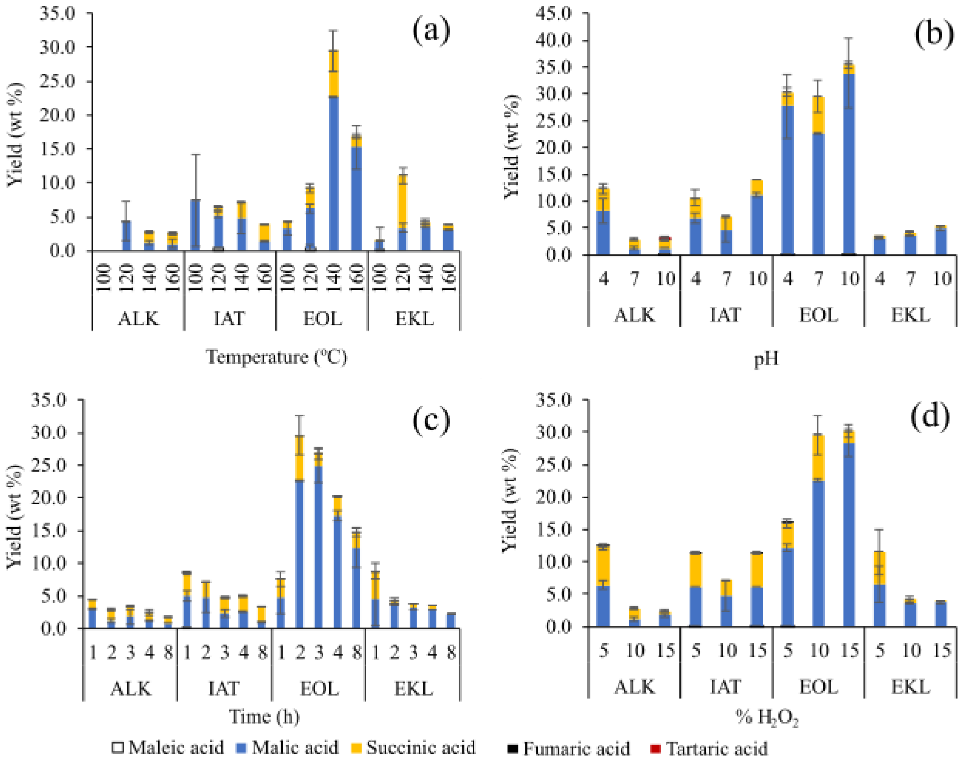

Figure 5.5 - C_4-DCA yield in the non-catalytic wet peroxide oxidation. Effect of: **(a)** Temperature; **(b)** pH; **(c)** time; **(d)** H_2O_2 percentage.

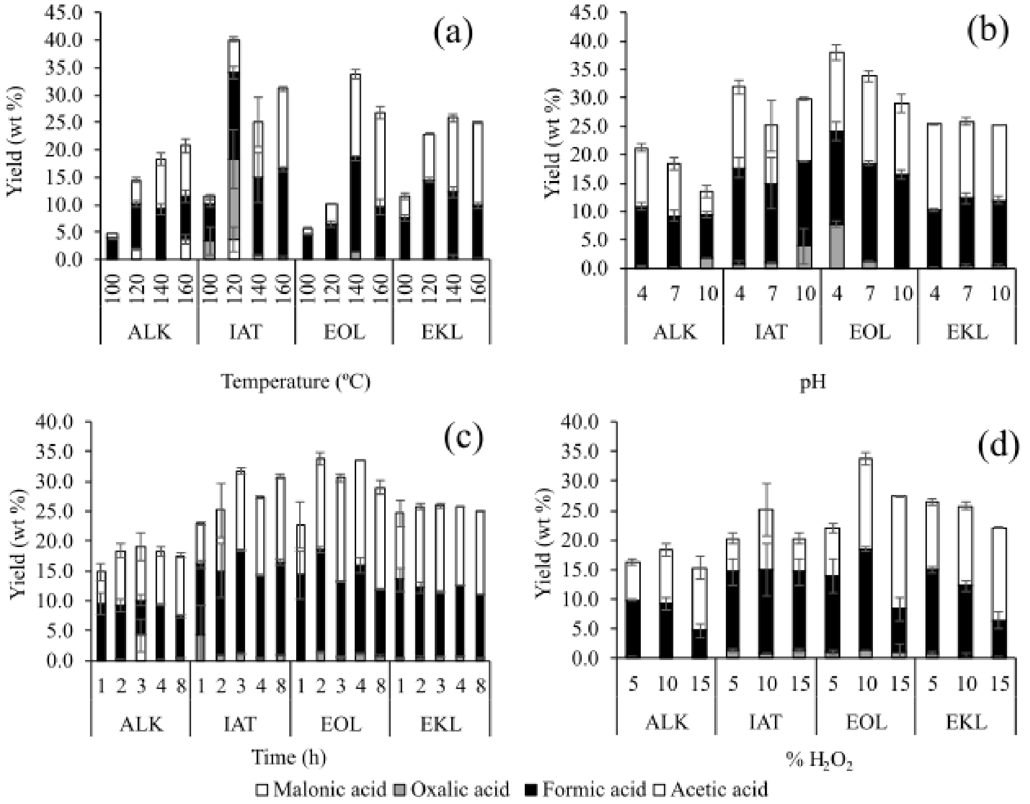

Figure 5.6 - Degradation acids yield in the catalytic wet peroxide oxidation. **(a)** Temperature effect; **(b)** pH effect; **(c)** time effect; **(d)** H_2O_2 percentage effect.

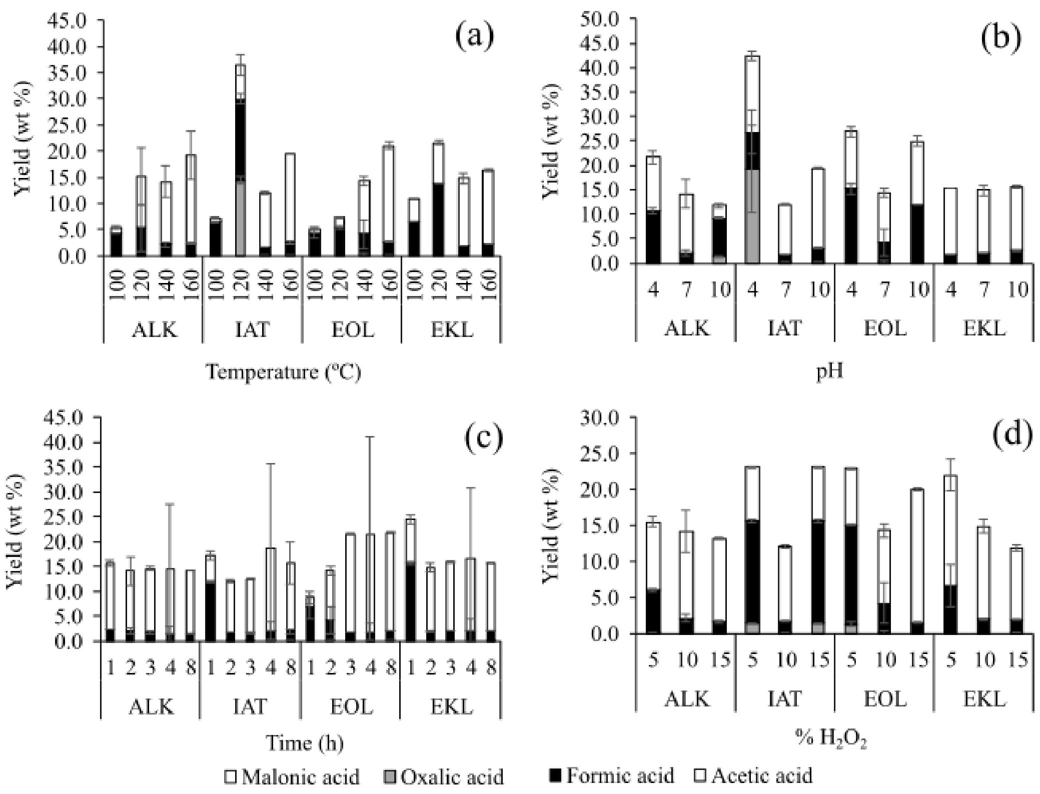

Figure 5.7 - Degradation acids yield in the non-catalyzed wet peroxide oxidation. **(a)** Temperature effect; **(b)** pH effect; **(c)** time effect; **(d)** H_2O_2 percentage effect.

It can be concluded that the best temperature to achieve succinic and malic acid at the highest yields was 140ºC, which is in agreement with the studies in Chapter 3 using lignin model compounds. A temperature higher than 140ºC over-oxidised the products, causing degradation of the produced C_4 acids, mainly the succinic acid, which had been reported to be oxidised to acetic acid (Suzuki et al., 2006), whose yield was much higher at 160ºC.

Alkaline pH led to lower C_4-DCA yields, especially for ALK lignin (Figure 5.4b). In acidic and neutral pH, the yields were similar. It has been reported that the amount of demethoxylation increased with pH decreasing (Gierer et al., 1992). Since the demethoxylation is one of the first steps to the further aromatic ring oxidation and to ring-opening reactions, as explained in Chapter 4, the use of a lower pH increased lignin conversion to lower-molecular weight compounds, confirmed by the higher lignin conversion and C_4-DCA yields in acidic pH. However, since lignin is usually insoluble in acidic pH, performing the oxidation under these conditions can put constrains to the productive process since lignin deposits in the catalyst and mass-transfer limitations can appear. Neutral pH led to similar C_4-DCA yields, comparatively to acidic pH, with the advantage that lignin is much more soluble in this medium. Individual C_4-DCA yields showed no significant differences between acidic and neutral conditions.

The main reaction sites of the TS-1 catalyst are the Ti atoms, whose reactivity is modified by changing the pH. It has been reported that, at neutral pH, TiO_2 has zero charge (pH 6.25-6.8), having at this point the best adsorption capability for the reactants due to the neutral surface (Suttipornphaisalkul et al., 2020). Even lignin conversion was higher at acidic pH, C_4-DCA yield was similar to the one achieved at neutral pH, confirming that an enhanced oxidation at a neutral pH was achieved with the catalyst. It is also important to note that the presence of TS-1 catalyst improved succinic acid yield for all studied lignins at the three evaluated pH conditions. For the non-catalysed reaction, the presence of succinic acid was negligible (Figure 5.5b).

For the four analysed lignins the highest C_4-DCA yields were achieved after 2 hours, as can be seen in Figure 5.4c. However, the formed acids showed a different stability pattern against time. Malic acid yield decreased due to their oxidation to low-molecular compounds, such as acetic acid, whereas succinic acid revealed to be stable throughout time, showing very low degradation levels, which can be useful for a future biorefinery process.

A high amount of H_2O_2 caused mineralisation of the C_4-DCA, avoiding their production at valued yields. As seen in Figure 5.4d, the best yields were obtained for 10% H_2O_2, while the extra adding of peroxide caused a decrease in the obtained acids yield. The same effect was observed for the degradation products (formic and acetic acids), showing that they were utterly mineralised to CO_2 using high H_2O_2 concentration. This behaviour was also observed with lignin peroxide oxidations using different TiO_2 based catalysts (Suttipornphaisalkul et al., 2020). Therefore, it is necessary to evaluate and optimize the amount of H_2O_2 added to the reaction in lignin oxidation leading to C_4-DCA. The use of an oxidiser amount higher than the needed one would make the process more costly without any valuable advantages.

The best lignin for succinic acid production was IAT, but EOL conducted to the higher total C_4-DCA yields, while ALK and EKL showed similar low yields. As previously stated, technical lignins with a higher content of aryl-ether bonds indicate a not too aggressive pulping process, avoiding re-condensation reactions. Once the aryl-ether bonds are cleaved in the oxidation reaction, the aromatic rings are oxidized and opened, leading to C_4-DCA. EOL, a lignin proceeding from an Organosolv process, has a structure closer to the one of the native lignin, i.e., it preserved most of the aryl-ether linkages after the pulping process. As a hardwood lignin, it has the advantage of reacting faster due to its syringyl groups. Therefore, the oxidant cleaves the ether bonds and opens the aromatic rings without being consumed in the breaking of the C-C bonds of the condensed structures. This fact may led to the existence of some extra oxidant to oxidize more aromatic rings and continue oxidizing the formed dicarboxylic acids, giving rise to high percentages of malic acids. Kraft lignins have a more recalcitrant structure due to the used harsher pulping process, causing the cleavage of aryl-ether bonds and the re-condensation of the fragments, reducing the overall C_4-DCA yield. IAT is a softwood lignin whose guaiacyl moieties are easily oxidized to succinic acid, giving rise to a higher yield for this compound. EKL as a hardwood lignin shows higher reactivity towards oxidation, expecting that higher C_4-DCA yields were obtained. However, since this lignin is highly reactive, during the delignification process, it becomes partially degraded and condensed, as reported in previous works (Costa et al., 2014), reducing the possibility to achieve higher C_4-DCA yields. Finally, even though ALK is an alkali softwood lignin, and thus better yields were expected (as happened with IAT), its structure was heavily modified, with condensed structures found in this lignin, reducing the global C_4-DCA yield. Then, it can be stated that lignins with lower chemical modification, i.e. lignins with a structure closer to the one of native lignin, would be more suitable for C_4-DCA production, given that they still present aryl-ether linkages that can be cleaved and ring-opening before re-condensation occur, which will decrease reactivity. The fact that less modified lignins give better C_4-DCA yields could be especially helpful for biorefinery processes, where milder extraction processes are being used.

During the HPLC analysis, phenolic compounds were not identified, corroborating that at even low concentrations of H_2O_2, degradation of the lignin fragments through ring-opening reactions occurred, forming low-molecular-weight compounds and even reaching complete mineralisation, without leasing to individual phenolic monomers.

5.3.3 Evaluation of TS-1 catalyst in C_4-DCA production

5.3.3.1 Catalyst loading effect

Due to the catalytic effect of TS-1 in radical species production, it is important to evaluate the minimum catalyst load to be added to the reaction flask to ensure the highest C_4-DCA yields, avoiding increasing costs in the oxidation process. TS-1 has the advantage of not having noble metals in its structure, having a lower cost compared to other precious-metal-based catalysts. To examine the optimum catalyst load, oxidation reactions were performed using different amounts of catalyst, as seen in Figure 5.8.

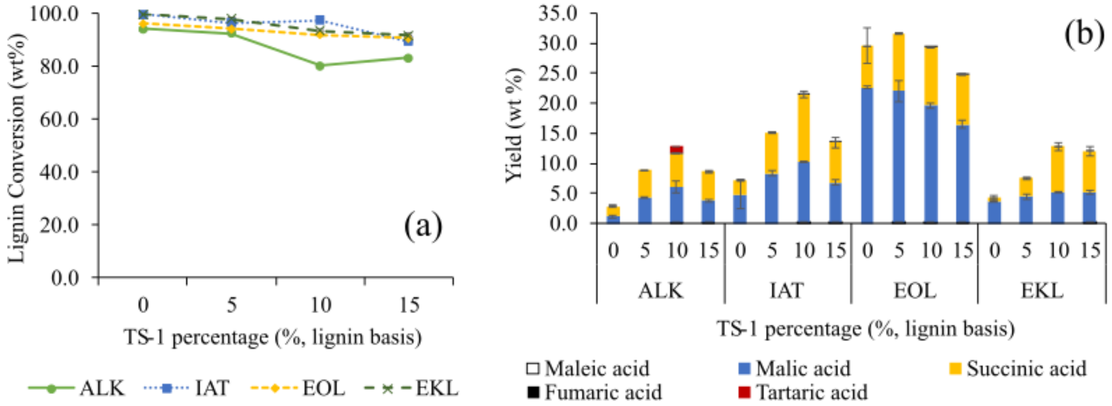

Figure 5.8 - Effect of TS-1 load on: **(a)** lignin conversion and **(b)** C_4-DCA yield.

Generally, all lignins were better converted using a lower amount of catalyst (Figure 5.8a) as the observed differences for the observed conversion data were statistically significant (confirmed by a one-way ANOVA test, P=0.05). However, when the C_4-DCA yield is analysed for the studied lignins, the non-catalysed reaction gave rise to lower yields, especially for succinic acid (Figure 5.8b). The higher succinic acid yield, for all lignins, was obtained using a 10% catalyst load (lignin-basis). The behaviour for malic acid was similar, except for EOL, where it was produced at a higher yield when less catalyst was presented. Loads higher than 10% caused a decrease in C_4-DCA yields, suggesting that the ideal load is 10%. Previous works where furfural was oxidised using TS-1 showed an ideal load of ~5 wt%, allowing a better maleic acid yield, while loads higher than 10% load intensified the over-oxidation (Alonso-Fagúndez et al., 2014). However, due to the lignin complex structure, in this work the over-oxidation was only observed after a catalyst load of 10% wt.

5.3.3.2 TS-1 reusability

To examine the reusability of the TS-1 catalyst in the C_4-DCA production, the same catalyst sample was consecutively used in 5 runs under the same experimental conditions. For these oxidation tests, the chosen conditions were the ones leading to the best succinic acid yield in the individual parameter evaluation, which were achieved with IAT lignin, at pH 7, 140ºC, 2 h, 10% H_2O_2, and 10% TS-1.

After each oxidation run, the reaction mixture was centrifuged, and the liquid removed using a pipette. Some of the catalyst remained suspended in the solution leading to a losing every run. This problem was due to the small size of the catalyst particles (0.3-0.5 µm), impeding sedimentation even after long centrifugation times (30 min at 3500 rpm). After 5 runs, the remaining catalyst was quantified as 46% of the original amount, confirming that the small size affected its recovery by centrifugation. A higher particle size catalyst is recommended for further studies, facilitating its full recovery after centrifugation.

As seen in Figure 5.9a, lignin conversion was preserved through the continuous runs, while the total CA (which involves C_4-DCA, acetic, oxalic and formic acids) yield decreased from 43 wt% to 36 wt%. Specifically, C_4-DCA yield decreased from 19 wt% to 15 wt%. A variation in the different acid yields in each run (Figure 5.9b) was observed, with more significant changes for maleic, fumaric, and formic acids. After 5 runs, malic and succinic acids yields were still 89% and 70% of the first run value, respectively. This variation could be explained by the catalyst loss as previously described. At the 5th run, the amount of TS-1 was practically half of the original amount, and the results matched the experiments where 5% TS-1 catalyst was used compared to 10% TS-1 (Figure 5.8).

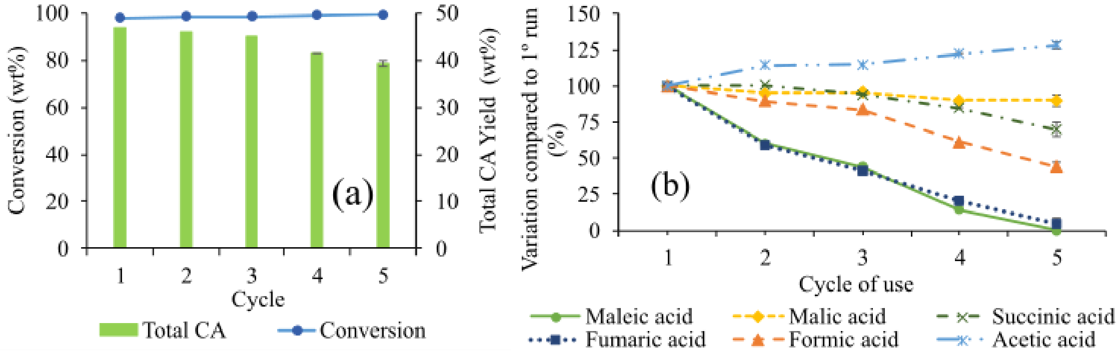

Figure 5.9 - Catalyst reusability after 5 successive oxidation runs. **(a)** Lignin conversion, **(b)** Carboxylic acids (CA) yield evolution along the 5 consecutive runs, comparatively with the first oxidation.

Deactivation has been reported for TS-1 catalysed oxidations, mainly due to the deposition of the reaction by-products over the surface and within the pores, even when using pure and simple feedstock such as furfural (Rodenas et al., 2018). In this work, after the first run, a slight change of colour was observed, which was expectable due to the deposition of lignin fragments associated with its complex reactivity and structure. These deposits can affect catalyst activity since they can block the pores and catalyst's surface, which is the main factor for TS-1 deactivation (Shi et al., 2013; Wang et al., 2007). Regeneration of catalysts contaminated with carbonaceous species can be done by calcination, being reported as a solution for deactivated TS-1 after several cycles (Alba-Rubio et al., 2017; Rodenas et al., 2018). In this work, the catalyst was only washed with acidified water between cycles. In other studies, the catalyst was repeatedly washed with organic solvents and dried before use, therefore removing more effectively the deposited contaminations from the pores (Alba-Rubio et al., 2017; Rodenas et al., 2018). As seen in Figure 5.10, the physical structure of TS-1 was not modified after 1 cycle. After 5 runs, some slight physical modifications are perceived on particle’s surface, with their whole structure remaining intact. EDS analysis showed that the atomic Si/Ti ratio (44.9±0.7) remained stable with 1 cycle (45±3). A change to 34±3 was observed after 5 cycles, suggesting a decrease in the Si content, probably due to some damages in the MFI surface structure. However, the activity experiments indicate that the main reason for C_4-DCA yield decrease was the loss of catalyst during the washing step and not the deactivation of the catalyst itself.

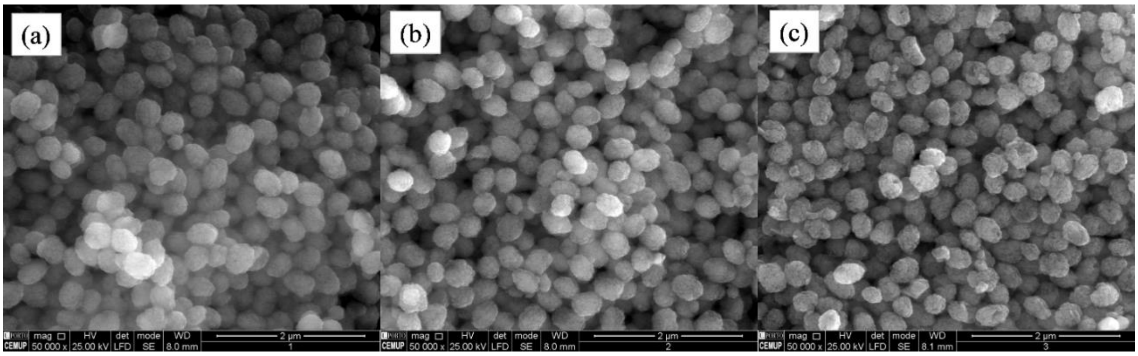

Figure 5.10 - SEM images of the original and reutilized catalyst: **(a)** original TS-1, **(b)** after 1 oxidation cycle, **(c)** after 5 oxidation cycles.

5.4 Conclusions

Lignin catalytic peroxide oxidation using TS-1 catalyst proved that C_4-DCA could be obtained at attractive yields. Succinic and malic acids were the main products, while maleic, fumaric, and tartaric acids were present but at small amounts. Comparatively with the alkali lignin, Kraft and organosolv lignins lead to higher conversion towards C_4-DCA. Succinic acid, a valuable product for bio-based polymers, was obtained at higher yields for the catalysed reaction in comparison with the non-catalysed one, being Indulin AT lignin the best studied case, leading to a yield four times higher than the one achieved without catalyst. Overall, the succinic acid yield followed the order IAT>EOL>EKL>ALK. while the best C_4-DCA total yields were achieved by EOL, suggesting that organosolv lignins (and lignins with a structure closer to native lignin) would have a more efficient oxidation activity towards C_4-DCA. Evaluating oxidation reaction key parameters was determinant to achieve good conversions without reaching over-oxidation, with the best conditions achieved for each individual parameter study, for the considered lignins, being 140ºC (temperature effect), neutral pH (pH effect), 10% TS1, lignin basis (catalyst effect), and 10 % H_2O_2 load (oxidant load effect). Values differing from these give rise to low lignin conversions, or over-oxidation products, like acetic and formic acids. This study considered the study of one parameter at a time and thus the overall best conditions were not achieved. Even so, the data presented here can be the basis for a deeper study, namely by using different statistical tools, like surface response methodology.

The optimum amount of TS-1 was determined to be 10wt% (lignin-basis) and the catalyst was found to be reusable. In the analysed consecutive cycles, a decrease in succinic and malic acids yield was observed, justified mainly due to the catalyst loss during the centrifugation step, which was linked to its small particle size and not to the deactivation caused by the carbonaceous deposits.

5.5 References

Abdelaziz, O.Y., Ravi, K., Mittermeier, F., Meier, S., Riisager, A., Lidén, G., Hulteberg, C.P., 2019. Oxidative Depolymerization of Kraft Lignin for Microbial Conversion. ACS Sustain. Chem. Eng. 7, 11640–11652. https://doi.org/10.1021/acssuschemeng.9b01605

Ahmad, Z., Dajani, W.W. Al, Paleologou, M., Xu, C., 2020. Sustainable process for the depolymerization/oxidation of softwood and hardwood kraft lignins using hydrogen peroxide under ambient conditions. Molecules 25, 1–19. https://doi.org/10.3390/molecules25102329

Alba-Rubio, A.C., Fierro, J.L.G., León-Reina, L., Mariscal, R., Dumesic, J.A., López Granados, M., 2017. Oxidation of furfural in aqueous H_2O_2 catalysed by titanium silicalite: Deactivation processes and role of extraframework Ti oxides. Appl. Catal. B Environ. 202, 269–280. https://doi.org/10.1016/j.apcatb.2016.09.025

Alonso-Fagúndez, N., Agirrezabal-Telleria, I., Arias, P.L., Fierro, J.L.G.G., Mariscal, R., Granados, M.L., 2014. Aqueous-phase catalytic oxidation of furfural with H_2O_2: High yield of maleic acid by using titanium silicalite-1. RSC Adv. 4, 54960–54972. https://doi.org/10.1039/c4ra11563e

Ansaloni, S., Russo, N., Pirone, R., 2017. Wet Air Oxidation of Industrial Lignin Case Study: Influence of the Dissolution Pretreatment and Perovskite-type Oxides. Waste and Biomass Valorization 0, 1–15. https://doi.org/10.1007/s12649-017-9947-4

Bao, H., Sagues, W.J., Wang, Y., Peng, W., Zhang, L., Yang, S., Xiao, D., Tong, Z., 2020. Depolymerization of Lignin into Monophenolics by Ferrous/Persulfate Reagent under Mild Conditions. ChemSusChem 13, 6582–6593. https://doi.org/10.1002/cssc.202002240

Bhargava, S.K., Tardio, J., Prasad, J., Föger, K., Akolekar, D.B., Grocott, S.C., 2006. Wet oxidation and catalytic wet oxidation. Ind. Eng. Chem. Res. 45, 1221–1258. https://doi.org/10.1021/ie051059n

Bi, Z., Li, Z., Yan, L., 2018. Catalytic oxidation of lignin to dicarboxylic acid over the $CuFeS_2$ nanoparticle catalyst. Green Process. Synth. 7, 306–315. https://doi.org/10.1515/gps-2017-0056

Boeriu, C.G., Bravo, D., Gosselink, R.J.A., van Dam, J.E.G., 2004. Characterisation of structure-dependent functional properties of lignin with infrared spectroscopy. Ind. Crops Prod. 20, 205–218. https://doi.org/10.1016/j.indcrop.2004.04.022

Cabral Almada, C., Kazachenko, A., Fongarland, P., Da Silva Perez, D., Kuznetsov, B.N., Djakovitch, L., 2020. Oxidative depolymerization of lignins for producing aromatics: variation of botanical origin and extraction methods. Biomass Convers. Biorefinery. https://doi.org/10.1007/s13399-020-00897-6

Cateto, C.A., Barreiro, M.F., Rodrigues, A.E., Belgacem, M.N., 2009. Optimization Study of Lignin Oxypropylation in View of the Preparation of Polyurethane Rigid Foams. Ind. Eng. Chem. Res. 48, 2583–2589. https://doi.org/10.1021/ie801251r

Cheng, C., Wang, J., Shen, D., Xue, J., Guan, S., Gu, S., Luo, K.H., 2017. Catalytic oxidation of lignin in solvent systems for production of renewable chemicals: A review. Polymers (Basel). 9, 38–50. https://doi.org/10.3390/polym9060240

Clerici, M.G., 2015. The Activity of Titanium Silicalite-1 (TS-1): Some Considerations on Its Origin. Kinet. Catal. 56, 453–458. https://doi.org/10.7868/s045388111504005x

Constant, S., Wienk, H.L.J., Frissen, A.E., Peinder, P. De, Boelens, R., Van Es, D.S., Grisel, R.J.H., Weckhuysen, B.M., Huijgen, W.J.J., Gosselink, R.J.A., Bruijnincx, P.C.A., 2016. New insights into the structure and composition of technical lignins: A comparative characterisation study. Green Chem. 18, 2651–2665. https://doi.org/10.1039/c5gc03043a

Costa, C.A.E.E., Pinto, P.C.R., Rodrigues, A.E., 2014. Evaluation of chemical processing impact on E. globulus wood lignin and comparison with bark lignin. Ind. Crops Prod. 61, 479–491. https://doi.org/10.1016/j.indcrop.2014.07.045

Costa, C.A.E.E., Pinto, P.C.R.R., Rodrigues, A.E., 2018. Lignin fractionation from E.

Globulus kraft liquor by ultrafiltration in a three stage membrane sequence. Sep. Purif. Technol. 192, 140–151. https://doi.org/10.1016/j.seppur.2017.09.066

Cronin, D.J., Zhang, X., Bartley, J., Doherty, W.O.S.S., 2017. Lignin Depolymerization to Dicarboxylic Acids with Sodium Percarbonate. ACS Sustain. Chem. Eng. 5, 6253–6260. https://doi.org/10.1021/acssuschemeng.7b01208

Demesa, A.G., Laari, A., Sillanp, M., Koiranen, T., 2017. Valorization of lignin by partial wet oxidation using sustainable heteropoly acid catalysts. Molecules 22, 1–11. https://doi.org/10.3390/molecules22101625

Demesa, A.G., Laari, A., Turunen, I., Sillanpää, M., 2015. Alkaline Partial Wet Oxidation of Lignin for the Production of Carboxylic Acids. Chem. Eng. Technol. 38, 2270–2278. https://doi.org/10.1002/ceat.201400660

Di Marino, D., Jestel, T., Marks, C., Viell, J., Blindert, M., Kriescher, S.M.A., Spiess, A.C., Wessling, M., 2019. Carboxylic Acids Production via Electrochemical Depolymerization of Lignin. ChemElectroChem 6, 1434–1442. https://doi.org/10.1002/celc.201801676

Faisal, I., 2009. Oxidation of Phenolic Wastewater by Fenton’s Reagent. Iraqi J. Chem. Pet. Eng. 10, 1–5.

Faix, O., 1992. Fourier Transform Infrared Spectroscopy, in: Stephen Y., L., Carlton W., D. (Eds.), Methods in Lignin Chemistry. Springer, Berlin, Heidelberg, pp. 83–109. https://doi.org/10.1007/978-3-642-74065-7_7

Figueirêdo, M.B., Deuss, P.J., Venderbosch, R.H., Heeres, H.J., 2019. Valorization of Pyrolysis Liquids: Ozonation of the Pyrolytic Lignin Fraction and Model Components. ACS Sustain. Chem. Eng. 7, 4755–4765. https://doi.org/10.1021/acssuschemeng.8b04856

Gamba, A., Tabacchi, G., Fois, E., 2009. TS-1 from First Principles. J. Phys. Chem. A 113, 15006–15015. https://doi.org/10.1021/jp905110s

Gierer, J., 1986. Chemistry of Delignification- Part 2: Reactions of lignins during bleaching. Wood Sci. Technol. 20, 1–33. https://doi.org/10.1007/BF00350692

Gierer, J., Yang, E., Reitberger, T., 1992. The Reactions of Hydroxyl Radicals with Aromatic Rings in Lignins, Studied with Creosol and 4-Methylveratrol. Holzforschung 46, 495–504.

Hasegawa, I., Inoue, Y., Muranaka, Y., Yasukawa, T., Mae, K., 2011. Selective Production of Organic Acids and Depolymerization of Lignin by Hydrothermal Oxidation with Diluted Hydrogen Peroxide. Energy & Fuels 25, 791–796. https://doi.org/10.1021/ef101477d

Jong, E. de, Higson, A., Walsh, P., Wellisch, M., 2011. Biobased Chemicals - Value Added Products from Biorefineries, IEA Bioenergy-Task 42 Biorefinery. https://doi.org/10.1126/science.1179713

Junghans, U., Bernhardt, J.J., Wollnik, R., Triebert, D., Unkelbach, G., Pufky-Heinrich, D., 2020. Valorization of Lignin via Oxidative Depolymerization with Hydrogen Peroxide: Towards Carboxyl-Rich Oligomeric Lignin Fragments. Molecules 25. https://doi.org/10.3390/molecules25112717

Kamm, B., Gruber, P.R., Kamm, M., 2008. Biorefineries-Industrial Processes and Products: Status Quo and Future Directions, Biorefineries-Industrial Processes and Products: Status Quo and Future Directions. https://doi.org/10.1002/9783527619849

Kang, J., Irmak, S., Wilkins, M., 2019. Conversion of lignin into renewable carboxylic acid compounds by advanced oxidation processes. Renew. Energy 135, 951–962. https://doi.org/10.1016/j.renene.2018.12.076

Kienberger, M., Maitz, S., Pichler, T., Demmelmayer, P., 2021. Systematic Review on Isolation Processes for Technical Lignin. Processes 9, 804. https://doi.org/10.3390/pr9050804

Kim, J.S., Lee, Y.Y., Kim, T.H., 2016. A review on alkaline pretreatment technology for bioconversion of lignocellulosic biomass. Bioresour. Technol. 199, 42–48. https://doi.org/10.1016/j.biortech.2015.08.085

Li, C., Zhao, X., Wang, A., Huber, G.W., Zhang, T., 2015. Catalytic Transformation of Lignin for the Production of Chemicals and Fuels. Chem. Rev. 115, 11559–11624. https://doi.org/10.1021/acs.chemrev.5b00155

Liu, C., Wu, S., Zhang, H., Xiao, R., 2019. Catalytic oxidation of lignin to valuable biomass-based platform chemicals: A review. Fuel Process. Technol. 191, 181–201. https://doi.org/10.1016/j.fuproc.2019.04.007

Lotfi, S., Boffito, D.C., Patience, G.S., 2016. Gas–solid conversion of lignin to carboxylic acids. React. Chem. Eng. 1, 397–408. https://doi.org/10.1039/C6RE00053C

Lotfi, S., Boffito, D.C., Patience, G.S., 2015. Gas-Phase Partial Oxidation of Lignin to Carboxylic Acids over Vanadium Pyrophosphate and Aluminum-Vanadium-Molybdenum. ChemSusChem 8, 3424–3432. https://doi.org/10.1002/cssc.201501036

Ma, R., Guo, M., Zhang, X., 2018a. Recent advances in oxidative valorization of lignin. Catal. Today 302, 50–60. https://doi.org/10.1016/j.cattod.2017.05.101

Ma, R., Guo, M., Zhang, X., 2014. Selective Conversion of Biorefinery Lignin into Dicarboxylic Acids. ChemSusChem 7, 412–415. https://doi.org/10.1002/cssc.201300964

Ma, R., Zhang, X.X., Wang, Y., Zhang, X.X., 2018b. New insights toward quantitative relationships between lignin reactivity to monomers and their structural characteristics. ChemSusChem 11, 2146–2155. https://doi.org/10.1002/cssc.201800550

Mathias, A.L., 1993. Produção de vanilina a partir da lenhina : Estudo cinético e do processo. Dep. Chem. Eng. University of Porto, Faculty of Engineering, Porto.

Rodenas, Y., Mariscal, R., Fierro, J.L.G.G., Martín Alonso, D., Dumesic, J.A., López Granados, M., 2018. Improving the production of maleic acid from biomass: TS-1 catalysed aqueous phase oxidation of furfural in the presence of γ-valerolactone. Green Chem. 20, 2845–2856. https://doi.org/10.1039/C8GC00857D

Rodrigues, A.E., Pinto, P.C. de O.R., Barreiro, M.F., Esteves da Costa, C.A., Ferreira da Mota, M.I., Fernandes, I., 2018. An Integrated Approach for Added-Value Products from Lignocellulosic Biorefineries. Springer International Publishing, Cham. https://doi.org/10.1007/978-3-319-99313-3

Rodrigues Pinto, P.C., Borges da Silva, E.A., Rodrigues, A.E., 2011. Insights into Oxidative Conversion of Lignin to High-Added-Value Phenolic Aldehydes. Ind. Eng. Chem. Res. 50, 741–748. https://doi.org/10.1021/ie102132a

Shi, H., Wang, Y., Wu, G., Feng, W., Lin, Y., Zhang, T., Jin, X., Wang, S., Wu, X., Yao, P., 2013. Deactivation and regeneration of TS-1/SiO_2 catalyst for epoxidation of propylene with hydrogen peroxide in a fixed-bed reactor. Front. Chem. Sci. Eng. 7, 202–209. https://doi.org/10.1007/s11705-013-1328-3

Sigma-Aldrich, 2006. Certificate Of Analysis - Lignin, alkali, low sulfonate content.

Silva, E.A.B. da, Zabkova, M., Araújo, J.D., Cateto, C.A., Barreiro, M.F., Belgacem, M.N., Rodrigues, A.E., 2009. An integrated process to produce vanillin and lignin-based polyurethanes from Kraft lignin. Chem. Eng. Res. Des. 87, 1276–1292. https://doi.org/10.1016/j.cherd.2009.05.008

Su, J., Yang, L., Liu, R.N., Lin, H., 2014. Low-temperature oxidation of guaiacol to maleic acid over TS-1 catalyst in alkaline aqueous H_2O_2 solutions. Chinese J. Catal. 35, 622–630. https://doi.org/10.1016/S1872-2067(14)60039-5

Sun, Y., Argyropoulos, D.S., 1996. A comparison of the reactivity and efficiency of ozone, chlorine dioxide, dimethyldioxirane and hydrogen peroxide with residual kraft lignin. Holzforschung 50, 175–182. https://doi.org/10.1515/hfsg.1996.50.2.175

Sun, Z., Fridrich, B., De Santi, A., Elangovan, S., Barta, K., 2018. Bright Side of Lignin Depolymerization: Toward New Platform Chemicals. Chem. Rev. 118, 614–678. https://doi.org/10.1021/acs.chemrev.7b00588

Suttipornphaisalkul, M., Wright, P., Kamwilaisak, K., 2020. Succinic acid production from lignin by photo-oxidation. Eng. Appl. Sci. Res. 47, 36–46. https://doi.org/10.14456/easr.2020.3

Suzuki, H., Cao, J., Jin, F., Kishita, A., Enomoto, H., Moriya, T., 2006. Wet oxidation of lignin model compounds and acetic acid production. J. Mater. Sci. 41, 1591–1597. https://doi.org/10.1007/s10853-006-4653-9

Upton, B.M., Kasko, A.M., 2016. Strategies for the conversion of lignin to high-value polymeric materials: Review and perspective. Chem. Rev. 116, 2275–2306. https://doi.org/10.1021/acs.chemrev.5b00345

Wang, Q., Wang, L., Chen, J., Wu, Y., Mi, Z., 2007. Deactivation and regeneration of titanium silicalite catalyst for epoxidation of propylene. J. Mol. Catal. A Chem. 273, 73–80. https://doi.org/10.1016/j.molcata.2007.03.068

Werpy, T., Petersen, G., 2004. Top Value Added Chemicals from Biomass: Volume I -- Results of Screening for Potential Candidates from Sugars and Synthesis Gas., U.S. Department of energy. United States. https://doi.org/10.2172/926125

Xiang, Q., Lee, Y.Y., 2000. Oxidative cracking of precipitated hardwood lignin by hydrogen peroxide. Appl. Biochem. Biotechnol. 84–86, 153–162. https://doi.org/10.1385/ABAB:84-86:1-9:153

Yin, G., Jin, F., Yao, G., Jing, Z., 2015. Hydrothermal Conversion of Catechol into Four-Carbon Dicarboxylic Acids. Ind. Eng. Chem. Res. 54, 68–75. https://doi.org/10.1021/ie5036447

Zeng, J., Yoo, C.G., Wang, F., Pan, X., Vermerris, W., Tong, Z., 2015. Biomimetic fenton-catalyzed lignin depolymerization to high-value aromatics and dicarboxylic acids. ChemSusChem 8, 861–871. https://doi.org/10.1002/cssc.201403128

Zhang, X., Zhao, Y., Liu, Y., Wang, J., Deng, Y., 2020. Recent progress on bio-based production of dicarboxylic acids in yeast. Appl. Microbiol. Biotechnol. 104, 4259–4272. https://doi.org/10.1007/s00253-020-10537-8

6. Microwave-assisted lignin wet peroxide oxidation

Modern and innovative methodologies for lignin valorisation are being suggested as a strategy to achieve higher productivity with better energy efficiency. Microwave energy can heat the reaction mixture quickly and homogeneously, accelerating chemical reaction.

In this chapter microwave heating was tested in the peroxide oxidation of three kraft lignins obtained from different sources (Indulin AT, Lignol, and *E. globulus* lignins). The effect of temperature, time, and catalyst type (TS-1 and Fe-TS1) was evaluated in the production of C_4 dicarboxylic acids. A comparison of microwave heating against conventional heating was carried out and discussed to assess the best heating methodology. The TS-1 catalyst improved the succinic acid yields in both heating techniques. Microwave heating showed a rapid lignin conversion, but in prolonged times, the conventional heating led to better results. The microwave heating specifically enhanced Lignol conversion to C_4 dicarboxylic acids even without a catalyst, showing a promissing possibility for future valorization of organosolv lignins.

6.1 Introduction

Lignin is a biopolymer present in plants, in percentages varying from 15 to 36 wt%. It is formed by three main monomers, namely *p*-hydroxyphenyl (H), guaiacyl (G), and syringyl (S) units, at different ratios depending on the type of plant (Kamm et al., 2008). Those units are linked by aryl ether bonds (*β-O-4, α-O-4*) and C-C bonds (*β-5, β-β, 5-5* and others), forming a three-dimensional complex matrix (C. Li et al., 2015). Pulping processes (e.g., kraft, sulphite, soda, and organosolv) are used to extract lignin from the biomass matrix, generating an annual amount of 130 million tons of kraft lignin (Berlin and Balakshin, 2014; Huang et al., 2020; Rinaldi et al., 2016). The final lignin has a chemical structure and properties that depend not only on the plant origin but also on the pulping process. Currently, only vanillin, dimethyl sulphide, and dimethyl sulfoxide are produced commercially from lignin. In general, lignin, a renewable feedstock, is still underutilized (Upton and Kasko, 2016).

Lignin can be valorized through various approaches, yielding different products. Gasification, pyrolysis, acid/base hydrolysis, reductive and oxidative conversion are the main strategies used to upgrade lignin to added-value compounds (Wang et al., 2019). Specifically, oxidative depolymerization produces aromatic and aliphatic compounds by cleaving the main bonds present in lignin (Cao et al., 2019; Pandey and Kim, 2011). Oxidation usually follows a radical pathway leading to three possible main reactions: side-chain cleavage (releasing aromatic aldehydes, acids, and quinones), aromatic ring cleavage (producing aliphatic dicarboxylic acids), and condensation products (Ma et al., 2015; Vangeel et al., 2018).

The production of aromatic aldehydes (e.g., vanillin, syringaldehyde) has been widely studied due to their direct valorization (Rodrigues et al., 2018). However, recently, an increased interest in dicarboxylic acids, especially C_4 dicarboxylic acids (C_4-DCA) like succinic, maleic, and fumaric acids arose given their current industrial use and their possibility to act as future building blocks derived from biomass (Gérardy et al., 2020; Werpy and Petersen, 2004). To achieve an aromatic ring-opening reaction, it is necessary to use harsh reaction conditions, namely strong oxidants (usually H_2O_2, O_3, or organic peroxides) helped by heterogeneous catalysts (Rinaldi et al., 2016).

Traditionally, oxidative conversion of lignin has been carried out using conventional heating, usually by applying high temperatures and pressures, and toxic or expensive solvents and catalysts. Nevertheless, there has been an increasing interest in non-conventional methods, such as microwave heating, mechanochemistry, sonication, photocatalysis, and electrocatalysis, which use milder conditions (Behling et al., 2016).

Microwave (MW) is a non-ionizing radiation that does not interact with the chemical bonds, producing heat by enhancing the kinetic energy of the molecules. Heat can propagate through two mechanisms, ionic conduction and bipolar rotation. The first one refers to the movement of ions trying to follow the electric current, causing shocks with other molecules and releasing heat. The second one is caused by the fast alignment of polar molecules to the electric field, causing friction and releasing heat. This second mechanism has a strong relationship with the dielectric properties of the compounds (Aguilar-Reynosa et al., 2017). Considering all factors, the microwave heating of materials depends on three properties: electric, dielectric, and magnetic (Palma et al., 2020).

MW heating has several advantages comparatively with conventional heating. The main ones are: faster heat transfer, shorter reaction times, non-localized heating (volumetric heating) avoiding surfaces overheating, the vessel avoids heat loss, the system can be turned on or off immediately, high temperatures over the boiling point can be achieved in pressurized systems, and a more efficient use of energy is possible. However, among the main disadvantages are the cost of the equipment, the non-uniformity of heat in materials that are not homogeneous, the low penetration of MW radiation, and the changes of the dielectric properties with temperature, affecting the MW affinity. Also, commercial MW equipment is not widely available, and more advances are still pending in this field (Aguilar-Reynosa et al., 2017; Palma et al., 2020).

MW heating has been used in lignin conversion processes, especially in pyrolysis reactions, obtaining bio-oils rich in phenolic compounds. However, fast pyrolysis of lignin using MW resulted in lower bio-oil yields comparatively with traditional fast pyrolysis (Bartoli et al., 2020; Fan et al., 2019; Palma et al., 2020). Moreover, as lignin has a low dielectric loss factor, more energy is needed to achieve the best conditions, thus only if bio-oil is upgraded to high added-value compounds the technique will be feasible (H. Li et al., 2015).

Lignin oxidation using MW has been introduced as a new way to improve the production of added-value compounds, such as aromatic aldehydes and acids (e.g., vanillin and syringaldehyde). Many oxidation studies have been performed using lignin model compounds to understand how the MW influences the reaction pathways. Gu et al. (2010) oxidized a lignin phenolic model compound (3-methoxy-4-hydroxybenzyl alcohol) using La-SBA-15 catalyst and H_2O_2. The catalyst improved oxidation to aromatic acids and quinones, and the oxidation was faster than with the conventional heating (CH). Lignin dimers (2-phenoxy-1-phenylethanol) and monomers (vanillyl alcohol and 4-hydroxybenzyl alcohol) were oxidized by Pan et al. (2015) using different metal salts, and the most effective ones were $CrCl_3$ and $MnCl_2$, while MW radiation resulted in better yields than CH. Zhang et al. (2016) used an electrodeless lamp combined with MW and H_2O_2 to enhance the photooxidation of guaiacol. The main formed acids were formic, acetic, and oxalic, and their yields were dependent from pH, time, and concentration of guaiacol and H_2O_2. Zhu et al. (2017) evaluated two lignin model dimers to study C_α-C_β bond cleavage, which is more difficult to break than the *β-O-4* bond. The authors found that MW improved the cleavage of the C_α-C_β bond, especially for phenolic dimer and organosolv lignin, releasing more aromatic monomers. Qu et al. (2020) oxidized phenolic and non-phenolic lignin monomers with *β-O-4* bonds using H_2O_2 and CuO. When comparing MW and CH systems, the authors found that the same reaction products were formed, but at different rates, since some oxidation steps were accelerated or not by MW. For example, the oxidation of vanillin to vanillic acid was accelerated, but the demethylation step and the ring-opening reaction not. This work was the first study reporting C_4-DCA production, including succinic, maleic, malic, and fumaric acids, from lignin model oxidation using MW.

Oxidation using real lignin samples showed different results, depending on the used lignin type and experimental conditions. Ouyang et al. (Ouyang et al., 2010) oxidized soda lignin with H_2O_2 using MW, achieving better degradation of high molecular-weight lignins to lower molecular weight fragments when compared to CH. Nevertheless, MW facilitated also the re-condensation reactions. The degradation and re-condensation were affected by the used temperature, time, and oxidant load. In a subsequent study, the authors verified that acidic conditions, high temperatures, and a correct amount of H_2O_2 were needed to maximize degradation (Ouyang et al., 2015). They also observed that MW oxidation gave rise to fewer products, mainly aliphatic alkanes, alcohols, acids, and esters, due to the cleavage of aromatic rings and deprivation of the side chains. In contrast, with CH, a more complex mixture of products, composed mainly of aromatic compounds, was observed. Kim and Park (2013) oxidized sulfonated lignin using MW and KOH. The obtained compounds when using MW were different from CH-assisted oxidation, namely, they include guaiacol, vanillin, homovanillic acid, acetovanillone, phenol, and syringol.

Heterogeneous catalysts can be used with MW heating since they are good MW absorbers, thus they can be heated very quickly, and reaching, in some cases, a higher temperature than the liquid phase due to special thermal effects (also known as hot spots) (Li et al., 2020). Alkaline-fractionated lignin depolymerization using different catalysts (CuO, $Cu(OH)_2$, Fe_2O_3, Cu_2O) in MW-assisted peroxide oxidation yielded vanillin and acetosyringone as the main products, which were produced at higher amounts when $Cu(OH)_2$+Fe_2O_3 catalyst was used, accompanied by other aromatic compounds, quinones and carboxylic acids at lower quantities (Panyadee et al., 2018). In addition, it was confirmed that Cu^{2+} promoted the cleavage of the side chains and the ether linkages, while Fe^{3+} enhanced H_2O_2 oxidation performance and the monophenols formation yields (Ouyang et al., 2014). Finally, peroxide oxidation of three lignins using $CuSO_4$ showed that the conversion was affected by the oxidant concentration, $CuSO_4$ presence, reaction time, and high temperatures. $CuSO_4$ has an essential role in the $\cdot OH$ radicals production, and the MW accelerated this reaction. The main products were aromatic compounds (acids, aldehydes) related to the initial type of lignin (Dai et al., 2018).

In this research, three different lignins were oxidized using titanium silicalite-1 (TS-1) and Fe-TS1 modified catalyst, and H_2O_2 as the oxidant. TS-1 has shown promising results, improving the amount of succinic acid in the peroxide oxidation of lignin, as already shown in Chapter 5 using conventional heating. This catalyst also improved the hydrogen peroxide conversion in the MW-mediated *n*-hexane oxyfunctionalisation (Kooyman et al., 1996). Given the importance of MW as a more efficient way to heat the reaction medium, it is crucial to evaluate this methodology together with the use of the TS-1 catalyst. The MW heating results will be also compared with the CH results to evaluate which heating system is better for C_4-DCA production.

6.2 Materials and methods

6.2.1 Materials

All chemical reagents were purchased from commercial sources and used without further purification: sulfuric acid (Chem-labs, 95-97% p.a.), sodium hydroxide (Merck, p.a.), hydrogen peroxide solution (Fluka, >30% p.a.), N,N-dimethylformamide (VWR, ≥99.9%), $FeSO_4 \cdot 7H_2O$ (Panreac, 97% p.a.), deuterated dimethyl sulfoxide (DMSO-d_6; VWR, 99.80%), and lithium chloride (VWR, AnalaR NORMAPUR). Catalyst TS-1 (ref. #: MSTS1001, lot number: 130117; H^+ cation) was acquired from ACS Materials, LLC. Fe-TS1 was obtained by modifying the original TS-1 by wet impregnation, as performed and detailed in Chapter 3.

Three different lignins were studied: Indulin AT (IAT), commercialized by MeadWestvaco Corporation, USA; a lignin isolated in May 2021 from an industrial black liquor obtained from a Portuguese *Eucalyptus globulus* Kraft pulping mill (The Navigator Company, Portugal) (EKL); and a lignin produced by an ethanol organosolv process from *Eucalyptus globulus* (EOL), supplied by Lignol Innovations, Canada.

6.2.2 Lignin characterization

Lignin characterization comprised the determination of ashes, carbohydrates, acid-insoluble, and acid-soluble lignin. Ashes were quantified by incinerating 0.5 g of lignin at 600ºC until a constant mass was achieved. Carbohydrates content was determined by suspending 15 mg of lignin in 2 mL of a 2 mol/L HCl methanolic solution with the acid methanolysis occurring for 4 h, at 100ºC. After cooling, pyridine and sorbitol (internal standard) were added, and the solution was evaporated under reduced pressure. The methanolysates were derivatized using trimethylchlorosilane (TMCS). Then, quantification was performed using GC-FID. A complete description of the procedure can be found elsewhere (Costa et al., 2018). Insoluble lignin was quantified by dissolving the lignin sample in an alkaline solution until complete dissolution was achieved, then acidified with H_2SO_4 2 mol/L until pH 2; heating at 40ºC to coagulate the lignin, then followed by centrifugation at 3500 rpm for 30 min. The insoluble lignin was dried at

100ºC overnight and weighted. The acid-soluble lignin content was considered as 100% - ashes content (%)- carbohydrates content (%)- acid-insoluble lignin content (%).

Quantitative ^{13}C NMR analysis was performed using a Bruker AVANCE III 400 spectrometer, operating at 400 MHz, at 45ºC for 72 h. For that, lignin samples (170 mg) were dissolved in 0.5 mL of deuterated dimethyl sulfoxide (DMSO-d_6). The quantitative conditions used for ^{13}C NMR measurements were: simple 1D pulse sequence, recycling time of 12 s, 1400 scans, and 1D sequence with power gated coupling using 90º flip angle. More details about the applied method can be found elsewhere (Costa et al., 2018).

Gel permeation chromatography (GPC) was used to evaluate lignin molecular weight and polydispersity index. Calibration was done using polystyrene (PS) standards, in the molecular weight range comprised between 162 and 50 000 g/mol (the calibration curve can be consulted in Fig A.3, in Appendix A). A Shimadzu Ultra-Fast Liquid Chromatography (UFLC) equipment, equipped with a Diode Array Detector (280 nm) was used with two Agilent columns in series: firstly an OligoPore column (300 x 7.5 mm, 6 µm nominal particle size) followed by a MesoPore column (300 x 7.5 mm, 3 µm nominal particle size). Before this arrangement, an OligoPore pre-column (300 x 7.5 mm) was placed. Analysis was performed at 70ºC, using dimethylformamide with 0.5 wt% LiCl, at 0.8 mL/min. More details about the applied method can be found elsewhere (Costa et al., 2018).

Attenuated total reflectance- Fourier transform Infrared Spectroscopy (ATR-FTIR) measurements were carried out using a JASCO FT/IR-6800 spectrometer (JASCO Analytical Instruments, USA), equipped with a MIRacle™ Single Reflection (ZnSe crystal plate; PIKE Technologies, USA). The analysis was performed by co-adding 256 scans in the range 4000-700 cm^{-1}, using a resolution of a 4 cm^{-1}.

6.2.3 Oxidation Procedure

Lignins were oxidised using a Biotage Initiator+ microwave reactor (Figure 6.1). For that, a lignin solution (2.5 mL, 10 g/L, pH 7.0, dissolved in water) was placed inside a 2-5 mL microwave vial with a stirring bar, then added with 0.250 mL of a 30 wt% H_2O_2 solution and 2.5 mg of catalyst when applied. The reactors were pre-stirred at 780 rpm for 30 s, the magnetron was turned on, and the heating started using the *Very high* absorption level, reaching the desired temperature around 90 seconds after starting the heating. Stirring was maintained during the oxidation to avoid hot spots in the solution that would produce localized over-oxidation. At the end of the reaction time, the microwave vial was immediately cooled with compressed air, reaching 40ºC around 2 minutes after the end of the reaction. The effect of temperature (140-170ºC), reaction time (0-3 h), type of catalyst (TS-1, Fe/TS-1), and type of lignin (Indulin AT, Lignol, and *E. globulus* kraft lignins) was studied. Experiments were done in duplicate.

Figure 6.1 - Biotage Initiator+ microwave reactor.

The data of conventional heating, used for comparison purposes, were extracted from Chapter 5. The information related to the used methodology can be found in subsection *5.2.2. Oxidation procedure*, from the *Materials and Methods* section in Chapter 5.

6.2.4 Oxidized lignin quantification

Oxidized lignin samples were acidified to pH~2, heated at 40°C to coagulate the acid-insoluble lignin, then centrifuged at 3500 rpm for 30 minutes. The acidic supernatant was used for carboxylic acid and acid-soluble lignin quantification. The insoluble lignin was resolubilised in an alkaline solution. Acid-soluble and insoluble lignin solutions were analysed by UV spectrophotometry at 240 nm and quantified based on a calibration curve done with the acid-soluble and insoluble lignin obtained from the respective original lignin, respectively. Lignin conversion was calculated as the sum of the acid-insoluble and the acid-soluble lignins. Calibration curves for acid-soluble and insoluble lignins can be found in Fig A.1, in Appendix A.

6.2.5 Carboxylic acids quantification

Carboxylic acids were quantified by high-performance liquid chromatography (HPLC) analysis using a Shimadzu UFLC, equipped with a Diode Array Detector (210 nm), a refractive index detector (RI), and a Phenomenex® Rezex™ ROA H^+ column (300 mm x 7.8 mm) and precolumn (50 mm x 7.8 mm). The analysis was performed at 50°C using isocratic mode (4 mmol/L H_2SO_4) at a 0.5 mL/min flow rate and an injection volume of 20 μL. Carboxylic acids were identified by comparison with retention times and quantified using calibration curves of individual standards. Samples were acidified, diluted as needed, and filtered through a 0.22 μm pore-size filter before injection. Calibration curves can be found in Table A.3, in Appendix A.

Quantified acids are expressed as *C_4-DCA* (sum of succinic, malic, maleic, fumaric, and tartaric acids) and *TCA* (total carboxylic acids: C_4-DCA plus oxalic, acetic, and formic acid).

6.3 Results and discussion

6.3.1 Lignin characterization

The studied lignins were characterized by FTIR, ^{13}C-NMR, GPC, and by quantifying the major components (acid-soluble and insoluble lignin, carbohydrate, and ash contents) to better understand their composition and chemical structure. This information is useful to get insights into the relationship between structure and peroxide oxidation behaviour.

As seen in Table 5.1, lignins IAT and EOL are commercial products with high purity (i.e. high lignin content and a low content of contaminants (carbohydrates and ashes)). On the contrary, EKL, a lignin isolated from a black liquor obtained from a Portuguese pulping plant using *E. globulus* as feedstock, presented a high content of carbohydrates and ashes (i.e. it is a low purity lignin). This sample was isolated in the laboratory, resulting in difficulties in the washing of the precipitated lignin. Even after washed 3 times with ultrapure water, plenty of the ashes remained in the lignin, mainly Na_2SO_4. However, the EKL was used to evaluate the oxidative conversion of this lignin, as an analysis of the possible valorisation of low-purity lignin obtained from pulp and paper production.

Table 6.1 – Composition of lignins (IAT, EOL, and EKL), presented in %w/w_{lignin}.

Lignin	Acid-insoluble lignin content (%*w/w*)	Acid-soluble lignin content (%*w/w*)[1]	Carbohydrate content (%*w/w*)	Ash content (%*w/w*)
IAT	92.1	1.93	2.43	3.54
EOL	95.3	3.2	1.41$^{(\bullet)}$	0.11$^{(\bullet)}$
EKL	65.0	3.7	3.2	28.1

Note: marked data was obtained from $^{\bullet}$ Costa et al., 2014. [1]Acid-soluble lignin is obtained by difference.

The three lignins were studied by gel permeation chromatography to compare the molecular weight, as seen in Table 6.2. EOL presented the higher M_w and M_n, as well it is the most polydisperse ($Đ_M$) lignin. IAT and EKL showed lower M_w and M_n. As both IAT and EKL are kraft lignins, it is expected that the harsh extraction process conditions might reduce the lignin size, compared to the milder extraction conditions of the organosolv process (EOL). As the IAT is a softwood lignin (high percentage of G units), the available site at C_5 position allows an easy condensation during the extraction process, which corroborates the high degree of condensation, comparatively with the other two lignins (hardwood lignins). This fact is also associated to the *β-O-4* content, given that this bond is mainly cleaved in the extraction process. Naturally, this bond has an abundance of 45-50% (softwood) or 60-62% (hardwood) (H. Li et al., 2015). Due to the extraction process conditions this value decreases, but EOL still keeps a high content, while kraft lignins show lower values, especially IAT.

Table 6.2 – Structural properties of the studied lignins (IAT, EOL, and EKL).

Lignin	M_w (g/mol)	M_n (g/mol)	$Đ_M$	S:G:H ratio	DC (%)	*β-O-4* units (per 100 a.r)
IAT	12285$^{(\blacktriangle)}$	4288$^{(\blacktriangle)}$	2.86$^{(\blacktriangle)}$	18:77:05	58	20
EOL	14458$^{(\blacktriangle)}$	4496$^{(\blacktriangle)}$	3.22$^{(\blacktriangle)}$	70:30:0$^{(\bullet)}$	35$^{(\bullet)}$	34
EKL	11595	4243	2.73	69:28:03	26	29

Note: marked data was obtained from $^{\bullet}$ Costa et al., 2014, $^{\blacktriangle}$ Chapter 5

The ATR-FTIR analysis (Figure 6.2) evidences the characteristic peaks of lignin as reported by Faix (1992) and Cateto et al. (2008). All lignins presented bands associated with OH stretching (3400 cm^{-1}) and C-H stretching of methyl and methylene groups (2934 and 2836 cm^{-1}). Vibrations associated with aromatic rings were present in all lignins, at approximately 1594 cm^{-1}, 1512 cm$^{-1,}$ and 1422 cm^{-1}. IAT presented only softwood characteristic vibrations (for guaiacyl units) at 1266 cm^{-1} and 855 cm^{-1}, while EOL and EKL also showed signals for syringyl groups, in the 1323-1326 cm^{-1} and 816-830 cm^{-1} regions. Also, the band at 1030 cm^{-1} was more intense in softwood lignins, while bands at 1456 cm^{-1} and 1108-1123 cm^{-1} were more intense in hardwood lignins. All these bands are associated with C-H deformations. Finally, the band at 1213 cm^{-1}, associated with a combined effect of C-C, C-O, and C=O stretching, was more intense in hardwood lignins.

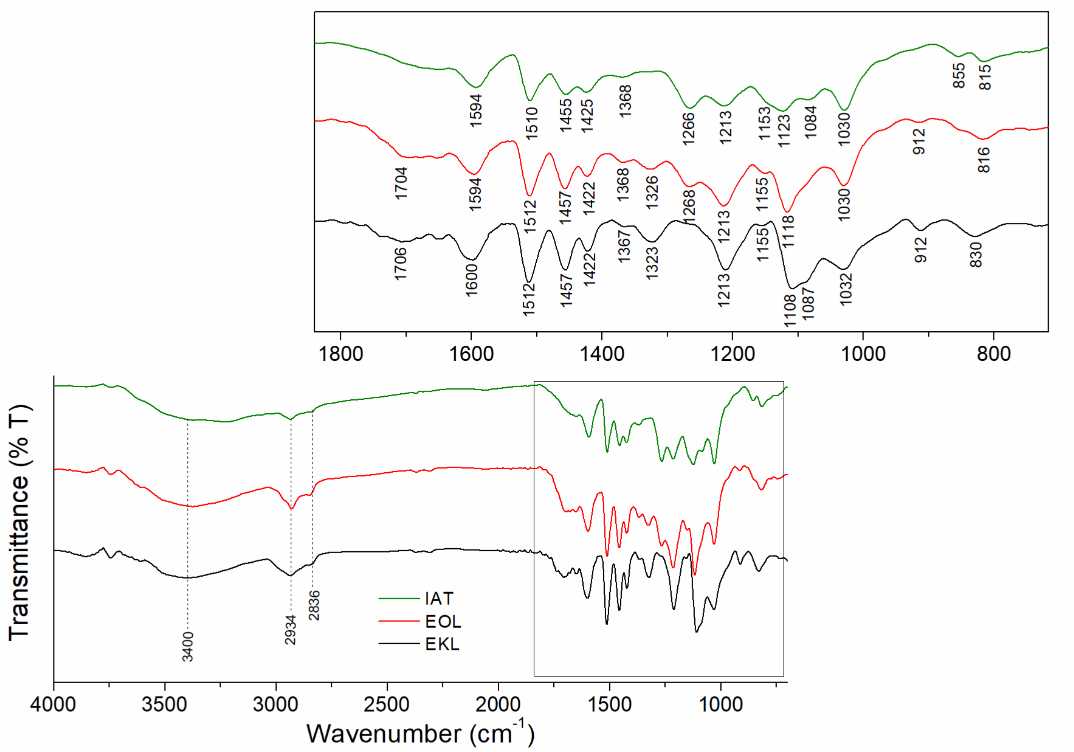

Figure 6.2 - ATR-FTIR analysis for the studied lignins

A ^{13}C-NMR analysis was performed to get information concerning lignin structure, including chemical bonds. The assignments were based in Costa et al. (2014) work, and the results are included in Table 6.3. EOL proved to be the lignin with higher *β-O-4* bonds. However, all lignins showed lower *β-O-4* values comparatively with the expected values for these type of lignins, probably due to a more vigorous depolymerization process, while the *β-5* + *β-β* units were in the expected ranges (H. Li et al., 2015). The condensation reactions are easier in softwood lignins (IAT) since G units have an available position (C_5) that can be linked with other units. In contrast, hardwood lignins (EKL and EOL) have methoxyl groups in both C_3 and C_5 positions, diminishing the possibility of condensation reactions. This relation can also be confirmed in the aromatic OCH_3 groups, higher for EOL and EKL lignins, and lower for IAT. Another important fact is that EOL shows no *p*-hydroxyphenyl units (H) while EKL shows only 3% H and IAT has 5% H units in their structure. The H units are more difficult to be oxidized to DCA due to the absence of methoxyl groups, since these substituents activates the aromatic ring to further oxidation (as stated in Chapter 3).

Table 6.3 – Assignments and quantification of structures/linkages and functional groups, identified by ^{13}C NMR (number per aromatic ring)

Lignin	Amount (number/Ar)		
	IAT	EOL$^{(\bullet)}$	EKL
β-5 and *β-β* structures (δ 51.0-53.8 ppm)	0.07	0.10	0.13
Aromatic OCH_3 (δ 54.3-57.3 ppm)	0.82	1.40	1.36
C_γ in *β-O-4* structures without C_α=O (δ 59.3-60.8 ppm)	0.13	0.26	0.14
C_γ in *β-5* and *β-O-4* structures with C_α=O; C_γ in *β-1* (δ 62.5-63.8 ppm)	0.05	0.07	0.16
C_α in *β-O-4* structures; C_γ in pinoresinol/syringaresinol and *β-β* structures (δ 70.0-76.0 ppm)	0.26	0.34	0.79
C_β in *β-O-4* structures; C_α in *β-5* and *β-β* structures (δ 80.0-90.0 ppm)	0.27	0.44	0.42
Aromatic C_{Ar}-H (δ 103.0-123.0 ppm)	2.19	1.95	2.02
Aromatic C_{Ar}-C (δ 123.0-137.0 ppm)	1.72	1.75	1.77
Aromatic C_{Ar}-O (δ 137.0-156.0 ppm)	2.05	2.30	2.19
C_4 in H units (δ 157.0-162.0 ppm)	0.04	0.00	0.03
CHO in benzaldehyde structures (δ 191.0-192.0 ppm)	0.02	0.04	0.03
CHO in cinnamaldehyde structures (δ 193.5-194.5 ppm)	0.01	0.04	0.03
CO in aldehydes and ketones (δ 195.0-210.0 ppm)	0.20	0.47	0.41

Note: marked data were obtained from $^\bullet$ Costa et al., 2014

6.3.2 Microwave-assisted oxidation

MW-assisted reactions can enhance lignin oxidation, but there is a direct connection between degradation and the reaction conditions, like pH, temperature, oxidant load, and time (Ouyang et al., 2015). In this work the effect of temperature, time, and catalyst type in the lignin oxidation towards C_4-DCA was evaluated.

6.3.2.1 Effect of temperature

As presented in Chapter 5, lignin oxidation depends significantly on the used lignin type, especially in what concerns origin and pulping method. As a starting point, IAT was selected to evaluate the best temperature for MW-assisted oxidation since this lignin originated the highest succinic acid when oxidized using conventional heating.

For IAT non-catalysed oxidation, the temperature had a strong effect on the C_4-DCA yields (sum of succinic, malic, maleic, fumaric, and tartaric acids). In Figure 6.3.a, the maximum C_4-DCA yield moved towards shorter times and higher yields with increasing temperature. The reaction using the lowest temperature (140ºC) took 2.0 h to reach the highest yield (8.2 wt%), while at 160ºC, the C_4-DCA yield achieved 18.3 wt% just in 30 minutes. The highest tested temperature (170ºC) showed its maximum yield at 15 minutes, then decreased, indicating that the acids were degraded after this point. The same behaviour was observed for the other tested temperatures, showing a slow decrease after the C_4-DCA maximum. Succinic and malic acids shared the same increasing-decreasing maximum yield behaviour, as observed in Figure 6.3.c and Figure 6.3.d, respectively. These acids represented more of the 98% of the quantified C_4-DCA. Interestingly, succinic acid yield did not significantly increase with temperature, with the highest yield achieved at shorter times. Malic acid yield, on the contrary, increased with temperature, going from 4.4% (140ºC) to 14.3% (160ºC). Probably, the temperature of 170ºC did not increase malic acid yield due to a fast degradation of the already-produced acids. Also, higher temperatures increased, considerably, the degradation to low-molecular-weight compounds, like formic and acetic acids (Figure 6.3.e and f, respectively). Formic acid was rapidly degraded to CO_2 at high temperatures, while acetic acid remained stable without decreasing its percentage even at high temperatures. Probably, succinic acid was not produced at higher yields because it was converted to malic acid and other compounds under oxidative conditions (Bensalah et al., 2012; Chan et al., 2014), confirming the increase in malic acid yield. Succinic and malic acids were degraded to formic and acetic acids, confirming the decrease of the C_4 acids after the maximum. As expected, lignin conversion strongly depended on temperature, as seen in Figure 6.3.b. It was needed at least 2 h to achieve a lignin conversion higher than 97% at 140ºC, while at 170ºC, it only took 30 minutes, confirming the important effect of temperature in the oxidation of lignin to added-value compounds. This effect has already been confirmed in other publications regarding lignin oxidation in MW reactors (Kim and Park, 2013; Ouyang et al., 2015; Qu et al., 2020).

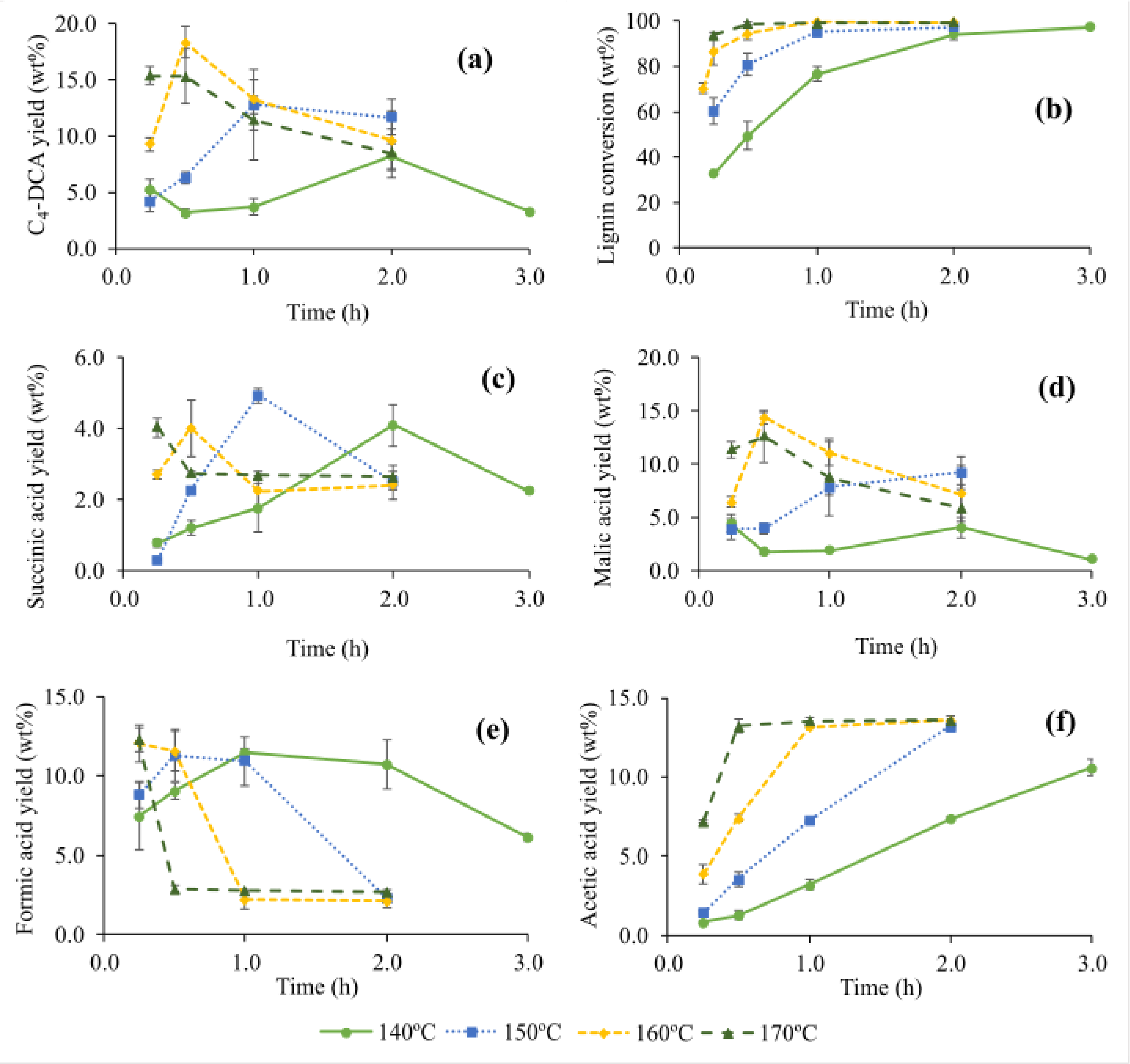

Figure 6.3 - Non-catalyzed microwave-assisted oxidation of IAT: Effect of temperature on **(a)** C_4-DCA yield, **(b)** lignin conversion, and yields for **(c)** succinic acid, **(d)** malic acid, **(e)** formic acid, and **(f)** acetic acid.

The experiments performed at 170ºC showed some technical problems due to the rapid reaction inside the vessel, since peroxide oxidation released O_2 from H_2O_2 disproportion and CO_2 from complete lignin mineralization, causing a rapid increase in pressure. This rise exceeded the safety recommendations for pressure rise (max. 5 bar/s) and caused several reactions to be stopped for safety measures. Even though a temperature of 170ºC generated the fastest oxidation, it is not recommended for safe and reproducible oxidation. Thus, the highest temperature selected for further experiments was 160ºC.

6.3.2.2 Catalytic effect: TS-1 and modified Fe-TS1

Catalysts have been used to improve the conversion and selectivity of lignin oxidations towards added-value compounds (Upton and Kasko, 2016). Titanium silicalite-1 (TS-1) was used for lignin peroxide oxidation (Chapter 5), and the obtained yields for succinic acid were higher when the catalyst was present. To evaluate if the same effect is observed when using MW as the heat source, experiments were performed using three lignins from different origins: Indulin AT (IAT, a softwood kraft lignin), Lignol (EOL, a hardwood organosolv lignin), and a lignin isolated from *Eucalyptus globulus* black liquor (EKL, a hardwood kraft lignin). The three lignins were oxidized at 160ºC under three catalytic conditions: TS-1 catalyst, a modified TS-1 with Fe (as reported previously in Chapter 3), and a non-catalysed reaction used for comparison. Lignin conversion was slightly lower when TS-1 was used, as can be seen in Figure 6.4, while the non-catalysed reaction reached complete conversion after 2.0 h for the three tested lignins. The same behaviour was observed previously when conventional heating was applied (Chapter 5). It has been reported that TS-1 stabilizes the hydrogen peroxide, avoiding very severe oxidation and slowly releasing the ·OH radicals (Kooyman et al., 1996). Interestingly, when Fe-TS1 was used in EKL and EOL lignins, the conversion was higher at shorter times, indicating that the Fe atoms in the catalyst structure enhanced the hydroxyl radical formation, increasing lignin depolymerization to lower-molecular-weight compounds (Ouyang et al., 2014).

Succinic and malic acids were the main C_4 acids obtained after the oxidation, with very low yields for fumaric and maleic acids (<0.10 % wt and <0.20 %wt, respectively), and no tartaric acid detected. Even maleic acid was not found at significant quantities, it is a fundamental intermediate after ring-opening reaction to produce malic and succinic acid, as described in Chapter 4, Figure 4.11. It was found in very low quantities due to its high reactivity in oxidative conditions, being converted quickly to other compounds.

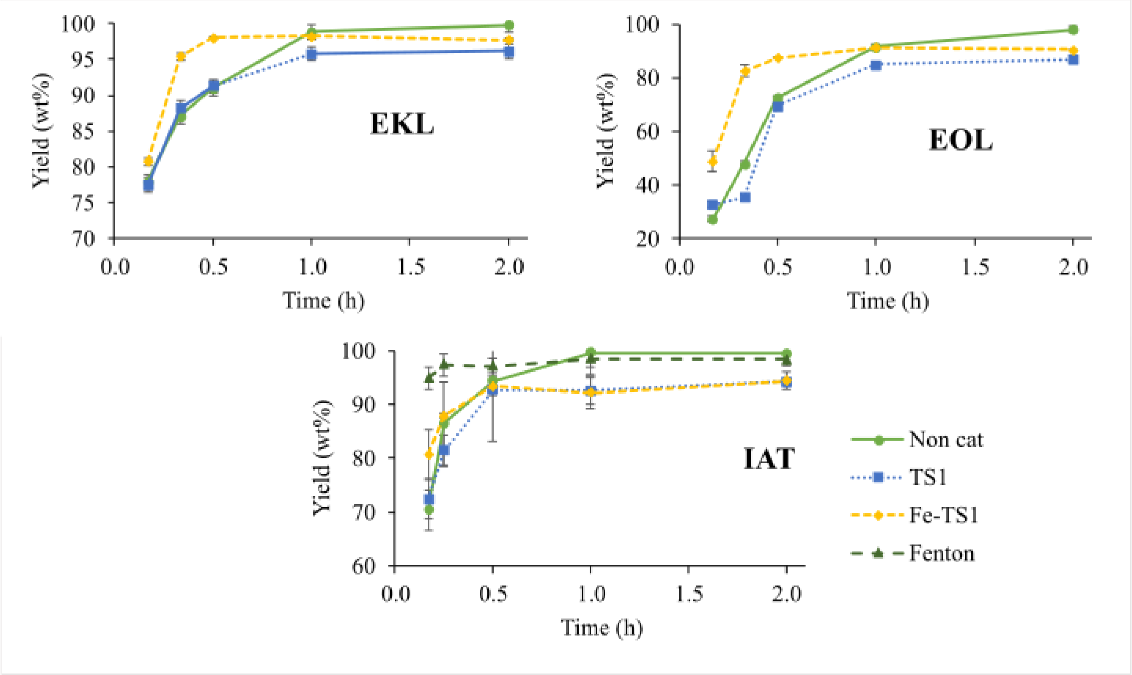

Figure 6.4 - Evolution of lignin conversion through time in the microwave-assisted oxidation, for EKL, EOL and IAT lignins (T=160ºC)

As seen in Figure 5.2a, the non-catalysed reaction showed a maximum for succinic acid yield, then decreasing slowly. The time to achieve the maximum yield depended on the used lignin. For the TS-1 catalysed reaction a continuously increasing yield was observed; only IAT reached a plateau after 1.0 h (yield - 6.3%). In general, the EOL lignin gave rise to the highest succinic acid yields (9.4 % for TS-1, 7.8% for Fe-TS1, 5.2% for non-catalyst). The kraft lignins (EKL and IAT) resulted in lower yields, which depended strictly on the used catalyst. For EKL and IAT, the succinic acid yield was more than twice higher than the yield for the corresponding non-catalysed reaction. With the Fe-TS1 catalyst, the succinic acid production was faster in the first 30 minutes for the studied lignins, but after 1.0 hour, the non-modified TS-1 conducted to similar yields or even higher. This information confirms that the modified Fe-TS1 only accelerated succinic acid production in the first minutes of the reaction, compared to TS-1, not increasing the maximum yield. Also, it can be seen that the catalytic oxidations avoid over-oxidations of the succinic acid, confirming milder reaction conditions, while the non-catalytic oxidation lead to harsher conditions degrading the succinic acid. Moreover, even though EKL was a lignin with lower purity, it produced an interesting amount of succinic acid, especially with the presence of catalyst, showing that impurities present in the lignin did not influence the conversion to succinic acid.

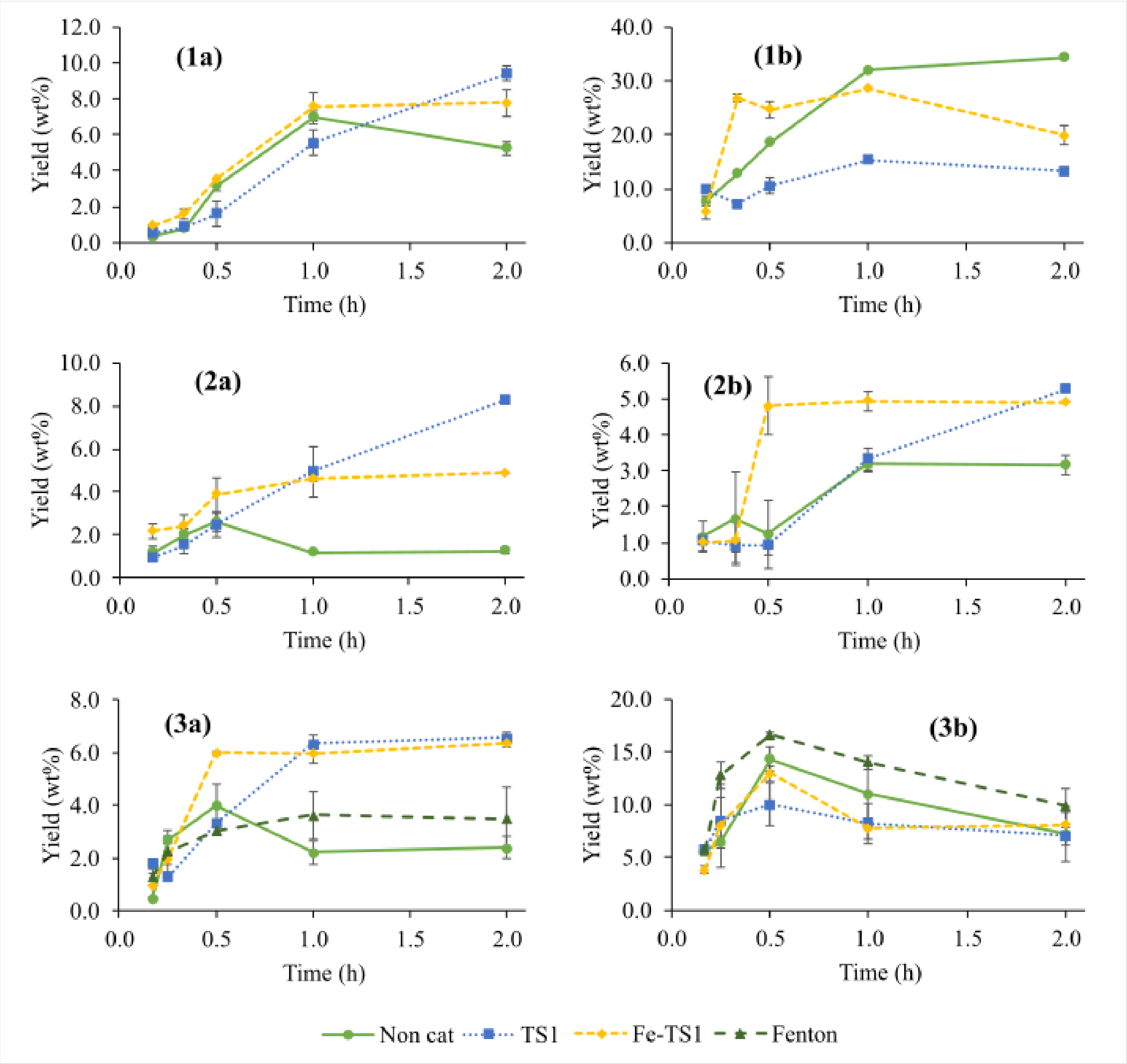

Figure 6.5 - Evolution of C_4-DCA yields through time in the microwave-assisted oxidation. **(a)** Succinic acid and **(b)** malic acid yields for **(1)** EOL, **(2)** EKL, and **(3)** IAT (T=160ºC).

EOL lignin gave rise to the highest yield for malic acid, reaching up to 34% in the non-catalysed reaction, while EKL was the lignin originating the lowest yield (max. 5.2%). For EKL and EOL, the malic acid yield increased rapidly with Fe-TS1. For the EKL, it was needed 2.0 h to be exceeded by the TS1 catalyst. For IAT, malic the maximum acid yield occurred after 0.5 h, then decreased. Both non-catalysed and Fe-TS1 catalysed reactions behaved very similarly, while TS-1 conducted to lower yields.

EOL showed higher yields of succinic and malic acids, but also acetic and formic acids (Figure 6.6.1a,b). Overall, quantified acids after 1.0 h-reaction for EOL accounted up to 56.9% (non-catalysed), 47.9% (TS-1) and 54.5% (Fe-TS1). EOL is an organosolv lignin with a mild pulping process and higher content of easily cleaved ether bonds (as seen in Table 6.2). Therefore, in EOL, the oxidant is mainly used to break the ether bonds, releasing the available hydroxyl groups in the phenolic ring, which facilitates the opening of the aromatic ring to produce the C_4-DCA. As the oxidation is more efficient with this lignin, the amount of C_4-DCA is higher. The easier degradation to C_4-DCA was also observed when conventional heating was used (Chapter 5). The C_4-DCA yields were similar with and without the catalyst for EOL, showing that for an organosolv lignin, the MW facilitates the oxidation that could be accomplished successfully even without catalyst.

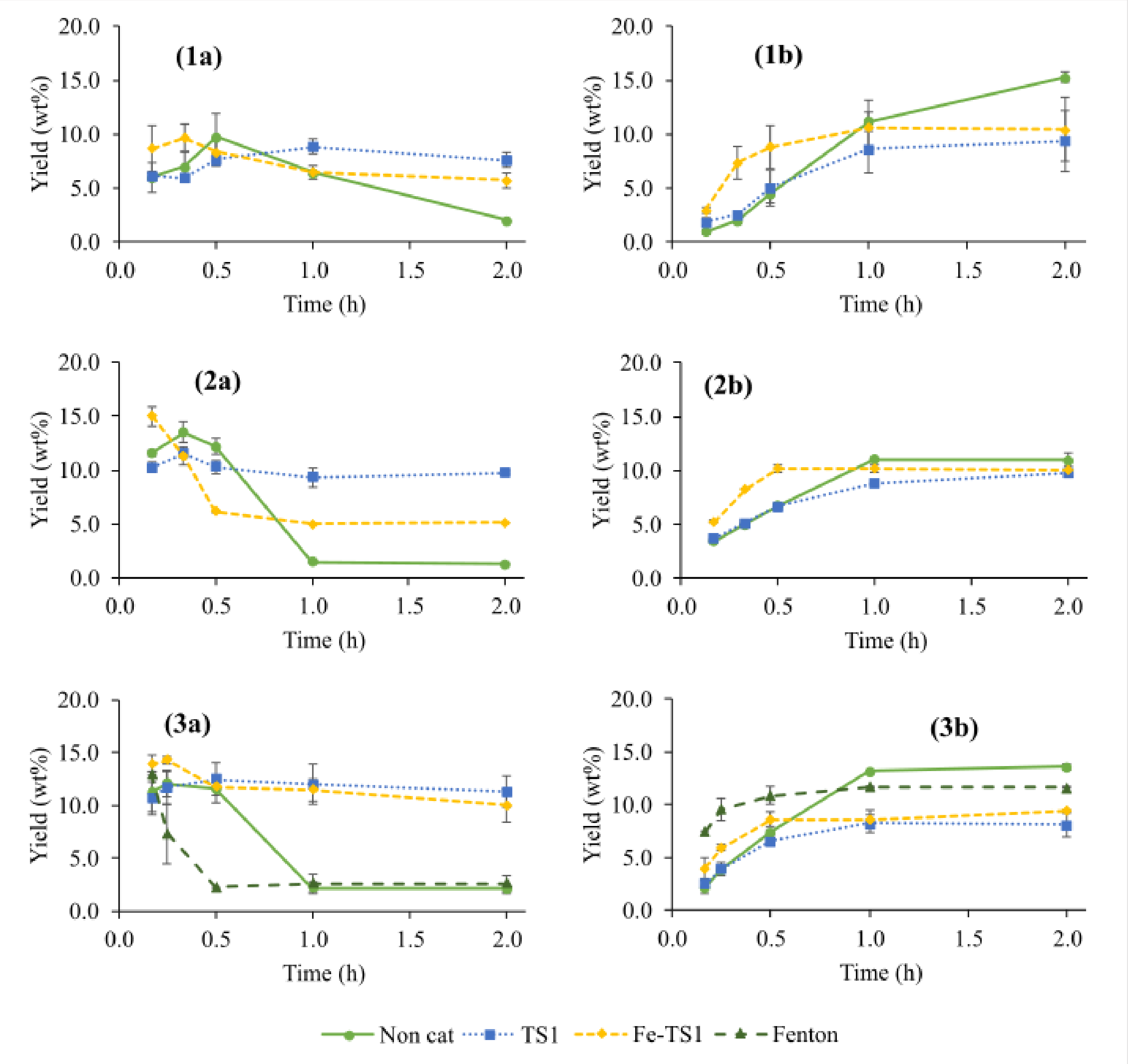

Figure 6.6 - Evolution of **(a)** Formic acid and **(b)** acetic acid yields through time in the microwave-assisted oxidation for **(1)** EOL, **(2)** EKL, and **(3)** IAT (T=160ºC).

Oxidation using only Fe^{2+} as a homogeneous catalyst (Fenton's reagent) was applied to IAT lignin to evaluate if a combined effect of the Fe atoms and the TS-1 structure justifies the differences between TS-1 and Fe-TS1, or if it is just caused by the Fe atoms placed at the catalyst surface. Fenton oxidation lead to a faster lignin conversion (Figure 6.4), given that Fe ions enhance the oxidation ability of H_2O_2, breaking the lignin structure faster, opening the aromatic ring, and producing oxidized low molecular weight compounds (Ouyang et al., 2014). It was noted in Figure 5.2.3a that Fe-TS1 produced more succinic acid in 0.5 h, but the TS-1 reaction reached a similar yield after 1.0 h. The Fenton's catalysed reaction behaved similarly to the non-catalysed reaction, resulting in low yields, while both TS-1/Fe-TS1 catalysts resulted in higher yields. Regarding malic acid, the best yield was achieved for the Fenton's reaction, followed closely by the non-catalysed reaction and the Fe-TS1. In all cases, the highest malic yield acid was achieved in the first 30 minutes, then decreasing. As proposed in Chapter 4 (Figure 4.11), once maleic acid is formed, it can be oxidized to malic acid or hydrated to succinic acid. As the TS-1/Fe-TS1 catalysts behaved similarly, resulting in high succinic acid yield, and Fenton's reagent behaves similarly to the non-catalysed reaction for malic acid yield, it can be inferred that the TS-1 and the Fe-TS1 catalysts preferably follow the pathway to succinic acid. On contrary, Fenton's catalyst and the non-catalysed reaction prefer the oxidation of maleic acid to malic acid. Thus, TS-1 and Fe-TS1 allow more selective oxidation towards succinic acid production.

It has been reported that H_2O_2 adsorbs in the tetrahedral Ti active sites in the TS-1 form the Ti-OOH species, which has an increased nucleophilic attack capability, compared to the H_2O_2 molecules (Xia et al., 2017). These species later interact with organic compounds that are close to the catalyst surface. Since the radicals are released in a controlled way, the lignin is oxidized by opening the aromatic ring and releasing the dicarboxylic acids (mainly maleic acid). However, as the acids are released to the aqueous medium, it is more difficult for them to interact with the acid catalyst surface to hydrate the double bond to form succinic acid. In the non-catalysed reaction, the free ·OH radicals are produced directly by the disproportion of H_2O_2 in the aqueous medium becoming available to attack the lignin structure, the already formed products, or to combine with other radicals. The Fe atoms in the Fe-TS1 structure disproportioned H_2O_2 instantly to free radicals, having the Fe-TS1 catalyst a mix behaviour between the stability of the TS-1 oxidation and the quick oxidation of the non-catalysed reaction, producing good succinic and malic acid yields. It can be concluded that the Fe-TS1 catalyst shows a combined effect of the Fe atoms along with the specific catalytic effect of the TS-1. Among TS-1 and Fe-TS1, Fe-TS1 achieves higher results in the first 30 minutes, but is quickly matched by the TS-1, and the difference in productivity is very slight.

6.3.3 Comparison with conventional heating

One of the significant advantages of using microwave radiation as a heating source against CH is the fact that reactions usually are achieved using milder conditions (e.g., shorter times or lower temperatures) due to the rapid heating process and efficient energy absorption (Kim and Park, 2013). Oxidations using the same lignins (IAT and EOL) were compared under different heating systems (conventional *vs*. microwave heating). The conventional heating system consisted of a Teflon vessel placed inside a pre-heated steel reactor (Figure 6.7.a), which was placed over a heating plate and protected with an insulation material. The microwave reactor consisted of a glass reactor, sealed after placing the samples and the stirring rod inside and placed directly inside the microwave equipment (Figure 6.7.b) without further preparation. The same reaction conditions (temperature, pH, lignin concentration, stirring, H_2O_2 concentration and catalyst load) were used in both reactors for comparison.

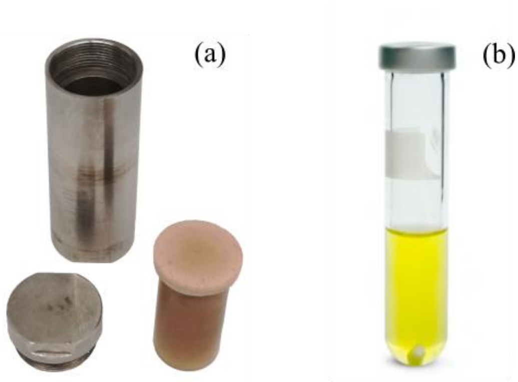

Figure 6.7 - Reactors used for **(a)** conventional heating (CH) and **(b)** microwave (MW)

When IAT lignin was oxidized using both methods at 140ºC (10% H_2O_2, 10% TS-1 (lignin-basis), stirring 800 rpm), it was found that in both catalyzed and non-catalyzed reactions, the MW heating gave rise to higher C_4-DCA yield at shorter times, but after 1.0 h, the CH become more effective leading to higher yields (Figure 6.8). The slower heating in the CH reactors avoided the rapid disproportion of H_2O_2 to H_2O and O_2 observed in the MW reactors in the first minutes. Therefore, the H_2O_2 was slowly activated in the CH compared to the MW, justifying why the conversion was faster in the first 30 minutes in the MW, but after 1 h, the oxidation was superior in the CH. Moreover, in both CH and MW C_4-DCA yields improved with the presence of the TS-1 catalyst.

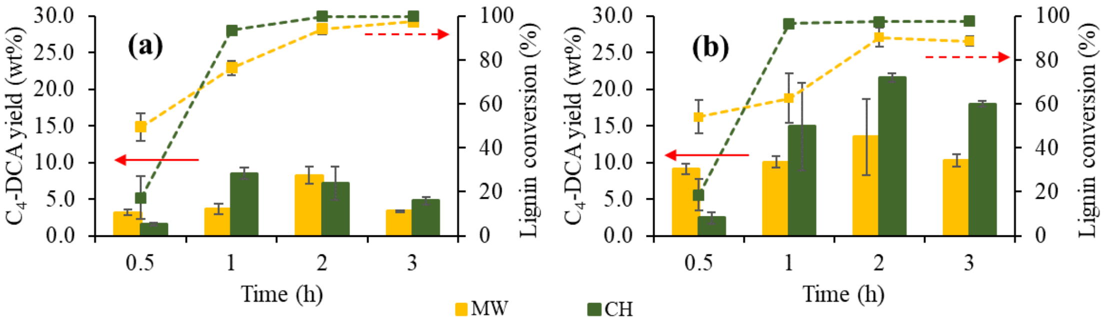

Figure 6.8 - Comparison between microwave (MW) and conventional heating (CH) oxidation, for C_4-DCA yields (columns) and lignin conversion (dashed line) in **(a)** non-catalysed and **(b)** TS-1 catalysed oxidation. (IAT lignin, reaction at 140ºC)

Since TS-1 is a hydrophobic catalyst with a low amount of OH groups, it does not absorb MW radiation. Therefore, it does not heat directly, only by heat transferred from the solvent, the H_2O_2, and the remaining products in the solution, which are quickly heated by MW radiation (Kooyman et al., 1996). However, the already adsorbed materials are heated quickly, and desorption from the catalysts occurs more rapidly (Kim and Ahn, 2012). The H_2O_2 conversion rate is higher when using MW heating, so more H_2O_2 is decomposed when using MW, comparatively with CH leading to a lower oxidation efficiency (Kooyman et al., 1996). The H_2O_2 activation can go through two mechanisms: the free radical mechanism (releasing free ·OH radicals in solution) and the interaction with the catalyst to form Ti-OOH, which interact with the lignin in the catalyst surface. It was also observed that the free radical mechanism has a higher contribution in the MW heating than in the CH, which could explain the lower lignin conversion in MW, and the non-considerable increment in the C_4-DCA yield, which decreased in some cases.

When the two studied lignins are compared concerning CH and MW using the same conditions (2 h, 160ºC, 800 rpm), some differences are evident, as seen in Figure 6.9. In the non-catalyzed reaction (Figure 6.9.(1,2a)), the succinic acid yield was similar for IAT, while for EOL it improved considerably (from 1.6% in CH to 5.2% in MW). Malic acid also increased EOL (from 15.3% in CH to 34.3% in MW) and IAT (from 1.4% in CH to 7.2% in MW). The increase in EOL was evident, since C_4-DCA yield increased from 16.8% (CH) to 39.6% (MW).

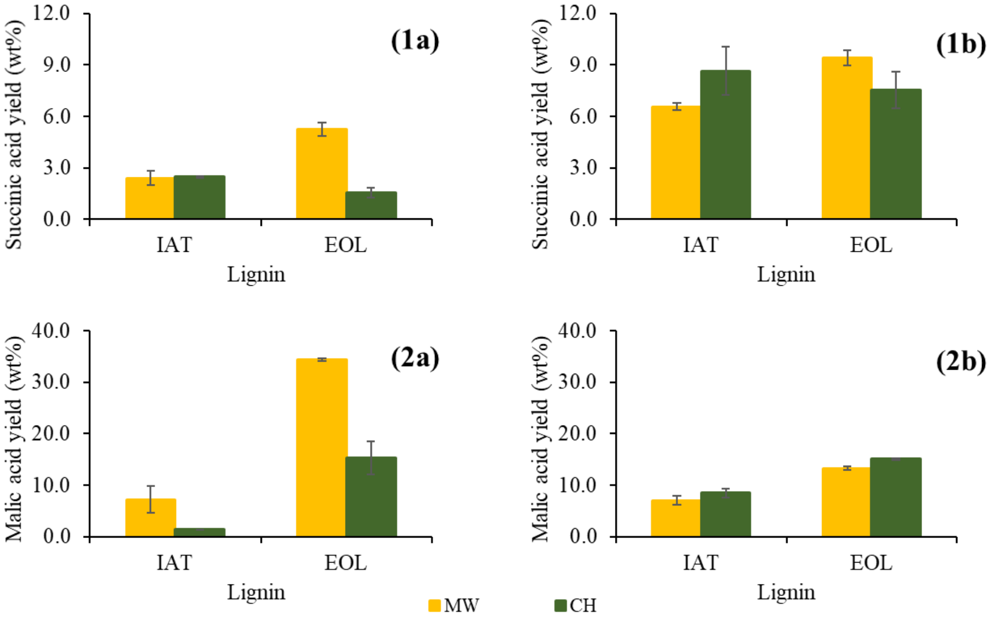

Figure 6.9 - Comparison between microwave (MW) and conventional heating (CH) oxidation using different lignins, for **(1)** succinic acid and **(2)** malic acid, in **(a)** non-catalysed and **(b)** TS-1 catalysed oxidation. (2 h reaction, 160ºC)

In general, MW enhanced the lignin non-catalyzed oxidation, especially with EOL. It has been reported that MW irradiation enhances the cleavage of β-*O-4* bonds (Ouyang et al., 2010) and C_α-C_β bonds (Zhu et al., 2017), thus facilitating lignin fractions and monomers conversion to C_4-DCA. Since EOL has a higher amount of β-*O-4* bonds (Table 6.2), the enhancement is higher for this lignin, explaining why EOL showed a higher C_4-DCA yield in the non-catalyzed reaction.

In the TS-1 catalysed reaction, a slight increase in succinic acid yield for EOL was evident after an MW reaction, while malic acid yield was lower in all cases for MW reactions (Figure 6.9.(1,2b)). However, the increasing effect on succinic acid yield caused by TS-1 was maintained in both CH and MW heating, while the malic acid yield did not show an apparent effect between both heating methods.

MW and CH differences regarding the produced compounds and the oxidation mechanism has contradictory evidences, as found in previously published works. In some works, the authors say that the lignin mechanism of peroxide oxidation does not change when using CH or MW, but only the reaction rate is affected (Qu et al., 2020), while other authors suggest that different mechanisms can occur when switching the heating method, being selective for cleaving specific bonds (Kim and Park, 2013; Ouyang et al., 2015; Zhu et al., 2017). However, the evidence is scarce since very few studies address the oxidative depolymerization of lignin and its comparison against conventional heating. Also, the exact conditions in both studies (CH vs. MW) were not exactly the same; there is a possibility that the change in the reaction conditions can trigger a modification in the mechanism (Qu et al., 2020).

Recently, Qu et al. (2020) performed a reaction with lignin model compounds using the exact reaction conditions and only changing the heating system. The author observed that an MW-mediated reaction accelerated the C_α-C_β bond cleavage into aromatic compounds, but no acceleration in the aromatic ring cleavage was observed, thus producing the same type of dicarboxylic acids at similar yields. The authors stated that microwaves interact only with intermediates sensitive to electromagnetic waves, and aromatic ring cleavage was not the case. This conclusion is still based on model compounds, and no experiments were performed with lignin using the same conditions, thus it is not easy to extrapolate this finding to the lignin oxidation due to its complex structure. However, in this study, it was possible to infer that EOL had a strong increasing effect with MW (without the catalyst effect), confirming that MW can enhance the production of certain dicarboxylic acids, depending on the structure of the used lignin and the number of labile ether bonds (*β-O-4* linkages).

6.4 Conclusions

Microwave-assisted reaction is an efficient process to conduct lignin peroxide oxidation towards C_4 dicarboxylic acids. Indulin AT non-catalytic oxidation increased when higher temperatures were selected, and C_4-DCA were obtained faster. When TS-1 and Fe-TS1 were used, higher yields of succinic and malic acids were obtained for the catalysed reactions with EKL and IAT. For EOL a similar behaviour in catalysed and non-catalysed reactions was observed. Since EOL is an organosolv lignin, the higher amount of *β-O-4* bonds allowed a faster oxidation, even in the absence of catalyst, because MW facilitates the cleavage of this linkage. The Fe-TS1 gave rise to faster oxidations than TS-1 catalyst, given the combined effect of the TS-1 and the Fe atoms deposited on its surface.

When comparing microwave and conventional heating, it was found that microwave enhanced the non-catalytic oxidation of lignins, especially with EOL, whose succinic and malic acids yields were two times higher with MW oxidation. However, when TS-1 was used, the MW results were lower since H_2O_2 is easily disproportioned to O_2, and the oxidative efficiency become slower.

Overall, it can be concluded that organosolv lignins show a very interesting possibility for future valorization using MW heating since they have bonds easily cleaved by MW leading to high conversion of added-value products. Also, MW showed good energy efficiency, achieving good results for short times. However, it was found that each lignin must be evaluated for both technologies (MW and CH-assisted reaction) to confirm the best process for the compounds of interest.

6.5 References

Aguilar-Reynosa, A., Romaní, A., Ma. Rodríguez-Jasso, R., Aguilar, C.N., Garrote, G., Ruiz, H.A., 2017. Microwave heating processing as alternative of pretreatment in second-generation biorefinery: An overview. Energy Convers. Manag. 136, 50–65. https://doi.org/10.1016/j.enconman.2017.01.004

Bartoli, M., Rosi, L., Frediani, P., Frediani, M., 2020. Bio-oils from microwave assisted pyrolysis of kraft lignin operating at reduced residual pressure. Fuel 278, 118175. https://doi.org/10.1016/j.fuel.2020.118175

Behling, R., Valange, S., Chatel, G., 2016. Heterogeneous catalytic oxidation for lignin valorization into valuable chemicals: What results? What limitations? What trends? Green Chem. 18, 1839–1854. https://doi.org/10.1039/c5gc03061g

Bensalah, N., Louhichi, B., Abdel-Wahab, A., 2012. Electrochemical oxidation of succinic acid in aqueous solutions using boron doped diamond anodes. Int. J. Environ. Sci. Technol. 9, 135–143. https://doi.org/10.1007/s13762-011-0007-5

Berlin, A., Balakshin, M., 2014. Industrial Lignins, in: Gupta, V.K., Tuohy, M.G., Kubicek, C.P., Saddler, J., Xu, F. (Eds.), Bioenergy Research: Advances and Applications. Elsevier, Amsterdam, pp. 315–336. https://doi.org/10.1016/B978-0-444-59561-4.00018-8

Cao, Y., Chen, S.S., Zhang, S., Ok, Y.S., Matsagar, B.M., Wu, K.C.-W.C.W., Tsang, D.C.W., 2019. Advances in lignin valorization towards bio-based chemicals and fuels: Lignin biorefinery. Bioresour. Technol. 291, 121878. https://doi.org/10.1016/j.biortech.2019.121878

Cateto, C.A.B., 2008. Lignin-based polyurethanes: Characterisation, synthesis and applications. Dep. Chem. Eng. University of Porto, Faculty of Engineering, Porto.

Chan, M.N., Zhang, H., Goldstein, A.H., Wilson, K.R., 2014. Role of Water and Phase in the Heterogeneous Oxidation of Solid and Aqueous Succinic Acid Aerosol by Hydroxyl Radicals. J. Phys. Chem. C 118, 28978–28992. https://doi.org/10.1021/jp5012022

Costa, C.A.E.E., Pinto, P.C.R., Rodrigues, A.E., 2014. Evaluation of chemical processing impact on E. globulus wood lignin and comparison with bark lignin. Ind. Crops Prod. 61, 479–491. https://doi.org/10.1016/j.indcrop.2014.07.045

Costa, C.A.E.E., Pinto, P.C.R.R., Rodrigues, A.E., 2018. Lignin fractionation from E. Globulus kraft liquor by ultrafiltration in a three stage membrane sequence. Sep. Purif. Technol. 192, 140–151. https://doi.org/10.1016/j.seppur.2017.09.066

Dai, J., Styles, G.N., Patti, A.F., Saito, K., 2018. $CuSO_4/H_2O_2$-Catalyzed Lignin Depolymerization under the Irradiation of Microwaves. ACS Omega 3, 10433–10441. https://doi.org/10.1021/acsomega.8b01978

Faix, O., 1992. Fourier Transform Infrared Spectroscopy, in: Stephen Y., L., Carlton W., D. (Eds.), Methods in Lignin Chemistry. Springer, Berlin, Heidelberg, pp. 83–109. https://doi.org/10.1007/978-3-642-74065-7_7

Fan, L., Song, H., Lu, Q., Leng, L., Li, K., Liu, Y., Wang, Y., Chen, P., Ruan, R., Zhou, W., 2019. Screening microwave susceptors for microwave-assisted pyrolysis of lignin: Comparison of product yield and chemical profile. J. Anal. Appl. Pyrolysis 142, 104623. https://doi.org/10.1016/j.jaap.2019.05.012

Gérardy, R., Debecker, D.P., Estager, J., Luis, P., Monbaliu, J.-C.M., 2020. Continuous Flow Upgrading of Selected C 2 –C 6 Platform Chemicals Derived from Biomass. Chem. Rev. 120, 7219–7347. https://doi.org/10.1021/acs.chemrev.9b00846

Gu, X., He, M., Shi, Y., Li, Z., 2010. La-Containing Sba-15/H_2O_2 Systems for the Microwave Assisted Oxidation of a Lignin Model Phenolic Monomer. Maderas. Cienc. y Tecnol. 12, 181–188. https://doi.org/10.4067/s0718-221x2010000300003

Huang, D., Li, R., Xu, P., Li, T., Deng, R., Chen, S., Zhang, Q., 2020. The cornerstone of realizing lignin value-addition: Exploiting the native structure and properties of lignin by extraction methods. Chem. Eng. J. 402, 126237. https://doi.org/10.1016/j.cej.2020.126237

Kamm, B., Gruber, P.R., Kamm, M., 2008. Biorefineries-Industrial Processes and Products: Status Quo and Future Directions, Biorefineries-Industrial Processes and Products: Status Quo and Future Directions. https://doi.org/10.1002/9783527619849

Kim, H.G., Park, Y., 2013. Manageable conversion of lignin to phenolic chemicals using a microwave reactor in the presence of potassium hydroxide. Ind. Eng. Chem. Res. 52, 10059–10062. https://doi.org/10.1021/ie400719v

Kim, K.-J., Ahn, H.-G., 2012. The effect of pore structure of zeolite on the adsorption of VOCs and their desorption properties by microwave heating. Microporous Mesoporous Mater. 152, 78–83. https://doi.org/10.1016/j.micromeso.2011.11.051

Kooyman, P.J., Luijkx, G.C.A., Arafat, A., Van Bekkum, H., 1996. Microwave heating in the TS-1 catalyzed oxyfunctionalisation of n-hexane. J. Mol. Catal. A Chem. 111, 167–174. https://doi.org/10.1016/1381-1169(96)00206-3

Li, C., Zhao, X., Wang, A., Huber, G.W., Zhang, T., 2015. Catalytic Transformation of Lignin for the Production of Chemicals and Fuels. Chem. Rev. 115, 11559–11624. https://doi.org/10.1021/acs.chemrev.5b00155

Li, H., Qu, Y., Xu, J., 2015. Microwave-Assisted Conversion of Lignin. pp. 61–82. https://doi.org/10.1007/978-94-017-9612-5_4

Li, H., Zhang, C., Pang, C., Li, X., Gao, X., 2020. The Advances in the Special Microwave Effects of the Heterogeneous Catalytic Reactions. Front. Chem. 8, 1–8. https://doi.org/10.3389/fchem.2020.00355

Ma, R., Xu, Y., Zhang, X., 2015. Catalytic Oxidation of Biorefinery Lignin to Value-added Chemicals to Support Sustainable Biofuel Production. ChemSusChem 8, 24–51. https://doi.org/10.1002/cssc.201402503

Ouyang, X., Huang, X., Ruan, T., Qiu, X., 2015. Microwave-assisted oxidative digestion of lignin with hydrogen peroxide for TOC and color removal. Water Sci. Technol. 71, 390–396. https://doi.org/10.2166/wst.2014.535

Ouyang, X., Lin, Z., Deng, Y., Yang, D., Qiu, X., 2010. Oxidative Degradation of Soda

Lignin Assisted by Microwave Irradiation. Chinese J. Chem. Eng. 18, 695–702. https://doi.org/10.1016/S1004-9541(10)60277-7

Ouyang, X., Tan, Y., Qiu, X., 2014. Oxidative degradation of lignin for producing monophenolic compounds. J. Fuel Chem. Technol. 42, 677–682. https://doi.org/10.1016/S1872-5813(14)60030-X

Palma, V., Barba, D., Cortese, M., Martino, M., Renda, S., Meloni, E., 2020. Microwaves and heterogeneous catalysis: A review on selected catalytic processes. Catalysts 10. https://doi.org/10.3390/catal10020246

Pan, J., Fu, J., Lu, X., 2015. Microwave-Assisted Oxidative Degradation of Lignin Model Compounds with Metal Salts. Energy & Fuels 29, 4503–4509. https://doi.org/10.1021/acs.energyfuels.5b00735

Pandey, M.P., Kim, C.S., 2011. Lignin Depolymerization and Conversion: A Review of Thermochemical Methods. Chem. Eng. Technol. 34, 29–41. https://doi.org/10.1002/ceat.201000270

Panyadee, R., Posoknistakul, P., Jonglertjunya, W., Kim-Lohsoontorn, P., Laosiripojana, N., Matsagar, B.M., Wu, K.C.W., Sakdaronnarong, C., 2018. Sequential Fractionation of Palm Empty Fruit Bunch and Microwave-Assisted Depolymerization of Lignin for Producing Monophenolic Compounds. ACS Sustain. Chem. Eng. 6, 16896–16906. https://doi.org/10.1021/acssuschemeng.8b04246

Qu, C., Ito, K., Katsuyama, I., Mitani, T., Kashimura, K., Watanabe, T., 2020. Directly Microwave-Accelerated Cleavage of C−C and C−O Bonds of Lignin by Copper Oxide and H_2O_2. ChemSusChem 13, 4510–4518. https://doi.org/10.1002/cssc.202000502

Rinaldi, R., Jastrzebski, R., Clough, M.T., Ralph, J., Kennema, M., Bruijnincx, P.C.A., Weckhuysen, B.M., 2016. Paving the Way for Lignin Valorisation: Recent Advances in Bioengineering, Biorefining and Catalysis. Angew. Chemie - Int. Ed. 55, 8164–8215. https://doi.org/10.1002/anie.201510351

Rodrigues, A.E., Pinto, P.C. de O.R., Barreiro, M.F., Esteves da Costa, C.A., Ferreira da Mota, M.I., Fernandes, I., 2018. An Integrated Approach for Added-Value Products from Lignocellulosic Biorefineries. Springer International Publishing, Cham.

https://doi.org/10.1007/978-3-319-99313-3

Upton, B.M., Kasko, A.M., 2016. Strategies for the conversion of lignin to high-value polymeric materials: Review and perspective. Chem. Rev. 116, 2275–2306. https://doi.org/10.1021/acs.chemrev.5b00345

Vangeel, T., Schutyser, W., Renders, T., Sels, B.F., 2018. Perspective on Lignin Oxidation: Advances, Challenges, and Future Directions. Top. Curr. Chem. 376, 30. https://doi.org/10.1007/s41061-018-0207-2

Wang, H., Pu, Y., Ragauskas, A., Yang, B., 2019. From lignin to valuable products–strategies, challenges, and prospects. Bioresour. Technol. 271, 449–461. https://doi.org/10.1016/j.biortech.2018.09.072

Werpy, T., Petersen, G., 2004. Top Value Added Chemicals from Biomass: Volume I -- Results of Screening for Potential Candidates from Sugars and Synthesis Gas., U.S. Department of energy. United States. https://doi.org/10.2172/926125

Xia, C., Peng, X., Zhang, Y., Wang, B., Lin, M., Zhu, B., Luo, Y., Shu, X., 2017. Environmental-Friendly Catalytic Oxidation Processes Based on Hierarchical Titanium Silicate Zeolites at SINOPEC, in: Karamé, I. (Ed.), Green Chemical Processing and Synthesis. InTech, pp. 119–150. https://doi.org/10.5772/intechopen.68389

Zhang, D., Sun, B., Duan, L., Tao, Y., Xu, A., Li, X., 2016. Photooxidation of Guaiacol to Organic Acids with Hydrogen Peroxide by Microwave Discharge Electrodeless Lamps. Chem. Eng. Technol. 39, 97–101. https://doi.org/10.1002/ceat.201500251

Zhu, G., Jin, D., Zhao, L., Ouyang, X., Chen, C., Qiu, X., 2017. Microwave-assisted selective cleavage of C_A-C_B bond for lignin depolymerization. Fuel Process. Technol. 161, 155–161. https://doi.org/10.1016/j.fuproc.2017.03.020

7. Conclusions and Suggestions for Future Work

7.1 Main Conclusions

The main objective of this work was to obtain C_4 dicarboxylic acids (C_4-DCA) from lignin oxidation. As lignin has a very complex structure, initial tasks were performed with lignin model compounds [*p*-hydroxybenzoic acid (pHBA), vanillic acid (VA), and syringic acid (SA)]. The objective was to understand the chemical pathways to C_4-DCA production to improve the reaction conditions. TS-1 catalyst was firstly evaluated using these compounds targeting an efficient conversion to succinic acid. Later, lignin was oxidized using TS-1 using both conventional heating (CH) and microwave heating (MW) to determine the best system for C_4-DCA production. Hence, the principal conclusions of this work are described below.

i) Methoxy substituents effect on lignin oxidation

It was important to understand how methoxy substituents influenced the reactivity and C_4-DCA selectivity in the peroxide oxidation. Initial studies were performed using lignin model compounds, thereafter followed by lignin samples. The main conclusions are:

- Methoxy substituents act as electron donors of the aromatic ring, stabilizing the hydroxyl radical and activating the structure towards peroxide oxidation. As pHBA has no methoxy substituents, it had the lowest reactivity, while SA presented the highest.
- The methoxy substituents affected the produced C_4-DCA, being succinic acid the main produced acid for the three oxidation compounds (pHBA, SA and VA), but with different yields and selectivities among the model compounds.
- The pathway of ring-opening reactions to C_4-DCA was studied. One of the first steps was the demethoxylation to achieve hydroxyl-free units, which can be further oxidized to quinones. These quinones are easily opened to form muconic acid derivatives, later decarboxylated to produce C_4 dicarboxylic acids.
- Hardwood lignin gave rise to the higher succinic acid yields (3.2 wt%), comparatively with softwood lignin (2.5 wt%) due to the higher reactivity caused by S units presenting more methoxy substituents. Therefore, lignin's internal structure affects the type and yield of the produced C_4-DCA, and an in-depth

evaluation of lignins is recommended to establish the best feedstock for succinic acid production.

ii) Lignin model compounds oxidation using TS-1 catalyst

Heterogeneous catalysts are an efficient way to improve oxidative lignin conversion. Vanillic acid, a lignin model compound, was oxidized using TS-1 to evaluate different reaction conditions towards C_4-DCA, and the main conclusions are:

- Different variables affected the produced acid and its yield. High temperatures (145°C) were needed to achieve the ring-opening reaction, but extended times ($t>2h$) and high temperatures caused C_4-DCA degradation.
- Acidic pH results more in a more selective oxidation towards succinic acid (7.4 mol%), while alkaline pH allows an easier hydroxylation to form malic acid (15.1 mol%). At alkaline pH, H_2O_2 is degraded, and the catalyst structure become damaged. However, as lignin is insoluble in acidic pH, mass transfer problems can hinder a good oxidation. Thus, a neutral pH was recommended for lignin oxidation.
- Modification of TS-1 with metallic ions (Cu, Co, and Fe) showed no improvement in alkaline conditions. In acidic conditions, only Fe-TS1 catalyst improved, slightly, the succinic acid yield, while Co and Cu-modified catalysts diminished the oxidant power of H_2O_2. Only Fe-TS1 was stable without leaching, being the only catalyst that could be used in subsequent experiments.

iii) Lignin oxidation using TS-1 catalyst

Further experiments used real lignin samples to evaluate the catalytic effect of TS-1. Four different lignins were chosen: Alkali lignin (softwood alkali, ALK), Indulin AT (softwood kraft, IAT), Lignol (organosolv hardwood, EOL), and *E. globulus* lignin (hardwood kraft, EKL). The main conclusions are:

- The main produced acids were malic and succinic acids, with traces of fumaric, maleic, and tartaric acids. The best conversions were observed for the kraft and the organosolv lignins. The best catalytic effect for succinic acid production was observed with IAT lignin, where TS-1 improved up to four times the succinic acid yield.

- Concerning the lignin type, it was found that IAT conducted to the highest succinic acid yield (11.3 wt%), followed, closely, by EOL (9.7 wt%). However, EOL showed the highest C_4-DCA total yields, with very high values of malic acid (19.5 wt%). As the organosolv pretreatment is a milder extraction process than the kraft process, EOL kept more *β-O-4* bonds and less condensed structures, confirming its use as a better feedstock for C_4-DCA production.
- The best conditions for C_4-DCA production were acidic and neutral pH, with lower yields at alkaline pH. High temperatures (140°C) were needed to achieve the ring-opening reaction, but very high temperatures (160ºC) and prolonged times ($t>2h$) caused acids degradation and condensation reactions of the remaining lignin fragments. The reaction depended on the H_2O_2 load added to the reaction medium since low amounts resulted in modest yields, while higher oxidant amounts caused over-oxidation of the products, decreasing the final yields.
- The catalyst was tested for several cycles without losing the catalytic properties after 5 cycles. The decrease in the total carboxylic acid yield was caused by the catalyst loss during the centrifugation step, given its small particle size.

iv) Lignin microwave-assisted oxidation towards C_4 dicarboxylic acids

Microwave (MW) heating was tested to evaluate how the peroxide oxidation of lignin was performed when using TS-1 and Fe-TS1. A comparison against conventional heating (CH) was also included. The main conclusions are:

- Temperature increase reduced the needed time to achieve the highest lignin conversion and C_4-DCA yield, but acids degradation occured after the maximum yield. At 170°C, the heating caused a rapid disproportionation of H_2O_2 to O_2 with a rapid increase in pressure and reduced oxidation potential.
- Catalyst effect in MW depended on the lignin type. TS-1 and Fe-TS1 enhanced succinic acid yield for EKL and IAT, while for EOL a similar behaviour was observed for the catalysed and non-catalysed reaction. Fe-TS1 accelerated the lignin conversion and C_4-DCA production in the first 30 minutes, being later matched by the TS-1 catalyst. TS-1 and Fe-TS1 helped to stabilize the oxidant that slowly release the radicals, avoiding a fast and uncontrolled oxidation favouring

C_4-DCA instead of degradation products. Interestingly, malic acid was obtained a high levels for EOL (34 wt%) in the non-catalysed reaction. Overall, this work showed a higher yield for succinic and malic acids compared to previous works.

- The non-catalytic oxidation was enhanced by using MW, compared to CH, especially for EOL lignin. TS-1 oxidation was better for CH since TS-1 enhanced the disproportionation of H_2O_2 in MW, reducing the oxidative power. The lignin conversion and C_4-DCA yields were higher in the first 30 minutes for MW, but CH matched MW for higher times.
- EOL showed outstanding results, as the organosolv mild extraction process produces low condensed lignins with a high amount of *β-O-4* bonds, facilitating the depolymerization and improving the aromatic ring cleavage towards C_4-DCA. In MW heating, this was crucial since MW enhances the cleavage of *β-O-4* bonds, and the increase of succinic acid yield (5.2 wt%) was substantial compared to CH (1.6 wt%), even without a catalyst.
- A careful study of the reaction conditions is needed to improve the production of the targeted C_4-DCA, as each lignin has a specific structure, comprising diverse bonds with different susceptibility to be cleaved.

The results presented in this work have contributed to reduce the research gap between lignin conversion and C_4-DCA production. C_4-DCA are building blocks widely used in diverse industrial fields and the studied productive route offers high potential for a future bioeconomy. Moreover, this work deepened the involved chemical pathways knowledge and provided positive evidence of lignin successful conversion to valuable C_4-DCA.

7.2 Suggestions for Future Work

Although this work tried to deepen the study of lignin valorization into C_4-DCA, there are still some opportunities to be improved through new research lines, looking forward to a competitive and efficient oxidation process. The provided suggestions are separated in two main groups: the improvement of the proposed process and the inclusion of the developed strategies into the global LSRE-LCM lignin valorization integrated process.

7.2.1 Improvement of the proposed process

The process used in this work is an initial approach for lignin valorization, which can be subjected to improvements. Some suggestions for future works are as follow:

- The use of batch reactors with higher capacity to study the kinetics and increase productivity. Higher volumes of reaction mixture would also allow separation and crystallization of the C_4-DCA. Studies for separation and crystallization have already been performed in the research group for vanillin (Gomes, 2019), so the available technology and knowledge can be addopted.
- The use of TS-1 with a larger particle size must be evaluated to determine the best separation process for efficient catalyst recovery. Also, it is pending the study of the regeneration of the spent catalyst, as several works have already suggested calcination (Alba-Rubio et al., 2017; Rodenas et al., 2018).
- It is advisable to perform a comparison between MW and CH using more similar conditions. Namely, the glass vials used as MW reactors could be used in CH by submerging the closed vial in an oil bath at the target temperature. Once the comparison is made, an economic analysis of the two processes is essential to evaluate the future application of the process.
- It is recommended to extend this study using more organosolv lignins from different feedstocks, mainly if obtained from a biorefinery processes since they proved to be especially advantageous for depolymerization towards C_4-DCA.
- Additional studies could be performed using heterogeneous catalysts with metallic ions with two oxidation states since they could improve oxidation performance and selectivity towards C_4-DCA. Many of these heterogeneous catalysts are already known but have not been used yet on lignin depolymerization to C_4-DCA (Das et al., 2012; Li et al., 2015; Schutyser et al., 2018).
- It would be interesting to extend the performed tests to the black liquor stream of the pulping plants without performing lignin precipitation and purification steps. This possibility shows an increasing challenge since this stream has a very alkaline pH and impurities can reduce peroxide efficiency and complicate the subsequent purification and separation steps. Moreover, as TS-1 is not stable in alkaline pH, a different catalyst should be proposed or adopt the non-catalyzed oxidation route.

7.2.2 Incorporation into the global LSRE-LCM lignin valorization integrated process

The LSRE-LCM lignin research group has studied an integrated process, where lignin is converted by wet O_2 oxidation to vanillin and syringaldehyde. This process generates two mains streams: high molecular weight lignins that are used as a raw material for lignin-based polyurethanes, and a phenolates-rich stream, that is purified to obtain aldehydes (Costa et al., 2021). However, the aromatic acids (e.g., vanillic and syringic acids) are not exploited due to over-oxidation of the valuable aldehydes. Still, they can be used for C_4-DCA production (as was proven in Chapters 3 and 4), enhancing the valorization given to lignin. Also, the lignin fraction-rich stream, which has higher condensation degree, could be used as feedstock for C_4-DCA production besides polyurethane production. All these solutions suit the new scope of biorefineries with good carbon efficiency and low residues production.

7.3 References

Alba-Rubio, A.C., Fierro, J.L.G., León-Reina, L., Mariscal, R., Dumesic, J.A., López Granados, M., 2017. Oxidation of furfural in aqueous H_2O_2 catalyzed by titanium silicalite: Deactivation processes and role of extraframework Ti oxides. Appl. Catal. B Environ. 202, 269–280. https://doi.org/10.1016/j.apcatb.2016.09.025

Costa, C.A.E., Vega-Aguilar, C.A., Rodrigues, A.E., 2021. Added-Value Chemicals from Lignin Oxidation. Molecules 26, 4602. https://doi.org/10.3390/molecules26154602

Das, L., Kolar, P., Sharma-Shivappa, R., 2012. Heterogeneous catalytic oxidation of lignin into value-added chemicals. Biofuels 3, 155–166. https://doi.org/10.4155/BFS.12.5

Gomes, E.D., 2019. Development of a continuous process for the production of vanillin and syringaldehyde from kraft black liquor. Dep. Chem. Eng. University of Porto, Faculty of Engineering, Porto.

Li, C., Zhao, X., Wang, A., Huber, G.W., Zhang, T., 2015. Catalytic Transformation of Lignin for the Production of Chemicals and Fuels. Chem. Rev. 115, 11559–11624.

https://doi.org/10.1021/acs.chemrev.5b00155

Qu, C., Ito, K., Katsuyama, I., Mitani, T., Kashimura, K., Watanabe, T., 2020. Directly Microwave-Accelerated Cleavage of C−C and C−O Bonds of Lignin by Copper Oxide and H_2O_2. ChemSusChem 13, 4510–4518. https://doi.org/10.1002/cssc.202000502

Rodenas, Y., Mariscal, R., Fierro, J.L.G.G., Martín Alonso, D., Dumesic, J.A., López Granados, M., 2018. Improving the production of maleic acid from biomass: TS-1 catalysed aqueous phase oxidation of furfural in the presence of γ-valerolactone. Green Chem. 20, 2845–2856. https://doi.org/10.1039/C8GC00857D

Schutyser, W., Renders, T., Van den Bosch, S., Koelewijn, S.F., Beckham, G.T., Sels, B.F., 2018. Chemicals from lignin: an interplay of lignocellulose fractionation, depolymerisation, and upgrading. Chem. Soc. Rev. 47, 852–908. https://doi.org/10.1039/C7CS00566K

Appendix A.

A.1. Calibration Curves

Calibration curves were established for carboxylic acids and lignin quantification at different moments during this project. Since the calibration curves were performed for each main objective, the data for each calibration is presented.

A.1.1. Carboxylic acid calibration curves

The carboxylic acids standards for the calibration curves were prepared with analytical grade reagents in ultrapure water, in concentration ranges where linearity has been reported and was checked during the calibration. For each calibration curve, at least 7 points were established. Statistical analysis were performed for each calibration curve, and the following parameters are presented: slope (m), intercept (b), coefficient of determination (R^2), detection limit (L_D), quantification limit (L_Q), as well as the variance applied to the slope (s_m) and the intercept (s_b) of the curve. It is indicated the type of quantification used: DAD detector (working at 210 nm or 260 nm) or Refraction Index detector. In some cases, both detectors are reported.

Three calibration curves are presented (Tables A.1, A.2., A.3.), corresponding to the main calibration moments for the Chapters 3, 4, and 5, respectively. During the analysis, calibration was checked using the calibration standards.

Table A-1Carboxylic acid calibration curves, February 2019.

Acid	λ (nm)	C_{start} (mg/L)	C_{final} (mg/L)	m	b	R^2	s_m	s_b	s_y	L_D (mg/L)	L_Q (mg/L)
Oxalic	210	10.00	150.0	31076	76207	0.9982	588	53200	73485	7.1	24
Maleic	210	0.25	25.0	307695	-32288	0.9990	4290	60100	100147	1.0	3.2
Tartaric	210	5.02	400.2	3778	-8367	0.9997	28	5830	10356	8.2	27
Malic	210	10.09	499.7	2035	-14434	1.0000	18	5230	8419	12	41
Malonic	210	10.00	249.6	1919	6217	0.9904	84	11800	18899	30	98
Succinic	210	5.02	250.0	1232	-4135	0.9987	20	2830	4564	11	37
Lactic	210	5.00	200.2	1476	-1894	0.9999	7	737	1165	2.4	7.9
Formic	210	50	500.0	2174	-12536	0.9978	45	13600	18118	25	83
Fumaric	210	0.5	25.0	297362	-15448	1.0000	875	12300	20322	0.2	0.7
Acetic	210	4.99	199.6	1072	-4923	0.9971	26	2780	4389	12	41
Propionic	210	5.00	100.0	1253	-445.9	0.9987	20	1260	1753	4.2	14
p-hydroxybenzoic	210	1.00	30.02	225718	-40164	0.9998	1220	22100	31750	0.4	1.4
	260			239235	-5282	1.0000	657	11800	17021	0.2	0.7
Vanillic	210	0.99	30.04	263960	-30632	0.9993	3220	58100	83545	0.9	3.2
	260			157745	1547	0.9999	775	14000	20080	0.4	1.3
Syringic	210	0.95	28.81	302211	25360	0.9975	6760	117000	167980	1.7	5.6
	260			96177	193.9	0.9999	421	7280	10472	0.3	1.1
Vanillin	210	1.00	20.00	185996	-7204	0.9949	5980	64500	100408	1.6	5.4
	260			76575	-4812	0.9987	1260	13500	21094	0.8	2.7

Table A-2 Carboxylic acid calibration curves, February 2020.

Acid	Detection method	C_{start} (mg/L)	C_{final} (mg/L)	m	b	R^2	s_m	s_b	L_D (mg/L)	L_Q (mg/L)
Oxalic	UV 210 nm	9.97	149.9	32069	-25620.5	1.0000	98	8907	1.1	3.8
	RI			293.7	-2114	0.9985	5	460	6.5	22
Maleic	UV 210 nm	0.25	25.02	237577	52917	0.9992	2948	41367	0.9	2.9
	RI			40.8	-21.4	0.9701	4	69	4.8	16
Tartaric	UV 210 nm	4.98	400.2	3575	-5118	0.9999	13	2719	4.1	14
	RI			279.2	-280.9	1.0000	1	179	3.4	11
Malic	UV 210 nm	19.88	993.8	1872	-3009	1.0000	6	3160	8.2	27
	RI			38.5	28.3	0.9998	0.3	142	18	60
Malonic	UV 210 nm	10.01	250.0	2189	-4957	0.9988	34	4752	10	35
	RI			235.5	-652	0.9997	2	256	5.2	17
Succinic	UV 210 nm	5.07	251.5	1531	31.5	0.9994	17	2368	7.5	25
	RI	25.15		38.0	22.4	0.9991	1	86	8.8	29
Lactic	UV 210 nm	5.27	210.9	1299	-1923.96	0.9999	7	785	2.9	9.5
	RI	26.37		25.4	97.0	0.9974	1	79	12	39
Formic	UV 210 nm	50.00	500.0	2175	48.8	0.9998	15	4515	8.3	28
	RI			113.8	-1056	0.9996	1	319	11	37
Fumaric	UV 210 nm	0.50	24.98	335333	73771	0.9997	2697	37811	0.6	1.9
	RI	4.99		47.1	10.83816	0.9824	4	60	3.7	12
Acetic	UV 210 nm	4.99	199.6	1286	-2060	0.9991	17	1831	6.7	22
	RI			148.3	-670.463	0.9976	3	353	11	38
p-HBA	UV 260 nm	1.02	30.02	216181	707.0	1.0000	607	10957	0.2	0.7
Vanillic	UV 260 nm	1.00	29.96	142412	-7140	0.9999	465	8376	0.3	0.8
Syringic	UV 260 nm	0.96	29.96	83586	-5173	0.9999	422	7613	0.4	1.3

Table A-3 Carboxylic acid calibration curves, April 2021.

Acid	Detection method	C_{start} (mg/L)	C_{final} (mg/L)	m	b	R^2	s_m	s_b	L_D (mg/L)	L_Q (mg/L)
Oxalic	UV 210 nm	10.0	149.97	32439	-26896	0.9999	117	10599	1.4	4.5
	RI			324.5	-366.5	0.9997	2.49	226	2.9	10
Maleic	UV 210 nm	0.247	24.7	241540	-13170	0.9999	884	12262	0.3	0.8
	RI			288.8	-75.68	0.9994	3.05	42.3	0.7	2.4
Tartaric	UV 210 nm	4.982	400.1	3633	-10117	0.9999	18.5	3853	5.7	19
	RI			284.3	-189.8	1.0000	0.71	147	2.8	9.2
Malic	UV 210 nm	19.8	990	1940	-18054	0.9996	17.8	9916	25	82
	RI			261.3	-714.3	0.9999	0.86	478	8.8	29
Succinic	UV 210 nm	4.99	248	1321	-8091	0.9977	28.3	3944	14	48
	RI			244.4	-119.0	0.9997	1.94	270	5.3	18
Formic	UV 210 nm	50.0	500.0	2132	127.1	0.9999	10.1	3023	5.7	19
	RI			111.1	98.95	0.9999	0.58	173	6.2	21
Fumaric	UV 210 nm	0.492	24.8	335826	54566	0.9999	1405	19542	0.3	1.0
	RI			337.9	-72.73	0.9995	3.54	49.3	0.7	2.4
Acetic	UV 210 nm	4.948	197.9	1473	-3586	0.9951	46.1	4912	16	53
	RI			165.1	89.24	0.9996	1.48	158	4.5	15

A.1.2. Soluble and insoluble lignin calibration curves

The lignin calibration curves were prepared as following:

Lignin samples (Indulin AT - IAT, Lignol - LIG, *E. globulus* kraft lignin - EKL, Alkali - ALK) were dissolved in an alkaline solution (pH~11), then acidified to pH~2 using H_2SO_4 2 mol/L, heated at 40°C to coagulate the acid-insoluble lignin, then centrifuged at 3500 rpm for 30 minutes. The acidic supernatant was used for acid-soluble lignin quantification. The acid-insoluble lignin was re-solubilized in an alkaline solution (phosphate buffer, pH~8-9). ALK lignin was completely soluble in acid, and no acid-insoluble lignin was determined.

Both acid-soluble and acid-insoluble lignin solutions were used for calibration curves preparation. Both calibration curves were analyzed by UV spectrophotometry at 240 nm.

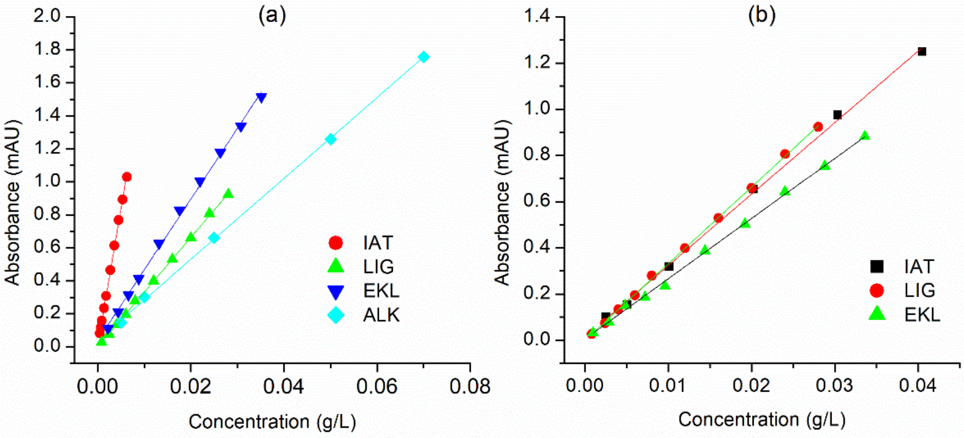

Figure A-1 Calibration curves for (a) acid-soluble lignin and (b) acid-insoluble lignin.

A.1.3. Gel permeation chromatography calibration curves

The gel permeation chromatography standards for the calibration curves were prepared with two different GPC grade standards: Agilent GPC/SEC (series number 0006149180, Mp 162- 4910 g/mol) and Sigma Aldrich #48937 (series number , Mp= 2340-55000 g/mol). The standards were prepared at a 5 mg/mL concentration, dissolved in the eluent (DMF, 0.5% LiCl). The standards were measured at 268 nm.

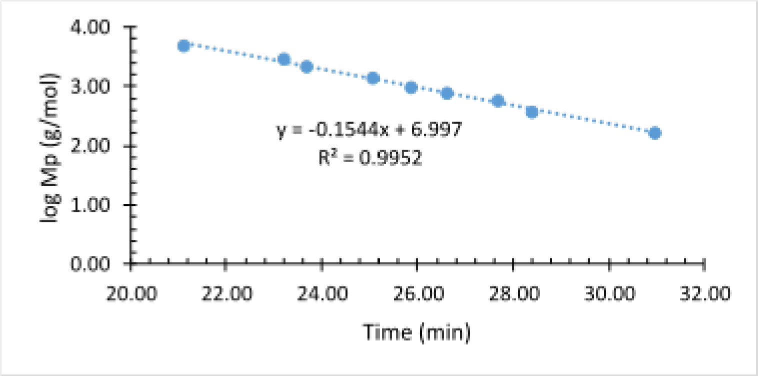

Figure A-1 Calibration curve for GPC analysis, December 2019

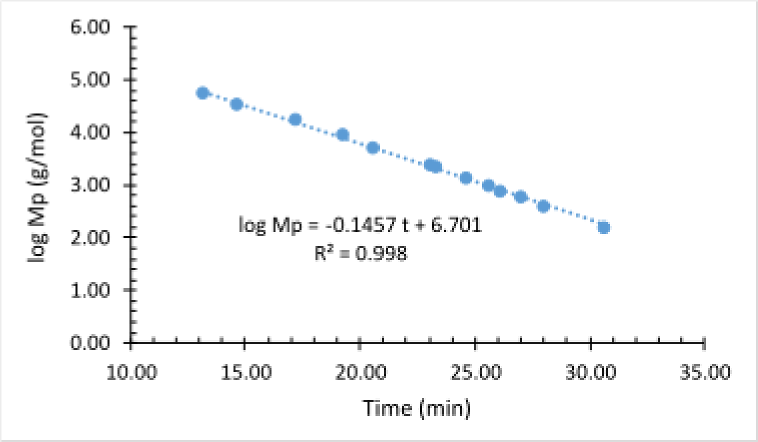

Figure A-2 Calibration curve for GPC analysis, April 2021

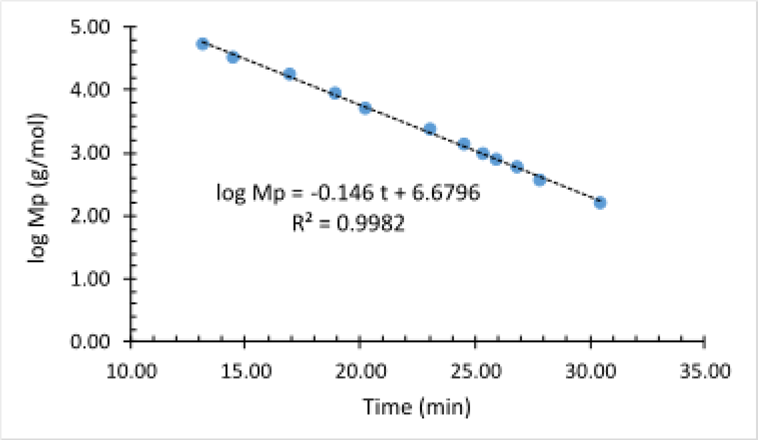

Figure A-3 Calibration curve for GPC analysis, July 2021

Appendix B.

B.1. Lignin oxidation protocol at Büchi reactor

This protocol is based in the Operation Manual (EXCL / QEQPRS / 0308 / 2012 : Batch Reactor), written by Rodrigues and Faria (2014). Additional information was included to use the reaction specifically for lignin oxidation with H_2O_2.

B.1.1. System description

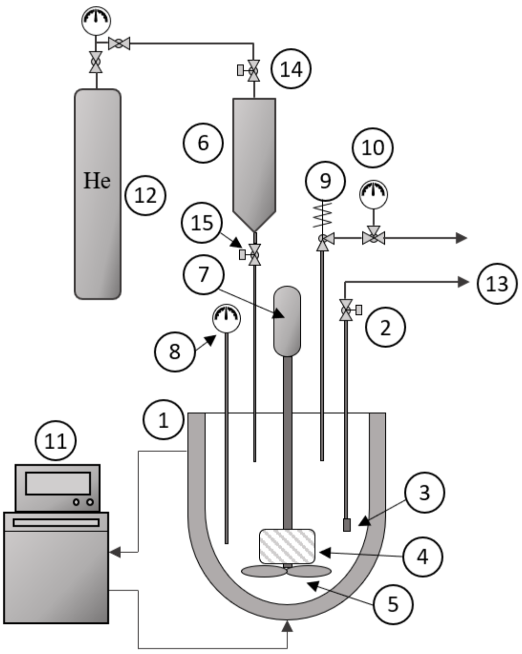

1. Batch reactor
2. Manual sampling valve
3. Sampling filter
4. Catalyst basket
5. Stirring blades
6. Feed container
7. Rotor
8. Thermocouple
9. Relief valve
10. Pressure transducer
11. Thermostatic bath
12. Helium bottle
13. Sampling port
14. Automatic valve
15. Manual valve

Figure B-1 Schematic representation of the experimental set-up.

The batch reactor (Büchi Laboratory Equipment, 45.10005.0000) has a 1 L capacity, a 12-bar maximum operating pressure, and a 200°C maximum operating temperature. All other materials can support up to 12 bar and 200°C.

For more technical details of the reactor individual parts, check the Batch Reactor Manual (Rodrigues and Faria, 2014)

B.1.2. Reactor preparation

1. Perform the following verification list:

Table B-1. Verification list for reactor preparation

#	Checklist	Status
1	All the electric components are correctly connected and have an adequate power supply.	
2	All the automatic valves are supplied with energy.	
3	The pressure of the Helium bottle used to pressurize the reactor is high enough to reach the set point intended by the user and keep it for the entire experiment.	
4	The level of the heating/refrigerating liquid of the thermostatic bath is appropriate.	
5	The sample line is clean and closed	
6	The thermocouple is ready to start measuring	
7	The pressure transducer is ready to start measuring and correctly calibrated	
8	The feed container is empty and clean and the manual valve at its outlet is completely opened	
9	The sampling filter is correctly installed	
10	The O-ring is placed at the top of the stirring shaft	
11	The feed container inlet manual valve is closed and the outlet manual valve is opened	
12	The *BatchReactor_V2.1* software is running*	

* For starting BatchReactor_V2.1 software, follow the next steps:

2. Open the BatchReactor_V2.1 Software. You will find the following window.

Save File As: C:\Users\WT\Documents\BatchReactor\New Text Document.txt

Measurements Rate (s): 1

Saving data Rate (s): 1

Relay Board Port: COM2

Calib. Curve Slope: 2,9582

Sampling Lines Cleaning Time (s): 5

GC Analysis Time (min): 5

Multi-Loop Valve Port: COM3

Calib. Curve Intercept: -0,725

Total Time (min): 180

Experiment Description

Username:
Project:

Reaction Scheme:
A + B <---> C + D

Exp. ID:
Temperature Set-Point:
Pressure Set-Point:
Stirring Speed:
Reactants Molar Ratio:
Catalyst:
Catalyst Amount:

1. Save File As
2. Measurements Rate (s)
3. Saving data Rate (s)
4. Relay Board Port
5. Sampling Lines Cleaning Time (s)
6. GC Analysis Time (min)
7. Multi-Loop Valve Port
8. Sampling Settings
9. Experiment Description
10. Calib. Curve Slope
11. Calib. Curve Intercept
12. Pressure Sensor Calibration
13. Start

Figure B-2 BatchReactor_V2.1 software main window

a. In Save File As (1), select the location and name of the desired text file. Place the .txt at the end.
b. Place the Measuring Rate (2) at 2 s (to avoid heavy data files).
c. Place the Saving Data Rate (3) at 2 s (to avoid heavy data files).
d. Place the Sampling Lines Cleaning Time (5) at 1 s.
e. Place the GC Analysis Time (6) at 1 min (without selecting any number here, the software won't run)
f. In Sampling Settings (8), select the "Manual Sampling" tab, and place any number at Total Time (min), but always superior to the total reaction time (including heating).
g. In Experiment Description, write any details of the experiment that will be saved in the text file.
h. After all information is placed, click Start (13).
i. The system will show an Alert Window, to check if every detail was introduced. Press OK.
j. The following window will be shown.

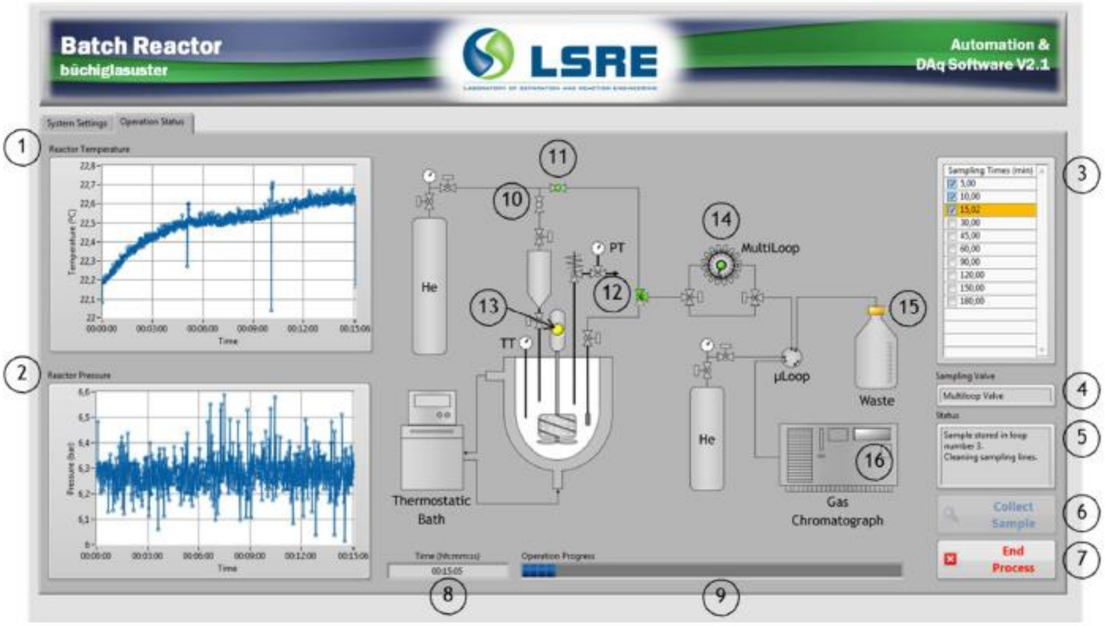

Sampling Times (min)
☑ 5,00
☑ 10,00
☑ 15,02
☐ 30,00
☐ 45,00
☐ 60,00
☐ 90,00
☐ 120,00
☐ 150,00
☐ 180,00

Sampling Valve: Multiloop Valve

Status: Sample stored in loop number 3. Cleaning sampling lines.

1. Batch Reactor Temperature Plot
2. Batch Reactor Pressure Plot
3. Sampling Times (min)
4. Sampling Valve
5. Status
6. Collect Sample
7. End Process
8. Time (hh:mm:ss)
9. Operation Progress Bar
10. AV1 Control/Indicator
11. AV2 Control/Indicator
12. AV3 Control/Indicator
13. Rotor Control/Indicator
14. Multiloop Valve Indicator
15. Waste Flask Indicator
16. GC Indicator

Figure B-3. BatchReactor_V2.1 software Experiment window

3. Weight the precise mass of the catalyst and load the catalyst basket.
4. Position the catalyst basket at the bottom of the stirring shaft, and place the stirring blades at the bottom of the stirring shaft, which supports the catalyst basket. The stirring blades and the basket must be well secure.
5. Load the batch reactor vessel with the precise amount of the lignin/model compound solution (minimum 400 mL).
6. Position and close the batch reactor.
7. Pressurize the reactor vessel by opening AV1, up to 3 bar. Close the AV1 and the Helium bottle pressure reducer when the pressure is stable. The pressure shown in the Helium tank manometer is +0.75 bar than the pressure recorded by the software.
8. Check if pressure is kept stable for several minutes. If it is well sealed, continue with the experiment. If it is not well sealed, reopen the reactor and close it again, checking for leaks.
9. Purge the reactor, then pressurize it again. Repeat twice to release all O_2 inside the reactor.

10. Pressurize the reactor vessel to 0.5 bar (to avoid having boiling inside the reactor at temperatures higher than 100ºC). Close the feed container outlet valve, the AV1, and the Helium bottle pressure reducer when the pressure is stable.
11. Open the feed container inlet valve to release pressure inside the feed container.
12. Switch the thermostatic bath on and set the temperature to the desired value. There is a difference of approximately 21ºC between the thermostatic bath and the reactor (the reactor is colder than the thermostatic bath), which must be taken into account when selecting the temperature
13. Switch on the rotor. Slowly increase speed to the desired value. If speed is increased too fast, the stirring blades could loosen from the stirring shaft and fall, causing damage to the glass reactor. This can only be done if the catalyst does not react with the lignin/model compound in absence of oxidant (H_2O_2). If the catalyst reacts with the lignin/model compound, the basket should be placed on the top of the shaft, and the stirring must starts precisely when the oxidant is added.
14. Wait until the desired temperature reaches the set point. During this time, pressure increases, and the solution must never boil.

B.1.3. Performing a reaction

Once the temperature achieved steady-state, the reaction can be started by adding the oxidant. All samples are taken manually.

1. Add the oxidant to the feed container, and close the inlet valve.
2. Pressurize the feed container, by opening the pressure reducer in the Helium tank and the AV1 valve. The pressure in the feed container must be higher than the reactor vessel's actual pressure, at least +0.5 bar. The difference between the pressure transducer and the read pressure in the software should be taken in place to calculate the pressure inside the feed container. As a rule of thumb, the feed container should be pressurized +1.25 bar higher than the software pressure.
3. Close the Helium tank outlet valve.
4. Place the clean, dry tubes for collecting samples on an ice-water bath, plus one or two additional tubes for cleaning the sampling line.
5. Open the outlet manual valve of the feed container, allowing the oxidant inside the reactor vessel. Start to count the reaction time.

6. At the desired sampling time, place the cleaning tube at the Sampling Line, and open the Sampling Line Manual Valve for 1-2 s, for cleaning the line. Then switch to another clean tube and collect the sample, sampling for about 1-2 s. **CAREFUL!** Samples exit the reactor at high pressure and high temperature! All security measures must be taken to avoid any accident.
7. Continue to take samples according to the desired sampling time. The temperature and pressure will be recorded by the software, but not the sampling time, which should be recorded manually.
8. Once the last sample is taken out, the equipment will not finish automatically, but the user must stop the process by pressing the “End Process” button in the “User Interface: Operation Status” tab. Once the “End Process” button is pressed, the data gathering stops, and the data file is recorded automatically. However, it is recommended to perform the closing procedure while the process is still running, to be able to see the current pressure and temperature inside the reactor.

B.1.4. Finishing the experiment and cleaning the reaction

Once the experiment is concluded, the following procedure will guide the user to release all pressure and temperature, clean the equipment and leave it in conditions for a new experiment. It is recommended to perform the closure procedure with the data-gathering swift on, to see the current pressure and temperature inside the reactor vessel.

1. Set the thermostatic bath temperature to a value sufficiently low to assure that all (or the majority) of the compounds present at the batch reactor vessel are in the liquid phase.
2. Check that the Helium tank outlet valve and the pressure reducer valve are both closed.
3. Once the temperature is lower than 60ºC, carefully release the pressure by opening the feed container inlet valve until complete depressurization.
4. Slowly reduce speed in the rotor, until it stops completely. Turn off the rotor.
5. Press the “End Process” button in the “User Interface: Operation Status” tab. At this moment, all data-gathering will be stopped and the information will be recorded in the data file. Also, all automatic valves are closed at this moment.

6. Carefully open the batch reactor, eliminate/store the content when the temperature is adequate to handle it, using the appropriate disposal procedure.
7. Remove the catalyst basket, eliminate/store the solid inside the basket using the appropriate disposal procedure.
8. Remove the catalyst basket and the stirring blades. Clean them with warm water to eliminate any residue.
9. Clean the reactor vessel using hot water, to eliminate any residue.
10. Clean all equipment that was in contact with the reaction solution using warm water.
11. Close the feed container outlet valve and pour warm water into the feed container. Open the outlet valve to clean the feed container. Repeat.
12. With a syringe, clean with water the sampling line, opening the sampling manual valve.
13. The reactor is now clean to perform another reaction.

If no reaction is going to be performed, then the *BatchReactor_V2.1* software is closed. Automatic valves should be automatically closed but should be checked if they are currently closed. The easiest way to check if the valves are closed if carefully touching them, and ensure they are cold. If they are still hot, they still have energy and are open. If the automatic valves are still opened, then after closing the *BatchReactor_V2.1* software, open the software *K8090 Demo,* located on the computer desktop. Select port "COM2" and click on "Connect". Turn off number 7 and 8. Check if the valve got disconnected. And finally, click on "Disconnect". Close the software.

B.1.5. References

Rodrigues, A.E., Faria, R., 2014. EXCL / QEQPRS / 0308 / 2012 : Batch Reactor - Manual V1.0.